REGULATION OF CENTROMERIC AND PERICENTRIC HETEROCHROMATIN

Dissertation zur Erlangung des Doktorgrades

der Naturwissenschaften

an der

Fakultät für Biologie

der

Ludwig-Maximilians-Universität München

vorgelegt von Silvia Dambacher

aus Mayen

München, Januar 2013

Dissertation eingereicht am: 10. Januar 2013

Mündliche Prüfung am: 04. April 2013

1. Gutachter: Prof. Peter Becker

2. Gutachter: Prof. Heinrich Leonhardt

3. Gutachter: P.D. Anna Friedl

4. Gutachter: Prof. Dirk Eick

5. Gutachter: Prof. Wolfgang Frank

6. Gutachter: Prof. Marc Bramkamp

Eidesstattliche Erklärung

Ich versichere hiermit an Eides statt, dass die vorgelegte Dissertation von mir selbständig und ohne unerlaubte Hilfe angefertigt wurde.

München, den ....

Silvia Dambacher

Erklärung

Hiermit erkläre ich, dass ich mich nicht anderweitig einer Doktorprüfung ohne Erfolg unterzogen habe.

München, den ....

Silvia Dambacher

Wesentliche Teile dieser Arbeit sind in folgenden Publikationen veröffentlicht:

Hahn M.*, **Dambacher S.*,** Dulev S., Anastasia Yurievna Kuznetsova, Simon Eck, Stefan Wörz, Dennis Sadic, Maike Schulte, Jan-Philipp Mallm, Andreas Maiser, Lothar Schermelleh, Pierre Debs, Harald von Melchner, Heinrich Leonhardt, Karl Rohr, Karsten Rippe, Zuzana Storchova, Schotta G. 'Suv4-20h2 mediates chromatin compaction and is essential for cohesin recruitment to heterochromatin.' Genes and Development 2013 Apr 15;27(8):859-72. doi: 10.1101/gad.210377.112

Dambacher S*, Deng W*, Hahn M*, Sadic D, Fröhlich J, Nuber A, Hoischen C, Diekmann S, Leonhardt H, Schotta G. 'CENP-C facilitates the recruitment of M18BP1 to centromeric chromatin.' Nucleus. 2012 January 1; 3(1): 101–110. doi: 10.4161/nucl.18955

Dambacher S.*, Hahn M.*, Schotta G. 'Epigenetic regulation of development by histone lysine methylation.' Heredity (Edinb). 2010 Jul;105(1):24-37. doi: 10.1038/hdy.2010.49. Epub 2010 May 5. Review

Hahn M.*, **Dambacher S.***, Schotta G. 'Heterochromatin dysregulation in human diseases.' J Appl Physiol. J Appl Physiol. 2010 Jul;109(1):232-42. doi: 10.1152/japplphysiol.00053.2010. Epub 2010 Apr 1. Review.

* These authors contributed equally to this work

TABLE OF CONTENTS

ABSTRACT

Constitutive heterochromatin in mammalian cells is present at repeat regions of telomeres, centromeres and at pericentric regions of the chromosome. This work focuses on centromeric and pericentric heterochromatin. Chromatin compaction keeps these genomic domains transcriptionally inert. How the compaction of chromatin is achieved is not completely understood. Dysregulation of heterochromatin organization leads to severe diseases and developmental defects (Hahn et al. 2010). Therefore it is important to understand the mechanisms that establish, regulate and maintain pericentric heterochromatin. Another function of pericentric heterochromatin emerged during the last few years. Centromeres are flanked by large blocks of heterochromatin, which, in *S. cerevisiae* (Folco et al. 2008; Kagansky et al. 2009) and *D. melanogaster* (Olszak et al. 2011), are required for the establishment of functional centromeres. It is currently not clear whether the compact structure of pericentric heterochromatin abolishes the integration of the centromere specific H3 variant CenpA. Heterochromatin might be important to define the border to centromeric regions and therefore ensures centromere identity. Furthermore heterochromatin-associated proteins might play direct roles at centromeres. Pericentric and centric chromatin are both composed of satellite repeat sequences and carry characteristic histone modifications (H3K9me3 and H4K20me3) (Martens et al. 2005). We identified M18bp1, a protein involved in 'priming' centromeric chromatin for CenpA deposition, in a peptide pulldown enriched with the heterochromatin mark H3K9me3. M18bp1 co-localizes with CenpA and is recruited to pericentric heterochromatin in wild type mouse fibroblasts. We propose a novel mechanism explaining the recruitment of M18bp1 to centromeres. M18bp1 is recruited to centromeres via direct interaction of a central region in M18bp1, containing a conserved SANT domain, with the C-terminus of CenpC (Dambacher et al. 2012). Furthermore this study shows that the recruitment of M18bp1 to pericentric heterochromatin occurs in an HP1-dependent manner. M18bp1 directly binds HP1 isoforms *in vitro* and *in vivo*. Together the data provide first evidence, that components of heterochromatin, like HP1 proteins, have functions at centromeric chromatin.

M18bp1 is crucial for mouse development as mutant embryos die very early in the blastocyst stage (E3.5). Blastocyst cells show mitotic defects and enter apoptosis. Inducible M18bp1 knockout fibroblasts show proliferation defects, which is the consequence of two major phenotypes: a) 12h after induction of the deletion severe mitotic defects like decondensed mitotic chromosomes, misalignment in metaphase plate, lagging chromosomes and anaphase bridges probably lead to cell death. b) 3-5 days after depletion, CenpA levels are reduced. Conditional knockout mice with specific deletion of M18bp1 in germ cells show cyst formation in female ovaries and reduced testis size in male mice compared to control mice. We provide the first characterization of a M18bp1 knockout mouse and provide first evidence that M18bp1 is essential for development.

The characterization of proteins involved in the establishment of repressive histone modifications is the second part of this thesis. Three enzymes are involved in the modification of histone H4 on lysine 20. PrSet7 introduces the monomethylation in a replication-dependent manner, while Suv4-20h1 and Suv4-20h2 establish the di- and trimethylation mark. How these enzymes are regulated in establishing the marks is not clear. It has been proposed that PrSet7 monomethylates newly synthesized histones, which then serve as substrates for Suv4-20h enzymes to be converted into di- and trimethylation. Suv4-20h enzymes indeed show higher activity on nucleosomal arrays with monomethylated H4K20, providing first evidence for a sequential methylation pathway. Additionally, a novel interaction between PrSet7 and Suv4-20h2 was identified in GST pulldown experiments. The direct interaction of PrSet7 and Suv4-20h2 indicates a mechanism for interdependent regulation of H4K20 specific methyltransferases, which has to be further validated in subsequent studies.

Suv4-20h2 plays important roles in ensuring the compact chromatin structure, important for gene silencing at pericentric heterochromatin. As a scaffold protein it provides multiple binding sites for HP1 proteins and tethers the mobile HP1 proteins to heterochromatin. Chromatin structure is more accessible to MNase upon loss of Suv4-20h2 and shows extended nucleosomal repeat length, both indicating that Suv4-20h2 mediates chromatin compaction. Furthermore Suv4-20h2 is crucial for the recruitment of cohesin to pericentric heterochromatin. Based on this experiments the histone methyltransferase Suv4-20h2 is defined as a major structural constituent of heterochromatin that mediates chromatin compaction and cohesin recruitment.

1. INTRODUCTION

1.1 Heterochromatin in mammalian cells

The interphase nucleus of eukaryotic cells comprises chromatin with different levels of compaction. Based on this observation, chromatin was first divided by Heitz 1928 (Heitz E.; Das Heterochromatin der Moose') in less condensed euchromatin and highly condensed heterochromatin (Huisinga et al. 2006). Different kinds of heterochromatin have been defined: facultative and constitutive heterochromatin. The repressive state of facultative heterochromatin is reversible and dependent on the cell type and differentiation state. In contrast constitutive heterochromatin is stable and endues the major portion of repressive chromatin in the nucleus. It is present at telomere regions of the chromosome and at the centromeres (Brown 1966) (Figure1.1).

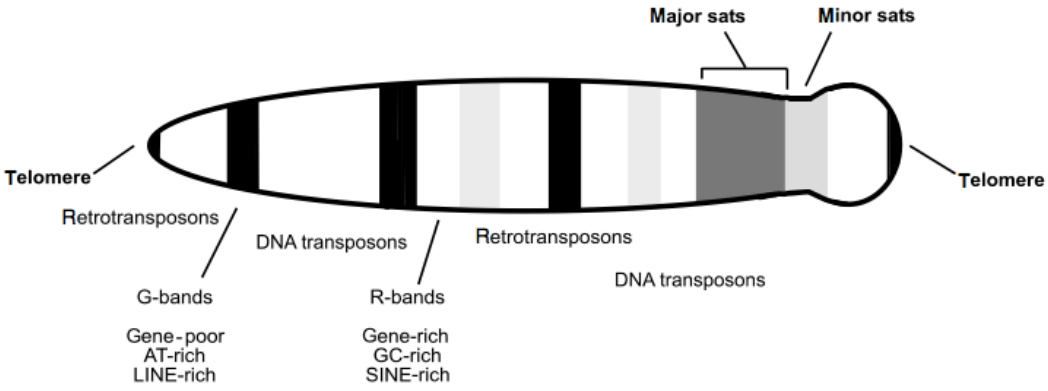

Figure 1.1. The chromatin landscape (Martens et al. 2005). Heterochromatin defines important genomic regions on the chromosome. Constitutive heterochromatin is present at highly repetitive regions like telomeres, minor and major satellite repeat regions.

The centromere represents the constricted region of the chromosome, which is important for ensuring chromosome inheritance. During mitosis kinetochore assembly occurs at the centromeres. The kinetochore complex serves as the platform for spindle-microtubule attachment in order to create the adequate force required for proper chromosome segregation. Together these mechanisms ensure the delivery of one copy of every single chromosome to each daughter cell during cell division. While the function of the centromere is evolutionarily conserved, the DNA sequence and the protein network present at centromeres are rapidly evolving. Two types of repetitive DNA sequences can be identified around centromeres in the mouse genome. The minor satellite repeats consist of 120 bp units and form a stretch of 600 kb, whereas the flanking major satellite repeats (6 megabases of 234 bp units) form the pericentric regions (Choo 2001; Martens et al. 2005; Bulut-Karslioglu et al. 2012) (Figure 1.2.). Together centric and pericentric heterochromatin form characteristic highly condensed clusters in interphase nuclei termed chromocenters. These compact chromatin structures can be easily visualized by DAPI staining.

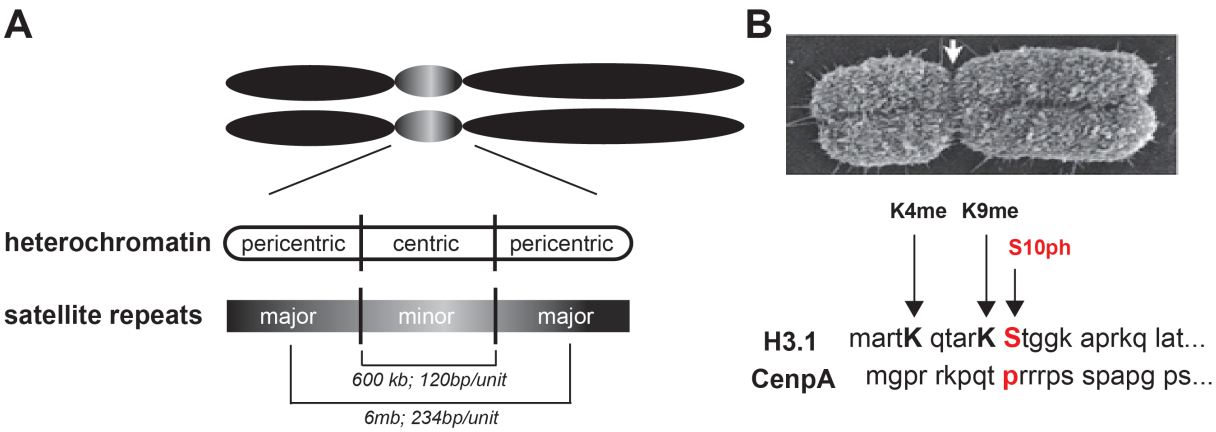

Figure 1.2. The centromeric region of the chromosome. A) Centromeres are at the constriction site of chromosomes. Minor satellite repeats are the underlying DNA at centromeric chromatin. They are flanked by major satellite repeats which form pericentric heterochromatin. **B)** Characteristic for centromeric chromatin is the Histone H3 variant CenpA. CenpA nucleosomes are interspersed with H3 containing nucleosomes.

The lack of a conserved DNA sequence provoked the hypothesis that epigenetic mechanisms determine the identity of centric and pericentric heterochromatin. Pericentric heterochromatin comprises repressive marks like hypoacetylation, DNA methylation and histone modifications like H3K9me3 and H4K20me3, which are typically associated with transcriptional silencing. In contrast centromeric chromatin collates heterochromatic and euchromatic characteristics. Kinetochores assemble on distinct chromatin regions that contain the histone H3 variant CENP-A and interspersed nucleosomes dimethylated on H3K4 (H3K4me2). The active mark H3K4me2 has been shown to be important for the recruitment of HJURP, the CenpA specific chaperone and the subsequent deposition of CenpA (Bergmann et al. 2011). Also other active histone modification marks are present at minor satellite repeats like H3K4me1 or H3K36me2, me3. Moreover ChIP experiments in mouse embryonic fibroblasts revealed that hypoacetylation (Honda et al. 2012), DNA methylation (Chen et al. 2003; Yamagata et al. 2007), and histone methylation (H3K9me3, H4K20me3) marks, which are characteristic for heterochromatin, are features of minor satellite repeat regions (Guenatri et al. 2004; Martens et al. 2005). Additionally proteins, characteristic for heterochromatin, like heterochromatin protein 1 (HP1) have been shown to localize to centromeric regions in metaphase (Hayakawa et al. 2003; Gopalakrishnan et al. 2009). According to that centromeric and pericentric heterochromatin share several common properties in mammalian cells. Studies in *S.cerevisiae* (Folco et al. 2008; Kagansky et al. 2009) and *D. melanogaster (Olszak et al. 2011)* suggest that heterochromatin is even crucial for the establishment and maintenance of functional centromeres. Heterochromatin in these organisms defines the border of centromeric chromatin (Pidoux and Allshire 2004; Sato et al. 2012). If this regulatory mechanism is conserved in higher organisms is completely unknown. However both centromeric and pericentric chromatin are important genomic regions which have to be tightly regulated. Any perturbation of the epigenetic balance can cause severe abberations like genomic instability, which can lead to cancer and other severe diseases (Shen 2011). Therefore it is very

important to learn more about the function and regulation of the complex system termed heterochromatin.

1.2 Formation of centromeric chromatin

Centromeres are crucial for proper chromosome segregation. Chromosome segregation defects may lead to loss or gain of one or more chromosomes, a condition known as aneuploidy which is a hallmark of malignant cells (Holland and Cleveland 2009). Thus cells have to strictly control the number of centromeres per chromosome. Chromosomes lacking a functional centromere show severe segregation defects (Amato et al. 2009), while in contrast chromosomes, which harbor more than one functional centromere face chromosome breakage due to asymmetric tension (Sato et al. 2012). CenpA loading onto chromatin is thought to be the crucial process to create a functional centromere, as CenpA is not present at inactive centromeres (Earnshaw and Migeon 1985). The loading itself is a very complex procedure, which can be separated in three different steps (Figure1.3):

a) Priming of centromeres for CenpA deposition

One central question in the context of centromeres is how centromere identity is achieved. Experiments revealed that HJURP, the chaperone incorporating CenpA into centromeric nucleosomes, requires the Mis18 complex consisting of Mis18alpha, Mis18beta, M18bp1 and RbAp46/48 proteins, for its recruitment to centromeres (Fujita et al. 2007). What could be possible mechanisms that drive the Mis18 complex to create a permissive chromatin state prone for CenpA deposition? Chromatin structure can be modified by specific epigenetic marks to allow incorporation of CenpA. One possibility to achieve an open chromatin state would be histone acetylation. Indeed several observations suggest that histone acetyltransferases may be required for functional CENP-A assembly and subsequent *de novo* kinetochore formation (Nakano et al. 2003; Okamoto et al. 2007; Ohzeki et al. 2012). In line with this the acetyltransferases p300 and PCAF have been found to both localize to functional, but not to inactive centromeres (Craig et al. 2003). Furthermore, upon depletion of Mis18 complex members, integration of newly synthesized CenpA is abrogated. Surprisingly this can be rescued by treating the cells with HDAC inhibitors like TSA or overexpression of HATs like p300 or PCAF (Fujita et al. 2007). According to this, an increase in centromeric H3 acetylation can be seen in G1 phase when M18bp1 is present at centromeres suggesting that M18bp1 recruits some HAT activity, which has not been identified yet. Interestingly mouse embryonic fibroblasts depleted for Mis18alpha show, apart from increased H3 acetylation, a decrease in H3K4me2, H3K9me2 and H3K9me3 as well as the loss of HP1 and a reduction of DNA methylation at minor satellite repeat regions. Direct interaction of DNMT3A and DNMT3B has been shown between Mis18 alpha (Kim et al. 2012) and CenpC (Gopalakrishnan et al. 2009). This interaction might be sufficient to recruit DNMT activity to centromeric chromatin. Furthermore it is currently unclear which methyltransferases are active at centromeres and how they are recruited. One possibility might be a HP1 mediated recruitment of centromere specific chromatin modifiers.

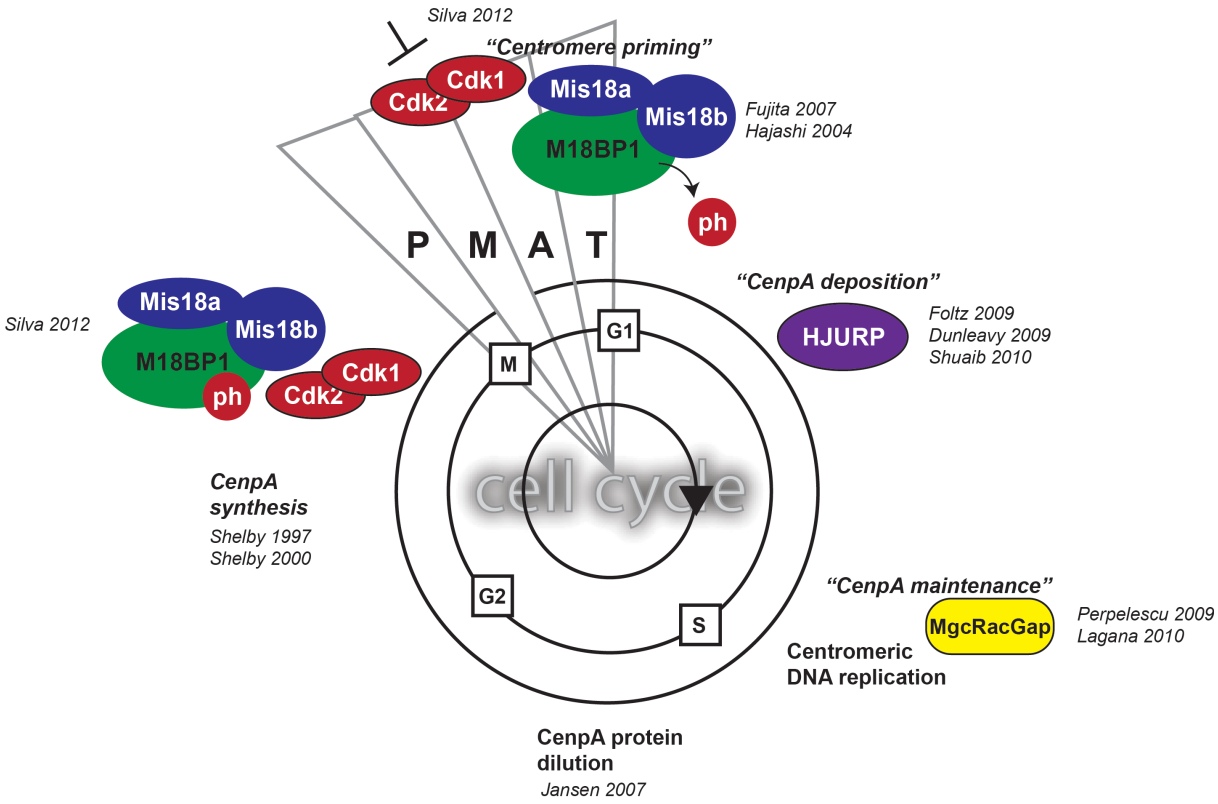

Figure 1.3. Cell cycle dependency of CenpA deposition. CenpA is diluted during DNA replication in S-phase as the existing amount is distributed equally onto both daughter strands. Highest levels of CenpA synthesis can be detected in G2 phase of the cell cycle, while newly synthesized CenpA is loaded much later in G1 phase. The CENP-A assembly machinery like the Mis18 complex is poised for activation throughout the cell cycle but kept in an inactive noncentromeric state by Cdk mediated phosphorylation during S, G2, and M phases. Cdk1/Cdk2 activity drops in anaphase and allows de-phosphorylation of M18bp1. In anaphase/telophase M18bp1 is recruited to centromeric chromatin and prepares chromatin for subsequent CenpA integration. In early G1 phase HJURP the CenpA specific chaperone deposits CenpA into chromatin, a process, which is error prone as CenpA deposition occurs also outside the centromeric regions. Therefore specific control mechanisms evolved to remove mis-integrated CenpA from non-centromeric regions while correctly integrated CenpA is maintained at centromeric regions in a process requiring M18bp1 and the small GTPase MgcGacGap.

b) Deposition of CenpA

In higher organisms CenpA deposition occurs in a replication independent manner. While in S phase the already existing CenpA nucleosomes are divided onto both daughter strands, the deposition of newly synthesized CenpA occurs only in early G1 phase by the histone chaperone HJURP (holiday junction recognition motif). This implicates that all proteins involved in this process have to be cell cycle regulated, which is ensured by an orchestrated cyclin/CDK network. Throughout G1 and S phase cyclins accumulate (increased CDK activity); at G2/M transition maximum CDK activity is necessary to guarantee that the majority of CDK substrates is phosphorylated. The CDK levels stay high until bi-orientation of all chromosomes at the metaphase plate is controlled by the spindle assembly checkpoint (SAC). After SAC is satisfied cyclins get rapidly degraded by the APC complex and the cell progresses to G1 with low CDK levels. Silva and colleagues could show (Silva et al. 2012) that CenpA deposition is regulated by the activity of Cdk1 and Cdk2. M18bp1 is phosphorylated by Cdk

proteins, which precludes its association with centromeric chromatin. Silva and colleagues proposed the following: After anaphase onset CDK activity drops, dephosphorylated M18bp1 is then able to associate with the centromere and recruits proteins, which are necessary for the CenpA loading. Interestingly they could also show that inhibition of Cdk leads to misintegration of CenpA outside of G1. This is an indication that Cdk regulated phosphorylation of M18bp1 is the major timing factor for CenpA deposition. Chromatin condensation efficiently performed by condensin complexes in mitosis is also suggested to be one criterion for CenpA deposition (Ribeiro et al. 2009; Samoshkin et al. 2009). Two independent affinity purification approaches in human cells using tagged CenpA (Dunleavy et al. 2009; Foltz et al. 2009) identified the prenucleosomal complex. HJURP, H4, Nucelophosmin1 (NPM1) as well as subunits of the CAF1 (H3.1 chaperone) and the HIRA complex (H3.3 chaperone) were found to be associated with CenpA. However it is still in question what the crucial steps in regulating the deposition of CenpA are.

c) Maturation and maintenance of centromeric chromatin

Newly synthesized CenpA is incorporated into chromatin by its chaperone HJURP- but this deposition is in a first place not fully specific for centromeric regions. After overexpression of CenpA, incorporation of CenpA occurs at kinetochore regions but also at genomic regions outside of minor satellite repeats, like the chromosome arms (Van Hooser et al. 2001). Therefore it was proposed that mechanisms exist which on the one hand remove misincorporated CenpA and on the other hand stabilize CenpA at centromeric regions or protect it from being removed by certain control mechanisms. The subunits of the remodeling and spacing factor (RSF) complex, Rsf1 and SNF2h interact with CenpA chromatin in mid-G1 phase and seem to be required for the maintenance of CenpA as HeLa cells depleted for Rsf1 show loss of CenpA (Perpelescu et al. 2009). Another study in HeLa cells (Lagana et al. 2010) revealed that the small GTPase MgcRacGap, Ect2, the small GTPases Cdc42 and Rac are important for stabilizing newly synthesized CenpA. MgcRacGap localizes to centromeres in late G1 phase of the cell cycle when CenpA loading is largely completed. Together with Ect2, MgcRacGap regulates the activity of the small GTPase Cdc42 in mitosis (Oceguera-Yanez et al. 2005). MgcRacGap is present at centromeres during late G1 phase and directly interacting with the licensing factor M18bp1, which in turn recruits Cdc42. As siRNA mediated knockdown of Cdc42 or Rac results in significant lower levels of CenpA at centromeres, it has been proposed that MgcRacGap-M18bp1-mediated Cdc42 activity is necessary to somehow modify CenpA. Either by adding or by removing a modification a separate identity for CenpA is generated, which marks it discriminably from old CenpA as a stable component of centromeric chromatin.

1.3 The complex network of centromere proteins

Once the centromere basis is established, a complex network of centromere proteins (more than 80 proteins have been identified until now) are recruited (Gascoigne and Cheeseman 2011) to form the kinetochore. The structural core of the kinetochore is composed of the KMN network consisting of

KNL-1 protein (Blinkin), the Mis12 complex and Ndc80 (Cheeseman and Desai 2008). Removal of any of the components of the KMN network leads to disruption of binding scaffolds for microtubules at outer kinetochore plates (Kline et al. 2006). To ensure proper chromosome alignment at the metaphase plate, each chromosome establishes bipolar attachments through its sister-kinetochores to microtubules protruding from opposite poles of the mitotic spindle (Tanaka 2008). The process of spindle attachment is a rather stochastic event and therefore error-prone. In order to control this crucial step eukaryotic cells have evolved a quality control mechanism: the spindle assembly checkpoint (SAC). SAC detects inappropriate kinetochore-microtubule attachments during chromosome congression from prometaphase to metaphase. Upon activation, additional control mechanisms are induced, which lead to delay of mitotic exit, allowing sufficient time for error correction and chromosome bi-orientation. During the early stages of mitosis (prometaphase), unattached kinetochores catalyze the formation of the mitotic checkpoint complex (MCC) composed of BubR1, Bub3, Mad2 and Cdc20. This leads in turn to inhibition of a downstream target of the SAC the anaphase promoting complex (APC/C). The APC/C is a E3 ubiquitin ligase that targets several proteins for proteolytic degradation, including mitotic cyclins (McLean et al. 2011) and therefore contributes to the strict cell cycle regulation and timing, crucial for proper chromosome segregation. Another important regulator of kinetochore assembly is the chromosomal passenger complex (CPC) consisting of Incenp, Borealin, Survivin and the kinase AuroraB. Importantly the CPC promotes chromosome bi-orientation by specifically destabilizing erroneous kinetochore attachments like syntelic and merotelic attachments by allowing the stabilization of correct bipolar attachments (Tanaka et al. 2002; Hauf et al. 2003; Lampson et al. 2004). Apart from its function in destabilizing incorrect attached spindle-microtubles, this complex comprises various other important functions in mitosis (Ruchaud et al. 2007; van der Waal et al. 2012). During cytokinesis the CPC localizes at the midbody where Aurora B initiates an abscission delay when two daughter cells are connected by a chromosome bridge. This mechanism protects the cells from tetraploidization (Steigemann et al. 2009). Altogether the CPC complex is an important factor in controlling cell division in spatial and temporal manner.

1.4 The functions of M18bp1 at centromeres

M18bp1 was first discovered in a temperature sensitive screen performed in fission yeast for mutants that mis-seggregated their chromosomes (Hayashi et al. 2004). In a subsequent study Mis18alpha and Mis18beta were identified to be present in a complex with M18bp1 (KNL2), RbAp46, RbAp48 (Fujita et al. 2007). Fujita and colleagues could show that upon siRNA knockdown of either Mis18alpha, Mis18beta or M18bp1 in HeLa cells the deposition of newly synthesized CenpA is impaired. Independently a study in C. elegans showed that the homologue of M18bp1 is required for the centromeric localization of CenpA (Maddox et al. 2007). The human M18bp1 localizes to centromeres at anaphase just before HJURP is present and remains there until mid G1 phase, suggesting a tightly cell cycle dependent regulation. MgcRacGap has been shown to directly interact with M18bp1 during

G1 phase (Lagana et al. 2010). Together with Ect2, MgcRacGap regulates the activity of the small GTPase Cdc42 in mitosis (Oceguera-Yanez et al. 2005). This interaction is crucial for the recruitment of active Cdc42 that somehow modifies CenpA leading to its maintenance at centromeric chromatin. A very recent study characterized the function of Mis18alpha in a mouse knockout model (Kim et al. 2012). Mis18alpha deficiency in mice leads to lethality at early embryonic stage (E6.5-E7.5). Further analyses of Mis18alpha knockout blastocysts and fibroblasts displayed severe defects like improper microtubule attachment to chromosomes, inappropriate chromosome condensation, mis-alignment in prometaphase, anaphase bridges, lagging chromosomes in telophase resulting in fragmented chromosomes. These results suggest that the Mis18 complex is required for proper chromosome segregation. The M18bp1 knockout in mice has not been analyzed yet and it is still unclear what the functions of M18bp1 at centromeres are and how M18bp1 is recruited to centromeric regions.

1.5 The sequential pathway to establish pericentric heterochromatin

Pericentric heterochromatin flanks the centromeric chromosome regions. Heterochromatin displays a highly compacted chromatin structure consisting of repetitive elements (major satellite repeat regions), which are kept in a transcriptionally inert state. The compact structure is achieved by specific chromatin modification patterns like DNA methylation, hypoacetylation and repressive histone modifications like H3K9me3 and H4K20me3, which provide a binding platform for specific sets of heterochromatin effector proteins. The heterochromatin organization differs in distinct cell types; correlating with the diffentiation state and varies due to the developmental stages (Probst et al. 2010). But how is heterochromatin established? Pericentric heterochromatin is established in a sequential pathway. Suv39h enzymes methylate chromatin at lysine 9 of histone H3 (H3K9me3). This creates a binding site for the recruitment of HP1 proteins to heterochromatin. In turn the presence of HP1 recruits more Suv39h enzymes leading to more H3K9me3 and further HP1 recruitment. Apart from Suv39h enzymes, HP1 directly binds to other important histone lysine methyltransferases (HMTs), Suv4-20h1 and Suv4-20h2, which introduces an additional repressive mark on histone H4 - H4K20me3 (Schotta et al. 2008) (Figure 1.4.). The accumulation of repressive marks and the potential of HP1 proteins to form homo- and heterodimers is thought to result in a chromatin cluster visible as dense chromocenter structures (Schwarzacher 1964; Bartova et al. 2002). Nevertheless a concrete mechanism leading to the specific heterochromatin structure is still under heavy debate. Cells lacking Suv39h enzymes loose both H3K9me3 and H4K20me3. Additionally due to the lack of H3K9me3 HP1 proteins are not recruited to pericentric heterochromatin (Peters et al. 2001). However Suv39h DKO cells still show chromocenter structures in the nuclei. As Suv39h DKO cells still show compacted chromatin, there might be additional proteins important for the structural integrity of heterochromatin.

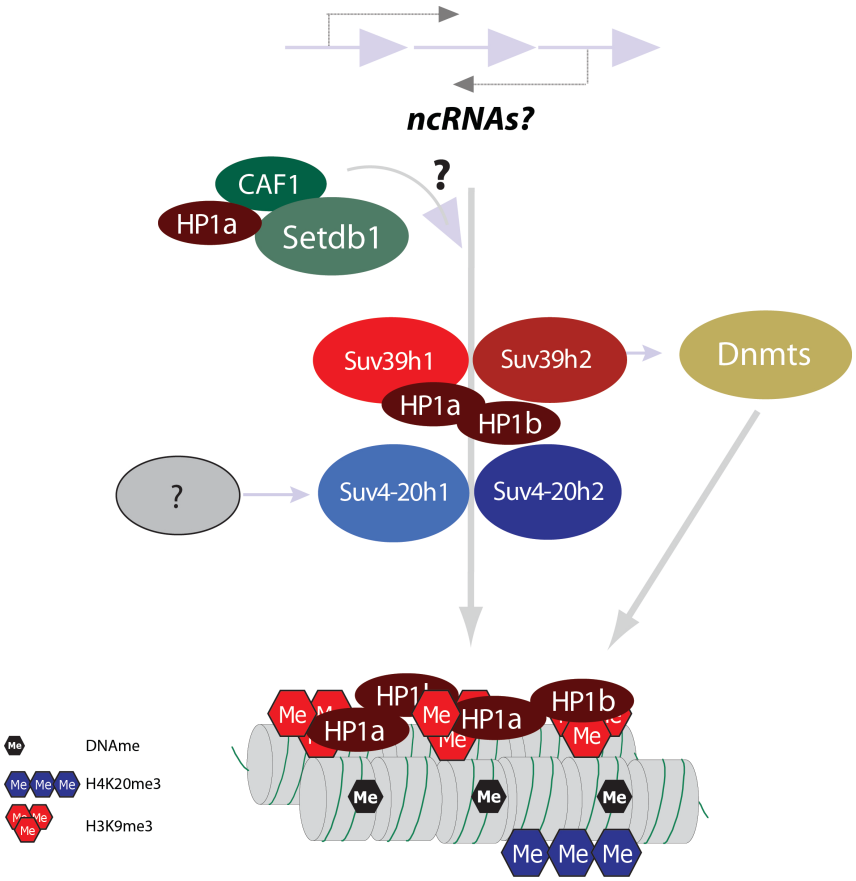

Figure 1.4. The sequential pathway to establish pericentric heterochromatin (adapted from (Schotta et al. 2004)). In a pathway, which is somehow regulated by ncRNAs the CAF1-HP1a-Setdb1 complex is recruited to pericentric heterochromatin. Setdb1 mono-methylates histone H3 at lysine 9 and provides a substrate for Suv39h enzymes. Suv39h1 and Suv39h2 are recruited to heterochromatin in an HP1 dependent manner and convert the monomethylation at H3K9 into trimethylation. Further HP1 molecules are recruited to pericentric heterochromatin and bind to H3K9me3. The high concentration of HP1 proteins recruits other HMTases like Suv4-20h proteins. Suv4-20h introduce the trimethylation of histone H4 at lysine 20. Additionally Suv39h proteins recruit DNA-methyltransferases (Dnmts), which modify major satellite repeats sequences. Additional proteins might contribute to the sequential pathway.

Chromocenter organization is maintained throughout the cell cycle with one exception during mitosis. This continuous presence of heterochromatin at major satellite repeats actually requires re-establishment of heterochromatin features after each round of replication. Pericentric heterochromatin as a rather closed and transcriptionally inert chromatin has to be reorganized during mitosis but also opened for the repair machinery to bind upon DNA damage (Goodarzi and Jeggo 2012). Therefore chromatin cannot be static. But in order to prevent cells from genomic instability it has to follow certain rules in protecting critical genomic regions from being transcribed at the wrong time. How this flexibility is ensured is not clear. There is some evidence that HP1 proteins might play important roles in the rearrangement of heterochromatin upon DNA damage (Ayoub et al. 2008; Ayoub et al. 2009; Baldeyron et al. 2011). Furthermore a recent study identified transcription factors that sequence-specificly recognize major satellite repeat regions and then recruit the required effector proteins (Bulut-Karslioglu et al. 2012), suggesting that regulation of heterochromatin comprises epigenetic and genetic aspects, which have to be further analyzed.

1.6 Regulation of histone lysine methylation

Heterochromatin displays a compact chromosomal structure with distinct histone and DNA modification patterns, important to control the transcription of repetitive elements. The characteristic methylation patterns at pericentric heterochromatin consisting of H3K9me3 and H4K20me3 are established by specific histone lysine methyltransferases (HMTs). Characteristic for nearly all histone lysine methyltransferases is the enzymatic domain, the SET domain (Tschiersch et al. 1994; Jenuwein et al. 1998; Trievel et al. 2002; Yeates 2002). Several proteins have been identified to methylate histone H3 at Lysine 9: G9a (Tachibana et al. 2002) and GLP (Tachibana et al. 2008) form dimers, which have been shown to introduce mono- and di-methylation at H3K9. Setdb1 (ESET) also possesses activity to methylate H3K9 (Yang et al. 2002). In a complex with HP1a and CAF1 it has been shown to be responsible for the monomethylation of H3K9. Monomethylated H3K9 serves as a substrate for Suv39h1 and Suv39h2, which convert the monomethylation into di- and trimethylation states at pericentric heterochromatin (Loyola et al. 2009). Suv39h enzymes are recruited to pericentric heterochromatin in a HP1- dependent manner (Rea et al. 2000). Three histone methyltransferases have been identified to methylate H4K20: PrSet7 (Nishioka et al. 2002), Suv4-20h1 and Suv4-20h2 (Schotta et al. 2004). PrSet7 (Setd8) introduces the monomethylation of H4K20 in a replication dependent manner. During replication, ‘old’ histones are distributed equally on both daughter strands and newly synthesized histones are incorporated into the nucleosomes. The monomethylation of newly synthesized H4 at lysine 20 is introduced in S-phase in close connection to the replication fork (Tardat et al. 2010). The expression of the PrSet7 protein is tightly regulated during cell cycle. Protein levels peak during G2/M and early G1 phase of the cell cycle (Oda et al. 2009). Various post- translational modifications have been identified including phosphorylation, sumoylation and ubiquitinylation (Abbas et al. 2010; Centore et al. 2010; Oda et al. 2010; Tardat et al. 2010; Spektor et al. 2011). PrSet7 has also been shown to interact with PCNA via a conserved PIP (PCNA interacting peptide) domain also called ‘PIP degron’ (Jorgensen et al. 2007; Huen et al. 2008; Havens and Walter 2009). This interaction is on the one hand crucial for the recruitment of PrSet7 to the replication fork, on the other hand it is important for the function of PrSet7 in DNA damage response and its cell cycle dependent regulation (Abbas et al. 2010; Centore et al. 2010; Oda et al. 2010). PrSet7 is a direct target for the E3 ligase complex CRL^{Cdt2}, which causes ubiquitin dependent degradation of its substrates. CRL^{Cdt2} activity is dependent on the interaction of PrSet7 with PCNA via its PIP degron.

Suv4-20h1 and Suv4-20h2 have been characterized as histone methyltransferases possessing specifc activity towards H4K20 methylation. Suv4-20h enzymes differ in their activities to induce either H4K20 methylation states as H4K20me2 is reduced in Suv4-20h1 knockout cells, whereas MEFs knockout for Suv4-20h2 almost loose H4K20me3. As different HMTases have been identified to methylate H3K9, Suv4-20h enzymes are the only methyltransferases, which show specific activity in introducing H4K20me2 and H4K20me3. They act downstream of Suv39h enzymes in a sequential

pathway (Schotta et al. 2004), as mouse fibroblasts depleted for Suv4-20h enzymes loose both H3K9me3 and H4K20 di- and trimethylation. Suv39h enzymes introduce H3K9 trimethyaltion, which in turn is bound by HP1 proteins. HP1 proteins recruit Suv4-20h enzymes to pericentric heterochromatin for establishing the trimethylation mark on H4K20. How the enzymatic activity of Suv4-20h enzymes is regulated is not known.

1.7 HP1 isoforms recruit multiple proteins to chromatin

HP1 was first discovered in *D. melanogaster* as a protein, which associates with pericentric heterochromatin. In mammals three isoforms have been identified HP1alpha, HP1beta and HP1 gamma. The proteins consist of three domains: The N-terminal chromo domain (CD) targets HP1 to heterochromatin as it allows direct binding to H3K9me3 (Lachner et al. 2001; Nielsen et al. 2002)A flexible hinge domain (Badugu et al. 2005) is implicated in the regulation of protein/RNA/DNA interactions. The C-terminal chromo shadow domain (CSD) is involved in homo- and heterodimerization of HP1 isoforms and mediates the binding to other proteins through a pentapeptide motif PxVxL (Thiru et al. 2004). HP1 proteins possess multiple functions at chromatin. It has been originally identified in *Drosophila* as a chromatin binding protein, which induces transcriptional repression at heterochromatin (Eissenberg et al. 1990). Additionally it plays a role in telomere maintenance (Canudas et al. 2011; Jiang et al. 2011), replication (Maison and Almouzni 2004) and DNA repair (Dinant and Luijsterburg 2009). HP1 is also present in euchromatic regions, but the mechanism for the recruitment of HP1 proteins to transcriptionally active chromatin is not clear as H3K9me3 is not present in these regions (Kwon and Workman 2011).

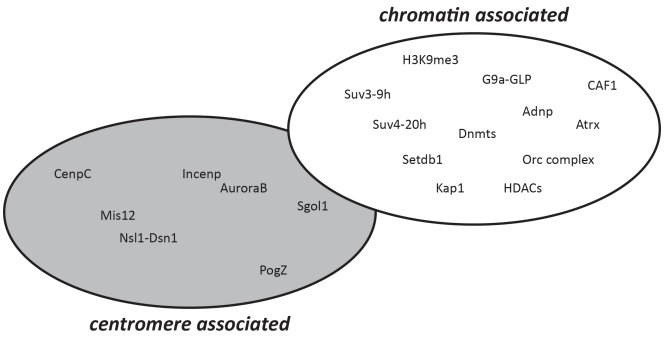

Figure 1.5. The interaction network of HP1 proteins adapted from (Kwon and Workman 2011). HP1 proteins interact with various proteins. Chromatin proteins, as well as proteins with described functions at centromeres have been identified to interact with HP1. Due to the complex interactome of HP1 isoforms they might serve as a hub to recruit different sets of proteins and complexes to specific loci and therefore regulate various functions.

As versatile as the functions are also the proteins that have been identified to directly interact with HP1, which rises the question how specificity is assured and how HP1 proteins are regulated. One suggestion would be that different HP1 isoforms or homo- heterodimers favor specific mechanism in the cell, e.g. all isoforms can be recruited to pericentric heterochromatin but HP1 gamma has been shown to be enriched with euchromatic regions. It has also been shown that localization of the different isoforms varies during cell cycle (Hayakawa et al. 2003). Additional levels of specification can be introduced by posttranslational modifications, proposed as ‘HP1-mediated subcode within the histone code’ (Lomberk et al. 2006). Detailed modification analyses could show that HP1 proteins are

hyperphosphorylated (Shimada and Murakami 2010) and sumoylated at the hinge domain (Maison et al. 2011). Several proteins have been identified to interact with HP1 proteins, which either are chromatin associated or non-chromatin proteins (Figure 1.5.). The diverse interaction partners of HP1 isoforms suggest that the protein might mediate several independent functions at chromatin and might even function as chromosomal hub for the recruitment of different effector proteins to specific chromosomal regions.

1.8 The function of cohesin at pericentric heterochromatin

Cohesin is a multi-subunit complex consisting of Smc1, Smc3, Scc1 (Rad21) and Scc3 (SA) responsible for sister chromatid cohesion in mitosis (Losada et al. 1998; Toth et al. 1999). ChIP experiments revealed that the presence of the complex correlates with genomic loci, which are occupied by CTCF. Cohesin and CTCF work together to mediate the long-range interactions that define the topology of a number of essential loci (Parelho et al. 2008; Wendt et al. 2008; Sanyal et al. 2012). The activity of the cohesin complex is highly cell cycle regulated. Initial recruitment of cohesin to chromatin occurs in telophase to G1 phase of the cell cycle. During S phase the cohesion between sister chromatids is established, a process dependent on Sororin, Esco1, and Esco2. With onset of prophase the bulk of cohesin is eliminated from the chromatin arms. Several proteins have been identified to contribute to the active removal process like Plk1, AuroraB, Condensin I, or Wapl. Exclusively pericentromeric cohesin remains and is protected from global removal by Shugoshin (Sgo1) and PP2A. Finally at metaphase to anaphase transition, separase is activated by the APC/C and cleaves centromeric cohesin as well as residual cohesin on chromosome arms, a process crucial to finally allow sister chromatid separation (Peters et al. 2008). In fission yeast, pericentromeric heterochromatin is directly responsible for the sister chromatid cohesion (Bernard et al. 2001). However Koch and colleagues could not show an interaction of Cohesin with HP1 proteins in higher organisms (Koch et al. 2008), although independent studies point towards a connection between cohesin and pericentric heterochromatin (Gartenberg 2009). Heterochromatin protein 1 has been shown to interact with Shugoshin (Yamagishi et al. 2008). As Shugoshin is known to preserve pericentromeric cohesin from active removal, heterochromatin might be involved in this protection.

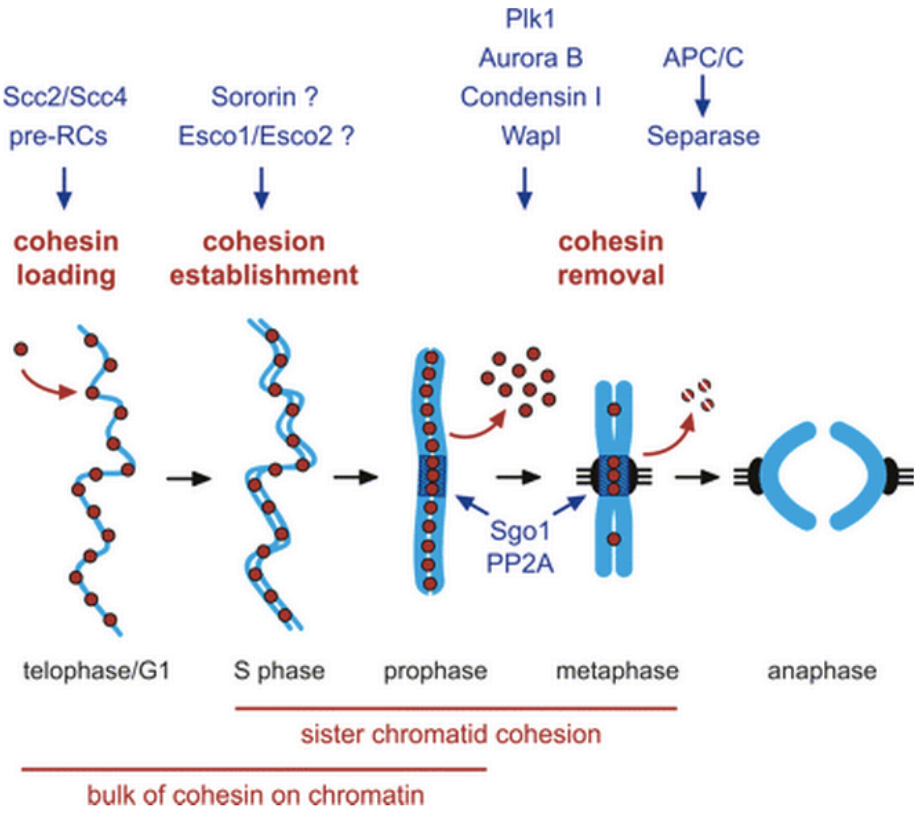

Figure 1.6. Cell cycle dependendent regulation of cohesin (Peters et al. 2008). Cohesin loading occurs in telophase/early G1 phase of the cell cycle, while cohesin establishment is mediated by Sororin and Esco1/Esco2 in S-phase during sister chromatid cohesin. Bulk cohesin is removed from chromosome arms and is protected at pericentromeric regions by Shugoshin proteins (Sgo1).

The Roberts-SC phocomelia syndrome is another example for a possible interdependency of cohesin and heterochromatin. This disease is an extremely rare genetic disorder caused by the mutation of the *ESCO2* gene on 8th chromosome. Esco2 is involved in establishment and activation of cohesin and localizes to pericentric heterochromatin exclusively during S phase (Whelan et al. 2012). Esco2 deficiency in mice causes mitotic defects (railroad chromosomes), which abolish development in very early stages. This phenotype is based on reduced Cohesin acetylation, improper sororin recruitment and the subsequent mis-localization of Cohesin at chromosomes causing defects in chromatid cohesion. Despite of some evidence predicting a correlation of Cohesin and heterochromatin it is currently unclear how Cohesin is recruited and maintained at heterochromatin. Additional studies failed to identify known heterochromatin factors like HP1 proteins to be responsible for the recruitment of Cohesin to regions of pericentric heterochromatin (Koch et al. 2008; Serrano et al. 2009). Therefore additional work is necessary to identify factors mediating the recruitment of Cohesin to pericentric heterochromatin.

AIMS OF THE THESIS

Pericentric and centric chromatin are important regions of the genome that have to be tightly controlled. A complex system of chromatin modifications combined with a complex network of protein interactions is necessary to guarantee identity and functionality of centromeres and pericentric heterochromatin. This enormous effort is necessary because any alteration in the structure causes severe phenotypes based on mitotic defects leading to genomic instability and resulting in cancer or other diseases. Although centromeres and pericentric heterochromatin have to be tightly controlled- they are permanently challenged to provide a system that is able to react to cell cycle dependent chromatin rearrangements and environmental changes. Therefore the chromatin has to be in a dynamic equilibrium and under permanent adaptation involving specific chromatin modifications and the dynamic recruitment of specific effector proteins and complexes. Centromeric and pericentric heterochromatin are tightly compacted structures, which ensure transcriptional inaccessibility. The mechanism by which this structural regulation is achieved and modulated throughout mitosis is completely unclear.

Our lab is interested in how centric and pericentric heterochromatin is established and regulated. In order to unravel the complex system responsible for the regulation of heterochromatin the interaction network of the H3K9me3 marks should be investigated. Therefore peptide pulldown approaches and subsequent high sensitive mass spectrometry analyses were performed to identify novel heterochromatin regulating proteins. From this initial peptide pulldown screen one protein especially draw our interest. M18bp1 (C79407, KNL-2) was specifically enriched with the trimethylation of H3K9. The fact that a protein with known functions in centromere establishment and maintenance somehow associated with the heterochromatic context was rather surprising.

A) Therefore I started the functional characterization of M18bp1 addressing the following questions:

How is M18bp1 recruited to centromeric regions?

M18bp1 was identified as a protein present at centromeric regions in a cell cycle dependent manner but it is unclear how it is targeted to this specific regions.

What are the functions of M18bp1 at chromatin?

Described as a protein involved in the priming of centromeres it was unclear what the precise function of the M18bp1 at centromeres is. Especially as M18bp1 was enriched with H3K9me3, a mark present in heterochromatin, it was obvious to ask for a potential function of M18bp1 at heterochromatin.

What happens to a cellular system or an organism when M18bp1 is missing?

The characterization of a mouse knockout model was basis for the functional characterization of the protein in the mammalian system.

B) Another aim was to characterize known key players involved in the establishment of pericentric heterochromatin like the HMTases Suv4-20h1 and Suv4-20h2 as well as HP1 proteins. Until now it is not clear how the compact structure at heterochromatin is established and maintained. HP1 dimer or multimeric complexes are suggested to be responsible for the structural features, but the concrete mechanism is not known.

How is the compact structure in heterochromatin achieved?

Suv4-20h2 has been reported to be tightly associated with heterochromatin, which was rather surprising for an enzyme. From this the hypothesis arose that Suv4-20h2 might display additional functions affecting the chromatin structure.

Histone H4 lysine 20 methylation is established in a sequential pathway. Dependent on the presence of H3K9me3 and HP1 proteins the HMTases (Suv4-20h1 and Suv4-20h2) are recruited to heterochromatic regions (Schotta et al. 2004). The monomethylation of H4K20 is mediated by PrSet7, which is a tightly cell cycle regulated enzyme. Up to now it is unclear how the enzymatic activity of Suv4-20h enzymes is regulated to induce either H4K20me2 or H4K20me3. It has been hypothesized that PrSet7 in a replication dependent manner monomethylates newly synthesized histone H4 at lysine 20, which is then converted to di- and trimethylation by the Suv4-20h enzymes. We aimed to question this hypothesis and asked:

How are H4K20 specific histone methyltransferases regulated?

2. RESULTS

2.1 The proteome of the histone H3 lysine 9 trimethylation mark in embryonic stem cells

The N-terminus of histones is a target for diverse posttranslational modifications like phosphorylation, acetylation, sumoylation and methylation. These modifications index the chromatin as part of the epigenetic control of gene expression and recruit specific sets of effector proteins. The trimethylation mark H3K4 localizes to promoter regions of actively transcribed genes, whereas repressive histone modifications are the hallmark of heterochromatin. Two histone modifications have been described to be associated with pericentric heterochromatin: H3K9me3 and H4K20me3. Proteins recognizing the different histone modification marks have conserved domains like Bromodomain, PHD finger or the Royal family domains (Tudor, PWWP, MBT and Chromodomain), which are a structurally related group of domains (Yap and Zhou 2010). While the bromodomain exhibits affinity to histone acetylation marks (Hassan et al. 2007), PHD finger and chromodomain have been shown to be associated with methylated histone tails (Musselman and Kutateladze 2011).

histone modification	reader	domain	function	reference
H3K9me3	HP1	chromo	heterochromatin	Lachner *et al*, 2001
	Tip60	chromo	DNA repair	Sun *et al*, 2009 Sun *et al*, 2010
	Chd7	chromo	chromatin remodeling	Takada *et al*, 2007
	Cdyl2	chromo	heterochromatin	Fischle *et al*, 2008
	Orc complex		replication	Vermeulen *et al*, 2010; Bartke T. *et al*, 2010

Figure 2.1. **Binders of H3K9me3 and their possible functions.** Overview of effector proteins identified for the H3K9 trimethylation mark, the interaction domain and the implicated function of the characterized interaction.

The trimethylation of H3K9 is recognized by HP1 proteins, which harbor a chromodomain (CD) and a chromoshadow domain (CSD). While the chromodomain directly interacts with the methylated H3K9, the CSD allows homo- or heterodimerization and binding to other effector proteins. In addition to HP1 proteins, also other mouse chromodomain proteins are reported to bind H3K9me3, some examples are depicted in Figure 2.1. The goal of this thesis was to reveal novel insights into the biological roles of histone methylation marks, which have been implicated in diverse biological processes ranging from regulation of pluripotency and development to cancer progression.

Starting point of this study was a peptide pulldown screen, which was performed using biotinylated peptides derived form the N-terminus of histone H3. As other studies (Bartke et al. 2010; Vermeulen et al. 2010) used similar approaches in a cancer cell line (HeLa cells) the focus here was the proteome of a pluripotent cell line. Therefore a protocol was established to prepare nuclear extracts from mouse embryonic stem cells (mES cells) (Figure 2.2.A). These cells are derived from the inner cell mass (ICM) of the pre-implantation embryo. ES cells are pluripotent, as they can give rise to all tissue lineages of the three primary germ layers.

Additionally, ES cells display a very interesting proteome containing 'stemness factors' like Oct4 or Nanog, which can be exclusively studied in this cell system.

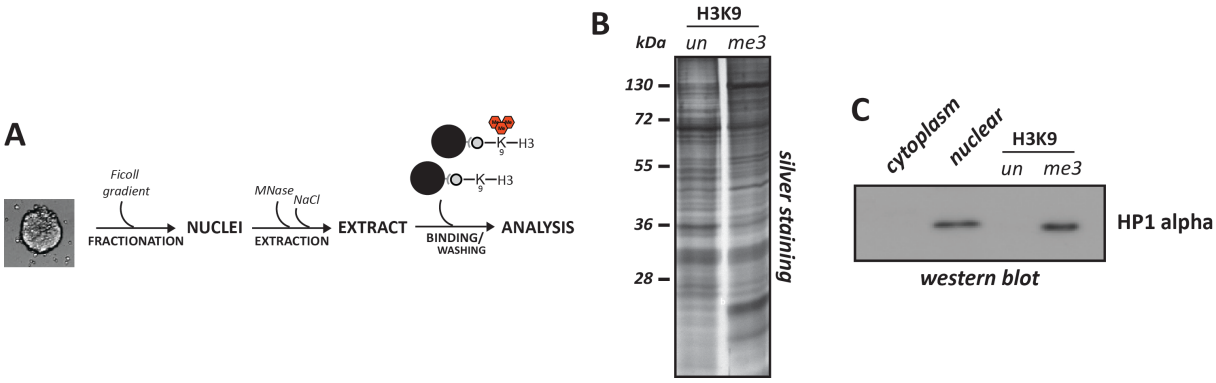

Figure 2.2. Peptide pulldown approach. A) Scheme of the peptide pulldown approach. mES cells were harvested and spinned through a Ficoll gradient to remove the cytoplasmic fraction and to isolate the nuclei. The DNA was digested with MNase and chromatin-associated proteins were extracted with high salt buffer. The resulting nuclear extract was then incubated with the biotinylated peptides immobilized on a streptavidine resin. Upon extensive washing steps to reduce unspecific binding proteins were separated on a SDS page. **B)** Silver gel of proteins bound to H3K9 unmodified and trimethylated peptide. **C.** Western blot probed with HP1a antibody.

Extracted ES cell proteins were precipitated with specific peptides, separated on a SDS page and visualized by silver staining (Figure 2.2.B). A well characterized protein with affinity for H3K9me3 is HP1. Therefore western blot with a HP1 antibody was performed to test for the quality of the nuclear extract and the washing conditions of the peptide pulldown (Figure 2.2.C). Several independent peptide pulldowns have been performed to guarantee reproducibility of the experiments. Depicted in Figure 2.3.A is a representative silver gel of an H3K9me3 peptide pulldown. Proteins, enriched with the H3K9me3 peptide compared to the unmodified control were identified by mass-spec analysis.

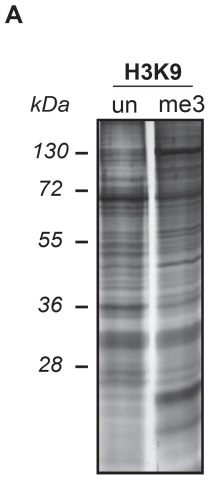

B

H3K9 peptide pulldown

protein	*un*	*me3*
Trim28	2	50
Trim24	0	17
HP1a	0	22
HP1b	1	14
HP1g	1	11
Atrx	0	8
M18bp1	0	4
Dnttip2	1	13
PogZ	0	20
Zfp828	0	3
Zfp462	0	11
Zfp280c	0	6

Figure 2.3 Interactome of histone H3 lysine 9 methylation mark. A) Silver stained SDS page of a representative peptide pulldown experiment. Individual lanes were cut in 10 pieces. Peptides from tryptic digest were analyzed in LC MS/MS. **B)** LC MS/MS analysis of silver gel samples after peptide pulldown. Mascot files were analyzed using Scaffold proteomics software to compare independent spectra. Numbers presented in the table are unique spectra found in peptide pulldown sample.

A list with the top hits is shown in Figure 2.3.B (a full list of identified proteins can be found in appendix table I.). All three HP1 isoforms were enriched with the H3K9me3 peptide confirming the western blot data and the specificity of the assay. Additionally, Trim28 (Kap1) was the top hit on this list of the proteins enriched with H3K9me3. Kap1 is a very complex protein involved in the genetic

silencing of repetitive genomic elements and acts as a scaffolding protein binding to several interactors like e.g. HP1 proteins (Iyengar and Farnham 2011). Interestingly aside of Kap1 many other proteins binding to H3K9me3 are known interactors of HP1 like Atrx and PogZ. Mass-spec analysis identified also several zink finger proteins like Zfp828, Zfp462, Zfp280c. Dnttip2 (ERBP; ERalpha binding protein) is a rather uncharacterized protein, which was enriched with the modified H3K9 peptide.

In summary, the H3K9me3 peptide pulldown screen resulted in a long list of potential binding factors for the different modifications. From these data however it was impossible to judge whether the association is based on a direct interaction of the candidate protein with the histone methylation mark or whether other proteins present in the nuclear extract mediate the interaction. Further analyses were necessary to characterize this association and to test for a possible function of these candidates at heterochromatin. As all proteins were precipitated with a modification characteristic for heterochromatin, they should be recruited to heterochromatin regions. Therefore localization studies in wild type mouse embryonic fibroblasts were performed using a set of candidate proteins. The cDNA was expressed from a mammalian expression vector containing an EGFP-tag. HP1b, a well characterized protein localizing to heterochromtic foci in the nucleus was transfected as a control. Both C2H2 zink finger proteins Zfp828 and PogZ showed a rather broad nuclear staining only excluding nucleolar regions. Importantly, some of the tested proteins showed clear heterochromatic localization like M18bp1 and Dnttip2, which were comparable to the localization of HP1b. Dnttip2 was additionally present in the nucleoli (Figure 2.4.).

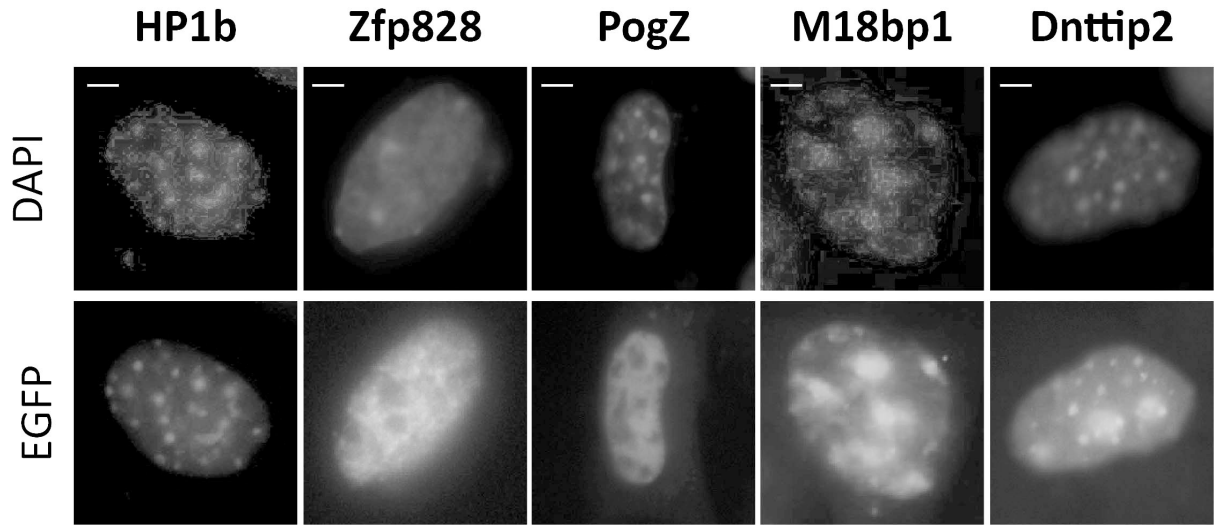

Figure 2.4. Localization of candidate proteins in mouse fibroblasts. Cellular distribution of different EGFP-tagged candidate proteins overexpressed in wild type mouse embryonic fibroblast cells. Scale bar is 5µm.

In a next step it was questioned whether the localization to heterochromatin is dependent on the H3K9me3 mark. Therefore localization studies were conducted in two knock-out cell lines: Suv4-20h DKO cells are depleted for Suv4-20h enzymes and therefore lack H4K20me3. Suv39h DKO cells are devoid of both H3K9me3 and H4K20me3, as the establishment of the H4K20me3 mark occurs in a sequential pathway and is therefore dependent on H3K9me3.

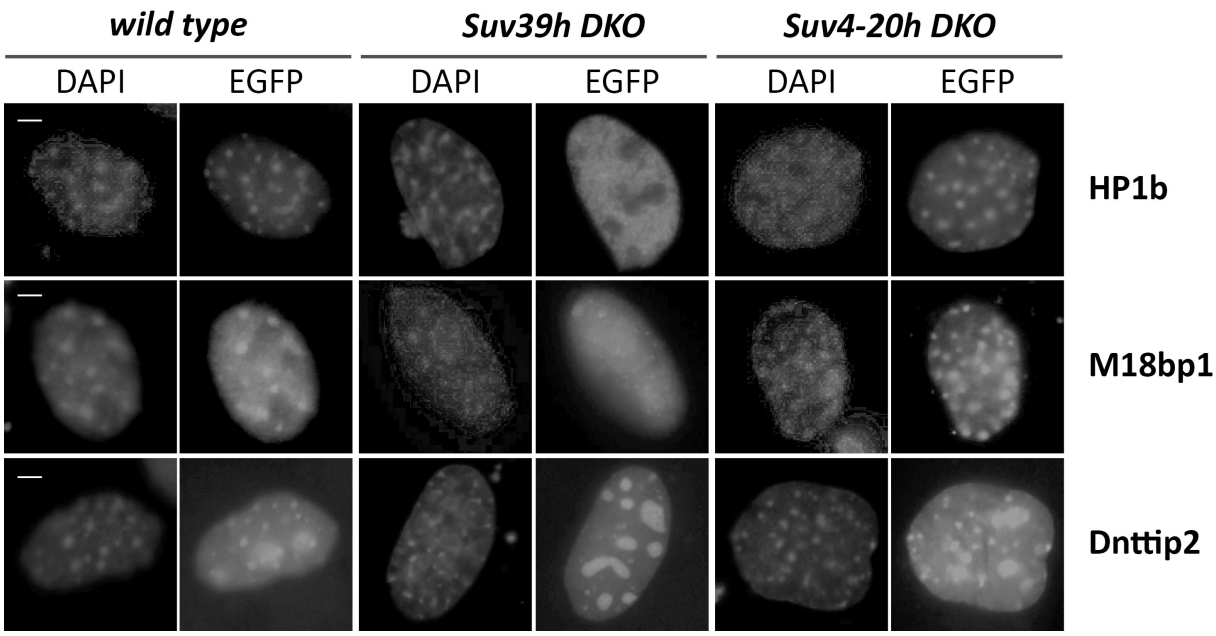

Figure 2.5. The localization of different candidate proteins is dependent on H3K9me3. Localization study of different EGFP-tagged candidate proteins overexpressed in wild type, Suv39h DKO and Suv4-20h DKO MEF cell lines. Scale bar is 5μm.

The localization of HP1b as a well-characterized H3K9me3 binder was clearly dependent on the presence of H3K9me3. HP1b was enriched at heterochromatic foci in wild type and Suv4-20h DKO cells but showed diffuse nuclear signal upon loss of H3K9me3. Interestingly a similar localization pattern could be observed in the case of two other candidate proteins: M18bp1 and Dnttip2. Cells overexpressing Dnttip2 showed EGFP signals in nucleoli and at regions of pericentric heterochromatin in wild type and Suv4-20h DKO mutant cells. Interestingly in cells lacking Suv39h enzymes Dnttip2 was still present in nucleoli but completely absent from heterochromatin. M18bp1 localized to heterochromatin in wild type and Suv4-20h DKO cells and showed diffuse nuclear EGFP signal in the Suv39h mutant fibroblast cells (Figure 2.5.).

2.2 The functional characterization of M18bp1

2.2.1. The function of M18bp1 at centromeres

M18bp1 was published as a protein, which is involved in 'priming' centromeric chromatin for CenpA deposition (Fujita et al. 2007). Confocal analysis of M18bp1 transfected mouse fibroblasts revealed that M18bp1 not only localized to pericentric heterochromatin but was also enriched at small foci in the nucleus (Figure 2.6). The small M18bp1-EGFP foci co-localized with centromeres, which were stained with an antibody specific for the centromere-specific histone H3 variant CenpA. But how is M18bp1 targeted to centromeric chromatin?

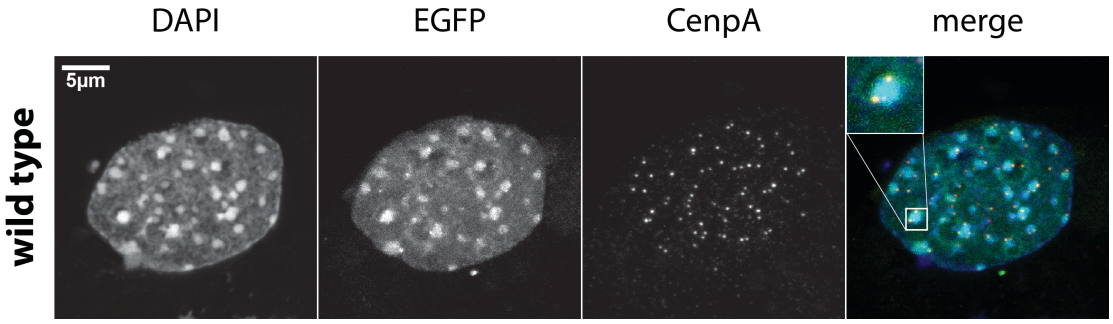

Figure 2.6. Centromeric localization of M18bp1 in mouse embryonic fibroblasts. Localization study of EGFP-tagged M18bp1 protein overexpressed in wild type mouse fibroblasts. Centromeric regions were stained with a specific antibody recognizing CenpA.

In order to identify proteins, which facilitate M18bp1 targeting to centromeres we tested several centromere proteins for interaction with M18bp1. In collaboration with Wen Deng in the group of Heinrich Leonhardt several Cenp proteins were tested for its interaction with M18bp1 in an F3H (fluorescent three-hybrid) interaction screen (Zolghadr et al. 2012). This assay allows an *in vivo* interaction test as a fluorescently labeled bait protein is tethered to a fixed location in the genome and analyzed for co-localization with a fluorescent prey fusion protein (Figure 2.7.A). In total 16 centromere proteins were tested for their binding affinity to M18bp1. CenpA as a prey protein was not recruited to the nuclear focus. Instead CenpC localized to the M18bp1 focus and showed strong interaction with M18bp1 (Figure 2.7.B).

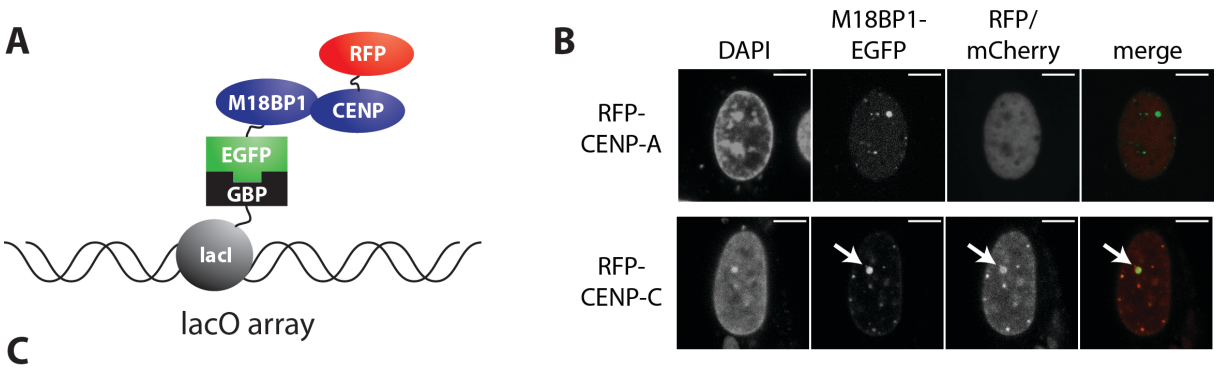

C

RFP /mCherry CENP-	A	B	C	H	I	L	M	N	O	P	Q	R	S	T	U	W
interaction	-	-	+	-	-	-	-	-	-	-	-	-	-	-	-	-

Figure 2.7. F3H interaction screen for M18bp1 interaction partners. A) Schematic drawing of the principle of a F3H assay. The F3H assay is an *in vivo* interaction assay based on a BHK cell line possessing a lac operator (lacO) repeat array stably integrated in the genome and fused to the EGFP binding protein (GBP). This cells line was further transfected with expression vectors encoding for the lac repressor (lacI), the bait protein (GFP-M18bp1) and different RFP/pmcherry tagged prey proteins (Cenp proteins). The lacI binds directly to the lac operator sequence and forms a LacI-GBP fusion protein. GBP recruits the EGFP-tagged M18bp1 to the lacO focus, which appears as green spot in the cell nucleus. Interactions of the tested prey proteins with M18bp1 are measured by the red/green ratio and are used as an indicator for the strength of the tested interaction **B)** Examples of microscope analysis of F3H assay. CenpA as prey protein did not localize with the lacO array binding M18bp1 but CenpC was recruited to the M18bp1 nuclear focus. **C)** Overview of tested Cenp proteins. Assay was performed by Wen Deng in the group of Heinrich Leonhardt. Scale bar is 5µm.

12 other Cenp proteins were tested in the F3H assay for interaction with M18bp1 but non of them was found to interact (Figure 2.7.C). Based on the initial F3H interaction screen, CenpC was identified to bind M18bp1. But which part of M18bp1 is required for the interaction with CenpC? M18bp1 is conserved in higher organisms and harbors two conserved domains, the SANT domain in the more C-terminal part of the protein and a SANTA domain located in the middle of the protein.

The SANT domain, initially identified as a 50-amino-acid motif that is present in nuclear receptor co-repressors, was subsequently found in the subunits of many chromatin-remodelling complexes. It was named after the first proteins, which were found to have such a domain: switching-defective protein 3 (Swi3), adaptor 2 (Ada2), nuclear receptor co-repressor (N-CoR) and transcription factor (TFIIIB) (Boyer et al. 2004). Sequence analysis revealed a strong similarity to the DNA-binding domain (DBD) of Myb-related proteins (Aasland et al. 1996). Many vertebrate proteins harboring a SANT domain possess also a SANTA (SANT Associated) domain, which has been identified based on a motif search (Zhang et al. 2006). The function of the SANTA domain is not characterized. To test if SANT and SANTA domains are participating in the interaction with CenpC several truncations of M18bp1 were generated and tested for interaction in the F3H assay (Figure 2.8.A). The N-terminus (M1 aa1-440) was not able to bind to CenpC while the C-terminus (M2 aa441-998) was sufficient to mediate an interaction with CenpC, suggesting that the SANTA domain alone is dispensable in this context. The

central region (M3 aa325-800) containing SANTA and SANT domain as well as a shorter fragment (M4) in which only the SANT domain was present showed clear interaction with CenpC, again suggesting that the SANTA domain is not crucial for the interaction (Figure 2.8.B).

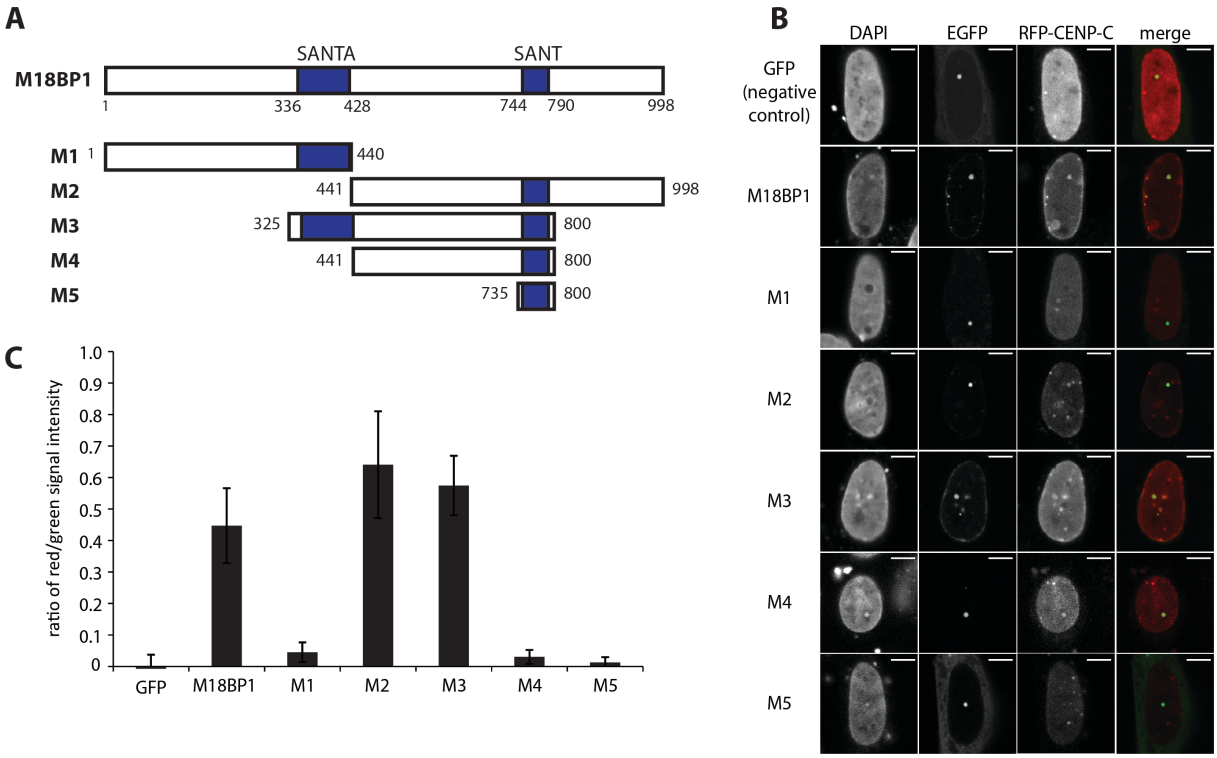

Figure 2.8. Mapping of the M18bp1 domain that interacts with CenpC. A) Scheme of the M18bp1 protein and conserved domains. Several truncations were derived: the N-terminus (M1), the C-terminus (M2), a central fragment containing both conserved domains (M3), a shortened M3 fragment lacking the SANTA domain (M4) and the SANT domain alone (M5). **B)** Microscopy analysis of the tested EGFP tagged M18bp1 fragments against RFP tagged CenpC. **C)** Statistical analysis of the interaction screen, based on automated quantification in several hundred cells per construct through red/green intensity values as a measurement of the strength of the tested interaction. Assay and analyses were performed by Wen Deng in the group of Heinrich Leonhardt. Scale bar is 5µm.

To test if SANT and SANTA domains are participating in the interaction with CenpC several truncations of M18bp1 were generated and tested for interaction in the F3H assay (Figure 2.8.A). The N-terminus (M1 aa1-440) was not able to bind to CenpC while the C-terminus (M2 aa441-998) was sufficient to mediate an interaction with CenpC, suggesting that the SANTA domain alone is dispensable in this context. The central region (M3 aa325-800) containing SANTA and SANT domain as well as a shorter fragment (M4) in which only the SANT domain was present showed clear interaction with CenpC, again suggesting that the SANTA domain is not crucial for the interaction (Figure 2.8.B). Statistical analysis of the interaction screen, based on automated quantification in several hundred cells per construct through red/green intensity values provided additional information concerning the strength of the tested interaction (Figure 2.8.C). In the case of M4 the average red/green signal ratio was rather low although in confocal imaging 73% of the analyzed cells showed co-localization with CenpC. One explanation for the discrepancy might be that the expression level of RFP CenpC is lower in cells co-expressing EGFP M4, compared to the other truncations. Based on

these results it seemed that the SANT domain somehow facilitates the interaction and therefore a small fragment containing solely the SANT domain was tested. This short truncation (M5) failed to interact with CenpC leading to the conclusion that apart form the SANT domain other regions of the protein are necessary to mediate the interaction. From this analysis it can be concluded that a central region of M18bp1 is needed to mediate a stable interaction with CenpC.

The interaction of M18bp1 and CenpC was further characterized in co-immunoprecipitation experiments. HEK cells were co-transfected with EGFP-tagged CenpC and myc-tagged M18bp1. CenpC was purified using nuclear extract with GFP-trap affinity resin. M18bp1 clearly co-immunoprecipitated with CenpC providing further evidence that M18bp1 and CenpC can interact in a different *in vivo* system (Figure 2.9.).

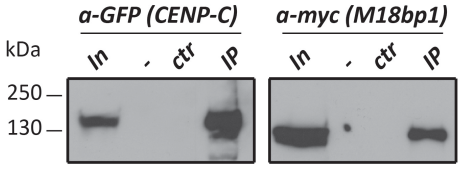

Figure 2.9. Co-immunoprecipitation of CENP-C and M18bp1. HEK293FT cells were transfected with expression plasmids for EGFP-CENP-C and myc-M18bp1. Nuclear extracts from these cells were incubated with agarose beads (control) and GFP-Trap affinity beads to enrich for EGFP-CENP-C and interacting bound proteins. Western blot analysis shows the nuclear extract (Inp), proteins bound to agarose beads (mock) and proteins that were enriched with GFP-Trap agarose beads (IP). An empty lane is indicated by "-". EGFP-CENP-C and myc-M18bp1 were detected using antibodies against GFP and myc, respectively.

CenpC is a conserved centromeric protein, whose very N-terminus has been shown to bind the Mis12 complex (Screpanti et al. 2011), a complex which together with Knl1 and Ndc80 is part of the (KMN) network forming the inner and outer kinetochore. The central region of CenpC is responsible for its direct binding to CenpA (Moree et al. 2011; Dambacher et al. 2012). Chromatin binding and dimerization activity has been shown for the C-terminus containing the cupin domain (Trazzi et al. 2002; Trazzi et al. 2009). A study in *X.laevis* (Moree et al. 2011) could show that the very C-terminus of CenpC is crucial for the interaction with the M18bp1 homologue. Therefore the goal was to define the region in CenpC crucial for its interaction with M18bp1. The cDNA of CenpC was divided into three constructs feasible for *in vitro* translation (Figure 2.10.A.). These sub-fragments were tested for their interaction with GST-tagged M18bp1 truncations (M1-M5). *In vitro* interaction studies showed that the N-terminal and the middle part of CenpC do not mediate the M18bp1 interaction. The N-terminal region of M18bp1 was also not required for the binding to CenpC. In contrast the C-terminus and a central region of M18bp1 showed direct interaction with the C-terminal fragment of CenpC. From the direct binding assay the C-terminal region of CenpC was identified to be required for the direct interaction with a central region of M18bp1 (Figure 2.10.B.).

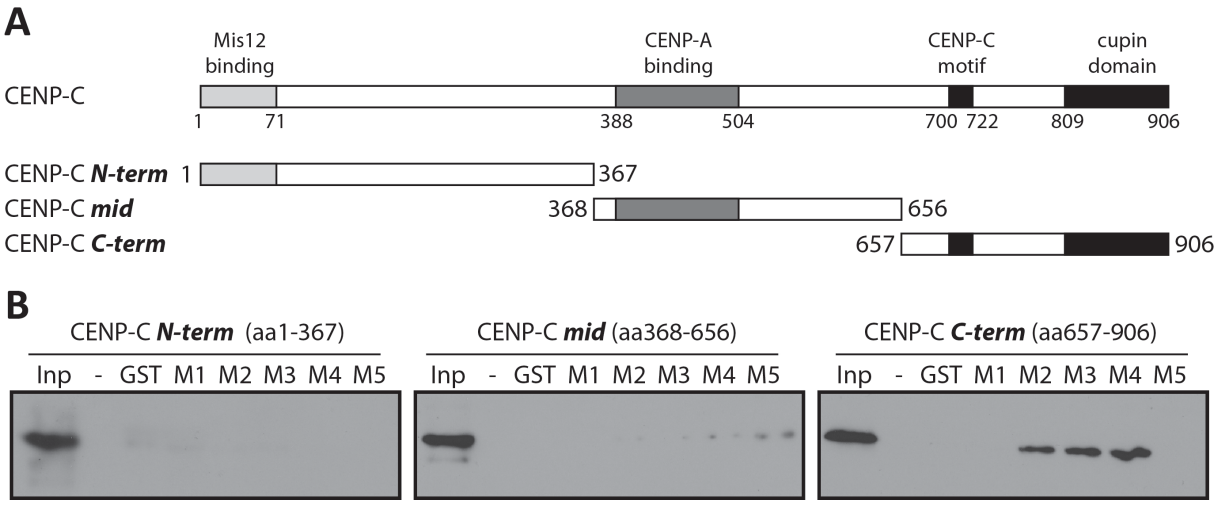

Figure 2.10. ***In vitro*** **interaction studies of M18bp1 and CenpC. A)** Scheme of the domain structure of mouse CenpC and the truncation constructs that were used in this assay. **B)** Recombinant GST-tagged M18bp1 truncations (M1-M5) were incubated with *in vitro* translated myc-tagged CENP-C truncation proteins and bound to GST beads. The bound CENP-C protein truncations were detected using myc antibody.

2.2.2. The characterization of M18bp1 knockout mice

To learn more about the *in vivo* functions of M18bp1, knockout mice provided by the EUCOMM project (Ayadi et al. 2012) were analyzed. Exon 4 of the M18bp1 gene was flanked by loxP sequences (Nagy 2000) and additionally a bGal cassette flanked with FRT sides was inserted into the locus. The targeting strategy results in a knockout first allele, which produces a beta-galactosidase (bGal) under control of the endogenous M18bp1 promoter (Figure 2.11.A). The heterozygous M18bp1$^{+/bGal}$ mice were phenotypically normal without showing any obvious defects in development, fertility or behavior. Intercrosses of M18bp1$^{+/bGal}$ mice were set up to obtain full mutant mice, however no living M18bp1 ko mice were observed, suggesting that M18bp1 is essential for viability (Figure 2.11.B.).

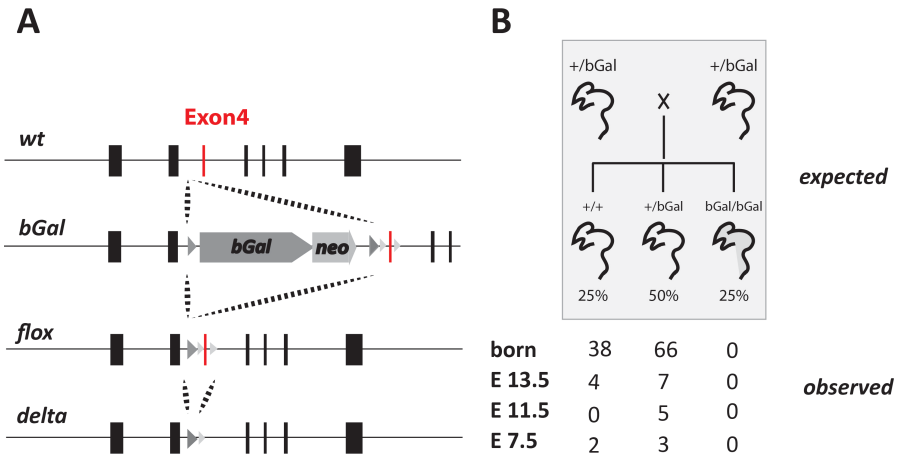

Figure 2.11. Genomic locus of M18bp1 and knockout strategy. A) Schematics of the M18bp1 ko strategy. The bGal allele carries an integration of a b-galactosidase gene, leading to a mutant allele. FRT-mediated recombination converted the bGal into a flox allele, which carries loxP sites around exon 4. Excision of exon 4 using Cre recombinase results in the loss-of-function delta allele. **B)** Intercrosses of M18bp1$^{bGal/+}$ mice revealed the early lethality of M18bp1 mutants.

To narrow down the time when these embryos die, embryos at different time points after fertilization (E7.5, E11.5, E13.5) were isolated. Genotyping revealed that not a single M18bp1 mutant embryo was generated after E7.5. These data clearly demonstrate that M18bp1 is an essential factor for early embryogenesis.

Notably, in the blastocysts (E3.5) from M18bp1$^{bGal/+}$ intercrosses, M18bp1$^{bGal/bGal}$ mutant embryos were detected, however, even these early embryos were developmentally retarded and displayed noticeable apoptotic bodies. Strikingly these early mutant embryos already showed developmental abnormalities while control blastocysts showed normal shapes and cellular structures. Individual cells showed an abnormal chromatin structure and the formation of apoptotic bodies (arrowhead) indicating ongoing cell death. Only a few mitotic cells could be monitored, which displayed segregation defects like misalignment of the metaphase plate (Figure 2.12.). Furthermore the generation of ES cell lines from these blastocysts failed suggesting that the outgrowth of the ICM, which gives rise to ES cells is also perturbed (data not shown). The malformation of the blastocyst implicates that the knockout of M18bp1 is lethal in the embryo at very early developmental stages at around E3.5.

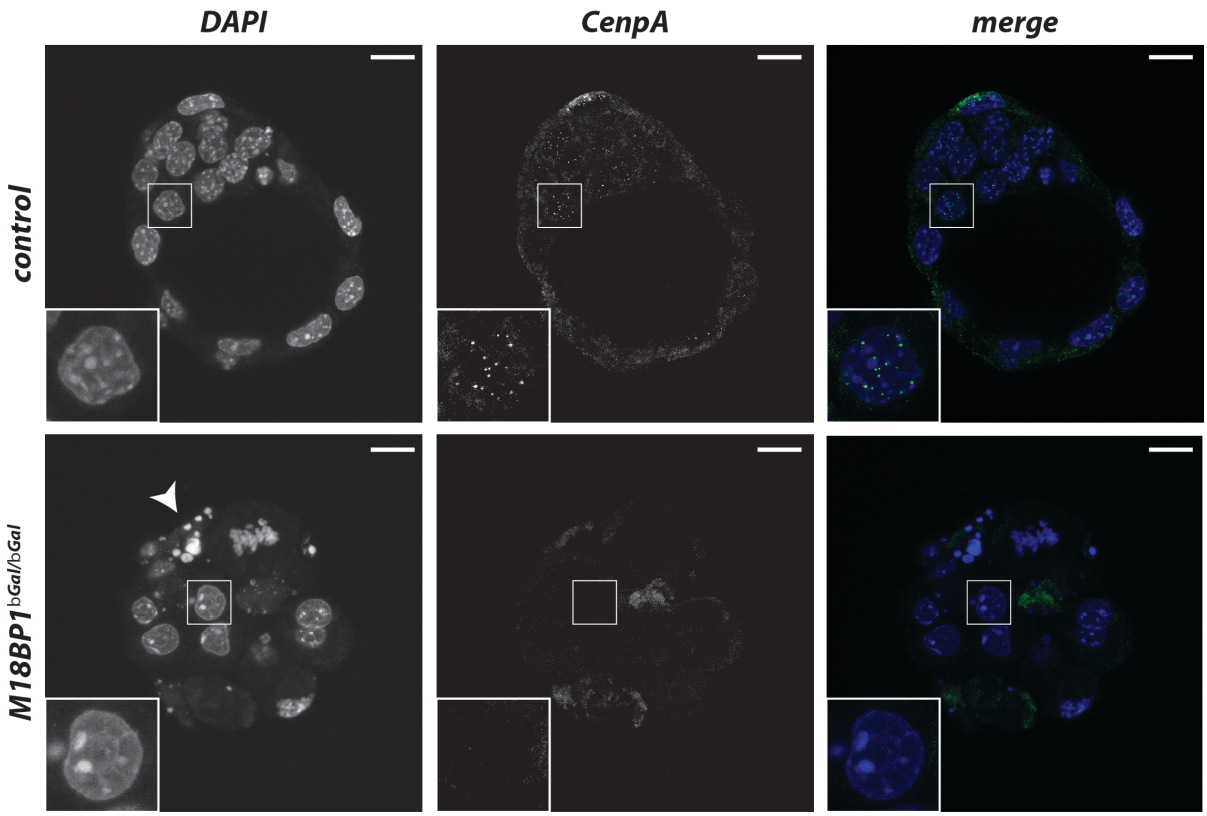

Figure 2.12. Phenotype of M18bp1 mutant blastocysts. Confocal section of an immunofluorescence analysis of control and M18bp1$^{bGal/bGal}$ blastocysts. The mutant blastocyst displays developmental retardation, reduced CenpA staining and the appearance of apoptotic bodies (arrowhead). Scale bar is 6µm.

To analyze whether defects in centromere organization might contribute to these developmental defects in the M18bp1 mutant blastocysts immunofluorescence analysis for CenpA was performed. While CenpA foci were well detectable in control blastocysts, mutant blastocysts showed reduced CenpA levels (Figure 2.12. middle). From these data it can be concluded that M18bp1 is essential for early embryogenesis through ensuring proper chromosome segregation by mediating CenpA incorporation into centromeric chromatin. As the straight knockout causes very early lethality conditional knockout mice were generated. For this purpose FLP recombination was used to remove the bGal cassette and to convert the M18bp1^{bGal} allele into a flox allele. The resulting flox allele allows expression of a full length M18bp1 protein and can then be converted into a M18bp1 delta allele using Cre recombinase. Cre-mediated recombination truncates the genomic sequence of M18bp1 from exon 3 onwards and leads to the expression of a short transcript, which could only give rise to a truncated non-functional protein. Dependent on the specific expression profile of the promoter driving the Cre recombinase expression, mutant alleles can be generated in a time- and tissue-specific manner. Expression data (biogps.org) describe M18bp1 as highly abundant in embryonic stem cells, hematopoietic stem cells and testis. As M18bp1 is highly expressed in testis, tissue-nonspecific alkaline phosphatase (TNAP) Cre recombinase (Lomeli et al. 2000) was used to generate a conditional knockout allele specifically in germ cells. Germ cells are defined as cells, which give rise to the gametes. Primordial germ cells (PGCs) cells in female mice enter into the prophase of the first meiotic

division in the ovary to become oocytes. In the testis of male mice PGCs become mitotically arrested to become prospermatogonia (Nakatsuji and Chuma 2001). M18bp1 was efficiently depleted in M18bp1$^{fl/fl}$, TNAP Cre mice obtained by crossing M18bp1$^{fl/fl}$ with M18bp1$^{fl/fl}$, TNAP Cre mice. The genotype of the offspring was comparable to the expected mendelian ratio. Mutant mice were born and did not show any obvious phenotype. Controlled matings revealed that female and male mice were still able to breed but breeding took longer as compared to wild type crossings.

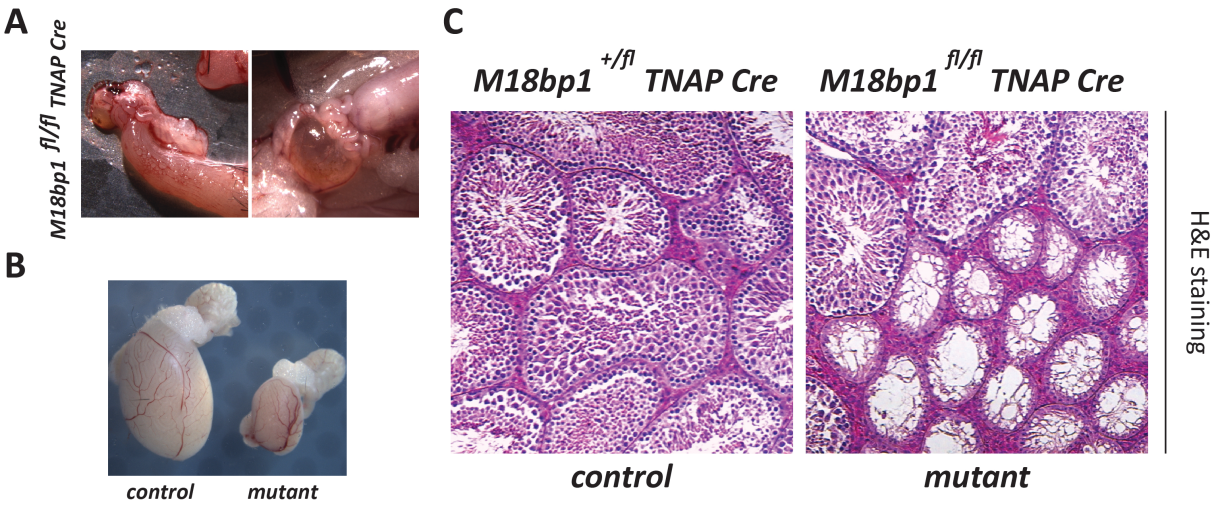

Figure 2.13. IHC analysis of ovaries and testis of M18bp1$^{fl/fl}$, TNAP Cre mice. A) Ovaries of M18bp1$^{fl/fl}$, TNAP Cre mice show ovarian cysts. **B)** Testis from control (M18bp1$^{+/fl}$, TNAP Cre) and mutant (M18bp1$^{fl/fl}$, TNAP Cre) mice show differences in size. **C)** Testicular histology was performed on material of 4 weeks old mice. H&E staining of control and mutant tissue as paraffin sections. Histology was performed by Alexander Nuber.

The effect of the M18bp1 depletion was investigated in ovaries and testis, as TNAP Cre specifically deletes in germ cells. Ovaries were isolated from adult female mutant mice. Whereas the overal morphology looked comparable to control ovaries, M18bp1 mutants showed ovarian cysts (Figure 2.13.A). Furthermore testes were dissected from mutant and control males. Compared to control mice the testes of mutant mice were severely reduced in size (Figure 2.13.B). Testicular histology was performed with material from 4 weeks old male mice. Male mice were fertile at 5-7 weeks. Paraffin sections of the 4 weeks old mice were stained with Hematoxylin and Eosin (H&E staining) to visualize structural tissue details. Stainings revealed that control mice showed the characteristic structural features of wild type tubles. In mutant mice some tubles showed normal structure while others were abnormally shaped with completely degenerated inner tuble structures (Figure 2.13.C).

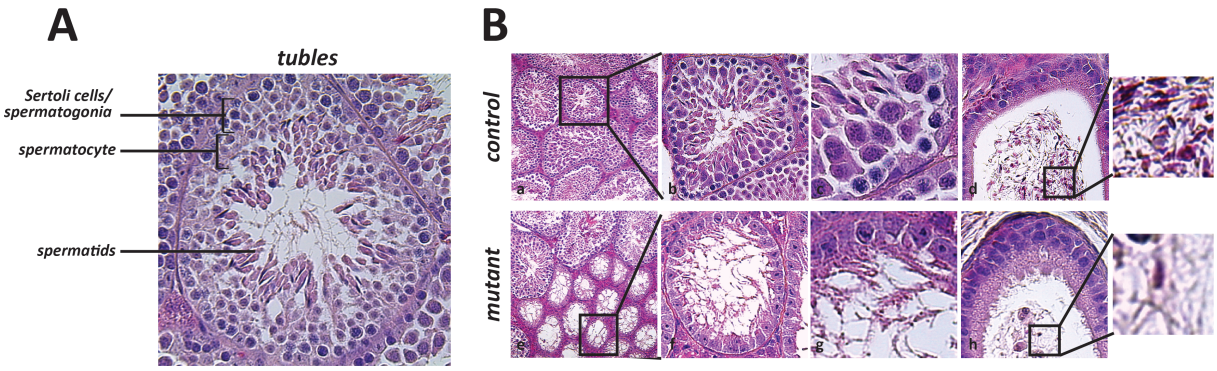

Figure 2.14. Testis phenotype of M18bp1$^{fl/fl}$, TNAP Cre mice A) Cellular composition of a seminiferous tuble, structures were visualized with H&E staining. **B)** Detailed histological analysis of H&E stained paraffin section of control and M18bp1$^{fl/fl}$, TNAP Cre mutant mice. Histology was performed by Alexander Nuber.

In the outer rim of the testicular tubles spermatogonia and Sertoli cells are present. Spermatogonia (spermatogonial stem cells) are germ cells, which in the mitotic (proliferative) phase undergo either self-renewal or differentiation into spermatocytes. In contrast Sertoli cells are not germ cells and have regulatory functions in spermatogenesis. Spermatocytes undergo two meiotic divisions and give rise to spermatids accumulating in the centre of the tubles (Figure 2.14.A). Detailed analysis of these paraffin sections revealed that the severely affected tubles lost spermatogonia, spermatocytes and spermatids completely and only Sertoli cells are still present at the outer rim of the structure. Sertoli cells as non-germ cells are not depleted for M18bp1 as TNAP Cre is not expressed in these cells. From these data it can be concluded that the loss of M18bp1 is essential for the survival of all germ cells and the lack of M18bp1 leads to total failure in spermatogenesis in most testis tubles. (Figure 2.14.B).

Due to the early embryonic lethality it was impossible to obtain primary mouse embryonic fibroblasts (pMEFs), which are normally isolated from E13.5 embryos. Therefore an inducible system was used, by combining the floxed allel with an inducible Cre recombinase. This Cre recombinase (Cre ERT2) is fused with the ligand-binding domain of the estrogen receptor. This fusion protein is constitutively expressed but localizes to the cytosol.

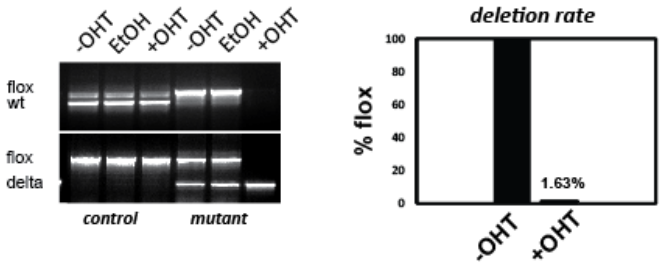

Figure 2.15. Deletion rate upon induction of the M18bp1 knockout using Tamoxifen. A) Endpoint PCR on genomic DNA from pMEFs of control (M18bp1$^{+/fl}$; Cre ERT2) and mutant (M18bp1$^{fl/fl}$; Cre ERT2) with specific primers detecting wt, floxed and delta allele in uninduced (- 4-OHT), control (EtOH) and Tamoxifen-induced (+ 4-OHT) cells. **B)** Quantitative PCR on genomic DNA of uninduced and induced mutant cell lines with specific primers detecting the floxed allele.

Upon treatment with tamoxifen (4-OHT), the Cre recombinase can enter the nucleus and converts the M18bp1 floxed to a deleted allele. MEFs were isolated from E13.5 embryos from intercrosses of M18bp1$^{fl/fl}$; Cre ERT2 mice. Cells were cultivated under low oxygen conditions and induced with Tamoxifen. Extensive titration experiments were necessary to adjust the Cre ERT2 system, as the Cre recombinase in control cells already caused some mitotic defects. Therefore the system was adjusted to a concentration of 4-OHT, which did not affect the control cells. The analysis of the cells was performed 12-24h after application of Tamoxifen. Genomic DNA was isolated to determine the deletion rate in mutant cell lines in standard endpoint PCR and qPCR (Figure 2.15.). Deletion after 24 hours was rather efficient as no flox allele was detected and the deletion rate was calculated to >95% from qPCR data. Additionally protein levels and turnover were analyzed comparing uninduced vs. induced mouse fibroblast extracts in western blot. For this purpose a M18bp1 specific antibody was raised in rabbit against peptides (see Materials and Methods). The antibody recognizes a protein band above 100kDa and an additional band at around 90kDa. The calculated size of M18bp1 is 113kDa, which matches with the upper band on the blot. This was confirmed as the band at >100kDa disappears upon induction of the deletion, suggesting a high turnover of M18bp1 (Figure 2.16.A).

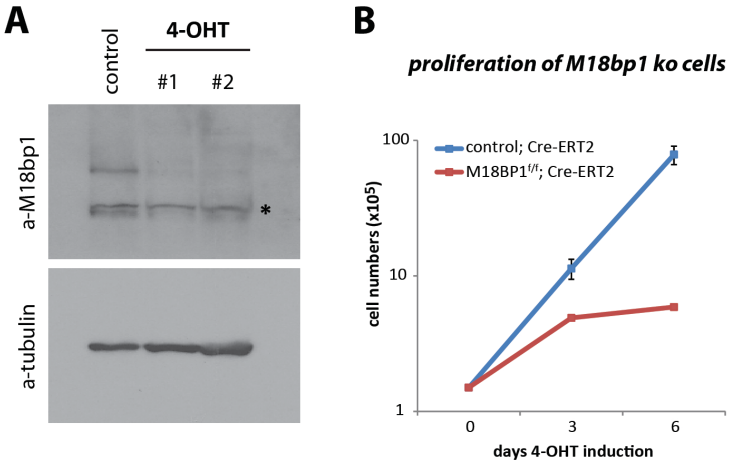

Figure 2.16. M18bp1 cko cells show proliferation defects upon induction of the deletion. A) Western blot of control and induced M18bp1$^{fl/fl}$; Cre ERT2 pMEFs (two cell lines) with a M18bp1 specific antibody. **B)** Proliferation curve of control and M18bp11$^{fl/fl}$; Cre ERT2 pMEFs after 4-OHT induction.

Proliferation rate of the cells was measured for up to six days after applying Tamoxifen. As the control cells show continuous proliferation, M18bp1$^{fl/fl}$; Cre-ERT2 fibroblasts grew considerably less well and stopped proliferation after day3 (Figure 2.16 B). Microscopy was used to further analyze the cellular phenotype upon deletion of M18bp1. The control cells exhibited characteristic morphology of wild type primary mouse fibroblasts while the mutant cells displayed severe changes in the nuclear structure 12h after Tamoxifen treatment. Two phenotypes could be observed in M18bp1$^{fl/fl}$; ESR Cre cells: an early phenotype visible 12h after depletion as M18bp1 ko cells show severe mitotic defects (Figure 2.17.) and a late phenotype appearing after 3-5 days of deletion when M18bp1 mutant cells show reduced CenpA levels. (Figure 2.18.) The early phenotype results in cells exhibiting anaphase

bridges, lagging chromosomes, micronuclei, blebbing of the nuclear lamina as well as less defined chromocenter structure. Furthermore many cells showed di- or multi-nucleation (Figure 2.17.).

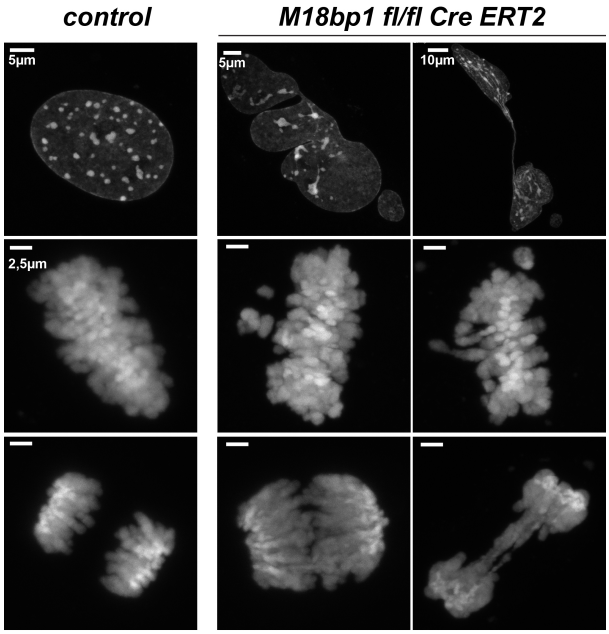

Figure 2.17. Mitotic defects upon M18bp1 depletion. Confocal analysis of pMEFs isolated from intercrosses of M18bp1$^{+/fl}$ x M18bp1$^{fl/fl}$;Cre ERT2. Deletion was induced by Tamoxifen treatment for 24h, when cells were fixed and DAPI stained.

High-resolution microscopy also revealed defects in chromosome condensation during mitosis. As M18bp1 was reported as a factor important for CenpA integration, CenpA levels were tested 12h and 3 days after depletion in control vs. mutant cells using a specific antibody. CenpA levels in M18bp1 mutant cells were well detectable 12h after depletion and comparable to control cells (data not shown). Interestingly 3 days after depletion, CenpA was hardly detectable in M18bp1 ko fibroblasts (Figure 2.18.).

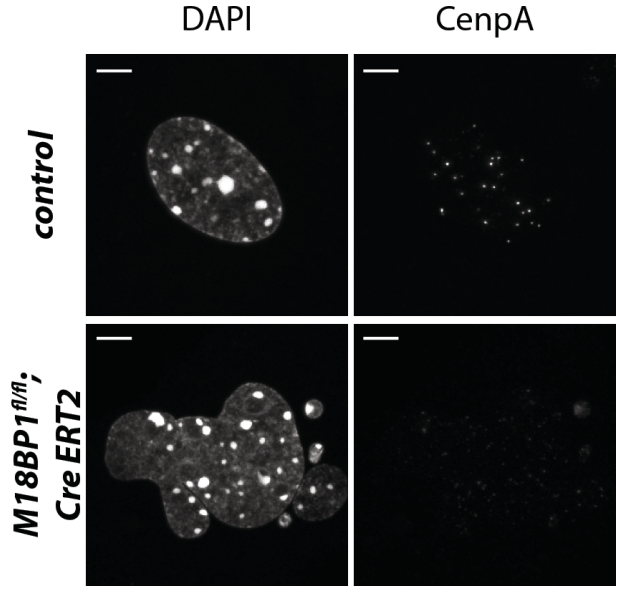

Figure 2.18. CenpA levels decrease upon M18bp1 depletion. Confocal analysis of pMEFs isolated from intercrosses of M18bp1 $^{wt/fl}$ x M18bp1 $^{fl/fl}$ ESR Cre. Mutation was induced by Tamoxifen treatment for 24h. Cells were fixed and stained with anti CenpA antibody. Scale bar is 5µm.

From these data it can be concluded that M18bp1 is involved in different cellular mechanisms: On the one hand M18bp1 may be directly involved in the regulation of mitosis and on the other hand M18bp1 is required for facilitating the deposition of newly synthesized CenpA onto centromeric chromatin in primary mouse fibroblasts.

M18bp1 ko fibroblasts show severe proliferation defects which are caused by failures during mitotic chromosome segregation. In order to detect alterations in the timing of mitosis M18BP1 ko fibroblasts expressing H2B-EGFP as nuclear marker were analyzed in live cell imaging. This method is a frequently used tool to monitor changes in the nuclear chromatin structure in living cells without compromising nuclear and chromosomal structures (Kanda et al. 1998).

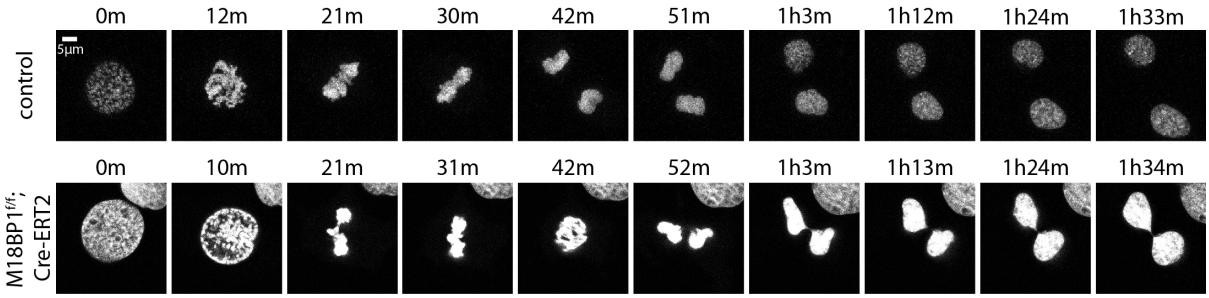

Figure 2.19. Time-lapse microscopy of M18bp1 knockout fibroblasts. Control and M18BP1$^{fl/fl}$; Cre ERT2 pMEFs which stably express H2B-EGFP were imaged for around 6 hours. Shown are time-series of selected mitotic cell divisions.

Upon induction with Tamoxifen aberrant cell divisions could be observed in M18bp1 mutant cells. Preliminary timescale analysis of cells revealed no obvious delay in mitotic progression, but further statistical analyses are necessary to conclude this observation (Figure 2.19.).

2.2.3 The interaction network of M18bp1

The depletion of M18bp1 results in a dramatic phenotype in mice as well as on the cellular level- but what are the precise molecular functions of M18bp1? One possibility could be that M18bp1 influences proteins, which are involved in centromere regulation. To identify potential candidates, a knock-in ES cell line was generated. Advantage of this system is, that the tagged M18bp1 is expressed under the control of the endogenous promoter and therefore protein levels are not altered in the cell (Figure 2.20.).

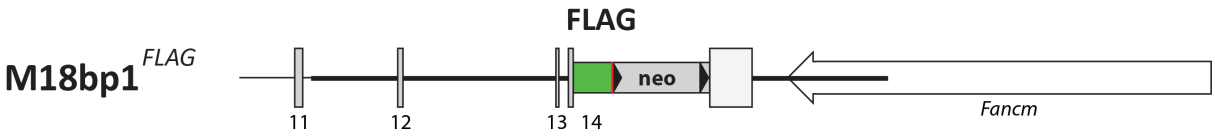

Figure 2.20. Knockin strategy for M18bp1^{FLAG}ES cells. Modification of the M18bp1 genomic locus in M18bp1 knock-in ES cells. These cells express a FLAG-tagged M18bp1 from the endogenous promoter.

Importantly no changes in proliferation rate or morphology in comparison to wild type ES cells were observed, suggesting that the integration of the targeting cassette did not cause any cellular defects. Six rounds of FLAG-immunoprecipitation experiments in wild type vs. M18bp1-FLAG cells were performed. Bound proteins of the immunoprecipitation (IP) experiments were separated on SDS page and silver stained (Figure 2.21.A). The efficient precipitation of the M18bp1-FLAG was tested in western blot using a FLAG- specific antibody (Figure 2.21. B).

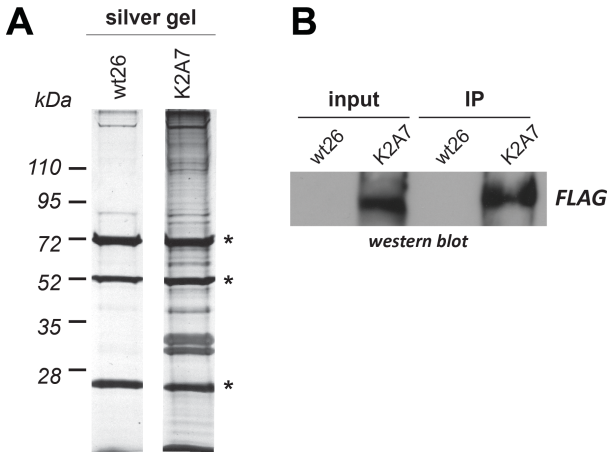

Figure 2.21. Immunoprecipitation of FLAG-tagged M18bp1 from ES cells. A) FLAG tagged M18bp1 was purified from knock-in ES cell nuclear extract with FLAG M2 antibody. As a control, wt ES cell extract was used to detect unspecific binding to the M2 antibody. Proteins were separated on SDS page and visualized by silver staining. **B)** Western blot analysis to check for successful precipitation of the tagged proteins with anti FLAG antibody.

Mass spectrometry analysis of proteins precipitated with FLAG- tagged M18bp1 revealed 446 enriched proteins. Some interesting clusters could be identified among these various proteins. Known interactors like Mis18alpha and Mis18beta, which have been proposed to form a stable complex with M18bp1 underline the cell line as a valid tool for the identification of interacting proteins. Importantly CenpC was also specifically enriched with M18bp1 confirming interaction data. Additional proteins,

which have been suggested to be associated with M18bp1 (Rbbp4 and Rbbp7), were present in the list of precipitating proteins. Moreover the small GTPase RacGap1, which was also described to be crucial for the regulation of M18bp1 has been identified (Lagana et al. 2010). Furthermore a number of novel putative interaction partners were identified. Two groups of proteins were particularly interesting in this context: On the one hand a class containing chromatin-associated proteins and on the other hand a class of proteins having functions at the centromere (Figure 2.22.).

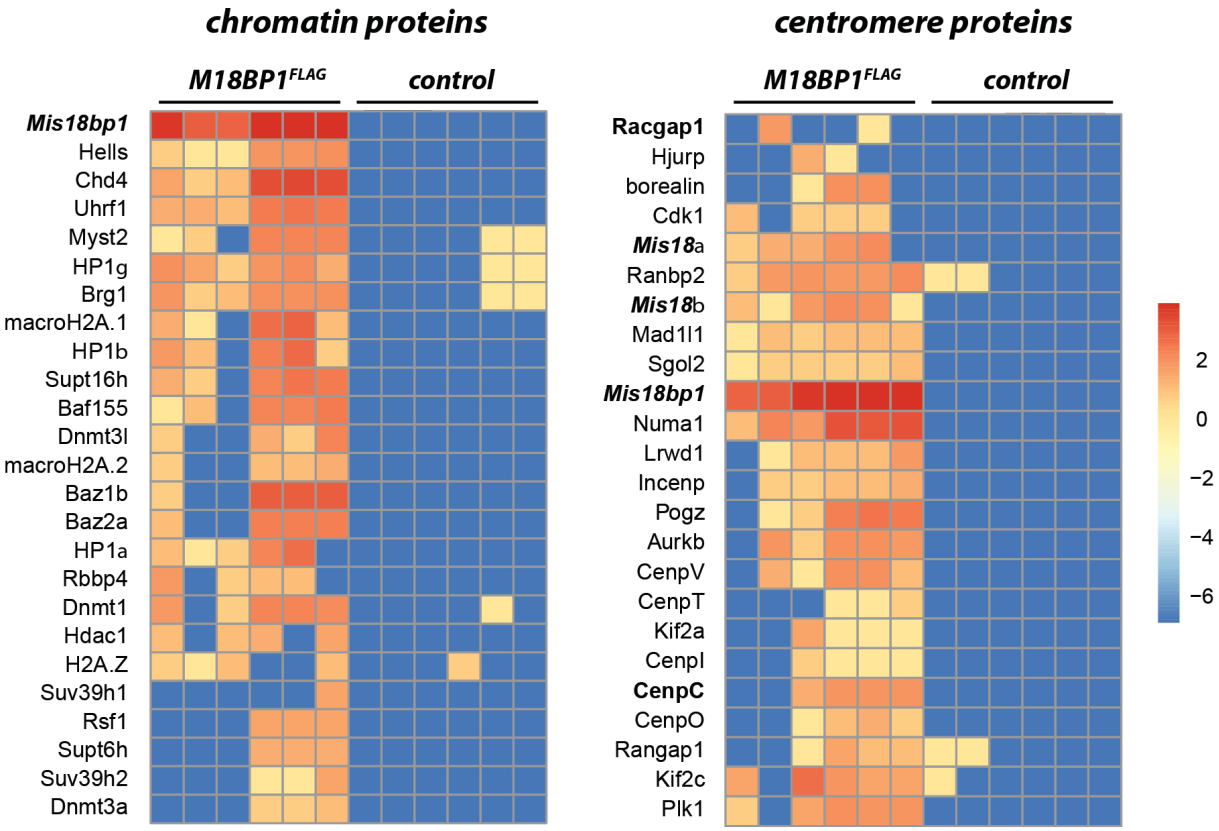

Figure 2.22. Interaction network of M18bp1 in knock in ES cells. Heat map of proteins identified in six independent FLAG-IP experiments from M18bp1^{FLAG} knock-in ES cells and wt ES cells as control. Proteins are clustered in chromatin proteins and centromere proteins.

The group of centromere proteins showed HJURP as the chaperone responsible for CenpA deposition onto chromatin and several centromere proteins associated with M18bp1. Apart from CenpC other Cenp proteins were present in the protein list, like CenpT, CenpO, and CenpV. CenpV was especially interesting as overexpression of CenpV causes hypercondensation of pericentromeric heterochromatin (Tadeu et al. 2008; Honda et al. 2009). CenpO was described as an important factor to prevent premature sister chromatid separation and is crucial for proper kinetochore function (Hori et al. 2008). Interestingly also other mitotic checkpoint proteins, like components of the chromosomal passenger complex (CPC), Aurora B, Incenp and Borealin, as well as Bub3 and Mad2 were present in this dataset.

Within the cluster of proteins having functions on chromatin, the three isoforms of HP1 (HP1alpha, beta and gamma) were abundant hits. HP1 proteins are well characterized in the context of heterochromatin. Importantly it has been reported that HP1 isoforms associate with centromeric chromatin in a cell cycle dependent manner (Hayakawa et al. 2003). The heterochromatin cluster of M18bp1 interacting proteins revealed also several histone variants like macro H2A.1 and macro H2A.2 and H2A.Z. Furthermore chromatin-modifying proteins like the DNA methyltransferases Dnmt1, Dnmt3a, HDAC1, the HAT Myst2 (Kap7) and the HMTases specific for H3K9me3, Suv39h1 and Suv39h2, have been identified. Interestingly Hells (Lsh) was also found in the list, which is a crucial factor for normal embryonic development and closely associated with pericentric heterochromatin (Muegge 2005). Lsh deficiency leads to abnormal heterochromatin organization, a loss of DNA methylation, and an altered pattern of histone-tail acetylation and methylation (Yan et al. 2003). In summary, M18bp1 interacts with both chromatin associated and centromere associated proteins, suggesting multiple functions of M18bp1, which have to be further analyzed.

2.2.4. The function of M18bp1 at pericentric heterochromatin

M18bp1 was one of the proteins specifically enriched with the H3K9me3 peptide in several independent experiments. Initial confocal analyses revealed that it localizes to chromocenters upon overexpression in mouse fibroblasts. In M18bp1-transfected cells the chromatin structure was altered extensively and looked rather compacted compared to non-transfected cells. Interestingly upon overexpressing the EGFP-tagged M18bp1 protein in Suv39h knockout MEFs the heterochromatic localization was lost showing a broad nuclear staining, but still lead to compaction of the chromatin structure (Figure 2.23.). These data suggest that the recruitment of M18bp1 to heterochromatin is dependent on the trimethylation of H3K9 or the enzymes inducing this mark (Suv39h1 and Suv39h2) and that overexpression of M18bp1 leads to a compacted chromatin structure.

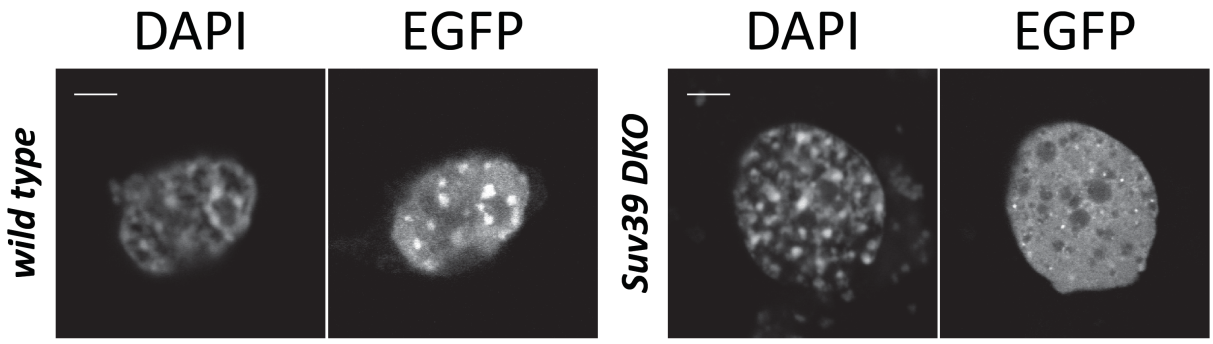

Figure 2.23. Heterochromatic localization of M18bp1 in mouse embryonic fibroblast cells. Confocal analysis of EGFP-tagged M18bp1 in wild type and Suv39h DKO mouse fibroblasts. Cells were transiently transfected and DAPI stained. Scale bar is 5µm.

Several truncation constructs have been created to map the heterochromatin- targeting domain in M18bp1. EGFP-tagged M18bp1 fragments divided the protein into an N-terminal part containing the

SANTA domain (M1) and a C-terminal part in which the SANT domain is present (M2). While the C-terminus was localizing to DAPI dense nuclear regions comparable to the full-length protein the N-terminus showed diffuse cytoplasmic and nuclear EGFP signal.

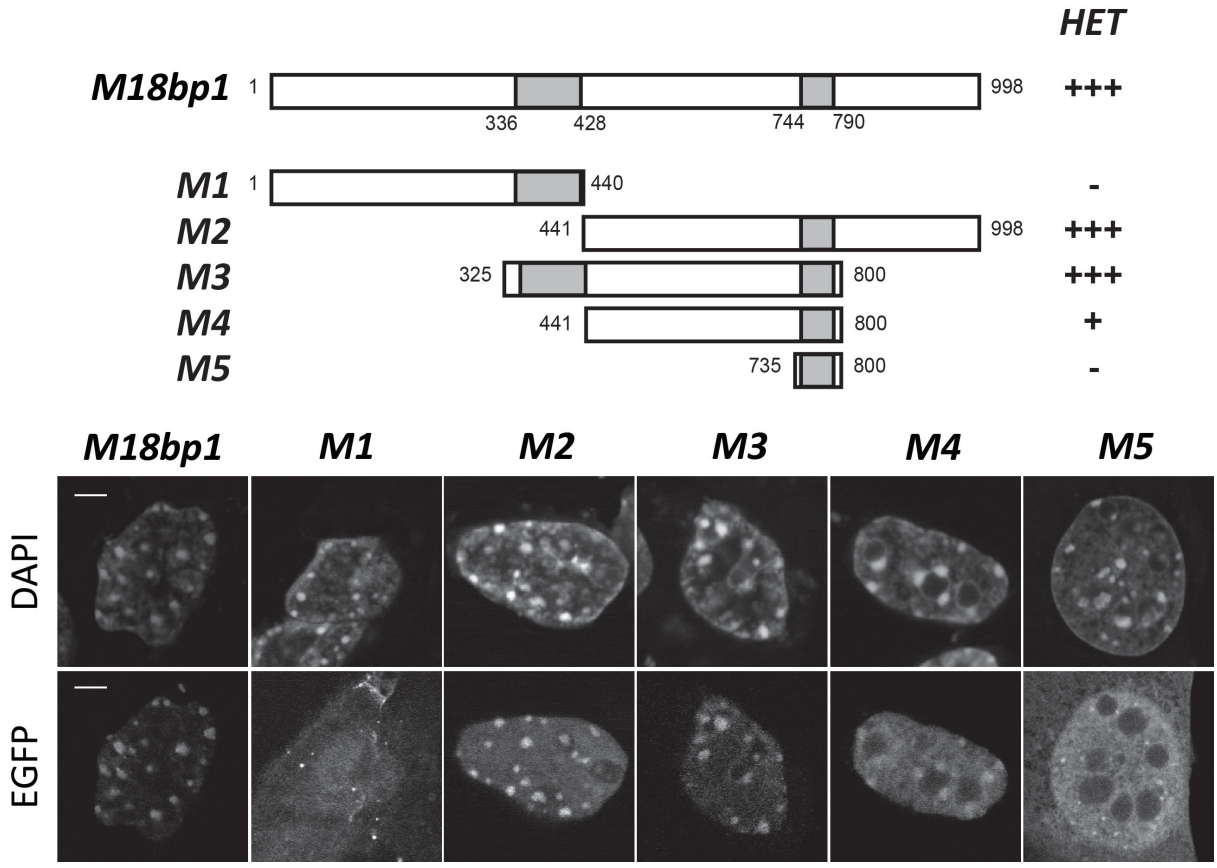

Figure 2.24. Localization analysis of M18bp1 truncations. Various truncations of M18bp1 (full length, M1-M5) were expressed as EGFP fusion proteins in wild type MEFs. Fixed cells were stained with DAPI and the nuclear distribution of the fusion proteins was monitored by confocal microscopy. DAPI-dense regions represent heterochromtic regions in the nucleus. Scale bar is 5μm.

A central region containing SANTA and SANT domain (M3) was found to localize to heterochromatic regions. Removing the SANTA domain from this region in fragment M4 did not alter the localization. Furthermore a very small sub-fragment comprising only the SANT domain was expressed and showed a broad nuclear distribution (Figure 2.24.).

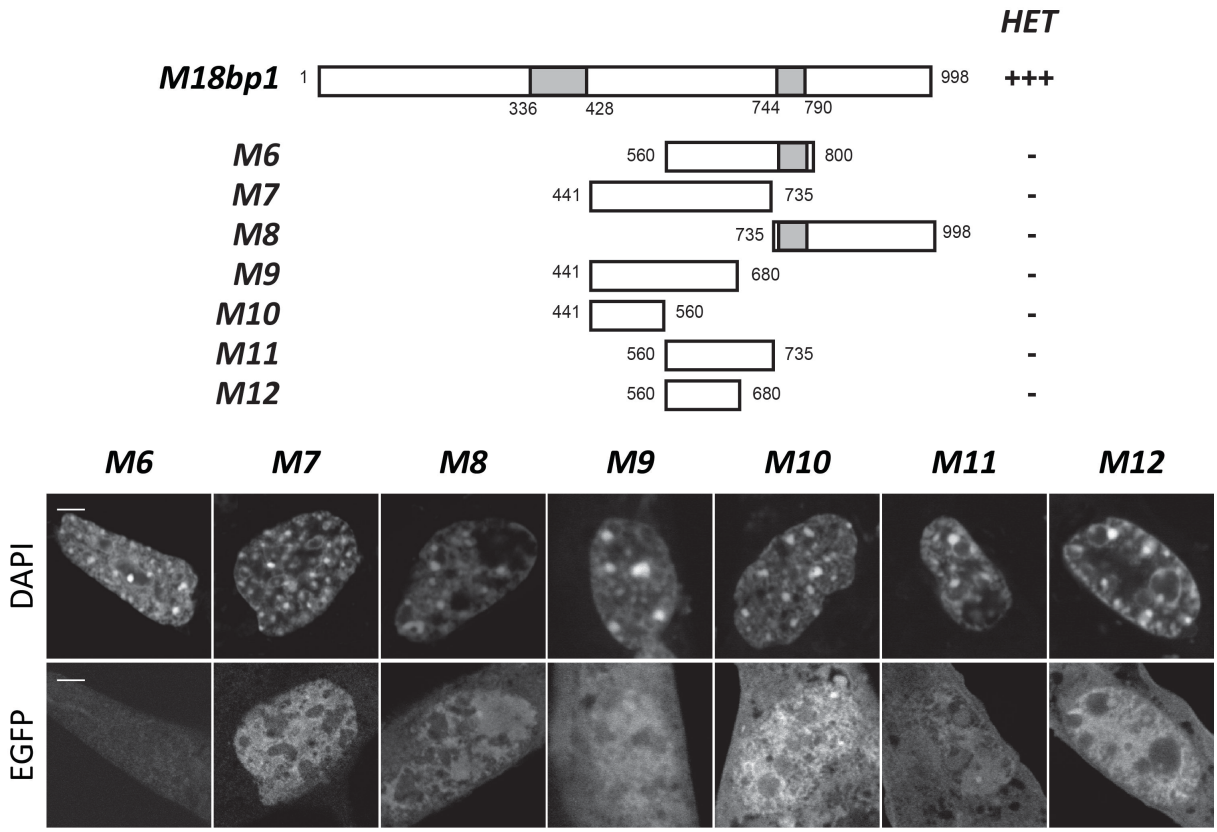

Figure 2.25. Mapping of the minimal heterochromatin targeting domain. Sub-fragments of M18bp1 (full length, M6-M12) were expressed as EGFP fusion proteins in wild type MEFs. Fixed cells were stained with DAPI and the nuclear distribution of the fusion proteins was monitored in confocal microscopy. DAPI-dense regions represent heterochromtic regions in the nucleus. Scale bar is 5µm.

Additional EGFP-tagged M18bp1 fragments were generated in order to map the minimal region necessary for the targeting of M18bp1 to heterochromatin. Unfortunately all tested fragments did not localize to heterochromatin (Figure 2.25.). Therefore the minimal region sufficient for the recruitment of M18bp1 to heterochromatin is M4, a 359aa long fragment from the C-terminus containing the SANT domain but not the SANTA domain. From these data it can be concluded that the C-terminus of M18bp1 is responsible for the targeting to heterochromatin. However it is unclear what targets M18bp1 to heterochromatin regions in the nucleus. As M18bp1 was associated with the H3K9me3 peptide direct interaction with these peptides was tested. Direct interaction assays were performed using *in vitro* translated myc- tagged M18bp1 and the differentially methylated H3K9 peptides. M18bp1 showed only weak binding affinity to the unmodified H3K9 peptide. Compared to the unmodified peptide, binding affinity towards methylated H3K9 peptides was higher. However M18bp1 was bound to all three methylation states mono-, di- and trimethylation, suggesting that M18bp1 has no specific affinity for the trimethylated peptide (Figure 2.26.A).

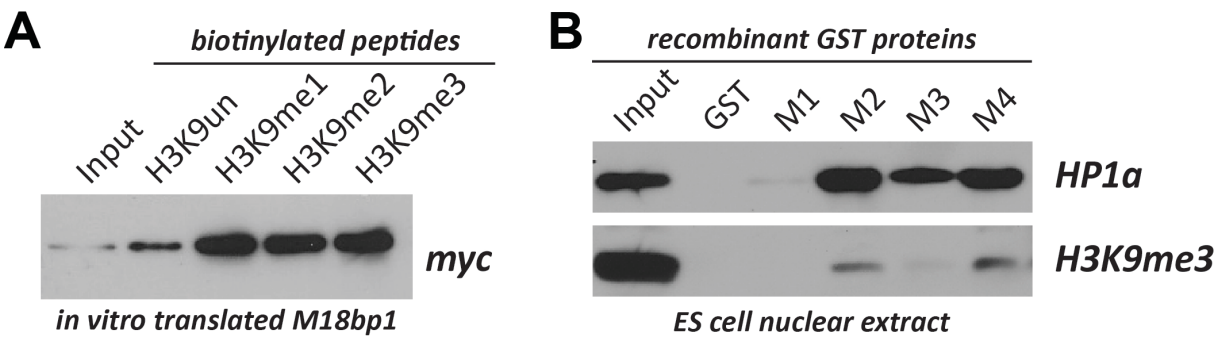

Figure 2.26. Interaction of M18bp1 with heterochromatin protein 1. A) Binding assay with H3 peptides and *in vitro* translated myc-tagged M18bp1 protein. **B)** Pulldown experiment with GST-tagged truncations of M18bp1 and GST as a control using nuclear extract from wild type ES cells.

Accordingly, if M18bp1 has basic affinity to H3K9 peptides other proteins might be necessary to modulate the specificity toward the trimethylation state. The most abundant proteins present at H3K9me3 are HP1 isoforms. They are also known to interact with many proteins, which have functions at heterochromatin. A GST pulldown assay was performed using recombinant GST-tagged M18bp1 truncations (M1-M4). ES cell extract from wild type cells was incubated with proteins coupled to Glutathione sepharose beads. HP1 alpha was detected in western blot to bind to the C-terminus (M2), the middle fragment (M3) and the heterochromatin-targeting domain (M4) of M18bp1 but not to the GST control or the N-terminus of the protein (M1). Furthermore nucleosomes carrying the H3K9me3 mark were also enriched with the C-terminal truncations (Figure 2.26.B).

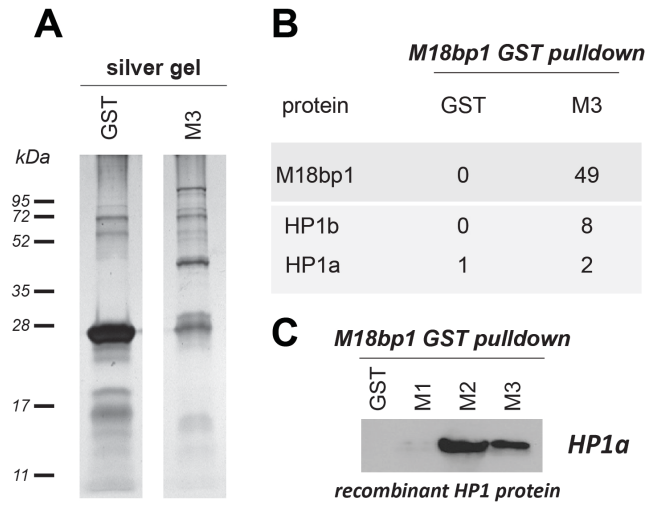

Figure 2.27. Interaction of M18bp1 with heterochromatin protein 1. A) Pulldown experiment with GST-tagged truncations of M18bp1 and GST as a control using nuclear extract from wild type ES cells. **B)** Mass-spec analysis of a GST pulldown experiment with a central M18bp1 fragment and wild type ES cell nuclear extract. **C)** Binding assay of recombinant GST-tagged M18bp1 truncations and recombinant HP1a protein.

These data were confirmed in mass-spec analyses using the M3 fragment and GST as a control. The recombinant M3 fragment precipitated the HP1 isoforms HP1b and HP1a. (Figure 2.27.B). As both experiments were performed with nuclear extract, other proteins present in the extract could mediate the interaction of M18bp1 with HP1. Therefore a direct interaction assay was performed, using recombinant tag-free HP1 alpha protein in a binding assay with three different C-terminal truncations

of M18bp1. Interaction was analyzed in western blot with a HP1 specific antibody. HP1 did not bind to the GST-tag suggesting that the assay condition was stringent. The N-terminus of M18bp1 did not bind to HP1, while HP1 was bound by the C-terminal part and the central region, which both contain the conserved SANT domain. (Figure 2.27.C).

The SANT domain is a conserved protein domain present in various proteins. The function of this motif is still unclear as no enzymatic activity or direct affinity has been shown until now. It has been suggested that the SANT domain might facilitate substrate recognition of different proteins.

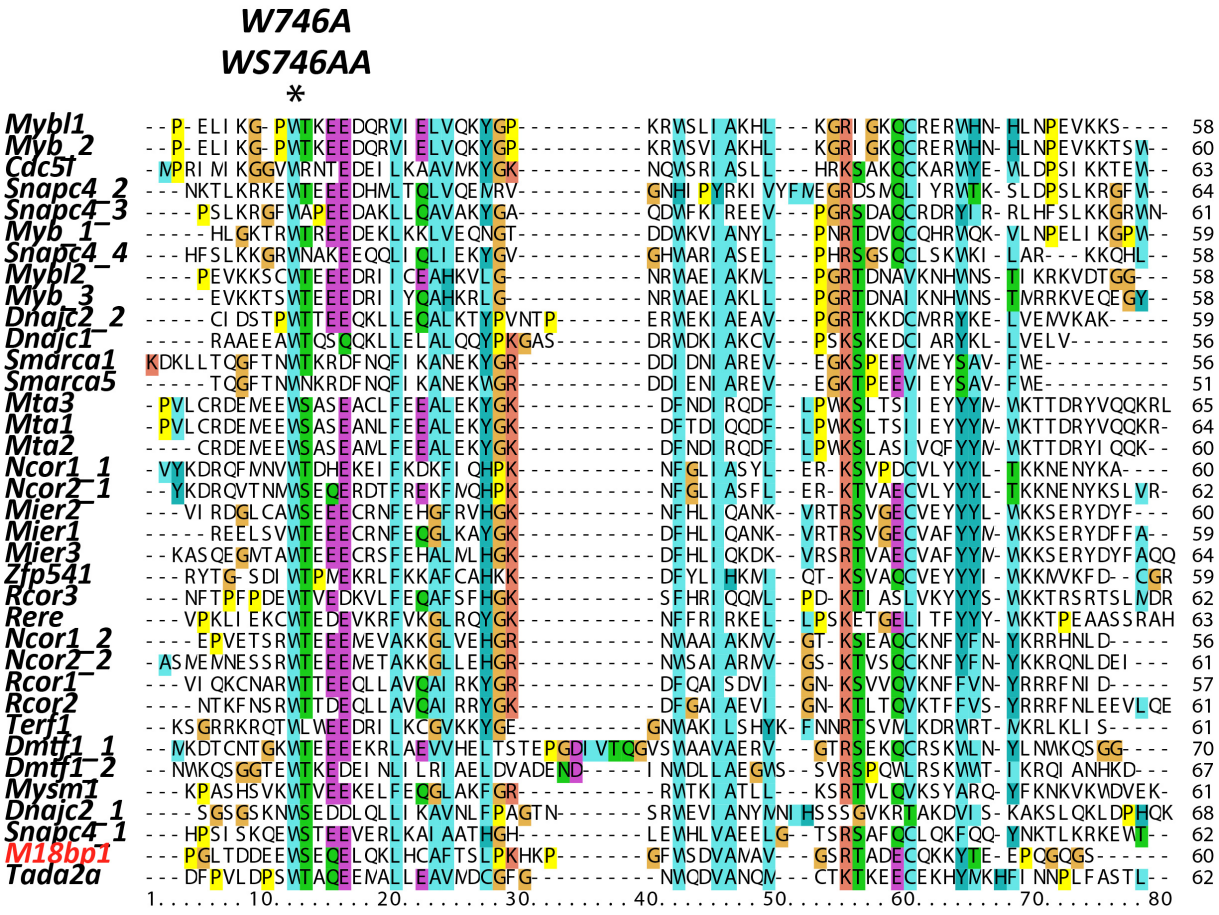

Figure 2.28. Alignments of mouse SANT domain proteins. Alignment of different SANT domain proteins, conserved in *M. musculus*. Highly conserved regions were selected for the PCR-mediated site-directed mutagenesis.

An alignment of the various SANT domain proteins conserved in *M. musculus* is depicted in Figure 2.28. Residues showing highest conservation were chosen for the introduction of an amino acid exchange to disrupt conserved structures in the SANT domain, which might be involved in its function. EGFP-tagged mutant constructs were transfected in wild type fibroblasts to monitor the localization of these mutant proteins (Figure 2.29.A).

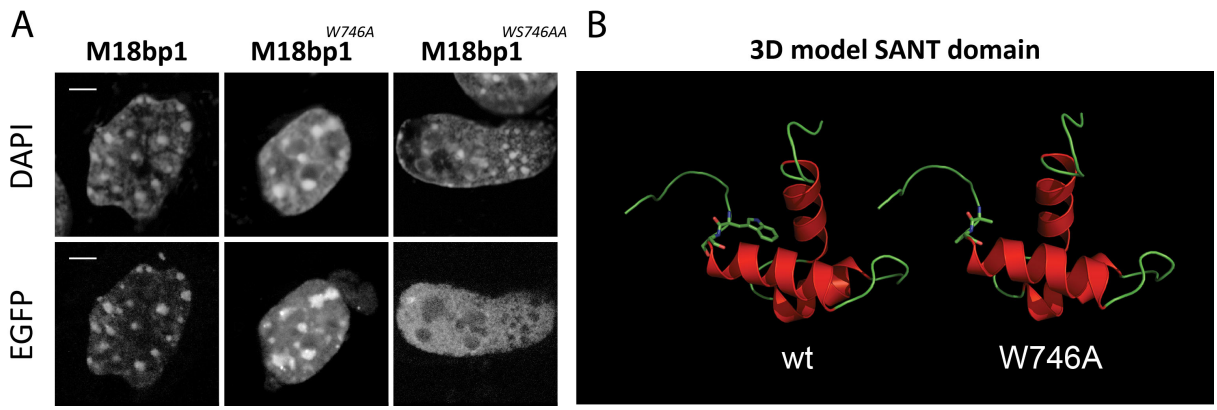

Figure 2.29. Localization of M18bp1 SANT mutant constructs. A) EGFP constructs of M18bp1 SANT domain mutants were analyzed for their localization in wild type mouse fibroblasts. **B)** Crystal structure model of the M18bp1 SANT domain before and after mutagenesis. Scale bar is 5µm.

In a first step a single mutation (M18bp1^{W746A}) resulting in an exchange of Tryptophan (W), containing an uncharged aromatic amino acid against Alanine (A), was generated by mutagenesis PCR. Testing the protein construct for its localization in wild type fibroblasts revealed that the single amino acid exchange in the SANT domain of M18bp1 did not alter the heterochromatic localization of M18bp1. As the neighboring amino acid Serine (S) was found to be also well conserved, a double mutant was generated (M18bp1^{WS746AA}). Interestingly the double mutant protein failed to localize to heterochromatin suggesting that this motif somehow influences the targeting to this regions. In summary a conserved residue in the SANT domain is crucial for the heterochromatic localization of M18bp1 in mouse fibroblasts (Figure 2.29 A). Modeling the crystal structure of M18bp1 revealed the formation of a cage like structure, which might be crucial for protein-protein interactions (Figure 2.29.B).

2.3. Characterization of H4K20 methyltransferases

Heterochromatin displays a compact structure with a distinct histone and DNA modification pattern, which is important to repress the transcription of repetitive elements. Heterochromatic regions possess hypermethylated DNA and are largely devoid of acetylation marks. The characteristic methylation pattern at heterochromatin is established in a sequential pathway. Suv39h enzymes introduce the methylation at H3K9, which is in turn bound by HP1 proteins. Suv4-20h1 and Suv4-20h2 have been characterized as the histone methyltransferases possessing specific activity towards H4K20 upon recruitment to heterochromatin via direct binding to HP1 proteins. Suv4-20h enzymes differ in their activities to induce H4K20 methylation states as H4K20me2 is reduced in Suv4-20h1 knockout cells, whereas MEFs deficient for Suv4-20h2 almost loose H4K20me3. Characteristic for all HMTases is their enzymatic domain, called SET domain. As different HMTases have been identified to methylate H3K9, Suv4-20h enzymes are the predominant methyltransferases, for introducing H4K20me2 and H4K20me3. The H4K20 monomethylation is specifically induced by another SET domain protein called PrSet7 (Setd8). During replication 'old' histones are distributed equally onto both daughter strands and newly synthesized histones are incorporated. PrSet7 induces monomethylation of newly-synthesized H4 in S phase in close connection to the replication fork protein PCNA. It has been proposed that in later stages of the cell cycle this mono-methyl mark is converted to either H4K20me2 or H4K20me3 dependent on the chromatin context. In order to test this hypothesis HMTase assays were performed.

The HMTases were purified form *E.coli* as recombinant GST-tagged proteins. PrSet7 was expressed as soluble protein, whereas the full length proteins of Suv4-20h1 and Suv4-20h2 were forming inclusion bodies in bacteria. Hence the N-termini containing the SET domains of either Suv4-20h1 and Suv4-20h2 were used for these assays (Figure 2.30.A.).

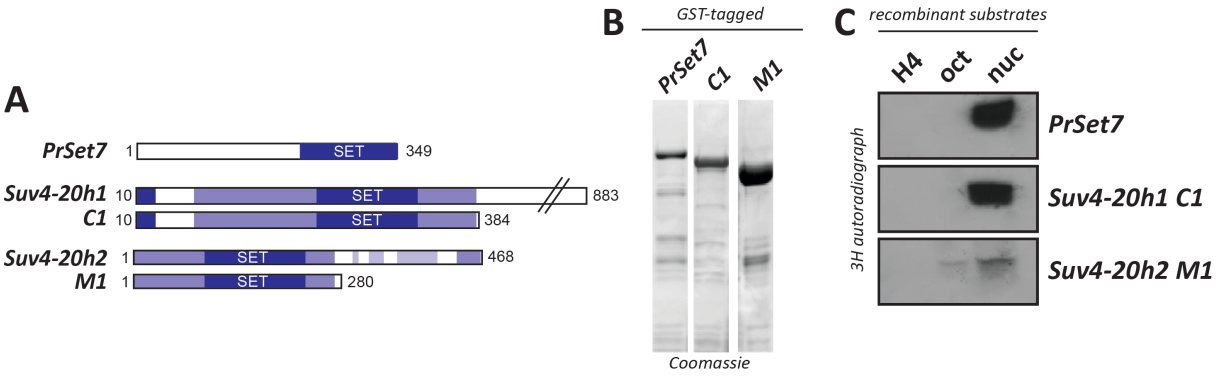

Figure 2.30. Substrate specificity of the different H4K20 methyltransferases. A) Scheme of the different H4K20 specific histone methyltransferases (PrSet7, Suv4-20h1 and Suv4-20h2). Depicted are the conserved motifs and the SET domain crucial for the enzymatic activity. **B)** Coomassie gel of purified recombinant GST tagged enzymes. **C)** Autoradiography of an HMTase assay with recombinant HMTases on different substrates (histone H4, octamers, nucleosomes) with ^{3}H labeled SAM (S-adenosyl methionine).

The purity of the proteins was monitored on a Coomassie stained SDS page (Figure 2.30.B). Subsequently the activity was tested in an HMTase assay using different substrates: histone H4, octamers or nucleosomes assembled on a 12x array of the 601 nucleosome positioning sequence (Routh et al. 2008). All three enzymes preferentially show methyltransferase activity towards H4, but only in the context of the nucleosomal substrates, not on histone H4 or octamers. Suv4-20h2 showed the weakest activity on unmodified recombinant nucleosomes (Figure 2.30.C). In conclusion the H4K20-specific methyltransferases possess activity on unmodified histone H4 exclusively in the nucleosomal context.

2.3.1 Suv4-20h enzymes prefer the monomethylated substrate to induce H4K20me3

The monomethylation of H4K20 requires PrSet7 whereas di- and trimethylation are introduced by the Suv4-20h enzymes. The higher methylation state might be achieved by converting the monomethylation state (Figure 2.31.A). Therefore it was tested whether nucleosomes carrying the monomethylation at H4K20 are preferred substrate for Suv4-20h1 and Suv4-20h2.

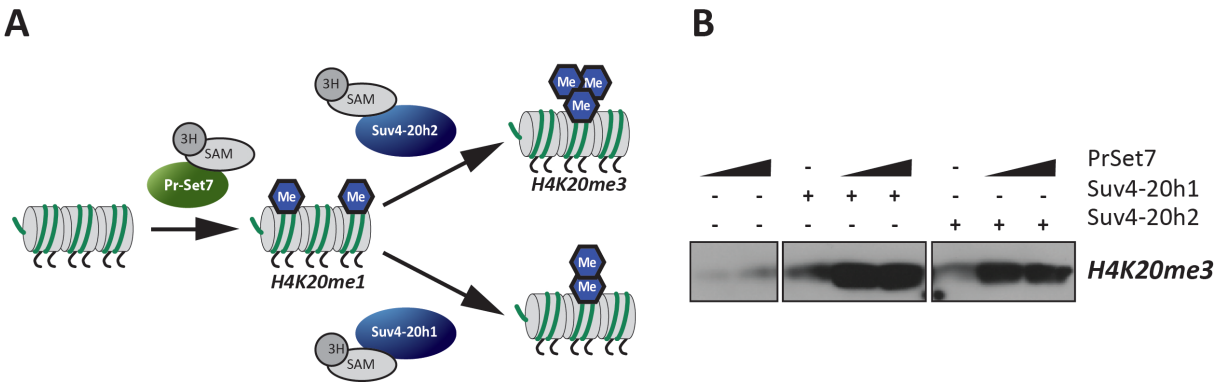

Figure 2.31. Suv4-20h enzymes prefer monomethylated substrates. A) PrSet7 monomethylates histone H4 in the nucleosomal context and provides a preferred template for the methylation by Suv4-20h1 and Suv4-20h2. **B)** HMTase assay using nucleosomal substrates and recombinant PrSet7, Suv4-20h1 and Suv4-20h2. Western blot of an HMTase assay using H4K20me3 specific antibody.

HMTase assays were performed on nucleosomal arrays comparing unmodified vs. premethylated substrates (Figure 2.31.B). Nucleosomal arrays were premethylated with PrSet7. PrSet7 did not induce significant amounts of H4K20 trimethylation. Suv4-20h1 and Suv4-20h2 induced trimethylation of H4K20 on unmodified nucleosomes. However both Suv4-20h1 and Suv4-20h2 showed increased methylation activity on the premethylated substrates, suggesting that Suv4-20h1 and Suv4-20h2 indeed prefer the H4K20me1 substrates to induce the trimethylation on histone H4.

2.3.2 PrSet7 interacts with the C-terminus of Suv4-20h2

PrSet7 has several important functions during the cell cycle; it is required for chromosome condensation, mitotic progression and proper DNA replication. The expression of PrSet7 is tightly regulated during the cell cycle, with highest expression during G2/M and early G1 phase while it is not expressed during S phase (Oda et al. 2009). Furthermore cell cycle regulation is achieved by several posttranslational modifications like phosphorylation, sumoylation and ubiquitination (Abbas et al. 2010; Centore et al. 2010; Oda et al. 2010; Tardat et al. 2010; Spektor et al. 2011). Additionally it harbors two PIP domains, a specialized type of PCNA interaction motif (PIP [PCNA-interacting peptide] domain) termed 'PIP degron', which allows the protein to be degraded through PCNA-coupled $CRL4^{Cdt2}$-mediated ubiquitination prior to S phase (Havens and Walter 2009; Oda et al. 2010). Interestingly the lack of PrSet7 in mice results in a severe phenotype. Embryos die very early in development in the eight cell stage (Oda et al. 2009). Compared to the phenotype of Suv4-20h DKO mice, which die perinatally, the PrSet7 phenotype is much stronger, leading to the hypothesis that the monomethylation mark of H4K20 is a crucial modification requiring strict regulation to ensure survival of cells.

GST pulldown experiments were performed to identify novel binding partners of PrSet7. Surprisingly two proteins were highly enriched with PrSet7. One was PCNA and the other one was Suv4-20h2 (Figure 2.32. and Appendix table IV.)

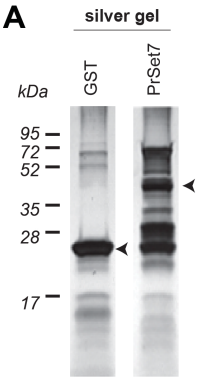

B

PrSet7 GST pulldown

protein	GST	PrSet7
PrSet7	0	63
PCNA	0	4
Suv4-20h2	1	10

Figure 2.32. GST pulldown with PrSet7. A) Silver staining of GST pulldown experiments with recombinant GST-tagged PrSet7 and wild type ES cell nuclear extract. GST was used as a control to monitor proteins, associated with the tag. **B)** LC MS/MS analysis of GST pulldown experiments. Numbers depicted in the table are the unique spectra achieved from Mascot analysis.

The direct interaction of PrSet7 and Suv4-20h2 was tested in binding assays. As full length Suv4-20h2 is not soluble upon expression in *E.coli* several truncation constructs were tested. The N-terminus (M1) containing the SET domain was not binding to PrSet7. The C-terminus (M2) showed clear interaction. Smaller fragments dividing the C-terminus (M4, M6) were also tested and could both bind to PrSet7 (Figure 2.33.).

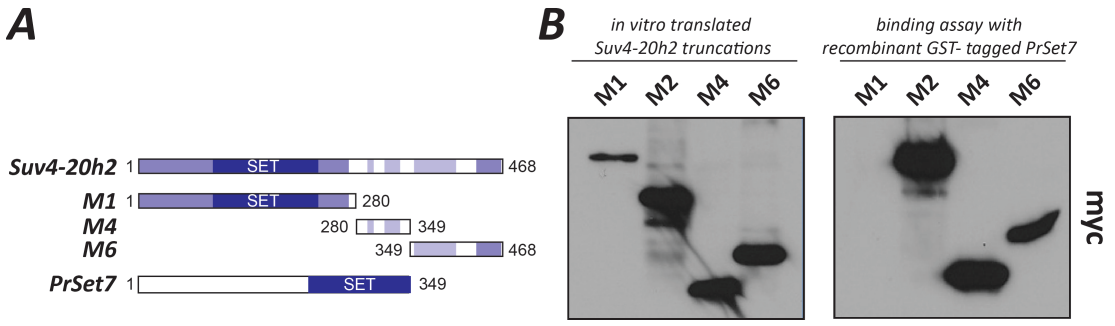

Figure 2.33. The C-terminus of Suv4-20h2 interacts with PrSet7. A) Map of PrSet7 and Suv4-20h2 truncation constructs used for *in vitro* translation. **B)** *In vitro* translated myc-tagged Suv4-20h2 truncations were tested for binding to GST-tagged PrSet7. Left panel shows myc- probed input of *in vitro* translation reactions. Right panel shows the bound proteins.

The binding assay revealed that PrSet7 and Suv4-20h2 directly interact *in vitro*. This interaction is mediated by the C-terminus of Suv4-20h2. From this assay it is not possible to further map interaction site(s) as both non overlapping C-terminal sub-fragments of Suv4-20h2 were binding to PrSet7.

2.3.3. The interaction network of Suv4-20h2

As Suv4-20h2 is an important player present at pericentric heterochromatin it was interesting to identify associated proteins, which might point towards additional functions of Suv4-20h2 and to improve the understanding of heterochromatin formation. Two different approaches were chosen to identify candidate proteins interacting with Suv4-20h2: a Yeast two-hybrid (Y2H) screen and a GST pulldown assay.

For the Y2H screen human SUV4-20H2 was cloned into a yeast expression vector. Yeast cells express the DNA binding domain (DB) of the Gal4 transcription factor fused to the bait protein. Human SUV4-20H2 as bait protein was fused to the DNA binding domain, which binds the upstream activating sequence (UAS). A human library of prey proteins was expressed as fusions to the Gal4-activating domain (AD). Bait-prey interaction induces expression of a downstream reporter gene (Koegl and Uetz 2007; Mohr and Koegl 2012). From three independent screens three proteins were reproducibly identified to interact with SUV4-20H2. HP1a, but not HP1b or HP1g was found to interact with Suv4-20h2. This interaction was already characterized, as HP1 proteins are required to recruit Suv4-20 proteins to heterochromatin, suggesting that the assay is feasible to identify proteins interacting with Suv4-20h2. However it was not clear why only one isoform of HP1 was identified, as all three isoforms were present in the prey library, suggesting that the screening approach was not driven to full saturation. The undescribed protein RHOXRI and the bol like protein Boll (Boule) were also identified in the Y2H screen to interact with SUV4-20H2 (Figure 2.34.). As a member of the DAZ (Deleted in AZoospermia) family of genes Boll is highly conserved among different species (Shah et al. 2010). Knockout mice of Boll show male infertility due to an arrest in spermatogenesis at the round spermatid stage (VanGompel and Xu 2010).

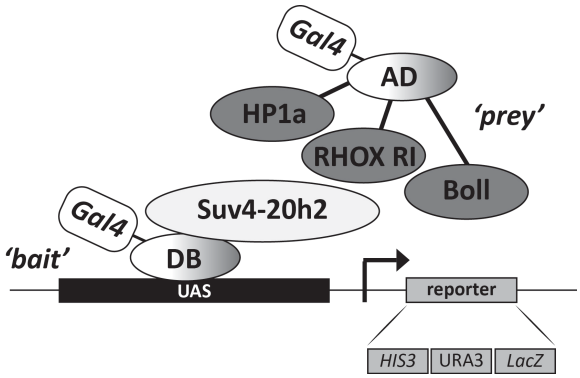

Figure 2.34. Yeast to hybrid screen to identify interactors of SUV4-20H2. Y2H screen was performed at the Yeast Two-Hybrid Protein Interaction Screening Service at the DKFZ (Prof. Kögl) in Heidelberg. Suv4-20h2 was used as bait for screening a human genomic cDNA library.

As the yeast two-hybrid screen identified only few candidates another approach was used. GST pulldown assays were performed using recombinant Suv4-20h2 C-terminal truncations and nuclear extract from mouse ES cells. GST served as control for background binding. Two Suv-20h2 truncations were tested: M7, a fragment from the very C-terminus, which is not recruited to heterochromatin and a central fragment, M5, which is targeted to heterochromatin via HP1 interaction motifs (Figure 2.35.).

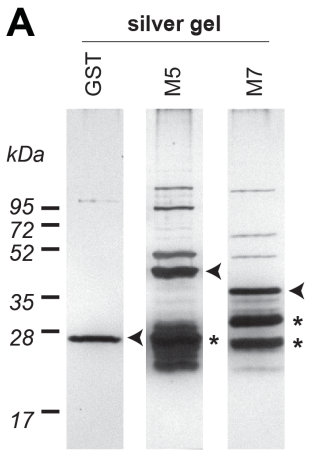

B

protein	*Suv4-20h2 GST pulldown* GST	M5 (aa 349-441)	M7 (aa 409-468)
Suv4-20h2	4	112	62
HP1a	0	41	0
HP1b	0	40	0
HP1g	1	40	0
Smc1	0	7	1
Smc3	0	3	0
PrSet7	0	8	2

Figure 2.35. Identification of proteins interacting with the C-terminus of Suv4-20h2. A) Silver staining of GST pulldown experiments with recombinant GST-tagged Suv4-20h2 truncations and wild type ES cell nuclear extract. GST was used as a control **B)** LC MS/MS analysis of GST pulldown experiments with recombinant GST-tagged Suv4-20h2 truncations and wild type ES cell nuclear extract. Numbers depicted in the table are the unique spectra achieved from Mascot analysis.

Upon mass-spec analysis all three HP1 isoforms were specifically enriched with the M5 fragment. Interestingly PrSet7 was also found associated with the C-terminus of Suv4-20h2. These data confirm the GST-pulldown results obtained by the reverse assay using PrSet7 as a GST pulldown bait. Additionally, several other proteins were found by mass-spec analysis like LaminB1, or subunits of the Orc complex involved in replication (Figure 2.35. and Appendix table III.). Two other proteins, which precipitated with the M5 fragment of Suv4-20h2 were particularly interesting: Smc1 and Smc3. Both proteins are subunits of the Cohesin complex, a multi-subunit complex consisting of Smc1, Smc3, Scc1 and Scc3. Cohesin is well known to be crucial for proper sister chromatid cohesion and chromatin structure organization.

The GST pulldown experiments were performed with nuclear extract, which still contained DNA and RNA. It is known that DNA and RNA can mediate protein-protein interactions. In order to test if the interaction between Suv4-20h2 and Smc is dependent on nucleic acids, pulldown experiments were repeated with either Benzonase treated nuclear extracts or in presence of EtBr, which, in both cases abolish interactions that are mediated through DNA or RNA. Benzonase is a very strong nuclease, which degrades RNA and DNA very efficiently, while EtBr is thought to block DNA interaction.

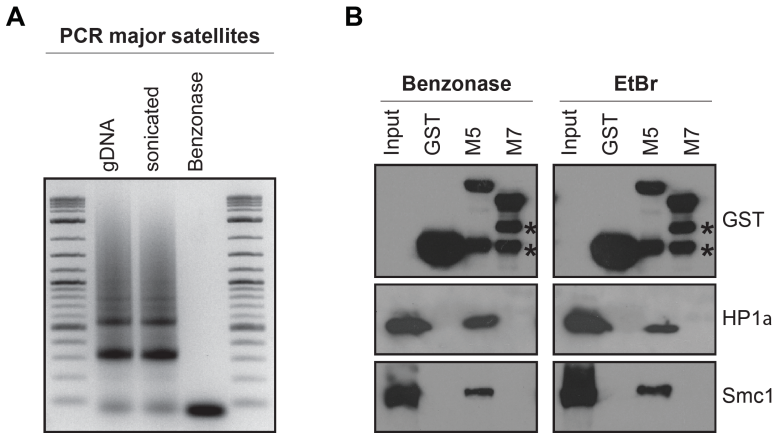

Figure 2.36. The interaction of Suv4-20h2 with cohesin and HP1 is DNA-independent. A) Endpoint PCR on genomic DNA. DNA isolated from sonicated nuclear extracts and Benzonase treated nuclear extract with primers specific for major satellite repeats. **B)** GST pulldown experiments with recombinant GST-tagged Suv4-20h2 truncations. In the left panel the nuclear extract from wt ES cells was treated with Benzonase to remove contaminating DNA and RNA. In the right panel the incubation of GST tagged Suv4-20h2 truncations and nuclear extract occurred in the presence of EtBr. Western blots for GST pulldown experiments using recombinant GST, Suv4-20h2-M5 and Suv4-20h2-M7 were probed for GST, HP1a and Smc1. The Input lane contains the nuclear extract. Degradation products of the GST tagged proteins are indicated by asterisks.

In both cases we could detect binding of Smc1 proteins to the Suv4-20h2-M5 fragment, demonstrating that the interaction is DNA- and RNA-independent (Figure 2.36.).

2.3.4. Suv4-20h2 interacts with subunits of the cohesin complex

Subunits of the Cohesin complex appeared as interactors of Suv4-20h2 truncations in the GST pulldown assay. Cohesin has been implicated in several important cellular functions. One of the most prominent is its role in ensuring sister chromatid cohesion during cell division. In order to confirm the interaction a Suv4-20h2$^{HA\text{-}Flag}$ knock-in ES cell line was generated for Co-Immunoprecipitation experiments. These cells express a HA-3xFLAG tagged fusion protein from the endogenous Suv4-20h2 promoter. Precipitation of Flag-tagged Suv4-20h2 from these cells co-precipitated the Cohesin subunits Smc1 and Smc3, suggesting that a minor fraction of Cohesin, associated with heterochromatin binds Suv4-20h2 *in vivo* (Figure 2.37.).

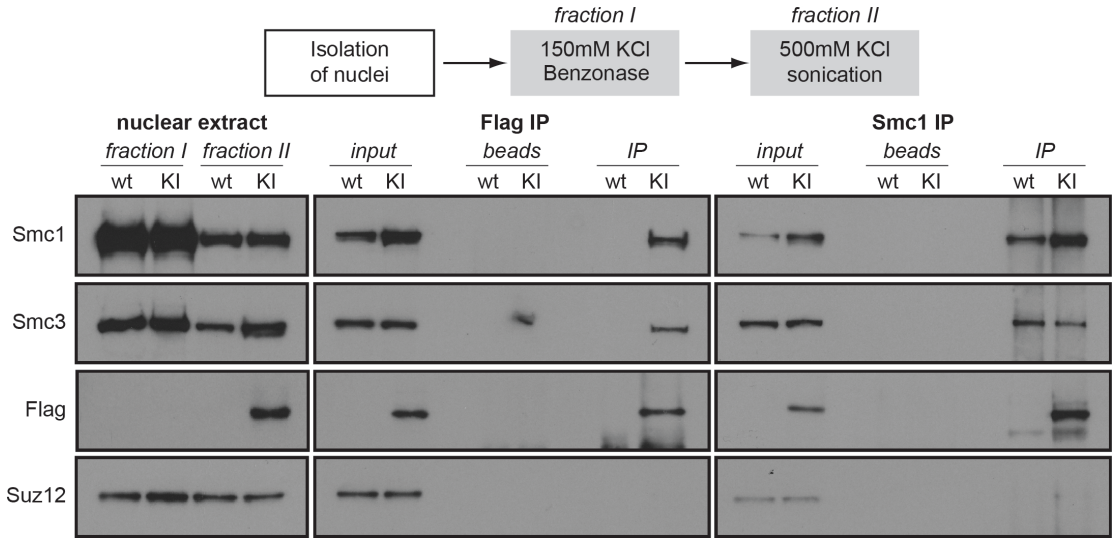

Figure 2.37. Suv4-20h2 and Cohesin interact *in vivo*. Fractionated nuclear extracts were prepared from wild type (wt) and Suv4-20h2$^{HA\text{-}FLAG}$ knock-in ES cells (KI). Suv4-20h2 and Smc1 were precipitated from fraction II extracts using FLAG and Smc1 antibodies, respectively. Bound proteins were visualized by western blotting using FLAG, Smc1, Smc3 and Suz12 antibodies

In the reverse experiment Cohesin subunit Smc1 was purified with a specific polyclonal antibody and could co-precipitate Suv4-20h2. To confirm the specificity of this assay a cohesin- independent chromatin protein (Suz12), which is known to associate with compacted chromatin was tested for its interaction with Suv4-20h2 and did not show any binding. In conclusion Suv4-20h2 associates with subunits of the Cohesin complex.

2.3.5. Suv4-20h2 mediates the compact heterochromatin structure

In addition to their enzymatic activity additional functions for the Suv4-20h proteins are not known. In (Souza et al. 2009) it has been shown that Suv4-20h2 is a rather immobile protein tightly associated with chromatin in HeLa cells. Furthermore earlier studies revealed (Schotta et al. 2004) that Suv4-20h2 is recruited to pericentric heterochromatin, as its C-terminus directly interacts with HP1 proteins. HP1 is present at heterochromatic regions and correlates with transcriptional silencing. It has been hypothesized that based on its ability to dimerize and to interact with several other chromatin proteins, HP1 proteins facilitate the formation of a higher order structure that is largely inaccessible for the transcription machinery. Surprisingly several independent studies could show that HP1 proteins are highly mobile proteins in FRAP analysis arguing against a structural function at heterochromatin (Schmiedeberg et al. 2004). So the question arises how can a mobile protein, which is not stably interacting with heterochromatin can induce such a compacted structure? There might be an additional factor involved in the structural role of HP1 proteins. As Suv4-20h2 inetracts with HP1 proteins and tightly associated with chromatin it might be a candidate. In order to address this hypothesis the HP1 interaction was further characterized *in vitro*. To map a minimal HP1 interaction domain several GST-tagged fragments of the Suv4-20h2 C-terminus were cloned and purified from bacteria. The already known targeting domain of the C-terminus M5 (aa349-441) and a fragment of the very C-terminus of

the protein M7 (aa 409-468) were purified with Glutathine sepharose. Additionally several GST-tagged sub-fragments were generated to subdivide the C-terminus into a 62aa long M12 fragment. Unfortunately the M12 fragment was not soluble from *E.coli* lysates therefore two subfragments were generated (M13, M14) (Figure 2.38.A). GST-tagged truncations and GST alone as a control were incubated with the three different isoforms of HP1 and bound to GST-beads. After several washes, bound proteins were analysed in western blot using specific antibodies against HP1 proteins. None of the HP1 isoforms was binding to the GST tag or fragment M7. The C-terminal M5 fragment precipitated all three HP1 isoforms.

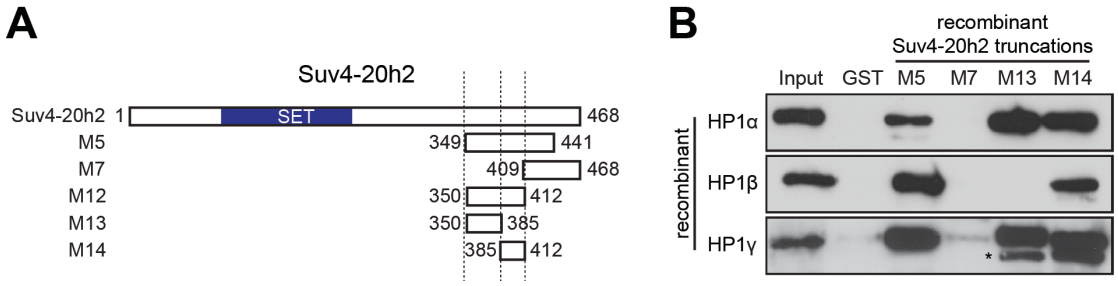

Figure 2.38. Suv4-20h2 contains several independent HP1 interaction motifs. A) Schematic of the Suv4-20h2 protein structure. The SET domain is located in the N terminus. The C-terminus harbors the heterochromatin targeting module M5, which can directly bind to HP1. Sub-fragments of this domain were generated as depicted here. **B)** GST-tagged protein truncations of Suv4-20h2 (M5, M7, M13 and M14) and recombinant GST were bound to glutathione sepharose and incubated with recombinant HP1a, HP1b, and HP1g. After extensive wash steps, bound proteins were separated on SDS-PAGE, and Western blots were probed with HP1 specific antibodies.

To test whether the targeting is mediated by interaction with HP1 proteins the short truncations were tested in *in vitro* binding assays. Direct binding of HP1a and HP1g to M13 and M14 was observed, whereas HP1b interacted exclusively with M14. Hence Suv4-20h2 displays several independent HP1 interaction sites within a small 62aa fragment of the C-terminus (Figure 2.38.B).

As Suv4-20h2 is tightly associated with heterochromatin it might indeed influence the structure of pericentric heterochromatin. To analyze this chromatin accessibility was examined using micrococcal nuclease (MNase) in wild type and Suv4-20h2 knockout cells. Initially, accessibility of chromatin from wild type, Suv4-20h2 KO and Suv4-20h DKO ES cell lines was monitored. Compared to wild type cells, Suv4-20h2-depleted cells show a chromatin structure, which is clearly more accessible to nucleases. DNA in the chromatin of cells lacking both Suv4-20h1 and Suv4-20h2 is even more exposed to MNase and shows therefore fast digestion. The genomic DNA originating from pericentric heterochromatin was visualized in Southern blot using a major satellite-specific probe (Figure 2.39).

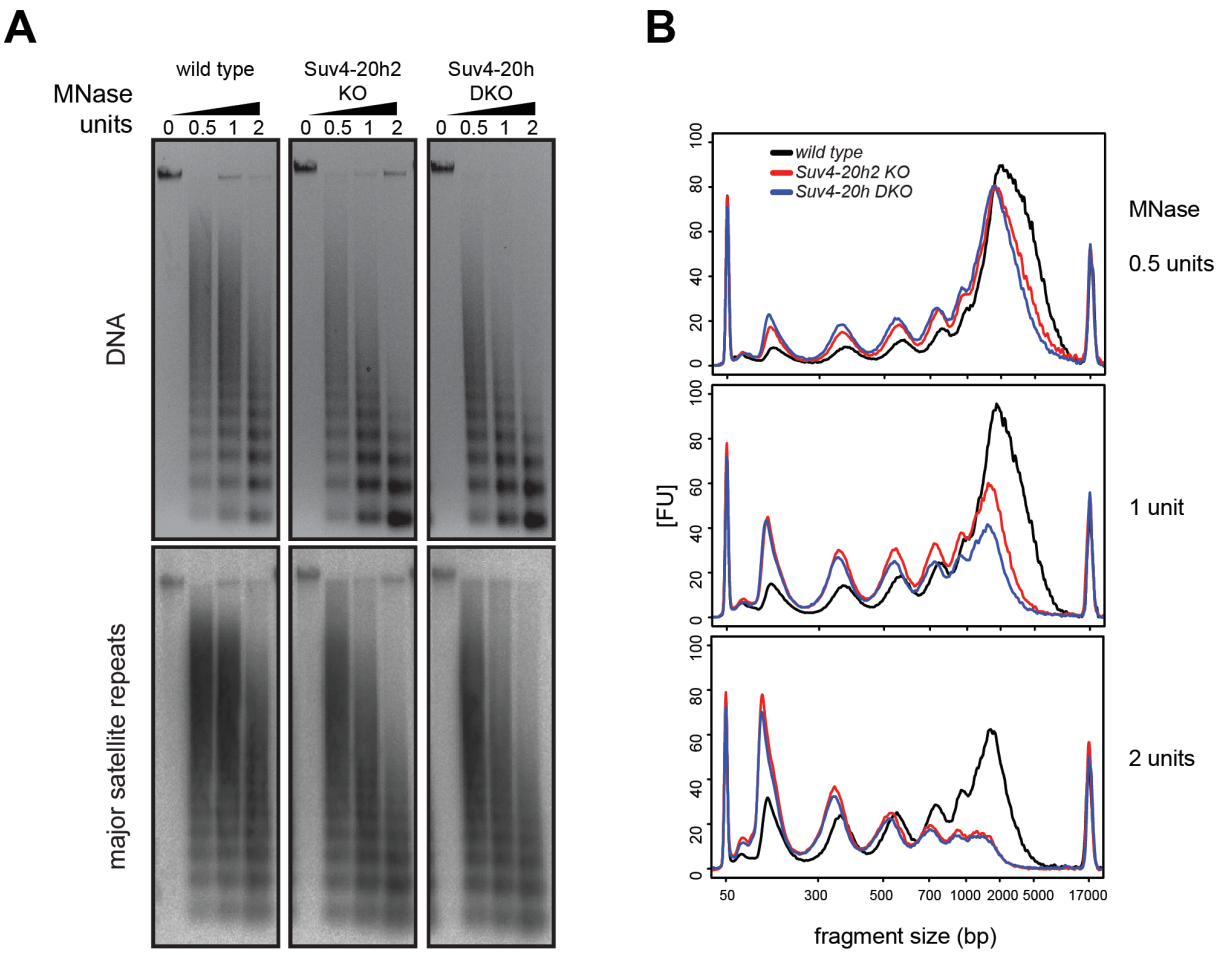

Figure 2.39. ES cells lacking Suv4-20h enzymes show higher MNase accessibility. A) Chromatin structure of wt, Suv4-20h2 KO and Suv4-20h DKO cells were analyzed in MNase accessibility assays. Chromatin was partially digested with different amounts of nuclease. Ladders of genomic DNA were separated on an agarose gel and EtBr stained (upper panel). Major satellite repeat DNA was monitored with specific probes in Southern blot (lower panel). **B)** DNA samples were analyzed on a Bioanalyzer, correlating concentration, size and repeat length in comparison with an internal standard.

Similar effects could be observed in mouse embryonic fibroblasts. Upon expression of Suv4-20h2 or M12 in Suv4-20h DKO MNase accessibility was comparable to wild type cells, proving that this re-expression clearly rescues the chromatin compaction phenotype (Figure 2.40). Additionally DNA digestion patterns show an increase in the nucleosomal repeat length in Suv4-20 DKO cells compared to wild type cells. Upon re-expression of Suv4-20h2 or M12 fragment nucleosomal repeat length is again comparable to patterns achieved upon MNase digestion of chromatin from wild type fibroblast cells. These data suggest that Suv4-20h2 plays a role in regulating chromatin structure, as it ensures chromatin compaction.

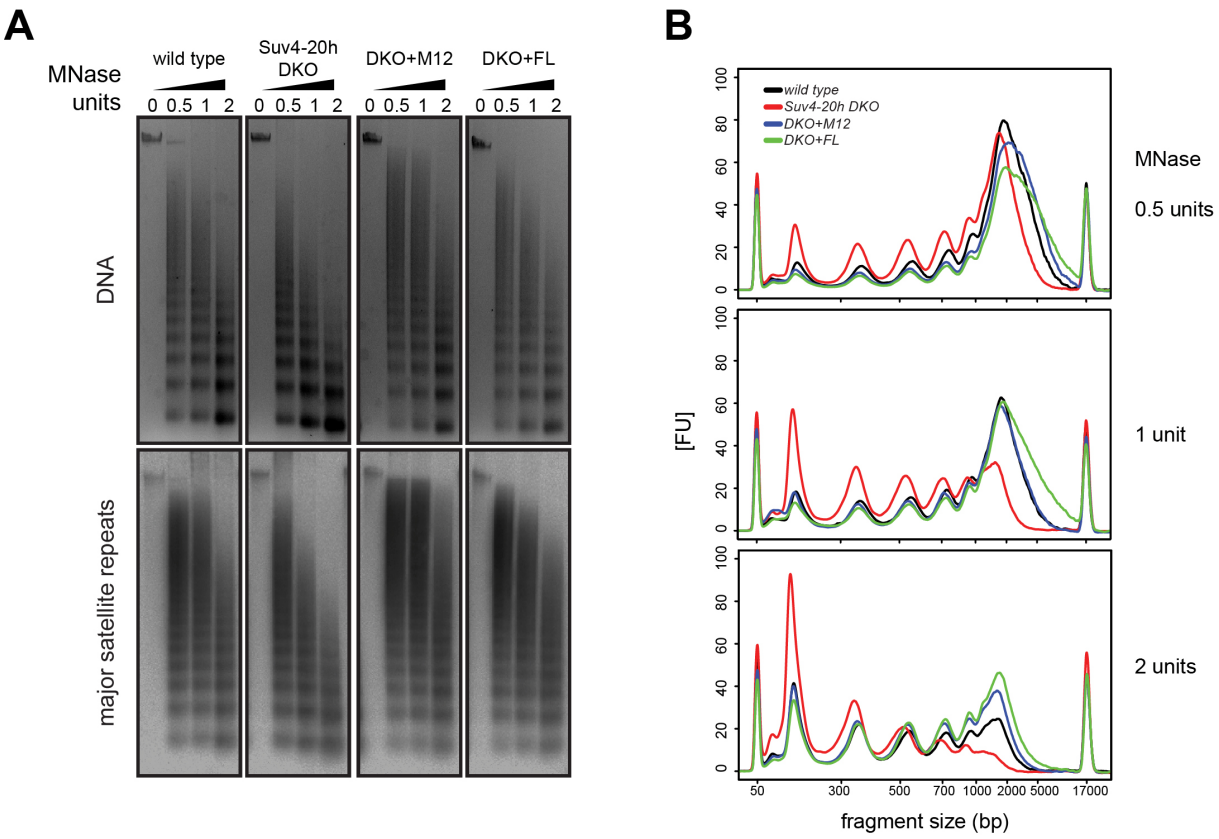

Figure 2.40. MEF cells lacking Suv4-20h enzymes show higher MNase accessibility. A) Chromatin structure of wt, Suv4-20h DKO cells and Suv4-20h DKO cells re-expressing either M12 or the full length Suv4-20h2 protein were analyzed in MNase accessibility assay. Chromatin was partially digested with different amounts of the nuclease. Genomic DNA was separated on an agarose gel and EtBr stained (upper panel). Major satellite repeat DNA was monitored with specific probes in Southern blot (lower panel). **B)** DNA samples were analyzed on a Bioanalyzer.

3. DISCUSSION

3.1. The proteome of the histone H3 lysine 9 trimethylation mark in embryonic stem cells

Pericentric heterochromatin has been associated with several important functions in the cell. It is involved in the regulation of gene repression and mediates chromosome segregation. But what specializes heterochromatin for its various functions? Pericentric heterochromatin is characterized by a unique histone modification pattern comprising the methylation marks H3K9me3 and H4K20me3. This chromatin modification state might generate affinities to recruit effector proteins, which provide specific activities and functions. One example is the well-characterized interaction of H3K9me3 and HP1 proteins (Bannister et al. 2001; Lachner et al. 2001). Recruitment of HP1 proteins mediates gene repression and chromatin compaction, but also additional functions might be mediated by this interaction (Singh 2010; Zeng et al. 2010). The identification of proteins with affinity towards the trimethylation of H3K9 helps to further understand the regulation of heterochromatin and to identify novel functions of repressive chromatin. As a screening system for novel proteins involved in the regulation of heterochromatin, a peptide- pulldown approach was chosen. This screen provided a list of candidate proteins with putative roles in heterochromatin. Well-characterized interactors for H3K9me3 HP1a, HP1b and HP1g were specifically precipitated with the trimethylated H3K9 peptide. Also several zink finger proteins like PogZ, Zfp828, Zfp462, Zfp280c were enriched with the trimethylated histone H3K9 peptide. All identified zink finger proteins belong to the C2H2 class of zink finger proteins. Cys2-His2 (C2H2) zinc finger domains were originally identified as DNA binding domains, but it has been shown that they can also bind RNA and mediate protein-protein interactions (Brayer and Segal 2008).

Interestingly the H3K9me3 interactome contains many proteins, which are known to interact with HP1 isoforms, like, for example, the transcriptional regulator Kap1 or the C2H2 zink finger proteins PogZ and Zfp828. The KRAB-associated protein 1 (Kap1, Trim28, Tif1b) was the most abundant hit in the H3K9me3 pulldown screen. Kap1 has been proposed as a scaffolding protein for transcriptional repression (Iyengar and Farnham 2011). The protein harbours several conserved domains: The N-terminal RBCC domain is necessary and sufficient for interaction with KRAB zink finger proteins, which can target Kap1 to genomic regions and mediates its oligomerization. In the central region the ‘HP1box’, containing the classical HP1 interaction motif PXVXL directly interacts with the chromoshadow domain of HP1 isoforms. This interaction seems to be crucial for the targeting of Kap1 to pericentric heterochromatin. Additionally a PHD finger and a bromodomain are located in the C-terminus of Kap1 and are required for the interaction of other effector proteins like the H3K9-specific methyltransferase Setdb1 (Schultz et al. 2002) or the NuRD complex. Kap1 is target for several posttranslational modifications, which regulate its various functions. Especially the phosphorylation of Kap1 at Serin 824 has been characterized in the context of a phospho-sumoylation switch (Li et al. 2007).

The PHD domain functions as an intramolecular E3 ligase for sumoylation of the adjacent bromodomain (Ivanov et al. 2007). ATM-stimulated Kap1 Ser824 phosphorylation leads to repression of Kap1 sumoylation, resulting in derepression of specific genes involved in cell cycle control and apoptosis. Kap1 is ubiquitously expressed throughout development (Cammas et al. 2000). Mice lacking Kap1 die as embryos (E5.5) suggesting that Kap1 is essential for early mouse development. Together, these data suggest that Kap1 is a multifunctional transcriptional regulator of target genes and comprises important functions at heterochromatin (Iyengar and Farnham 2011). Although Kap1 is well characterized in many functional aspects it is currently unclear whether the interaction of Kap1 with chromatin is a direct interaction or mediated by HP1 proteins.

The pogo transposable element-derived protein with zinc finger domain (PogZ) was one of the first proteins, which have been described to bind to HP1a not through the classical HP1 interaction motif (PXVXL), but through a zinc-finger-like motif (Nozawa et al. 2010). The interaction region of PogZ required for binding to the CSD in HP1a and was mapped to amino acid 791- 850 and called HPZ (HP1-binding zinc-finger-like). The HPZ motif is rich in cysteine (Cys) and histidine (His) residues. Interaction with HP1 proteins requires the HPZ motif, as mutation of all Cys and His residues in the HPZ region completely abolish the interaction with all the HP1 isoforms. Featuring this motif PogZ competes with proteins containing the PXVXL motif for the binding to HP1 and exhibits a regulatory mechanism to displace HP1 specifically. The binding of PogZ to HP1 forces dissociation of HP1 form mitotic chromosome arms, a process, which is required for normal mitotic progression. Additionally PogZ is required for the regulation of AuroraB function in M phase and thus serves as a major regulator of mitosis (Nozawa et al. 2010).

Zfp828 (CAMP; chromosomealignment-maintaining phosphoprotein) is a zink finger protein containing characteristic repeat motifs. The repeat motifs were named according to the consensus sequence identified: the SPE motif (consensus: PxxSPExxK), the WK motif (SPxxWKxxP), and the FPE motif (FPExxK). For the WK motif an interaction with MAD2L2 was shown in far-western analysis. MAD2L2 is involved in mitotic control mechanism as an inhibitor of the anaphase-promoting complex/cyclosome (APC/C) (Chen and Fang 2001; Pfleger et al. 2001). Zfp828 localizes to chromatin and the mitotic spindle in a cell cycle dependent manner and is target for CDK-mediated phosphorylation at multiple sites during mitosis. Upon knockdown of Zfp828, HeLa cells displayed severe mitotic defects (Itoh et al. 2011). These knockdown cells did not show any alterations in HP1 localization, however Zfp828 has been identified in interaction studies to associate with HP1 proteins (Vermeulen et al. 2010). These data provide evidence for a function of zink finger proteins as DNA binding factors, which might be responsible for recruitment of HP1 to specific genomic loci. A function of Zfp828 at heterochromatin has not been investigated yet.

Another protein enriched with the H3K9me3 peptide was Dnttip2 (deoxynucleotidyltransferase terminal-interacting protein 2, TdIF2). Dnttip2 was first identified in a yeast two-hybid screen as

interactor of the terminal deoxynucleotidyltransferase (TdT) (Fujita et al. 2003). TdT is a DNA polymerase required for the synthesis of extra nucleotides during V(D)J recombination (Komori et al. 1996). Dnttip2 binds core histones and binds to TdT through a C-terminal region. The formation of this complex inhibits TdT activity *in vitro*. Dnttip2 has been proposed to function as a chromatin remodelling protein, as it comprises binding affinity for DNA and releases histone H2A/H2B dimers from chromatin in a PCNA-dependent manner (Fujita et al. 2003). Dnttip2 shows nuclear and nucelolar localization. ChIP experiments for Dnttip2 in HEK cells expressing FLAG-tagged Dnttip2 revealed that it is associated with the promoter of human ribosomal RNA genes (Koiwai et al. 2011). Koiwai and colleagues furthermore identified another interaction partner, the acetyltransferase Tat interactive protein 60 (Tip60), using Dnttip2 as bait in Y2H screen. The direct interaction of Dnttip2 with Tip60 was suggested to be important for regulating HAT activity at ribosomal promoters. IF experiments revealed that it localizes to heterochromatin in a H3K9me3 dependent manner, however it is unclear what mediates the recruitment to pericentric heterochromatin and what might be the function.

Surprisingly M18bp1 (Knl2, C79407), a centromere-associated protein was precipitated specifically with the H3K9me3 peptide. M18bp1 is present at centromeres and is involved in priming of centromeric chromatin for CenpA integration (Hayashi et al. 2004; Fujita et al. 2007). M18bp1 localizes to centromeric and heterochromtic regions in the nucleus. As no function for heterochromatin-specific histone modifications like H3K9me3 at centromeric chromatin has been described in higher organisms, it was rather surprising to find M18bp1 in the H3K9me3 screen.

In summary interaction partners of the repressive histone methylation mark H3K9me3 were identified. Upon those are already known effector proteins at heterochromatin, indicating that the method is a powerful tool to identify proteins with important functions at repressive chromatin. Further evidence for the identification of H3K9me3-associated proteins was given by the analysis of the nuclear localization of some candidate proteins. Database search revealed also proteins, which are unnamed or not described yet. Furthermore many proteins have been identified which are not functionally characterized, or not known to play a role at heterochromatin. Future projects will deal with the characterization of those candidate proteins. As a basis for further studies various tools were developed to characterize the functions of these proteins. Immunofluorescence in different cell types can be used for initial localization studies. The generation of knock-in ES cells is feasible to follow the EGFP- tagged proteins at endogenous levels in mouse embryonic stem cells and provides the opportunity to perform co-immunoprecipitation experiments with affinity tags to examine the interaction network of candidate proteins. From the extensive data set, the characterization of M18bp1 in mouse was the central focus of this study.

3.2. The recruitment of M18bp1 to centromeres is mediated by CenpC

M18bp1 has been shown to be important in several aspects of centromere formation and has been originally characterized as a centromere priming factor (Fujita et al. 2007). Analysing the nuclear distribution of this protein in mouse embryonic stem cells clearly showed that M18bp1 is present at both centromeric and pericentric heterochromatin. Expression of M18bp1 in wild type fibroblast cells showed clear co-localization with the centromere-specifc histone variant CenpA. As we have shown in (Dambacher et al. 2012) the localization of M18bp1 to centromeres is highly cell-cycle-regulated. Confocal microscopy data in mouse embryonic stem cells clearly showed that M18bp1 is present at centromeres in a distinct window of the cell cycle. Co-localization with CenpA can be monitored from anaphase through to late G1phase the time frame when the loading of newly synthesized CenpA takes place (Dunleavy et al. 2009). The cell-cycle-dependent localization of M18bp1 is consistent with previous studies in human cells (Lagana et al. 2010) underlining the evolutionary conservation of the protein. Although M18bp1 is present at centromeres, it was still unclear how it is recruited to centromere regions. The current study proposes a mechanism that is responsible for the recruitment of M18bp1 to centromeric regions. A central region of M18bp1, which contains a conserved SANT domain directly binds to the C-terminus of CenpC *in vivo* and *in vitro*. Similar results have been obtained in *X. laevis* (Moree et al. 2011), suggesting that the direct interaction of M18bp1 with CenpC is conserved in higher organisms. The region identified to be responsible for the CenpC interaction is a rather big fragment M4 (359aa), containing the SANT domain. Testing a very short fragment (M5; 65aa) comprising solely the SANT domain did not show any affinity to CenpC, suggesting that either the interaction is mediated via a distinct structural feature, which cannot form upon truncating the protein. Another explanation would be that other protein regions are necessary to mediate the stable interaction with CenpC. Although the SANT domain is a conserved motif in several proteins (Boyer et al. 2004), for example chromatin remodeling factors, very little is known about concrete functions of these domain. Further experiments are required to examine whether the SANT domain is involved in the regulation of the M18bp1-CenpC interaction and to identify a specific function for the SANT domain. The introduction of point mutations in conserved motifs in the SANT domain of M18bp1 would allow the mapping of the minimal interaction domain, which still comprises all features crucial for the binding of M18bp1 to CenpC. Upon mapping of the interacting regions co-crystallization would give further information about the nature of the interaction. Additional mechanisms might exist that either regulate M18bp1 or CenpC recruitment to centromeric regions or that regulate the interaction of M18bp1 with CenpC. As CenpC belongs to the CCAN (Constitutive Centromere Associated Network) it localizes to centromeres throughout the cell cycle (Foltz et al. 2006; Perpelescu and Fukagawa 2011), while M18bp1 is only present from anaphase until G1 phase of the cell cycle. The regulation of CenpC might be ensured via posttranslational modifications. It has been shown that M18bp1, CenpA (Silva et al. 2012) and CenpC are indeed substrates for posttranslational modifications, e.g. phosphorylation and sumoylation (Chung et al. 2004; Nousiainen et al. 2006; Olsen

et al. 2006). (Silva et al. 2012) propose a Cdk-mediated phosphoswitch model: M18bp1 is phosphorylated by Cdk1/Cdk2 in G2, M and S phase of the cell cycle. This phosphorylation prohibits recruitment to centromeres and CenpA integration. When APC/C mediates the loss of Cdk activity in anaphase this leads to de-phosphorylation and subsequent localization of M18bp1 to minor satellite repeat regions. Also CenpA is dephosphorylated and loaded upon preparation of the chromatin mediated by M18bp1. Interestingly, upon transient expression of CenpC (Dambacher et al. 2012), some cells show clear centromere localization of CenpC, which does not co-localize with M18bp1. This observation suggests the hypothesis that there might be additional regulatory mechanisms, which control CenpC or the M18bp1-CenpC interaction. M18bp1 is recruited to centromeres in a CenpC-dependent manner, suggesting a pathway for centomere assembly beginning with CenpA as hallmark for active centromeres recruiting CenpC. CenpC then recruits the CenpA loading factor M18bp1 to centromeric regions to ensure constant CenpA levels at centromeres. Further evidence for such a pathway is provided by knockdown studies of CenpC in mES cells (Dambacher et al. 2012). Upon knockdown of CenpC in these cells, reduced CenpA levels at centromeres were observed, accompanied by an impaired M18bp1 recruitment to centromeric regions.

3.3. M18bp1 is essential for early mouse development and spermatogenesis

In order to further elucidate the functions of M18bp1, knockout mice were analyzed. The straight knockout in ($M18bp1^{bGal/bGal}$) was prenatally lethal as no embryos were observed after E7.5. Furthermore the generation of ES cell lines from blastocyst stage E3.5 out of $M18bp1^{bGal/+}$ intercrosses failed. Microscopy of fixed blastocysts showed that already in very early stages, mutant blastocysts show developmental retardation. Blastocyst cells showed mitotic defetcs and reduced CenpA levels. Furthermore, blastocysts possessed apoptotic bodies, a DNA structure pointing towards cells entering apoptosis.

Recently (Kim et al. 2012) described the Mis18alpha knockout mouse. Mis18alpha mutant embryos survive until E5.5, although knockout blastocysts showed reduced CenpA levels and apoptotic cells. Surprisingly, CenpA mutant mice survive until E6.5 (Howman et al. 2000), suggesting that embryos might tolerate reduced levels of CenpA up to a certain developmental stage. M18bp1 knockout mice show a much earlier and more severe phenotype compared to the defects described for CenpA and Mis18alpha knockout embryos. CenpA is diluted during replication as the existing CenpA amount is distributed between the two daughter strands. Newly synthesized CenpA is integrated in G1 phase to re-establish the full CenpA level. Therefore a phenotype caused only by defective CenpA deposition would appear later, as CenpA level have to be diluted to a critical level, like in CenpA mutant mice. The much earlier phenotype in M18bp1 ko mice might therefore have different reasons. Further s are necessary to distinguish between cause and consequence leading to the severe blastocyst phenotype observed in M18bp1 mutant mice. Intercrosses of M18bp1 ko mice and p53-deficient mice could be phenotypically analyzed to investigate whether apoptosis is dependent on the p53 pathway. If p53-

dependent pathways are responsible for apoptosis the blastocyst phenotype should be partially be rescued in mice lacking p53.

For the analysis of the cellular phenotype, inducible M18bp1$^{fl/fl}$; Cre ERT2 primary mouse embryonic fibroblasts (pMEFs) were established. Upon 4-OHT-induced depletion of M18bp1, M18bp1 ko fibroblasts showed strongly impaired proliferation and loss of proliferation was observed after 4-5 days. Two phenotypes can be observed upon induction of the knockout in primary mouse fibroblasts: a) very early mitotic defects leading to apoptosis and b) cells which survive show 3-5 days upon Cre-induction severe micro- and polynucleation, altered nuclear chromatin organization and the loss of CenpA. The earliest defects are visible 12h after depletion. Cells showed mitotic abnormalities, like anaphase bridges, lagging chromosomes and not properly aligned metaphase plates, which point towards segregation defects. These phenotypes probably lead to apoptosis and cell death. The chromosomes seem to be fussy and improperly condensed. But there are also cells, which are not affected so severely. The reason for this is not known. Some cells might have lower Cre recombinase activity, resulting in a partial or delayed deletion of M18bp1. The residual M18bp1 might be sufficient for the survival of the cells. It could also be possible, as M18bp1 is highly cell cycle regulated, that cells might be able to tolerate the loss of M18bp1 in specifc cell cycle stages. Surviving cells show micro and polynucleation, suggesting that cell division and cytokinesis are affected. Furthermore the chromatin structure in the nucleus is severely altered, as chromocenters are not stochastically distributed throughout the nucleus and do not have a defined shape, suggesting that the loss of M18bp1 affects chromosome compaction and organization. A potential function of M18bp1 in chromatin organization has to be addressed in further experiments. The data clearly demonstrate that M18bp1 is absolutely essential to ensure proliferation of fibroblast cells as only a minor fraction of mutant M18bp1 cells, could pass through mitosis with minor defects. However cells show a loss of CenpA as a later phenotype after 3-5 days of deletion. As M18bp1 is involved in the deposition of newly synthesized CenpA onto chromatin this mechanism is blocked upon lack of M18bp1, therefore the existing CenpA amount is diluted with every cell cycle. It has been shown that also the reduction in CenpA levels can cause severe mitotic defects (Howman et al. 2000; Regnier et al. 2005). Probably in the first mitosis, without M18bp1, segregation defects occur that lead to apoptosis. But what are the reasons for such a dramatic phenotype and what are precise molecular functions of M18BP1 in the above-mentioned processes? Due to the lethality of the M18bp1 deletion, it is hard to distinguish between cause and consequence of the described defects. Rescue experiment might help to distinguish the phenotypes. Furthermore it might be interesting to analyze whether known centromere proteins still localize to centromeric regions in the absence of M18bp1.

Interestingly it has been described that mitotic defects appearing in HeLa cells upon knockdown of M18bp1 could be rescued by either TSA treatment of the cells or overexpression of p300 (Fujita et al. 2007). It would be interesting to test this in the context of the inducible M18bp1 knockdown to

elaborate which phenotype is caused upon changes in acetylation patterns at centromeric chromatin. Furthermore it would be interesting to analyze if histone modification marks like H3K4me2, H3K9me3, H4K20m3 and H3S10ph are altered in M18bp1 ko fibroblasts. Life cell imaging could be used to distinguish the different phenotypes. Large-scale quantification of the different phenotypes in correlation with mitotic progression in wild type compared to M18bp1 mutant cells could be used to detect potential mitotic delay induced by the activation of specific mitotic checkpoint proteins. Additionally rescue cell lines re-expressing M18bp1 under the endogenous promoter, can be used to determine the different M18bp1-specific phenotypes. To be able to distinguish the defects caused by the loss of CenpA from CenpA- independent defects, M18bp1 depletion could be induced in cells arrested in G0 phase of the cell cycle. In non-dividing cells CenpA levels should be stable. Upon release from G0 arrest, Cenp-A independent mitotic functions of M18bp1 could be identified. Additionally, CenpA deposition defects in M18bp1 ko cells could be examined by expression of SNAP-tagged CenpA according to (Jansen et al. 2007; Lagana et al. 2010). The SNAP-tag is a covalent fluorescent labeling approach. Firstly the SNAP-tag allows pulse chase labelling to visualize all existing SNAP-tagged CenpA at the time of labelling and get information about CenpA maintenance. Secondly the signal of the SNAP-tagged CenpA can be quenched to allow monitoring of *de novo* synthesed SNAP-tagged CenpA, giving information about CenpA loading. Comparing wild type and M18bp1 knockout cells expressing SNAP-tagged CenpA can be used to detect M18bp1-dependent changes in CenpA levels during the cell cycle.

As M18bp1 knockout mice die very early in development, a conditional knockout system in which recombination occurs in adult tissues and independent of development was analysed. M18bp1$^{fl/fl}$; TNAP Cre mice were generated, deleting M18bp1 under a promoter specific for germ cells. The IHC analysis of M18bp1 mutant testis revealed two types of tubles: Some tubles looked normal and contained all different cell types important for proper spermatogenesis, but most tubles contained only Sertoli cells and showed complete abolishment of spermatogenesis, suggesting a role of M18bp1 in spermatogenesis. Sertoli cells are not germ cells and therefore no deletion should occur in these cells.

M18bp1 is an essential gene for mouse development. Expression data from mouse tissues reveal that the protein is highly abundant in embryonic stem cells, neuronal stem cells and also hematopoietic stem cells, as well as testis, suggesting important functions of M18bp1 in cell types with a high proliferation rate.

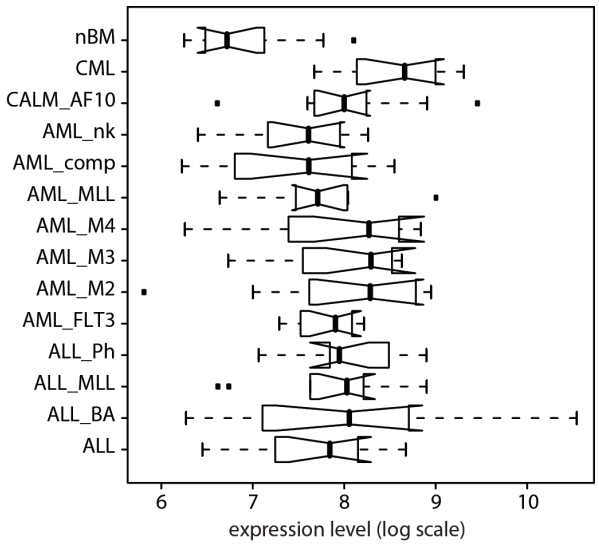

Figure 3.1. Expression levels of human M18BP1 in cancer. Affymetrix expression profiling of M18BP1 in normal bone marrow (nBM) and different hematopoietic malignancies (data kindly provided from S Bohlander).

M18bp1 plays essential roles for cell division and proliferation. According to this it is interesting that M18bp1 is overexpressed in various hematopoietic tumors (Figure 3.1.). These data suggest that tumor cells that need to ensure proliferation require high levels of M18bp1. Cancer cells have often up-regulated other mitotic genes, e.g. MAD1L1, MAD2L1, MAD2L2, BUB1, BUB1B, BUB3, CDC20, and TTK (Yuan et al. 2006). Mad1 mRNA is up-regulated in breast carcinomas (Yuan et al. 2006), small-cell lung cancer cell lines (Coe et al. 2006) and mantle-cell lymphoma cell lines (de Leeuw et al. 2004) and its up-regulation is a marker of poor prognosis. Mad1 is a component of the mitotic checkpoint that remains tightly bound to Mad2 throughout the cell cycle (Ryan et al. 2012). Another example is Hek1 (highly expressed in cancer 1). Hek1 is a subunit of the Ndc80 complex involved in microtubule binding by the kinetochore. Overexpression of Hec1 in an inducible mouse model results in mitotic checkpoint hyperactivation, aneuploidy and tumor formation *in vivo (Diaz-Rodriguez et al. 2008)*. Chromosome instability and deregulated proliferation of cells have been discussed in the context of cancer, as no oncogene has been shown to cause cancer on its own (Coschi and Dick 2012). A transgenic cell or mouse model could be generated to analyse the dose dependent tumorigenic potential of M18bp1. M18bp1 expression could be controlled in a TET-on or TET-off system according to (Gossen and Bujard 1992). The appearance of aneuploidy and tumorigenesis could be analysed in cells and in the *in vivo* mouse system.

3.4. Centromeric and pericentric interaction partners of M18bp1

Proteins, which interact with M18bp1 are likely to contribute to organizing centromeric as well as pericentric heterochromatin and might explain the severe phenotypes observed in M18bp1 knockout cells. A M18bp1^{FLAG} knock-in cell line was generated and used for FLAG immunoprecipitation experiments. Systematic analyses of candidate proteins from mass-spec data revealed two groups of proteins, which are particularly interesting in the context of M18bp1. On the one hand proteins

associated with heterochromatin have been identified and on the other hand, centromere proteins and mitotic regulators associated with M18bp1 have been detected. Importantly, proteins which were already known to associate with M18bp1 were also present in the mass-spec datasets. (Fujita et al. 2007) primarily described M18bp1 in a complex with Mis18alpha and Mis18beta. Based on knockdown experiments in HeLa cells, they concluded that the core members of the Mis18 complex are interdependent of each other. Upon absence of one component the remaining subunits are not able to localize to centromeres. Furthermore, they identified RbAp46/48 (Rbbp4, Rbbp7) to interact with hMis18 in a dynamic (nonstable) fashion. Mass-spec data derived from independent M18bp1 FLAG-IP experiments showed Mis18alpha, Mis18beta and CenpC consistently enriched with M18bp1. Also Rbbp4 was present in the list of proteins, which precipitate with M18bp1. Rbbp4 and its homologs can act as autonomous chaperones. Rbbp4 was found in the multi-chaperone complex CAF-1 as well as in chromatin-remodeling complexes, HAT or HDAC complexes (De Koning et al. 2007). Rbbp4 and Rbbp7 enhance the activities of these complexes. Histone H3/H4 dimers/tetramers can interact with Rbbp4 and Rbbp7 (Murzina et al. 2008). Conceivably, the partial unfolding of histone H4 when bound to Rbbp4 and Rbbp7 chaperones might facilitate the action of ATP-dependent chromatin-remodeling complexes. M18bp1 has been reported to 'prime' chromatin for CenpA deposition, which implicates the recruitment of different chromatin modulating activities to centromeric regions, like HDAC, HAT, chromatin remodelers. In this context Rbbp4 and 7 might be interesting candidates mediating chromatin reorganization functions. The reorganization of the chromatin structure at centromeres is probably required to allow HJURP- mediated deposition of CenpA. Furthermore another protein was found in the immunoprecipitation experiment, which has been previously reported to associate with M18bp1, the small GTPase activating protein MgcRacGap (Lagana et al. 2010).

The severe mitotic phenotypes upon depletion of M18bp1 suggest a function in mitotic regulation. Mitosis is crucial for the survival of organisms, as reproduction and cell division require proper replication and segregation of the genome (Lara-Gonzalez et al. 2012). Mitotic defects can alter genomic inheritance and lead to cells with altered karyotypes. Therefore cells developed several layers of control mechanisms ensuring that every daughter cell inherits one complement of the genetic information after cell division. Different mitotic checkpoints like the spindle assembly checkpoint (SAC), the chromosomal passenger complex (CPC) and the anaphase promoting complex (APC/C) monitor crucial steps of cell division. Interestingly we found components of these machineries associated with M18bp1: the inner centromere protein Incenp, the kinase AuroraB and Borealin (also known as Dasra) are components of the chromosomal passenger complex (CPC). Survivin is also present in the CPC (Carmena et al. 2012). The complex is highly regulated by different phosphorylation events, which also define its localization during cell cycle. Various functions have been reported for the CPC ranging from correcting chromosome-microtubule attachment errors and consecutive activation of the spindle assembly checkpoint (SAC), to regulation of chromosome condensation and cytokinesis. Interestingly depletion of CPC components in mice causes severe mitotic defects, which are comparable to the phenotypes in M18bp1 ko cells. Incenp mouse knockout

embryos die at a very early stage in development around E3.5. The analysis of E3.5 embryos shows compared to control embryos few cells, which were large and contained macronuclei with large chromosome complements. Addionally, cells show micronuclei formation, internuclear bridges and abnormal spindles (Cutts et al. 1999; Uren et al. 2000). AuroraB knockout cells show severe mitotic defects as prometaphases displayed several misaligned chromosomes and abnormal spindles (Fernandez-Miranda et al. 2010). The siRNA- mediated knockdown of Borealin in HeLa cells shows defective spindle attachment with multiple spindle poles leading to lagging chromosomes in anaphase and failures in cytokinesis (Gassmann et al. 2004). As members of the CPC were identified in the M18bp1 IP approach and additionally, phenotypes described from CPC mutant cells are comparable to M18bp1 ko cells, it would be interesting to test for a direct interaction of M18bp1 and CPC subunits. Misregulation of the CPC in M18bp1 mutant cells might explain the early phenotype.

Furthermore the lack of M18bp1 causes defects in chromosome condensation as knockout MEFs show de-condensed chromosomes during anaphase. Interestingly, Condensin-depleted cells show a similar phenotype (Vagnarelli et al. 2006). Upon conditional knockout of SMC2 in DT40 cells, chromosomes lose their compact structure and show severe segregation defects and chromosome bridges in anaphase. In this study, the chromosome architecture in anaphase could be rescued either by exogenous expression of EGFP-tagged cyclin B3 or a PP1 binding mutant of Repo-Man^{RAXA}. Repo-Man recruits a pool of PP1γ to chromatid arms at anaphase onset. Repo-Man^{RAXA} comprises a dominant negative mutant that localises to anaphase chromosomes and can block recruitment of PP1. They termed this activity critical for mitotic chromosome structure that is inactivated by Repo-Man–PP1 during anaphase ‘regulator of chromosome architecture’ (RCA). The similar phenotype of condensing-depleted cells and M18bp1 knockout cells suggest the hypothesis that misregulation in condensin causes chromosome decondensation in M18bp1 mutant cells. Additional evidence is provided by the mass-spec dataset derived from M18bp1 FLAG-IP as condensin subunits were found to be associated with M18bp1. Further experiments are necessary to characterize this association and to determine whether M18bp1 directly interacts with the condensin complex.

Active centromeres display a characteristic pattern of post-translatonal histone modification marks (Sullivan and Karpen 2004; Lam et al. 2006; Ribeiro et al. 2010; Bergmann et al. 2011). Several independent studies indicate that the local chromatin state is crucial for the maintenance of a functional kinetochore structure (Nakano et al. 2003; Nakashima et al. 2005; Nakano et al. 2008; Cardinale et al. 2009; Bergmann et al. 2011). The epigenetic control of centromeric regions has been investigated in an artificial system, human artificial chromosomes (HACs). These data suggest that different histone modification activities are recruited to centromeric regions. Not much is known about histone-modifying enzymes, which act at centromeric regions. However, ChIP experiments on minor satellite repeat regions showed clear enrichment for H3K9me3 at centromeric heterochromatin (Martens et al. 2005). Interestingly, several proteins, known from the sequential pathway involved in

the establishment of pericentric heterochromatin are enriched with the M18bp1 protein. Suv39h1 and Suv39h2, HP1a, b, g as well as Dnmts have been identified, suggesting that effector proteins at heterochromatin might display functions at centromeric chromatin. Another interesting candidate protein in this context might be CenpV. CenpV was especially interesting as overexpression of CenpV causes hypercondensation of pericentromeric heterochromatin. The phenotypes described by Tadeu *et. al.* upon knockdown of CenpV in HeLa cells are similar to the M18bp1 knockout phenotype: misalignment of metaphase chromosomes, lagging chromosomes in anaphase, cytokinesis defects and rapid cell death. Interestingly they describe the 'mislocalization and destabilization of the chromosomal passenger complex (CPC) and alterations in the distribution of H3K9me3 in interphase nucleoplasm' (Tadeu et al. 2008; Honda et al. 2009) providing further evidence for connected regulatory pathways in centromeric and pericentric heterochromatin.

3.5. M18bp1 is recruited to pericentric heterochromatin via direct interaction with HP1

Originally we got interested in M18bp1 from data of a peptide pulldown from ES cells, as M18bp1 was enriched with the repressive histone modification H3K9me3. Localization studies in mouse fibroblast cells revealed that M18bp1 localizes to heterochromatic foci. This localization was clearly Suv39h- or H3K9me3-dependent. The central region of M18bp1 (M4) was mapped to be sufficient for targeting the protein to pericentric heterochromatin through direct interaction with HP1 isoforms. Interestingly the overexpression of M18bp1 in fibroblasts seems to be toxic for the cells, as cells expressing high levels of M18bp1 show highly condensed chromatin and apoptosis. Cells with lower expression levels of M18bp1 show a compacted chromatin structure with less chromocenters. The cells expressing M18bp1 show less chromocenters, which are more compacted compared to non-transfected cells.

In order to understand the potential function of M18bp1 at major satellite repeats we screened the data from immunoprecipitation experiments performed with the FLAG-tagged M18bp1 from knock-in ES cells. These data contain several proteins with characterized functions at pericentric heterochromatin (Suv39h1, Suv39h and the three HP1 isoforms). Remarkably all three HP1 isoforms precipitate with M18bp1. The interaction of M18bp1 with HP1 proteins was characterized in direct binding assays. The region of M18bp1 interacting with HP1 was mapped to a central fragment, which we originally found to mediate the interaction with CenpC. The shortest M18bp1 fragment interacting with HP1 was M4 with more than 300aa. HP1 proteins are highly conserved heterochromatin-associated proteins. Each of the three isoforms possesses conserved domains: The chromodomain (CD) mediates interaction with heterochromatin, while the chromoshadow domain (CSD) mediates dimerization of HP1 and recruitment of a variety of other nuclear chromatin-modifying proteins. Many of these HP1 binding partners contain a consensus PXVXL motif (Smothers and Henikoff 2000; Thiru et al. 2004). M18bp1 sequence was analysed to identify a HP1 interaction motif. There was no classical consensus sequence- but one motif, which might mediate the binding to HP1 (Figure 3.2.). Mutagenesis of this

potential interaction motif might help to further characterize the M18bp1 interaction with HP1 proteins. The chromo shadow domain of HP1 proteins has been reported to mediate protein-protein interactions. Therefore this domain should be tested in direct binding assays with recombinant M18bp1 truncations.

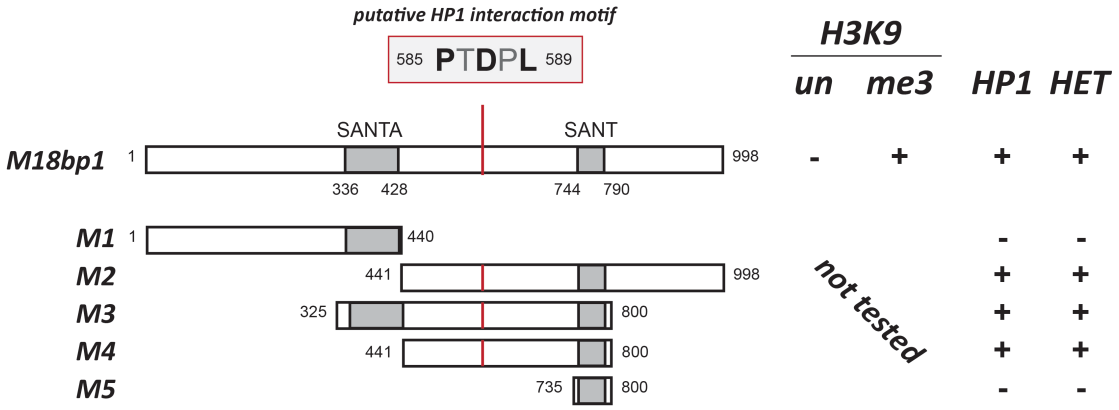

Figure 3.2. Summary of biochemical analyses of M18bp1 truncations. M18bp1 binds to histone H3 peptide trimethylated at lysine 9. A central region (M4) has been identified in binding assays to directly bind to HP1 isoforms and is also sufficient to target M18bp1 to heterochromatin in mouse fibroblasts. A putative HP1 interaction motif has been identified (aa585-589).

Alignment of the known mouse SANT domain proteins identified conserved amino acids within the SANT domain, which was used to introduce point mutations. The single point mutant M18bp1^{W746A} was able to localize to heterochromatin, the double mutant M18bp1^{WS746A} showed a diffuse nuclear localization pattern. The SANT domain has been crystalized from other proteins like the chromatin remodeler Chd1 (Ryan et al. 2011). Modeling the structure of the M18bp1 SANT domain based on these data revealed that the domain forms a cage-like structure with the conserved residues pointing towards the center of this cage. The structure itself might be important for mediating the binding of M18bp1 with other proteins. Further analyses are necessary to explain the functions of the SANT domain. This might also help to characterize the interaction of M18bp1 with HP1 proteins and its potential function at heterochromatic regions.

The binding of M18bp1 to HP1 proteins is sufficient to recruit M18bp1 to heterochromatin. But further analyses are necessary to investigate the function of M18bp1 at pericentric heterochromatin. There is some evidence from *S.cerevisiae* (Pidoux and Allshire 2005) and *D. melanogaster* (Olszak et al. 2011) that heterochromatin is crucial for proper centromere formation. If heterochromatin somehow affects centromeres in mammalian cells is currently unclear, although there is evidence that such a regulatory mechanism might exist. (Kim et al. 2012) observed epigenetic changes when Mis18alpha is missing. Mis18 alpha knockout fibroblasts show reduced CenpA levels and a decrease in H3K4me2. Furthermore, the loss of M18bp1 causes reduction in classical heterochromatin marks like decreased H3K9me3, increase in acetylation and a decrease in DNA methylation at minor satellite repeats. Also well-characterized proteins associated with pericentric heterochromatin like HP1a, HP1b and Suv39h1 are reduced at minor satellite repeat regions. These data suggest that the Mis18 complex

might be important for pericentric heterochromatin in mammalian cells. ChIP experiments are necessary to analyse changes in histone modification patterns and HP1 levels at minor and major satellite repeat regions in the absence of M18bp1.

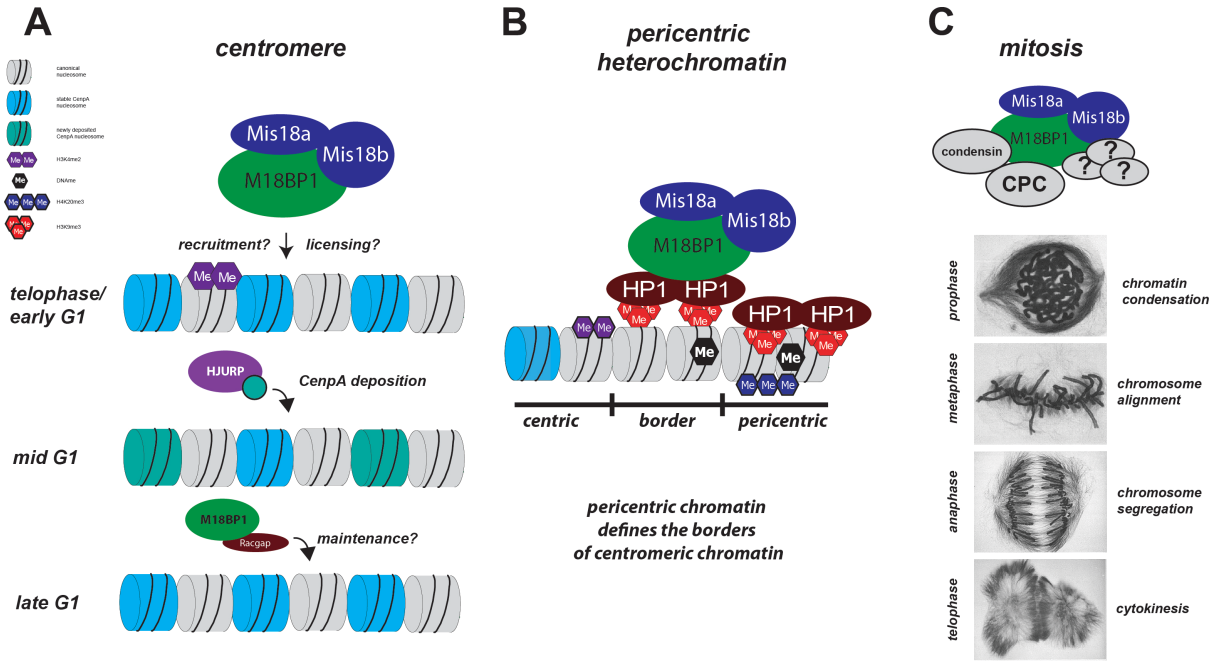

Figure 3.3. The various functions of M18bp1. M18bp1 possess various functions at centromeric and pericentric heterochromatin. **A)** M18bp1 is involved in several steps wihich are important for CenpA deposition. It is recruited to centromeric chromatin in early G1 phase in a complex with Mis18alpha and beta. M18bp1 somehow prepares the chromatin to allow CenpA deposition by the CenpA specific chaperone HJURP in mid G1 phase. In late G1 phase M18bp1 together with MgcRacGap is involved in the maintenance of newly integrated CenpA **B)** M18bp1 localizes to pericentric heterochromatin and binds to HP1 isoforms. It might be involved in defining the border of centromeric heterochromatin. **C)** Cells lacking M18bp1 show severe mitotic defects leading to cell death. M18bp1 is important for proper chromatin condensation during mitosis and might associate with the machinery of the mitotic checkpoint control like the chromosomal passenger complex (CPC) complex. Mitotic pictures adapted from http://alevelnotes.com/Eukaryotic-Cellular-Division-Process/147.

In summary M18bp1 might possess several functions on chromatin as depicted in (Figure 3.3.). A well-described function of M18bp1 is its contribution to centromere establishment through regulation of CenpA deposition and maintenance (Figure 3.3 A). Based on data achieved in this thesis M18bp1 might have additional functions at heterochromatin. The HP1-mediated recruitment to pericentric heterochromatin might define the border between pericentric and centromeric chromatin (Figure 3.3 A). Based on the analysis of the cellular phenotype in M18bp1 knockout fibroblasts, M18bp1 might interact with subunits of the chromosomal passenger complex, required for proper progression through mitosis (Figure 3.3.C).

3.6. Novel functions of Suv4-20h2

Three proteins have been identified to mediate the methylation of H4K20. PrSet7 has been characterized as the only HMTase responsible for the monomethylation of H4K20 (Nishioka et al. 2002). Suv4-20h1 and Suv4-20h2 are recruited to chromatin in an HP1-dependent manner to introduce the di-and trimethylation of histone H4 on lysine 20 (Schotta et al. 2008). While PrSet7 is highly cell-

cycle regulated and target for various posttranslational modifications, the regulation of Suv4-20h enzymes is rather unknown. The direct interaction of PrSet7 and Suv4-20h2 might indicate a synergistic regulation of both HMTases. In order to identify the functional context this interaction further experiments have to be done.

Heterochromatin is an important structure in the cell and involved in various functions. Defects in heterochromatin formation result in improper transcriptional regulation and cause chromosome instability. Heterochromatin is defined as rather transcriptionally inert and forms a very compacted structure. This compacted chromatin structure is hypothesized to be achieved by a network of multi-merized HP1 proteins. This hypothesis has been questioned as HP1 proteins appear to be highly mobile in FRAP analysis (Schmiedeberg et al. 2004). Additional proteins might therefore be required to mediate a compact chromatin structure. A known interactor of HP1 present at heterochromatin is Suv4-20h2 (Schotta et al. 2008). Interestingly Suv4-20h2 has been shown to be a stable component of heterochromatin in FRAP experiments (Souza et al. 2009).

The region in Suv4-20h2, harbouring the HP1 interaction motifs, was mapped to a 62aa fragment (M12) in the C-terminus. Each sub-fragment of M12 (M13 and M14) independently binds HP1 isoforms *in vitro*, suggesting that Suv4-20h2 comprises several independent HP1 interaction domains in the C-terminus of the protein. FRAP analyses in mouse embryonic fibroblasts expressing EGFP-tagged Suv4-20h2 and the M12, M13 and M14 truncations of Suv4-20h2 revealed that M12 is as stably bound to heterochromatin as the full length protein. M13 and M14 show higher mobility (unpublished data M.Hahn). The direct binding assays and the FRAP data provide evidence, that each of these single interactions might synergistically contribute to the stabilization of Suv4-20h2 through multiple HP1 proteins.

Additional evidence for a structural role of Suv4-20h2 at heterochromatin is provided by MNase accessibility assays. Chromatin from cells lacking both Suv4-20h1 and Suv4-20h2, or only Suv4-20h2 comprises a more open chromatin structure. Importantly, the re-expression of full-length Suv4-20h2, or the M12 fragment, is able to re-establish a compacted chromatin structure, comparable to chromatin from wild type cell. MNase digestion patterns show a shift in the nucleosomal repeat length upon loss of Suv4-20h enzymes. Changes in nucleosome repeat length might implicate changes in nucleosome linker length caused by reduced linker histone H1 levels. If this effect is mediated by Suv4-20h2 and specific for pericentric heterochromatin has to be further investigated. ChIP experiments quantifying H1 levels at major satellite repeat and control regions in wild type and Suv4-20h2 KO cells might provide further information. Long linker length correlates with a more open chromatin structure, whereas short linker sequences are present in compacted chromatin (Grigoryev 2012). The loss of H1 leads to global shortening of the spacing between nucleosomes in thymus nuclei from wild type and H1-triple-null mice (Fan et al. 2003). Upon MNase digest, chromatin from the H1-deficient mutant nuclei migrates faster than that from wild-type nuclei, which is comparable to the effect observed in

Suv4-20h mutant cells. Together, these data imply that Suv4-20h2 is a central component of heterochromatin regulating chromatin accessibility. As a scaffolding protein it binds multiple HP1 proteins, bridging H3K9me3- rich heterochromatin domains, which then might lead to the stable inaccessible structure of heterochromatin. Additionally, Suv4-20h2 might regulate additional proteins like linker histone H1, which facilitate the structural function of Suv4-20h2 at heterochromatin.

Cohesin is present at pericentric heterochromatin but it is not known how the recruitment to heterochromatin is mediated. In fission yeast it has been shown that Cohesin is recruited to heterochromatic regions by Swi6/HP1 proteins (Nonaka et al. 2002). In mammalian cells, Cohesin does not interact with HP1 proteins (Koch et al. 2008). Therefore it is currently not known which proteins are involved in recruitment and maintenance of Cohesin at pericentric heterochromatin. In GST pull- down experiments using a C-terminal GST-tagged Suv4-20h2 fragment, cohesin subunits (Smc1, Smc3) were precipitated. Co-immunoprecipitation experiments using either FLAG- tagged Suv4-20h2 or using Smc1 antibody provided additional evidence that Suv4-20h2 is associated with the Cohesin complex. Further indication that Suv4-20h2 might be involved in the recruitment of Cohesin to pericentric heterochromatin was provided by ChIP experiments. Comparing levels of cohesin subunits (Smc1 and Rad21) in wild type and Suv4-20h2 KO mouse embryonic fibroblasts, cohesin was selectively reduced at major satellite repeat regions in Suv4-20h2-deficient cells (unpublished data S. Dulev).

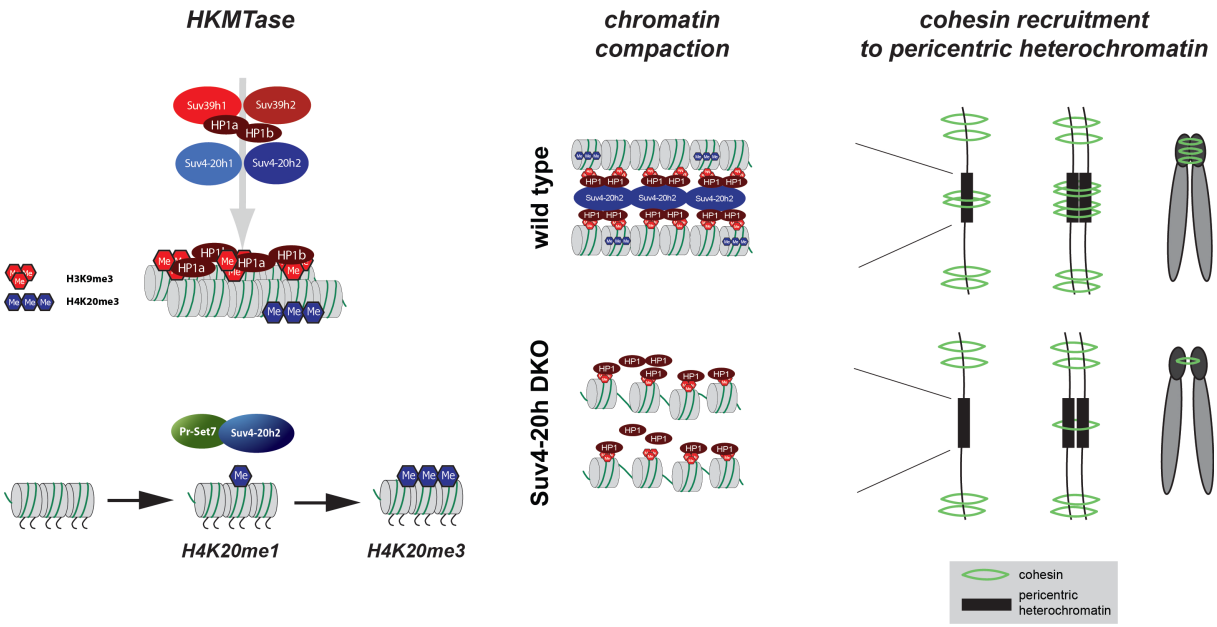

Figure 3.4. The functions of Suv4-20h2. A) Suv4-20h2 is part of the core protein network required for establishment of pericentric heterochromatin. Suv4-20h2 directly interacts with PrSet7 and converts the monomethylation of H4K20 into trimethylation. **B)** Suv4-20h2 is an important constituent of pericentric heterochromatin. It provides several HP1 binding sites to tether these proteins to heterochromatin and therefore to ensure a compact chromatin structure. **C)** Suv4-20h2 is required for the recruitment of cohesin to pericentric heterochromatin.

In summary several novel functions of Suv4-20h2 can be proposed based on the work of this thesis. Suv4-20h2 directly interacts with PrSet7, the enzyme responsible for the monomethylation at H4K20. It preferentially converts nucleosomes monomethylated at H4K20 into trimethylated nucleosomes, suggesting that PrSet7 and Suv4-20h2 are acting in a synergistic manner to introduce H4K20me3 at pericentric heterochromatin (Figure 3.4.A). Suv4-20h2 is a stable constituent of pericentric heterochromatin and is required to tether HP1 proteins to heterochromatin ensuring the highly compacted chromatin structure at pericentric heterochromatin (Figure 3.4.B). Data provided in this thesis furthermore propose Suv4-20h2 as crucial for the recruitment of cohesin to pericentric heterochromatin (Figure 3.4.C).

4. MATERIAL AND METHODS

4.1 Cell biology methods

Cultivation of mammalian cell

HEK cells were cultivated in High Glucose DMEM with L-Glutamine complemented with sodium pyruvate, penicillin/streptomycin (PAA) and fetal calf serum (Sigma). MEF and ES cells were cultivated in High Glucose DMEM with L-Glutamine complemented with sodium pyruvate, fetal calf serum (Sigma), beta-mercaptoethanol, non-essential amino acids (PAA) and penicillin/streptomycin (PAA) in a 37°C incubator at 5% CO2. For ES cell culture medium was supplemented with leukemia inhibitory factor (LIF) and gelatinized tissue culture dishes were used.

Transfection

Cells were transfected on slides using Lipofectamine 2000 (Invitrogen) or TransIT-LT1 (Mirus) according to the manufacturers instructions. ES cells were seeded on matrigel (BD Biosciences) coated slides 24h before transfection.

Immunofluorescence and microscopy

Immunofluorescence analyses were performed as described (Lehnertz et al. 2003) using the antibodies depicted in Table 4.5.

A Leica TCS SP5 confocal laser scanning microscope with a HCX PL APO CS 63x/1.3 NA glycerol immersion objective and a Zeiss LSM510 confocal microscope were used to obtain the images. Sequential excitation at 405nm, 488 nm, 543 nm and 633nm was provided by diode, argon and helium-neon gas lasers, respectively. Emission detection ranges of the PMTs were adjusted to minimize crosstalk between the channels. Images were further analysed using ImageJ software.

For live cell imaging, cells were cultivated in optical chambers (Ibidi) using pMEF medium buffered with 20mM HEPES under low oxygen conditions at 37°C for 24 hours. Then 3nM Tamoxifen was added and cells were monitored for 12h.

Knockin- ES cell lines

The Suv4-20h2-EGFP targeting constructs were obtained using the recombineering cloning technique described previously (Liu et al. 2003). To generate Suv4-20h2HA-FLAG knock-in cells, the NotI-linearized targeting vector was electroporated into feeder-independent wild type ES cells. Cells were selected in 180 µg/ml G418 (PAA) and 2 µM Ganciclovir (Invivogen). Single colonies were picked and screened by nested PCR to obtain the final ES cell clone.

The M18bp1-FLAG targeting constructs were obtained using the recombineering cloning technique described previously (Liu et al. 2003). To generate retrieval and mini-targeting vectors, PCR fragments were amplified from the BAC clone RP23-396P24 (Children's Hospital Oakland Research Institute). For the retrieval plasmid, PCR fragments were cloned into the pL253 plasmid using NotI, HindIII and SpeI. A genomic region of 7 kb, spanning the last exons of M18bp1, was retrieved from the BAC clone using recombineering in EL350 bacteria. The mini-targeting plasmid was constructed by generating PCR fragments flanking the M18bp1 stop codon. These PCR fragments were cloned together with the floxed Neo cassette from pL452 (EcoRI-BamHI fragment) into pBluescript IISK+ using NotI, EcoRI, BamHI and SalI. In a subsequent cloning step, the EGFP tag was inserted with EcoRI. For the final targeting vector, the 7 kb region was mini-targeted by recombineering with the NotI-SalI fragment containing the EGFP and floxed Neo from the minitargeting plasmid. To generate M18bp1 knock-in cells, the NotI-linearized targeting vector was electroporated into feeder-independent wild type mouse ES cells. Cells were selected in 180 µg/ml G418 (PAA) and 2 µM Ganciclovir (Invivogen). Single colonies were picked and screened by nested PCR to obtain the final ES cell clone (K2A7).

4.2 Molecular biology methods

Cloning of candidate proteins

cDNAs were obtained by PCR on genomic DNA template purified from either mouse fibroblasts or embryonic stem cells. Primers were designed with gateway att- side overhangs. Cloning was performed using gateway cloning system (Invitrogen) following the manufacturers instructions. Primers used for cloning are listed in Table 4.3.

Site directed mutagenesis PCR to create point mutations

Primers containing the DNA sequence leading to point mutation in the amino acid sequence of the protein were designed. Mutagenesis primer are listed in Table 4.3. The mutagenesis PCR was done following the manufacturers instructions for Quick change site directed mutagenesis kit using Pfu Polymerase (Stratagene). The template was digested with the restriction enzyme DraI (NEB). Chemically competent E.coli (Stellar) were transformed with 5ul of the reaction using heat shock procedure and selected on agar plates containing the adequate antibiotics. DNA was purified and mutagenesis was verified by sequencing.

RT-qPCR for monitoring M18bp1 expression levels

RNA of cells was harvested using RNeasy (Qiagen). 1.25 µg RNA was used for cDNA synthesis using Superscript III Kit (Invitrogen) and random hexameric primers (NEB). QPCR reactions were carried out in technical triplicates using a Roche Light Cycler 480 with FAST SYBR® Master Mix (Applied Biosystems), and gene-specific primers. Ct-values were normalized to the geometric mean of

Actin and Gapdh for each individual cDNA and fold changes where calculated by the 2-ΔΔCt-method (Vandesompele et al. 2002). qPCR primer are listed in Table 4.4.

4.3 Biochemical Methods

Determination of protein concentration

The concentration of proteins was determined using Bradford assay (Bradford 1976; Compton and Jones 1985).

SDS page

Separation of proteins by SDS-PAGE was performed in the PerfectBlue Dual gel Twin system (Peqlab) using precast gel cassettes (Invitrogen). Resolving and stacking gels were poured according to the manufacture's instructions using 30% (v/v) polyacrylamide solution (Rotiphorese, 37.5:1 acrylamide/bisacrylamide) and resolving gel buffer (375 mM Tris/HCl pH 8.8) or stocking gel buffer (125 mM Tris/HCl pH 6.8) respectively. Prior to loading samples were mixed with Roti Load1 (Roth) and heat-denatured for 7 min at 95°C. Various molecular weight protein standards were purchased from Bio-Rad/Peqlab. Electrophoresis was performed at 40 - 80 mA at RT for varying time. SDS gels were either used for Coomassie staining, silver staining or western blotting.

Coomassie staining of protein gels

Proteins were visualized in SDS page by incubating in staining solution [0.1% Coomassie R250, 10% acetic acid, 25% methanol] for 15 min at room temperature. Destain [8% acidic acid, 25% methanol in water] was used to remove excessive staining solution.

Silver staining of protein gels

SDS page was fixed in fixation solution [10% acetic acid, 30% isopropanol] for at least 2h or over night at room temperature. The gel was washed 3x 20min in 30% ethanol followed by sensitizing using 0.01% $Na_2S_2O_3$ for 1min at room temperature and washed 3x 30sec with water. Staining solution [0.1% $AgNO_3$ in H_2O] was applied for 1h at room temperature shaking. The gel was again washed 3x 30sec with water and incubated with the developer solution [3% NaCO3, 0.05% formaldehyde, 0.02% $Na_2S_2O_3$ in H_2O]. Reaction was stopped by adding 5% glycine solution. Rinsed in water and stored in water at 4°C.

Western blot

Proteins separated by SDS-PAGE were transferred to to a PVDF membrane (Roth). Transfer was achieved with a wet blot system (Criterion Blotter, Bio-Rad). Before the transfer, the polyacrylamide gel and the PVDF membrane was activated in MeOH and rinsed in blotting buffer [25 mM Tris, 192 mM glycine, 10% methanol]. The transfer was performed at 400mA for 1h at 4°C. The membranes were incubated in Blocking Buffer [1 x PBS, 3% BSA] for 1 h at RT in order to saturate free binding

sites on the membrane and hence minimize the non-specific background. After blocking the membranes were incubated either for 2.5h at RT or o/n at 4°C with an appropriate dilution of the primary antibody. The membranes were extensively washed for 3 x 20min in [PBS-T Buffer 1 x PBS, 0.05% (v/v Tween 20)]. The HRP-coupled secondary antibody was incubated for 1-1.5h at room temperature in the appropriate dilution in 3% skimmed milk in 1x PBS. The membranes were again washed 3x 20min in PBS-T and exposed to X ray films upon using ECL developer solution mix (Amersham biosciences).

Generation and purification of M18bp1 antibodies

M18bp1 antibody was raised with (Gramsch Laboratories) in rabbit immunized with two peptides derived from the mouse protein.

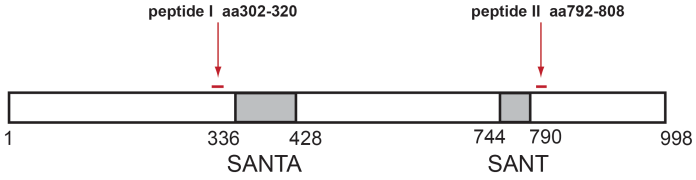

Figure 4.1. Peptides used for antibody generation.

Antibody serum was purified using Protein A/Protein G Agarose beads, eluted with glycine pH 2.5 and immediately neutralized by 1M Tris pH 12 and tested on extracts from mouse embryonic stem cells.

Generation of nucleosomal substrates

Recombinant human histones were expressed in Bl21 *E. coli* and purified according to (Morales et al. 2004). To obtain linear 601 arrays, the insert was cut out with *Eco*RI and *Hin*dIII. Plasmid DNA was digested by *Dra*I to 19, 692, 811 and 1113-bp fragments serving as competitor DNA. Nucleosomal arrays were assembled by continuous salt dialysis as described in (Huynh et al. 2005). Arrays were purified by precipitation with 5 mM $MgCl_2$ (Schwarz et al. 1996).

Expression and purification of GST tagged proteins from E. coli

GST fusion proteins were expressed from pGEX6P1 vector in E. coli Bl21 (Stratagene). Bacteria were induced at OD 0.6 by adding 1mM IPTG at 37°C for 3h or over night with at 25°C. Harvested cells were resuspended in Lysis buffer [20 mM Tris pH 7.5, 150 mM NaCl, 2 mM EDTA, 1mM DTT, complete (Roche)] and disrupted using a Branson sonicator. Suspension was adjusted to 1%Triton and incubated for 30min at 4°C. Cell debris was removed by centrifugation 60min 12000 rpm 4°C. GST tagged proteins were bound to Glutathione-S-Sepharose beads (Amersham Biosciences) for 1h 4°C rotating. After washing with 10x bed volume of wash buffer I [20mM Tris pH 7.5, 500 mM NaCl, 2 mM EDTA, 1% Triton-X-100 und 1mM DTT], wash buffer II (20 mM Tris pH 7.5, 150 mM NaCl, 2

mM EDTA, 0.1% TritonX-100 und 1mM DTT] und wash buffer III [20 mM Tris pH 7.5, 150 mM NaCl, 2 mM EDTA und 1mM DTT] bound proteins were eluted with elution buffer [10mM Tris [pH 8.0], 10 mM Glutathion], dialyzed against 1xPBS,20% glycerol snap frozen and stored at -80°C.

Peptide pulldown assay

50µg of biotinylated peptides were bound to 50µl streptavidine beads (Dynabeads C1 Invitrogen) for 1h at room temperature on a rotation wheel in binding buffer [50 mM Tris pH 7.5, 500 mM NaCl, 1 mM EDTA, 0.1% NP40]. Nuclear extract was prepared from ES cells using Ficoll gradient to remove cytoplasm followed by salt extraction with 500mM NaCl in binding buffer and sonication. Binding was allowed over night at 4°C in a rotating wheel. Unspecifically bound proteins were removed in 3 washing steps with wash buffer [50 mM Tris pH 7.5, 500 mM NaCl, 1 mM EDTA, 0.1% NP40]. Beads were resuspended in SDS sample buffer and protein separation was performed on SDS page. Proteins were visualized by silver staining.

GST pulldown assay

GST fusions of PrSet7, M18bp1 truncations and Suv4-20h2 truncations were expressed from pGEX6P1 vector in E. coli and purified using Glutathione-S-Sepharose beads (Amersham Biosciences). Nuclei of wild type ES cells were isolated by spinning through a Ficoll gradient. For the Benzonase treatment cells were resuspended in low salt IP buffer [50 mM Tris pH 7.5, 150 mM KCl, 1 mM EDTA, 20% glycerol, 0.1% NP40] and digested with Benzonase (Merck Chemicals) for 15 min at 30°C, then adjusted to 500 mM KCl, incubated on ice for 30 minutes followed by 3x 10 sec sonication at an amplitude of 30 in a Branson sonifier. For the salt extract, proteins were extracted with high salt IP buffer [50 mM Tris pH 7.5, 500 mM KCl, 1 mM EDTA, 20% glycerol, 0.1% NP40, proteinase inhibitor cocktail (Roche)] incubated on ice for 30 minutes, followed by 3x 10 sec sonication at an amplitude of 30 in a Branson sonifier. Both nuclear extracts were diluted to a final concentration of 250 mM KCl with no salt IP buffer; precipitated or non-soluble proteins were then removed by centrifugation. 5µg of either GST or the different GST-Suv4-20h2 fusion proteins were incubated with the Benzonase treated nuclear extract or salt extract supplemented with 50µg/ml EtBr over night at 4°C on a rotation wheel. Precipitates were again removed by centrifugation before 60µl Glutathione-S-Sepharose beads were added and incubated for another hour at 4°C. Beads were washed with IP buffer containing 300 mM KCl; subsequently, the bound proteins were eluted with 50µl SDS sample buffer. Proteins were separated on a SDS-polyacrylamid gel, visualized by silver staining and identified by mass-spectrometry analysis.

***In vitro* binding assay**

GST fusion proteins of M18bp1 (aa1-440), M18bp1 (aa441-998), M18bp1 (aa325-800), M18bp1 (aa441-800) M18bp1 (aa735-800) were expressed in *Escherichia coli* and purified on Glutathione-S-Sepharose (Amersham Biosciences). *In vitro* translation of CenpC proteins (CenpC (aa1-367), Cenpc

(aa368-656), CenpC (657-906)) was performed using TnT® Quick Coupled Transcription/Translation System (Promega). 10µl of the *in vitro* translated myc- tagged CenpC and 5µg GST protein coupled to Glutathione-S- Sepharose were incubated in IP buffer [50mM Tris pH7.5, 150mM NaCl, 1mM EDTA, 0.1%NP40, 20% glycerol and proteinase inhibitor cocktail (Roche)] o/n at 4°C on a rotating wheel. The beads were washed four times with IP buffer containing 1M NaCl and resuspended in 50 µl loading buffer. Bound proteins were separated on SDS-polyacrylamidgels and detected by immunoblotting using α-myc antibody (9E10).

HP1 interaction test

GST fusion proteins of M18bp1 and Suv4-20h2, HP1a, HP1b and HP1g were expressed in *E. coli* and purified using Glutathione-S-Sepharose beads (Amersham Biosciences). GST-tags of HP1a, HP1b and HP1g were removed by PreScission (GE Healthcare) cleavage. Interaction tests were performed by incubating 5µg GST-Suv4-20h2 fusion protein with 5µg of either HP1a, HP1b and HP1g in IP buffer [50 mM Tris pH 7.5, 150 mM NaCl, 1 mM EDTA, 0.1% NP40, 20% glycerol and proteinase inhibitor cocktail (Roche)] for 1h at room temperature on a rotating wheel. Then 60µl Glutathione-S- Sepharose beads were added and incubated for 1h at 4°C on a rotating wheel. The beads were washed three times with IP buffer containing 300 mM NaCl and eluted with 50 µl SDS sample buffer. Proteins were separated on SDS-polyacrylamidgels and detected by immunoblotting using isoform-specific HP1 antibodies (Euromedex).

Co-immunoprecipitation

Nuclei from wild type and Suv4-20h2-HA-FLAG ES cells were isolated by spinning through a Ficoll gradient. The nuclear pellet was resuspended in low salt IP Buffer [50mM Tris pH 7.5, 150mM KCl, 1mM EDTA, 20% glycerol, 0.1% NP40, proteinase inhibitor cocktail (Roche)]. Fraction I extract was isolated after digestion for 15 minutes at 37°C with Benzonase (Merck) in low salt IP buffer, followed by mild sonication 1x 10 sec at amplitude 20 in a Branson sonifier. Insoluble proteins were separated by spinning for 10 minutes at 13000 rpm at 4°C. The protein pellet was further extracted with high salt IP Buffer [50mM Tris pH 7.5, 500mM KCl, 1mM EDTA, 20% glycerol, 0.1% NP40, proteinase inhibitor cocktail (Roche)] on ice for 30 minutes followed by 3x 10 sec sonication at an amplitude of 30 in a Branson sonifier. Fraction II extract was then diluted to a final concentration of 250mM NaCl with no salt IP Buffer and precipitated or insoluble proteins were removed by centrifugation (30min, 13000rpm, 4°C). The different extracts were incubated with either 5µg Flag M2 antibody (Sigma) or Smc1 antibody (Bethyl Labs) coupled to ProteinA/G magnetic beads (Dynabeads Invitrogen) o/n at 4°C on a rotating wheel. The beads were washed in IP buffer containing 300mM KCl for five times and eluted with SDS sample buffer. Proteins were separated on SDS-polyacrylamidgels and analysed by western blotting using antibodies for Flag M2 (Sigma), Smc1 (Bethyl labs), Smc3 (Abcam) and Suz12 (Cell Signalling).

Immunoprecipitation of proteins co-expressed in HEK293FT cells

HEK293FT cells (Invitrogen) were co- transfected one day before with EGFP-C1-Cenpc and pCMV myc-M18bp1. After harvesting the cells by trypsinization, nuclei were isolated via spinning through a Ficoll gradient. The nuclear pellet was resuspended in high salt IP Buffer [50mM Tris pH 7.5, 500mM NaCl, 1mM EDTA, 20% glycerol, 0.1% NP40] with 4 strokes through 19.5G syringe needle. After incubation on ice for 30 minutes the solution was sonicated 3x 10" at an amplitude of 30 in a Branson sonicator. The nuclear extract was diluted to a final concentration of 150mM NaCl with no salt IP Buffer and precipitates were removed by centrifugation. The extract was incubated o/n at 4°C on a rotating wheel with either GFP binder beads [ChromoTek], covalently coupled myc 9E10 antibody on agarose Protein A/ProteinG beads or agarose beads only. The beads were washed in IP buffer containing 300mM NaCl for five times and afterwards denatured in SDS sample buffer. Proteins were separated on SDS-polyacrylamidgels and analyed by western blotting using α-myc and α-GFP.

Chromatin accessibility assay

Cytoplasm of wild type, Suv4-20h2 KO and Suv4-20h2 DKO ES cells and wild type, Suv4-20h DKO, DKO+FL and DKO+M12 fibroblast cell lines was removed by spinning through a Ficoll gradient. Isolated nuclei were resuspended in Ex100 buffer [10 mM HEPES pH 7.6, 100 mM KCl, 1.5 mM MgCl2 0.5 mM EGTA, 10% Glycerol, proteinase inhibitor cocktail (Roche)] and digested with different amounts of MNase (Sigma) in the presence of 3mM CaCl2. Digest was stopped after 9 min by addition of 1/10 volume MNase stop buffer [0.5 M EDTA, 10% SDS]. Genomic DNA was purified and then separated on a 1% agarose gel, followed by blotting onto a Nylon membrane [Roti-Nylon plus, Roth] via capillary transfer. Hybridization with a ^{32}P-labeled major satellite probe was performed using standard conditions. MNase digestion patterns were further analyzed using the Agilent 2100 bioanalyzer (Agilent Technologies). 100ng of each sample were loaded onto a DNA LabChip using the Agilent DNA 12000 kit and analysis was performed using the 2100 expert software (Agilent Technologies).

Southern blot

Sample DNA from MNase digests was purified using Phenol-Chloroform extraction followed by Isopropanol precipitation. Equal amounts were separated on an agarose gel in 1x TAE buffer and DNA was blotted onto Nylon membrane (Roth) by capillary transfer over night in 20x SSC buffer [3M NaCl, 0.3M sodium citrate]. After blotting overnight, membranes were baked at 80°C for 2 hours and prewashed at 68°C for 30minutes in 2xSSC and subsequently for 2 hours in 2x SCC 1xDenhardt's (0.5 % SDS, 1 mM EDTA, 0.02 % BSA, 0.02 % PVP-40, 0.02 % Ficoll). Before hybridization membranes were incubated for 1 hour at 68°C in pre-incubation solution (2XSSC, 1xDenhardt's an denatured salmon sperm carrier DNA). Membranes were subsequently incubated overnight at 68°C in a rotating cylinder with 5 ml pre-incubation solution containing a radioactively labelled probe major satellite

repeat probe. Membranes were washed three times with 3xSSC 1xDenhardt's for 30 minutes at 68°C and then analyzed by exposure to Fuji FLA3000 phosphoimager screens.

HMTase activity assay

Recombinant GST-tagged SET domain proteins (100ng-500ng) were incubated in 50mM Tris-HCl, pH 8.5, 20mM NaCl and BSA, with 1ul of 3H-labelled SAM (Hartmann adenosyl-Lmethionine, S-(methyl-3H)) or non radioactive SAM (NEB) and 1 ug of either recombinant human H4 or histone octamers (H2A, H2B, H3 and H4) or assembled nucleosomes for 1 h at 30°C. For scintillation counter analysis samples were spotted onto negatively charged Whatman filter analyzed in the Scintillation counter. Or samples were loaded on high percentage SDS page and probed with specific antibodies.

4.4 Mouse methods

Generation of conditional mouse knockout strains

Heterozygous mice with successful germ line transmission of the targeted allele were purchased from the EUCOMM project. C57BL/6J mice expressing Flp recombinase to remove the neomycin resistance cassette resulting in “flox”-alleles. To disrupt M18bp1 protein, heterozygous M18bp1$^{fl/+}$ and mice were crossed with different Cre lines.

Genotyping

Genomic DNA was isolated from tail biopsy. Proteinase K (Invitrogen) in tail buffer [50mM Tris pH 7.4, 100 mM EDTA, 100mM NaCl, 1% SDS] at 55°C over night was used to rmove proteins. DNA was precipitated by high salt in isopropanol and resuspended in 1x TE buffer. Genotyping was performed as standard endpoint PCR reaction in 25ul volume.

Isolation of blastocysts and primary mouse fibroblasts (pMEFs)

Blastocyst were isolated E3.5, pMEFs at E12.5 according to

Hogan, B., Beddington, R., Constantini, F., and Lacy, E. 1994. Manipulating the Mouse Embryo: A Laboratory Manual, 2nd ed. Cold Spring Harbor Laboratory Press, Cold Spring Harbor, NewYork.

Table 4.1. Cloning vectors

vector	company	description
pDonor Zeo	Invitrogen	Bacterial expression vector, containing att sides for gateway cloning
pEGFP N1	Invitrogen	Mammalian expression vector, C-terminal EGFP tag, CMV promoter, polyadenylation signal from SV40
pCMV myc	Invitrogen	Mammalian expression vector, N-terminal c-myc, HA tag, CMV promoter, polyadenylation signal from SV40
pGex6P1	Invitrogen	Bacterial expression vector, N-terminal GST tag, tac promoter, PreScission cleavage site
pET21	Novagen	Bacterial expression vector

Table 4.2. Bacteria strains

strain	company	genotype
DB3.1	Invitrogen	F- gyrA462 endA1 glnV44 Δ(sr1-recA) mcrB mrr hsdS20(rB-, mB-) ara14 galK2 lacY1 proA2 rpsL20(Smr) xyl5 Δleu mtl1
DH5 alpha	Promega	F- endA1 glnV44 thi-1 recA1 relA1 gyrA96 deoR nupG Φ80dlacZΔM15 Δ(lacZYA-argF)U169, hsdR17(rK- mK+), λ–
Stellar	clontech	F–, ara,Δ(lac-proAB) [Φ80d lacZΔM15], rpsL(str), thi, Δ(mrr-hsdRMS-mcrBC), ΔmcrA, dam, dcm
Bl21 (DE3)	NEB	F– ompT gal dcm lon hsdSB(rB- mB-) λ(DE3 [lacI lacUV5-T7 gene 1 ind1 sam7 nin5])

Table 4.3. Primer sequences.

cloning primer		
M12,M13+M14 pGex6P1 direct cloning		
Suv4-20h2 pGex6P1: 350f BamHI	f	GGGATCCgtcctccgcactgcctgtgt
Suv4-20h2 pGex6P1: 385f BamHI	f	GGGATCCcgctggaccccacaacag
Suv4-20h2 pGex6P1: 412r EcoRI	r	GGAATTCctaggctaggcgggtaagttc
Suv4-20h2 pGex6P1: 385r EcoRI	r	GGAATTCctagcgagtctgggggcgcag
M7	f	ggggacaagtttgtacaaaaaagcaggcttaaccatgacccgcctagccccagcc
	r	ggggaccactttgtacaagaaagctgggtctggctcaccactattgat
M12	f	ggggacaagtttgtacaaaaaagcaggcttaaccatggtcctccgcactgcctgt
	r	ggggaccactttgtacaagaaagctgggtcggctaggcgggtaagttc
M13	f	ggggacaagtttgtacaaaaaagcaggcttaaccatggtcctccgcactgcctgt
	r	ggggaccactttgtacaagaaagctgggtcgcgagtctgggggcgcag
M14	f	ggggacaagtttgtacaaaaaagcaggcttaaccatgcgctggaccccacaacag
	r	ggggaccactttgtacaagaaagctgggtcggctaggcgggtaagttc
HP1b	f	ggggacaagtttgtacaaaaaagcaggcttaactatggggaaaaagcaaaac
	r	ggggaccactttgtacaagaaagctgggtcattcttgtcgtctttttgtc
HP1g	f	ggggacaagtttgtacaaaaaagcaggcttaaaaatggcctccaataaaactac
	r	ggggaccactttgtacaagaaagctgggtcttgtgcttcatcttcaggac
HP1a	f	ggggacaagtttgtacaaaaaagcaggcttaagacatgggaaagaagacc
	r	ggggaccactttgtacaagaaagctgggtcgctcttcgcgctttctttttc
M18bp1	f	ggggacaagtttgtacaaaaaagcaggcttaactatgattgtaacacctttga
	r	ggggaccactttgtacaagaaagctgggtcgtcagaattggaaaagtaa
M1	f	ggggacaagtttgtacaaaaaagcaggcttaactatgattgtaacacctttga
	r	ggggaccactttgtacaagaaagctgggtctcttgctgtttcctgtctg
M2	f	ggggacaagtttgtacaaaaaagcaggcttaactatgcaggaaacagcaagag
	r	ggggaccactttgtacaagaaagctgggtcgtcagaattggaaaagtaa
M3	f	ggggacaagtttgtacaaaaaagcaggcttaactatgactgttgtaaaagaag
	r	ggggaccactttgtacaagaaagctgggtcatgttttcgggatccttgg
M4	f	ggggacaagtttgtacaaaaaagcaggcttaactatgcaggaaacagcaagag
	r	ggggaccactttgtacaagaaagctgggtcatgttttcgggatccttgg
M5	f	ggggacaagtttgtacaaaaaagcaggcttaactatggaccatctacctggtt
	r	ggggaccactttgtacaagaaagctgggtcatgttttcgggatccttgg
Dnttip2	f	ggggacaagtttgtacaaaaaagcaggcttaactatggtggtcaccaggtcc
	r	ggggaccactttgtacaagaaagctgggtcattgcgaaatttcttcttttc
PogZ	f	ggggacaagtttgtacaaaaaagcaggcttaactatggcggacaccgacctgtt
	r	ggggaccactttgtacaagaaagctgggtcgatctccatcagatcaagg
Zfp828	f	ggggacaagtttgtacaaaaaagcaggcttaactatggaagtgtgtcaggaatt
	r	ggggaccactttgtacaagaaagctgggtcaatctgctgctcctccaatg
Mutagenesis primer		
M18bp1W746A	f	GTTTAACTGATGATGAAGAAGCCAGTGAGCAAGAGTTACAGAAG
	r	CTTCTGTAACTCTTGCTCACTGGCTTCTTCATCATCAGTTAAAC
M18bp1W746A	f	GTTTAACTGATGATGAAGAAGCCGCCGAGCAAGAGTTACAGAAGC
	r	GCTTCTGTAACTCTTGCTCGGCGGCTTCTTCATCATCAGTTAAAC

primer for Suv4-20h2 knock-in cells		
MGC_tag_1f	f	CACTCCCACTGTCCTTTCCTAA
MGC_tag_1r	r	CAAACTCACAGAGAGCCACCTA
MGC_tag_2f	f	TCGCATTGTCTGAGTAGGTGTC
primer for genotyping of M18bp1 ko mice		
M18bp1 wt / M18bp1 flox	f	CCATGCCTGTTTATACCAGTTAGCA
M18bp1 wt / M18bp1 flox	r	GCCCATTTAAAGCACCAATTGTTAA
M18bp1 bGal	f	CCATGCCTGTTTATACCAGTTAGCA
M18bp1 bGal	r	CATCTCCCCTTCAGTCTTCCTGT
M18bp1 delta	f	CCATGCCTGTTTATACCAGTTAGCA
M18bp1 delta	r	GCGAGCTCAGACCATAACTTCGTAT
Flpe	f	GTGGATCGATCCTACCCCTTGCG
Flpe	r	GTCCAACTGCAGCCCAAGCTTCC
TNAP Cre	f	CCA CGA CCA AGT GAC AGC AAT G
TNAP Cre	r	CAG AGA CGG AAA TCC ATC GCT C
Cre ERT2	f	TCG CGA TTA TCT TCT ATA TCT TCA G
Cre ERT2	r	GCT CGA CCA GTT TAG TTA CCC
primer for M18bp1 knock-in cells		
cloning fragment AB	f	ATAGCGGCCGCCTAACTCAAATGCAAAACC
cloning fragment AB	r	CGCAAGCTTTGATTAATAGTTTTTCACTAT
cloning fragment YZ	f	TCCAAGCTTCCATGACTTGCTCACCTTG
cloning fragment YZ	r	TGCACTAGTTATGAAAGAACTCTCATAATG
cloning fragment CD	f	ATAGCGGCCGCTCTCCACCACCAACACGGA
cloning fragment CD	r	TCGGAATTCGTCAGAATTGGAAAAGTAAT
cloning fragment EF	f	CGAGGATCCTGATAGACGACTTGCAGGAAT
cloning fragment EF	r	TCTGTCGACAGTCCACAATCTTAACTCTG
nested PCR outer	f	ACCGCTTCCTCGTGCTTTAC
nested PCR outer	r	AAAGCCAAGCTCACTGTTTC
nested PCR inner	f	GATTGGGAAGACAATAGCAGGCATG
nested PCR inner	r	GCGCAAGTAAATCATCAAAAGGCTG

Table 4.4. Primers used for quantitative PCR

gene	**mRNA**	**direction**	**sequence in 5' to 3' direction**
beta actin	NM_007393.3	fw	ggtcatcactattggcaacg
		rw	tccatacccaagaaggaagg
M18bp1	NM_172578.2	fw	ctccaaaaggccagcatcacg
		rw	ttgccggaggtaggctgttcc
Gapdh	NM_008084.2	fw	tcaagaaggtggtgaagcag
		rw	gttgaagtcgcaggagacaa

Table 4.5. Antibodies used for immunoflourescence and western blot

antibody	**company**
CenpA	Cell Signalling
CenpC	Abcam
M18bp1	Gramsch Heidelberg, peptide antibody from rabbit
HP1a	Euromedex
HP1b	Euromedex
HP1g	Euromedex
Tubulin	Sigma
H4K20me3	Schotta et al 2004
Smc1	Abcam
Smc3	Bethyl
Suz12	Cell Signalling
myc	9E10
GFP	Roche

ABBREVIATIONS

CCAN: Constitutive Centromere Associated Network

Cko: conditional knockout

CPC: chromosomal passenger complex

DAPI: 4,6-Diamino-2-phenylindol

DNA: Desoxyribonucleinsäure

EGFP: enhanced Green Fluorescent Protein

GST: Glutathion-S-Transferase

H4K20me3 : trimethylation of histone H4 at lysine 20

H3K9me3: trimethylation of histone H3 at lysine 9

HP1: heterochromatin protein 1

HMTase: histone lysine methyaltransferase

kb: Kilobasen

kDa: Kilodalton

ko: knockout

SAM: S-adenosyl-[methyl-3H]-l-methionin

SANT: switching-defective protein 3 (Swi3), adaptor 2 (Ada2), nuclear receptor co-repressor (N-CoR) and transcription factor (TFIIIB)

SANTA: SANT associated

SET: suppressor of variegation, enhancer of zeste and trithorax

Suv39h1: suppressor of variegation 3-9 homolog 1

Suv39h2: suppressor of variegation 3-9 homolog 2

Suv4-20h1: suppressor of variegation 4-20 homolog 1

Suv4-20h2: suppressor of variegation 4-20 homolog 2

ACKNOWLEDGEMENTS

I would like to thank…

Prof Dr. Gunnar Schotta for giving me the opportunity to join his group and to work on all this interesting projects

Prof. Dr. Peter Becker for following up my work, for taking over the role of an official supervisor and for giving me the opportunity to work in the stimulating scientific environment of the Adolf Butenandt Institute

the members of my thesis advisory committee Axel Imhof, Felix Müller Planitz and Andreas Ladurner

the ZFP Lars Israel, Pierre Schilcher, Tilmann Schlunk und Marc Borath for many analyses of mass-spec samples, which are the basis for this work

the Schotta Lab for the nice atmosphere. Dennis for a lot of expertise and great discussions. Alex for a lot of help with the mice and the immunohistochemistry. Maike for a lot of help with cloning and biochemistry.

Florian Büddefeld for his help on the M18bp1 project

Prof. Dr. Heinrich Leonhardt and Wen Deng for the collaboration and the F3H assay

Prof. Dr. Stefan Bohlander for providing the Affymetrix expression profiling of M18BP1 in different hematopoietic malignancies

CURRICULUM VITAE

Personal information

Name	Silvia Dambacher
Date of birth	11.01.1980
Place of birth	Mayen
Nationality	German

University education

02/2008-ongoing **PhD in Molecular Biology**

Adolf Butenandt Institute, Ludwig-Maximilian University Munich

Professor Dr. Gunnar Schotta

09/2007 **Diploma in Biotechnology**

University of Applied Sciences, Mannheim

Diploma thesis: '*Identification of interaction partners of posttranslational modified nucleosomes*'

2007 **Academic Visitor**

Laboratory of Prof. Tony Kouzarides

Welcome Trust/Cancer Research UK Gurdon Institute, Cambridge- UK

2004 **Internship Max-Planck-Institute for Biochemistry**,

Department for Molecular Biology (Prof. Dr. Jentsch)

Research Group of Dr. Buchberger

project: *Identification of new interactors of the human "von Hippel-Lindau-tumor suppressor protein (pVHL) " via two hybrid screen in Saccharomyces cerevisiae*

School education

06/1999 **Abitur** (German advanced school leaving certificate)

Martin-von-Cochem Gymnasium, Cochem

Table I Mass-spec list of the H3K9 peptide pulldown assays. The number of unique spectra that were identified for each protein in the mass-spec analysis is indicated (Scaffold analysis).

name	H3K9un	H3K9me3
tripartite motif protein 28 [Mus musculus]	5	78
histone cluster 1, H2bd [Homo sapiens]	38	34
histone H2A type 1-F [Mus musculus]	26	28
Hist2h4 protein [Mus musculus]	40	29
histone H1.4 [Mus musculus]	31	30
Treacher Collins Franceschetti syndrome 1, homolog, isoform CRA_b [Mus musculus]	28	50
heterochromatin protein 1-beta [Homo sapiens]	4	35
PREDICTED: similar to ribosomal protein L23a [Mus musculus]	35	32
beta actin [Homo sapiens]	39	34
myb-binding protein 1a [Mus musculus]	43	31
histone H1.5 [Mus musculus]	23	22
RIKEN cDNA 9430010O03, isoform CRA_c [Mus musculus]	26	21
PREDICTED: similar to Nucleophosmin (NPM) (Nucleolar phosphoprotein B23) (Numatrin) (Nucleolar protein NO38) [Mus musculus]	24	18
histone cluster 1, H3a [Homo sapiens]	22	17
unnamed protein product [Mus musculus]	0	31
PREDICTED: similar to Fibrillarin isoform 2 [Mus musculus]	22	19
LINE-1 type transposase domain-containing protein 1 [Mus musculus]	18	25
PREDICTED: similar to Chromobox homolog 3 (HP1 gamma homolog, Drosophila) isoform 2 [Pan troglodytes]	0	18
unnamed protein product [Mus musculus]	25	17
lamin-B1 [Mus musculus]	24	20
nucleolar protein 58 [Mus musculus]	21	17
RecName: Full=Histone H1.3; AltName: Full=H1 VAR.4; AltName: Full=H1d	11	10
ribosomal L1 domain containing 1, isoform CRA_b [Mus musculus]	22	14
ribosomal protein L26 [Homo sapiens]	14	12
histone cluster 2, H2ac [Homo sapiens]	11	6
nucleolar protein 56 [Mus musculus]	17	9
mCG114749, isoform CRA_a [Mus musculus]	13	10
H2A histone family, member Z [Homo sapiens]	7	7
chromodomain-helicase-DNA-binding protein 4 [Mus musculus]	1	23
mCG1028606 [Mus musculus]	10	10
protease, serine, 1 [Mus musculus]	6	6
60S ribosomal protein L35 [Mus musculus]	10	9
lamina-associated polypeptide 2 isoform epsilon [Mus musculus]	9	10
putative rRNA methyltransferase 3 [Mus musculus]	16	10
histone H1.1 [Mus musculus]	10	7
RecName: Full=Nucleolar RNA helicase 2; AltName: Full=Nucleolar RNA helicase II; AltName: Full=Nucleolar RNA helicase Gu; AltName: Full=RH II/Gu; AltName: Full=Gu-alpha; AltName: Full=DEAD box protein 21	14	6
transcription intermediary factor 1-alpha [Mus musculus]	0	18
putative ribosomal RNA methyltransferase NOP2 [Mus musculus]	15	7
heterogeneous nuclear ribonucleoprotein A3 [Mus musculus]	12	9
ATP synthase, H+ transporting, mitochondrial F1 complex, alpha subunit, isoform 1, isoform CRA_e [Mus musculus]	7	11
unnamed protein product [Mus musculus]	8	5
EBNA1 binding protein 2 [Mus musculus]	11	4
BAP28 protein [Mus musculus]	8	6
unnamed protein product [Mus musculus]	6	6
mCG13479, isoform CRA_a [Mus musculus]	8	4

Pogz protein [Mus musculus]	0	16
PREDICTED: similar to ribosomal protein [Mus musculus]	4	3
unnamed protein product [Mus musculus]	5	6
60S ribosomal protein L12 [Mus musculus]	7	8
PREDICTED: similar to ribosomal protein L3 isoform 1 [Mus musculus]	10	5
PREDICTED: hypothetical protein [Mus musculus]	7	7
PREDICTED: hypothetical protein [Mus musculus]	11	5
60 kDa heat shock protein, mitochondrial [Mus musculus]	9	6
PREDICTED: hypothetical protein [Mus musculus]	7	5
mCG22088 [Mus musculus]	6	7
unnamed protein product [Mus musculus]	9	5
DEAD (Asp-Glu-Ala-Asp) box polypeptide 5 [Mus musculus]	7	6
unnamed protein product [Mus musculus]	6	5
heat shock protein 8 [Rattus norvegicus]	5	9
ribosomal protein L8 [Homo sapiens]	9	2
reduced expression 2 [Mus musculus]	0	7
mKIAA4193 protein [Mus musculus]	7	7
mCG20089, isoform CRA_a [Mus musculus]	3	10
nucleolar and coiled-body phosphoprotein 1, isoform CRA_a [Mus musculus]	9	4
mCG145163 [Mus musculus]	3	3
zinc finger protein 57 [Mus musculus]	0	6
unnamed protein product [Mus musculus]	5	4
Sf3b1 protein [Mus musculus]	5	3
RecName: Full=H/ACA ribonucleoprotein complex subunit 4; AltName: Full=Dyskerin; AltName: Full=Nucleolar protein family A member 4; AltName: Full=snoRNP protein DKC1; AltName: Full=Nopp140-associated protein of 57 kDa; AltName: Full=Nucleolar protei	5	6
histone H2A.x [Mus musculus]	3	3
RRS1 ribosome biogenesis regulator homolog [Mus musculus]	6	3
ribosome production factor 2 homolog isoform 1 [Mus musculus]	6	3
expressed sequence AA408556, isoform CRA_a [Mus musculus]	3	2
PREDICTED: similar to ribosomal protein L19 isoform 1 [Macaca mulatta]	4	3
unnamed protein product [Mus musculus]	0	6
Ribosomal protein, large, P0 [Mus musculus]	5	3
complement component 1 Q subcomponent-binding protein, mitochondrial [Mus musculus]	4	3
N-acetyltransferase 10, isoform CRA_a [Mus musculus]	4	3
unnamed protein product [Mus musculus]	4	4
U3 small nucleolar ribonucleoprotein protein IMP3 [Mus musculus]	4	3
ribosome biogenesis protein BRX1 homolog [Mus musculus]	7	2
pescadillo homolog [Mus musculus]	6	2
alpha thalassemia/mental retardation syndrome X-linked homolog (human) [Mus musculus]	1	6
DNA segment, Chr 13, Wayne State University 177, expressed [Mus musculus]	5	3
type II keratin 5 [Mus musculus]	7	1
putative ATP-dependent RNA helicase Pl10 [Mus musculus]	3	3
mCG133010, isoform CRA_c [Mus musculus]	3	3
keratin, type I cytoskeletal 10 [Mus musculus]	3	3
mCG127344, isoform CRA_b [Mus musculus]	4	3
mCG8513 [Mus musculus]	4	3
mCG120690 [Mus musculus]	3	3
PREDICTED: similar to ribosomal protein S24 [Macaca mulatta]	3	3
H/ACA ribonucleoprotein complex subunit 1 [Mus musculus]	2	3
mCG7617, isoform CRA_a [Mus musculus]	6	1
unnamed protein product [Mus musculus]	3	2
PREDICTED: similar to acidic ribosomal phosphoprotein P1 isoform 1 [Mus musculus]	2	2

peter pan homolog (Drosophila), isoform CRA_a [Mus musculus]	3	2
alpha-tubulin isotype M-alpha-2	4	2
keratin, type II cytoskeletal 73 [Mus musculus]	3	2
unnamed protein product [Mus musculus]	1	5
bromodomain adjacent to zinc finger domain protein 2A [Mus musculus]	3	3
PREDICTED: hypothetical protein [Mus musculus]	4	2
mCG1128, isoform CRA_a [Mus musculus]	4	2
ADP/ATP translocase 2 [Mus musculus]	4	1
RNA-binding protein 39 [Mus musculus]	2	3
40S ribosomal protein S19 [Mus musculus]	2	2
Atp5b protein [Mus musculus]	1	3
protein transport protein Sec61 subunit beta [Mus musculus]	3	2
Gtpbp4-pending protein [Mus musculus]	6	0
expressed sequence C79407 (M18bp1)[Mus musculus]	0	4
unnamed protein product [Mus musculus]	5	0
histone H2B type 1-H [Mus musculus]	2	1
ribosomal protein S14 [Mus musculus]	3	2
nucleoporin 93, isoform CRA_a [Mus musculus]	3	2
Chain A, N-Terminal Fragment Of Importin-Beta	2	3
unnamed protein product [Mus musculus]	3	2
SWI/SNF related, matrix associated, actin dependent regulator of chromatin, subfamily a, member 4, isoform CRA_a [Mus musculus]	1	4
heterogeneous nuclear ribonucleoproteins A2/B1 isoform 1 [Mus musculus]	2	3
splicing factor, arginine/serine-rich 7, 35kDa, isoform CRA_a [Homo sapiens]	2	3
ribosomal RNA processing protein 1 homolog A [Mus musculus]	2	3
mCG23455, isoform CRA_a [Mus musculus]	4	1
RecName: Full=Serine/arginine repetitive matrix protein 2	3	2
unnamed protein product [Mus musculus]	2	2
nucleolar complex protein 3 homolog [Mus musculus]	4	1
mCG122723 [Mus musculus]	3	1
mCG21756, isoform CRA_b [Mus musculus]	2	3
guanine nucleotide binding protein-like 3 (nucleolar), isoform CRA_a [Mus musculus]	3	2
block of proliferation 1 [Mus musculus]	4	1
lamin B receptor [Mus musculus]	2	3
unnamed protein product [Mus musculus]	1	3
heterogeneous nuclear ribonucleoprotein L, isoform CRA_b [Mus musculus]	3	0
unnamed protein product [Mus musculus]	2	2
nuclear pore complex protein Nup160 [Mus musculus]	2	2
histone H2B type 1-B [Mus musculus]	2	1
mCG16669, isoform CRA_e [Mus musculus]	2	2
mKIAA0187 protein [Mus musculus]	3	1
60S ribosomal protein L36	3	0
mCG12239 [Mus musculus]	0	4
zinc finger protein 828 [Mus musculus]	0	4
epithelial protein lost in neoplasm-a [Mus musculus]	1	2
gamma-aminobutyric acid receptor beta-2 subunit [Mus musculus]	2	1
nucleolar transcription factor 1 isoform 2 [Mus musculus]	1	2
Hist1h3e protein [Mus musculus]	2	1
unnamed protein product [Mus musculus]	1	2
Utp3 protein [Mus musculus]	1	2
60S ribosomal protein L38 [Mus musculus]	1	2
RNA-binding protein 25 [Mus musculus]	3	0
DNA segment, Chr 19, Brigham & Women's Genetics 1357 expressed, isoform CRA_b [Mus musculus]	3	0

PREDICTED: similar to Glyceraldehyde-3-phosphate dehydrogenase (GAPDH) [Mus musculus]	1	2
Eukaryotic translation elongation factor 1 alpha 1 [Mus musculus]	2	1
pinin [Mus musculus]	1	1
apoptosis antagonizing transcription factor, isoform CRA_b [Mus musculus]	2	0
DNA topoisomerase 2-alpha [Mus musculus]	2	1
RanBP2 protein [Mus musculus]	0	3
dynein, axonemal, heavy chain 11 [Mus musculus]	1	2
zinc finger protein 280c [Mus musculus]	0	3
RecName: Full=Ribosomal RNA processing protein 1 homolog B; AltName: Full=RRP1-like protein B	1	2
phospholipase C gamma 1 [Mus musculus]	2	1
Rangap1 protein [Mus musculus]	1	2
leukocyte receptor cluster (LRC) member 8, isoform CRA_a [Mus musculus]	2	1
ankyrin repeat and SOCS box-containing 15 [Mus musculus]	2	0
Acin1 protein [Mus musculus]	3	0
histone H1.2 [Mus musculus]	1	1
caspase recruitment domain-containing protein 9 [Mus musculus]	1	1
ribosomal protein L10a [Rattus norvegicus]	2	0
PREDICTED: hypothetical protein [Mus musculus]	1	2
PREDICTED: similar to putative integral membrane protein TMIE [Mus musculus]	0	2
Bclaf1 protein [Mus musculus]	1	1
mCG17415 [Mus musculus]	1	1
mCG121979, isoform CRA_b [Mus musculus]	0	2
putative pre-mRNA-splicing factor ATP-dependent RNA helicase DHX15 isoform 2 [Mus musculus]	2	0
WD repeat domain 36, isoform CRA_b [Mus musculus]	2	0
RecName: Full=60S ribosome subunit biogenesis protein NIP7 homolog; AltName: Full=PEachy; AltName: Full=kDa93	2	0
retinoblastoma-binding protein mRbAp48	0	2
lymphocyte-specific helicase [Mus musculus]	1	1
heterogeneous nuclear ribonucleoprotein H [Mus musculus]	0	2
nucleolar protein 10 [Mus musculus]	1	1
U3 small nucleolar RNA-associated protein 15 homolog [Mus musculus]	1	1
growth arrest and DNA-damage-inducible, gamma interacting protein 1 [Mus musculus]	0	2
mCG10343, isoform CRA_b [Mus musculus]	1	1
PREDICTED: similar to FUS interacting protein (serine-arginine rich) 1 [Macaca mulatta]	1	1
mCG23000, isoform CRA_a [Mus musculus]	2	0
Sec61 alpha 1 subunit [Homo sapiens]	2	0
MARCKS-like 1 [Mus musculus]	1	1
serine/arginine repetitive matrix 1 [Mus musculus]	2	0
hypothetical protein LOC66276 [Mus musculus]	1	1
poly(rC)-binding protein 1 [Mus musculus]	1	1
PRP19/PSO4 pre-mRNA processing factor 19 homolog (S. cerevisiae), isoform CRA_a [Mus musculus]	2	0
hnRNP-associated with lethal yellow [Mus musculus]	2	0
unnamed protein product [Mus musculus]	1	1
SET domain containing 3 [Mus musculus]	2	0
immunoglobulin heavy chain [Mus musculus]	1	1
mCG5393 [Mus musculus]	1	1
nucleolar complex protein 2 homolog [Mus musculus]	2	0
Suv39h2 protein [Mus musculus]	0	2
splicing factor, arginine/serine-rich 1 (ASF/SF2), isoform CRA_c [Mus musculus]	1	1
unnamed protein product [Mus musculus]	2	0
mCG5312, isoform CRA_a [Mus musculus]	0	2
sal-like 2 (Drosophila), isoform CRA_a [Mus musculus]	1	1
CKLF-like MARVEL transmembrane domain containing 6 [Mus musculus]	0	2

protein lin-28 homolog A [Mus musculus]	1	0
RIKEN cDNA 4932418E24 [Mus musculus]	2	0
A-kinase anchor protein 9 [Mus musculus]	1	1
PREDICTED: similar to ribosomal protein L28 [Mus musculus]	2	0
lymphoid-restricted membrane protein [Mus musculus]	0	2
RecName: Full=Septin-1; AltName: Full=Differentiation protein 6; Short=Protein Diff6; AltName: Full=Peanut-like protein 3	1	1
mCG120696 [Mus musculus]	0	1
nucleolar protein 7 [Mus musculus]	0	1
methyl-CpG binding domain protein 3, isoform CRA_a [Mus musculus]	0	1
MutS homolog 2 (E. coli) [Mus musculus]	0	1
mCG13856, isoform CRA_a [Mus musculus]	0	1
deoxynucleotidyltransferase terminal-interacting protein 2 [Mus musculus]	0	1
eukaryotic translation initiation factor 4A2, isoform CRA_c [Mus musculus]	0	1
promyelocytic leukemia, isoform CRA_a [Mus musculus]	0	1
mCG3370 [Mus musculus]	0	1
EMG1 nucleolar protein homolog (S. cerevisiae), isoform CRA_b [Mus musculus]	0	1
SWI/SNF complex subunit SMARCC1 [Mus musculus]	0	1
Ngdn protein [Mus musculus]	0	1
RecName: Full=Proline-, glutamic acid- and leucine-rich protein 1; AltName: Full=Modulator of non-genomic activity of estrogen receptor	1	0
isocitrate dehydrogenase 3 (NAD+) alpha, isoform CRA_b [Mus musculus]	1	0
mCG144546 [Mus musculus]	1	0
splicing factor 3B, 14 kDa subunit [Homo sapiens]	1	0
DEAD (Asp-Glu-Ala-Asp) box polypeptide 51 [Mus musculus]	1	0
Eftud2 protein [Mus musculus]	1	0
mCG120440 [Mus musculus]	1	0
unnamed protein product [Mus musculus]	1	0
RecName: Full=Heat shock protein HSP 90-beta; AltName: Full=HSP 84; AltName: Full=Tumor-specific transplantation 84 kDa antigen; Short=TSTA	1	0
nucleolar protein 14 [Mus musculus]	1	0
eukaryotic translation initiation factor 6 [Mus musculus]	1	0
Nucleolar complex associated 4 homolog (S. cerevisiae) [Mus musculus]	1	0
probable ATP-dependent RNA helicase DDX27 [Mus musculus]	1	0
60S ribosomal protein L32'	1	0
U3 small nucleolar RNA-interacting protein 2 [Mus musculus]	1	0
pleckstrin homology-like domain, family A, member 1 [Mus musculus]	1	0
unnamed protein product [Mus musculus]	1	0
Mphosph10 protein [Mus musculus]	1	0
unnamed protein product [Mus musculus]	0	1
mCG117568, isoform CRA_a [Mus musculus]	0	1
heterogeneous nuclear ribonucleoprotein A1 isoform b [Mus musculus]	0	1
ras-related protein Rab-5C [Mus musculus]	1	0
karyopherin (importin) alpha 2 [Mus musculus]	0	1
RecName: Full=B-Raf proto-oncogene serine/threonine-protein kinase	0	1
mCG140775 [Mus musculus]	0	1
zinc finger protein 518B [Mus musculus]	0	1
mCG132526 [Mus musculus]	1	0
mCG115615, isoform CRA_a [Mus musculus]	1	0
MEK kinase 2	1	0
RecName: Full=Sentrin-specific protease 3; AltName: Full=Sentrin/SUMO-specific protease SENP3; AltName: Full=SUMO-1-specific protease 3; AltName: Full=Smt3-specific isopeptidase 1; Short=Smt3ip1	1	0
MYST histone acetyltransferase 2, isoform CRA_a [Mus musculus]	0	1
M-phase phosphoprotein, mpp8 [Mus musculus]	0	1
unnamed protein product [Mus musculus]	1	0

unnamed protein product [Mus musculus]	0	1
tumor necrosis factor, alpha-induced protein 3 [Mus musculus]	1	0
ras-related protein Rab-32 [Mus musculus]	0	1
pentatricopeptide repeat domain 1 [Mus musculus]	1	0
anti-DNA immunoglobulin heavy chain IgG [Mus musculus]	0	1
DEAH (Asp-Glu-Ala-His) box polypeptide 9, isoform CRA_a [Mus musculus]	0	1
RecName: Full=Protein capicua homolog	0	1
hypothetical protein LOC227545 [Mus musculus]	1	0
unnamed protein product [Mus musculus]	1	0
mCG145590 [Mus musculus]	0	1
hypothetical protein LOC75964 isoform 2 [Mus musculus]	1	0
poly A binding protein, cytoplasmic 4 [Mus musculus]	0	1
olfactory receptor 1089 [Mus musculus]	1	0
hypothetical protein LOC240185 [Mus musculus]	0	1
mCG10523, isoform CRA_b [Mus musculus]	1	0
Tpr [Mus musculus]	0	1
Voltage-dependent anion channel 2 [Mus musculus]	1	0
myosin-7B [Mus musculus]	0	1
unnamed protein product [Mus musculus]	0	1
RecName: Full=Probable ATP-dependent RNA helicase DDX20; AltName: Full=DEAD box protein 20; AltName: Full=DEAD box protein DP 103; AltName: Full=Component of gems 3; AltName: Full=Gemin-3; AltName: Full=Regulator of steroidogenic factor 1; Short=ROS	1	0
unnamed protein product [Mus musculus]	1	0
CTTNBP2 N-terminal-like protein [Mus musculus]	0	1
collagen alpha-4(IV) chain precursor [Mus musculus]	0	1
PREDICTED: similar to electrogenic sodium bicarbonate cotransporter NBC4c isoform 3 [Mus musculus]	1	0
RIKEN cDNA 4930523C11 gene [Mus musculus]	0	1
dynein cytoplasmic 2 heavy chain 1 [Mus musculus]	0	1
SMEK homolog 3, putative [Mus musculus]	0	1
1700007B14Rik protein [Mus musculus]	0	1
heterogeneous nuclear ribonucleoprotein U, isoform CRA_b [Mus musculus]	1	0
mCG120998, isoform CRA_b [Mus musculus]	1	0
PREDICTED: similar to insulinoma protein (rig) isoform 1 [Mus musculus]	0	1
nuclear factor related to kappa B binding protein, isoform CRA_a [Mus musculus]	0	1
RIKEN cDNA 4930431B11, isoform CRA_a [Mus musculus]	1	0
Nuclear VCP-like [Mus musculus]	1	0
argininosuccinate lyase [Mus musculus]	0	1
unnamed protein product [Mus musculus]	1	0
chordin [Mus musculus]	0	1
RNA-binding protein PNO1 [Mus musculus]	1	0
unnamed protein product [Mus musculus]	1	0
Myb protein P42POP, isoform CRA_a [Mus musculus]	0	1
multiple ankyrin repeats, single KH-domain homolog [Mus musculus]	0	1
Cytoplasmic FMR1 interacting protein 1 [Mus musculus]	1	0
Plexin B2 [Mus musculus]	1	0
mCG130959 [Mus musculus]	0	1
suppression of tumorigenicity 5 protein isoform 1 [Mus musculus]	1	0
ATPase, class II, type 9A [Mus musculus]	0	1
zinc finger proten 607 [Mus musculus]	1	0
neuropilin 1, isoform CRA_a [Mus musculus]	0	1
unnamed protein product [Mus musculus]	0	1
PREDICTED: hypothetical protein [Mus musculus]	0	1
unnamed protein product [Mus musculus]	0	1

vimentin, isoform CRA_a [Mus musculus]	0	1
CDK105 protein [Rattus norvegicus]	1	0
heparan-alpha-glucosaminide N-acetyltransferase [Mus musculus]	0	1
mKIAA2013 protein [Mus musculus]	1	0
PREDICTED: hypothetical protein LOC68531 [Mus musculus]	1	0
PREDICTED: hypothetical protein LOC67170 [Mus musculus]	0	1
phosphoinositide 3-kinase regulatory subunit 6 isoform 1 [Mus musculus]	0	1
unnamed protein product [Mus musculus]	1	0
unnamed protein product [Mus musculus]	1	0
Nucleolin [Mus musculus]	1	0
succinate dehydrogenase complex, subunit C, integral membrane protein [Mus musculus]	0	1
proton-coupled amino acid transporter 1 [Mus musculus]	0	1
PREDICTED: similar to hCG1645909 [Mus musculus]	1	0
Msn protein [Mus musculus]	1	0
splicing factor 3B subunit 4 [Mus musculus]	0	1
mCG20427 [Mus musculus]	1	0
RNA polymerase II elongation factor ELL2 [Mus musculus]	1	0
non-receptor tyrosine kinase [Mus musculus]	1	0
uncharacterized serine/threonine-protein kinase SgK494 [Mus musculus]	0	1
arylacetamide deacetylase-like 3 [Mus musculus]	0	1
non-POU-domain-containing, octamer binding protein [Mus musculus]	1	0
mCG145123 [Mus musculus]	0	1
rotatin [Mus musculus]	1	0
ubiquitin carboxyl-terminal hydrolase isozyme L3 [Mus musculus]	1	0
PREDICTED: hypothetical protein [Mus musculus]	1	0
hypothetical protein B930041G04 [Mus musculus]	1	0
mCG1027331 [Mus musculus]	1	0
mCG12136, isoform CRA_d [Mus musculus]	0	1
5033413D22Rik protein [Mus musculus]	0	1
PREDICTED: hypothetical protein [Mus musculus]	1	0
mCG5258, isoform CRA_b [Mus musculus]	0	1
anti-DNA immunoglobulin heavy chain IgG [Mus musculus]	1	0
unnamed protein product [Mus musculus]	1	0
lethal(3)malignant brain tumor-like protein [Mus musculus]	1	0
mCG130077 [Mus musculus]	0	1
FYN binding protein, isoform CRA_b [Mus musculus]	1	0
Ankrd43 protein [Mus musculus]	1	0
mCG9260 [Mus musculus]	1	0
novel protein [Mus musculus]	1	0
serine/threonine-protein kinase N1 [Mus musculus]	1	0

Table II Mass-spec list of the M18bp1 FLAG IP. The number of unique spectra that were identified for each protein in the mass-spec analysis is indicated (Scaffold analysis).

gene	gene name	wt	K2A7	Diff
M18bp1	mis18-binding protein 1	0	184	184
Chd4	chromodomain-helicase-DNA-binding protein 4	0	69	69
Snrnp200	U5 small nuclear ribonucleoprotein 200 kDa helicase	0	61	61
Numa1	nuclear mitotic apparatus protein 1	0	54	54

Hnrnpm	heterogeneous nuclear ribonucleoprotein M	1	48	47
Baz1b	tyrosine-protein kinase BAZ1B	0	43	43
Spnb3	spectrin beta chain, brain 2	0	43	43
H2afy	core histone macro-H2A.1	0	37	37
CBX1	chromobox protein homolog 1	0	35	35
Nup160	nuclear pore complex protein Nup160	0	34	34
Rpl5	60S ribosomal protein L5	0	32	32
Tpr	nuclear pore complex-associated protein Tpr	0	32	32
Cbx5	chromobox protein homolog 5	0	30	30
Hist1h1d	histone H1.3	0	30	30
Ddx10	probable ATP-dependent RNA helicase DDX10	0	29	29
Flna	filamin-A	0	29	29
Oip5	protein Mis18-beta	0	29	29
Tjp1	tight junction protein ZO-1	0	29	29
Uhrf1	E3 ubiquitin-protein ligase UHRF1	0	29	29
Supt16h	FACT complex subunit SPT16	0	28	28
Trip12	thyroid hormone receptor interactor 12	0	28	28
Baz2a	bromodomain adjacent to zinc finger domain protein 2A	0	27	27
Utp18	U3 small nucleolar RNA-associated protein 18 homolog	0	27	27
Pogz	pogo transposable element with ZNF domain	0	26	26
Prpf40a	pre-mRNA-processing factor 40 homolog A	0	26	26
Smc3	structural maintenance of chromosomes protein 3	0	26	26
Utp15	U3 small nucleolar RNA-associated protein 15 homolog	0	26	26
Elavl1	ELAV-like protein 1	0	25	25
Pes1	pescadillo homolog	0	25	25
2610039C10Rik	protein Mis18-alpha	0	24	24
Atad2	ATPase family AAA domain-containing protein 2	0	24	24
Utf1	undifferentiated embryonic cell transcription factor 1	0	24	24
Igf2bp1	insulin-like growth factor 2 mRNA-binding protein 1	0	22	22
Orc1	origin recognition complex subunit 1	0	22	22
Rpl13a	60S ribosomal protein L13a	0	22	22
Tjp2	tight junction protein ZO-2	0	22	22
Gnb2l1	guanine nucleotide-binding protein subunit beta-2-like 1	0	21	21
Plk1	serine/threonine-protein kinase PLK1	0	21	21
Smarcc1	SWI/SNF complex subunit SMARCC1	0	21	21
Bms1	ribosome biogenesis protein BMS1 homolog	0	20	20
Cenpc1	centromere protein C 1	0	20	20
Fn1	fibronectin	0	20	20
Lin28a	protein lin-28 homolog A	0	19	19
Nol11	nucleolar protein 11	0	19	19
Zc3h18	zinc finger CCCH domain-containing protein 18	0	19	19
Aurkb	aurora kinase B	0	18	18
Ddx39	ATP-dependent RNA helicase DDX39A	0	18	18
Dhx37	probable ATP-dependent RNA helicase DHX37	0	18	18
Flii	protein flightless-1 homolog	0	18	18
Ruvbl2	ruvB-like 2	0	18	18
Cdca8	borealin	0	17	17
Cenpv	centromere protein V	0	17	17
Pcbp1	poly(rC)-binding protein 1	0	17	17

Rbm34	RNA-binding protein 34	0	17	17
Rrs1	ribosome biogenesis regulatory protein homolog	0	17	17
Smc1a	structural maintenance of chromosomes protein 1A	0	17	17
Syncrip	heterogeneous nuclear ribonucleoprotein Q	0	17	17
Utp3	something about silencing protein 10	0	17	17
Wdr12	ribosome biogenesis protein WDR12	0	17	17
Glyr1	putative oxidoreductase GLYR1	0	16	16
Hells	lymphocyte-specific helicase	0	16	16
Lamc1	laminin subunit gamma-1	0	16	16
Pabpc1	polyadenylate-binding protein 1	0	16	16
Rpl18	60S ribosomal protein L18	0	16	16
Sfpq	splicing factor, proline- and glutamine-rich	0	16	16
Slc25a5	ADP/ATP translocase 2	1	17	16
Actn1	alpha-actinin-1	0	15	15
Gnai2	guanine nucleotide-binding protein G(i) subunit alpha-2	0	15	15
Nol10	nucleolar protein 10	0	15	15
Nup155	nuclear pore complex protein Nup155	0	15	15
Terf1	telomeric repeat-binding factor 1	0	15	15
2610101N10Rik	U2 snRNP-associated SURP motif-containing protein	0	14	14
Lyar	cell growth-regulating nucleolar protein	0	14	14
Rpl7l1	60S ribosomal protein L7-like 1	0	14	14
Rps14	40S ribosomal protein S14	0	14	14
Rps16	40S ribosomal protein S16	1	15	14
SRSF10	serine/arginine-rich splicing factor 10	0	14	14
Vdac1	voltage-dependent anion-selective channel protein 1	0	14	14
Atrx	transcriptional regulator ATRX	0	13	13
Ddx56	probable ATP-dependent RNA helicase DDX56	0	13	13
Eif6	eukaryotic translation initiation factor 6	0	13	13
Emg1	ribosomal RNA small subunit methyltransferase NEP1	0	13	13
Hist1h1a	histone H1.1	0	13	13
Noc4l	nucleolar complex protein 4 homolog	0	13	13
Ptbp1	polypyrimidine tract-binding protein 1	0	13	13
Ruvbl1	ruvB-like 1	0	13	13
Vdac2	voltage-dependent anion-selective channel protein 2	0	13	13
Ahctf1	protein ELYS	0	12	12
Anxa6	annexin A6	0	12	12
D2Wsu81e	uncharacterized protein C9orf114 homolog	0	12	12
Ddx52	probable ATP-dependent RNA helicase DDX52	0	12	12
Eif3a	eukaryotic translation initiation factor 3 subunit A	1	13	12
Fxr1	fragile X mental retardation syndrome-related protein 1	0	12	12
Gnb2	guanine nucleotide-binding protein G(I)/G(S)/G(T) subunit beta-2	0	12	12
Impdh2	inosine-5'-monophosphate dehydrogenase 2	0	12	12
Polr2b	DNA-directed RNA polymerase II subunit RPB2	0	12	12
Rbbp4	histone-binding protein RBBP4	0	12	12
Rpf1	ribosome production factor 1	0	12	12
Skiv2l2	superkiller viralicidic activity 2-like 2	0	12	12
Trim27	zinc finger protein RFP	0	12	12
Lamb1	laminin subunit beta-1	0	11	11
Ngdn	neuroguidin	0	11	11

Psip1	PC4 and SFRS1-interacting protein	0	11	11
Rpl10	60S ribosomal protein L10	0	11	11
Rpl22	60S ribosomal protein L22	0	11	11
Set	protein SET	0	11	11
Snrnp70	U1 small nuclear ribonucleoprotein 70 kDa	0	11	11
Arglu1	arginine and glutamate-rich protein 1	0	10	10
Bysl	bystin	0	10	10
Cdh1	cadherin-1	0	10	10
Ezh2	histone-lysine N-methyltransferase EZH2	0	10	10
Hnrnpa0	heterogeneous nuclear ribonucleoprotein A0	0	10	10
Hsp90b1	endoplasmin	0	10	10
Imp4	U3 small nucleolar ribonucleoprotein protein IMP4	0	10	10
Larp7	la-related protein 7	0	10	10
Ppp1r9a	neurabin-1	0	10	10
Pycr2	pyrroline-5-carboxylate reductase 2	0	10	10
Rfc5	replication factor C subunit 5	0	10	10
Rpl24	60S ribosomal protein L24	0	10	10
Rrp1	ribosomal RNA processing protein 1 homolog A	0	10	10
Rsf1	remodeling and spacing factor 1	0	10	10
Srsf5	serine/arginine-rich splicing factor 5	0	10	10
Ssrp1	FACT complex subunit SSRP1	0	10	10
Stoml2	stomatin-like protein 2	0	10	10
Tkt	transketolase	0	10	10
Tmpo	lamina-associated polypeptide 2	0	10	10
Ywhag	14-3-3 protein gamma	0	10	10
1600021P15Rik	protein MB21D2	0	9	9
2310008H09Rik	protein C16orf88 homolog	0	9	9
Brix1	ribosome biogenesis protein BRX1 homolog	0	9	9
Incenp	inner centromere protein	0	9	9
Lrwd1	leucine-rich repeat and WD repeat-containing protein 1	0	9	9
Msh2	DNA mismatch repair protein Msh2	0	9	9
Myef2	myelin expression factor 2	0	9	9
Nup98	nucleoporin 98	0	9	9
Prpf19	pre-mRNA-processing factor 19	0	9	9
Rbm25	RNA-binding protein 25	0	9	9
Cacybp	calcyclin-binding protein	0	8	8
Cenpo	centromere protein O	0	8	8
Dcaf13	DDB1- and CUL4-associated factor 13	0	8	8
Ddx46	probable ATP-dependent RNA helicase DDX46	0	8	8
Dnmt3l	DNA (cytosine-5)-methyltransferase 3-like	0	8	8
Eif4a3	eukaryotic initiation factor 4A-III	0	8	8
Gar1	H/ACA ribonucleoprotein complex subunit 1	0	8	8
Gm6472	0	0	8	8
H2afy2	core histone macro-H2A.2	0	8	8
Hk2	hexokinase-2	0	8	8
Ilf2	interleukin enhancer-binding factor 2	0	8	8
Mad1l1	mitotic spindle assembly checkpoint protein MAD1	0	8	8
Mta2	metastasis-associated protein MTA2	0	8	8
Nop16	nucleolar protein 16	0	8	8

Phf17	protein Jade-1	0	8	8
Phip	PH-interacting protein	0	8	8
Polr2a	DNA-directed RNA polymerase II subunit RPB1	0	8	8
Ppp2r1a	serine/threonine-protein phosphatase 2A 65 kDa regulatory subunit A alpha isoform	0	8	8
Rps13	40S ribosomal protein S13	0	8	8
Snrpa1	0	0	8	8
Snrpb2	U2 small nuclear ribonucleoprotein B"	0	8	8
Supt6h	transcription elongation factor SPT6	0	8	8
Tdh	L-threonine 3-dehydrogenase, mitochondrial	0	8	8
Urb2	unhealthy ribosome biogenesis protein 2 homolog	0	8	8
Wdr18	WD repeat-containing protein 18	0	8	8
WDR5	WD repeat-containing protein 5	0	8	8
Zfp462	zinc finger protein 462	0	8	8
1110037F02Rik	protein virilizer homolog	0	7	7
2210011C24Rik	uncharacterized protein LOC70134	0	7	7
2810004N23Rik	uncharacterized protein C1orf131 homolog	0	7	7
Arpc1b	actin-related protein 2/3 complex subunit 1B	0	7	7
Cct6a	T-complex protein 1 subunit zeta	0	7	7
Coro1c	coronin-1C	0	7	7
Crnkl1	crooked neck-like protein 1	0	7	7
Ddb1	DNA damage-binding protein 1	0	7	7
Ddx3y	ATP-dependent RNA helicase DDX3Y	0	7	7
Dis3	exosome complex exonuclease RRP44	0	7	7
Exosc4	exosome complex component RRP41	0	7	7
Gsn	gelsolin	0	7	7
Hdac1	histone deacetylase 1	0	7	7
Hmga1	high mobility group protein HMG-I/HMG-Y	0	7	7
Hspg2	basement membrane-specific heparan sulfate proteoglycan core protein	0	7	7
Kif2a	kinesin-like protein KIF2A	0	7	7
Lbr	lamin-B receptor	0	7	7
Nup37	nucleoporin Nup37	0	7	7
Pcna	proliferating cell nuclear antigen	0	7	7
Ppih	peptidyl-prolyl cis-trans isomerase H	0	7	7
Rfc4	replication factor C subunit 4	0	7	7
Rps10	40S ribosomal protein S10	0	7	7
Rps23	40S ribosomal protein S23	0	7	7
Rrp15	RRP15-like protein	0	7	7
Senp3	sentrin-specific protease 3	0	7	7
Stk38	serine/threonine-protein kinase 38	0	7	7
Surf6	surfeit locus protein 6	0	7	7
Tcp1	T-complex protein 1 subunit alpha	0	7	7
Utp11l	probable U3 small nucleolar RNA-associated protein 11	0	7	7
Wdr43	WD repeat-containing protein 43	1	8	7
2310058A11Rik	0	0	6	6
Brd2	bromodomain-containing protein 2	0	6	6
Cdk1	cyclin-dependent kinase 1	0	6	6
Cdk105	ribosome biogenesis protein NSA2 homolog	0	6	6
D14Ertd668e	PHD finger protein 11	0	6	6
Diexf	digestive organ expansion factor homolog	0	6	6

Eif2s1	eukaryotic translation initiation factor 2 subunit 1	0	6	6
Eprs	bifunctional glutamate/proline--tRNA ligase	0	6	6
Hjurp	Holliday junction recognition protein	0	6	6
Ikbkap	elongator complex protein 1	0	6	6
Immt	mitochondrial inner membrane protein	0	6	6
Kpna2	importin subunit alpha-2	0	6	6
Krt71	keratin, type II cytoskeletal 71	0	6	6
Nacc1	nucleus accumbens-associated protein 1	0	6	6
Pak1ip1	p21-activated protein kinase-interacting protein 1	0	6	6
Rlf	zinc finger protein Rlf	0	6	6
RPS9	40S ribosomal protein S9	0	6	6
Sgol2	shugoshin-like 2	0	6	6
Slc25a4	ADP/ATP translocase 1	1	7	6
Stmn2	stathmin-2	0	6	6
Sugt1	suppressor of G2 allele of SKP1 homolog	0	6	6
Trim35	tripartite motif-containing protein 35	0	6	6
Usp9x	probable ubiquitin carboxyl-terminal hydrolase FAF-X	0	6	6
Wdr74	WD repeat-containing protein 74	0	6	6
Ywhah	14-3-3 protein eta	0	6	6
Zfp512	zinc finger protein 512	0	6	6
Zmym3	zinc finger MYM-type protein 3	0	6	6
Aars	alanine--tRNA ligase, cytoplasmic	0	5	5
Actr2	actin-related protein 2	0	5	5
Alyref	THO complex subunit 4	0	5	5
Cct3	T-complex protein 1 subunit gamma	0	5	5
Cct8	T-complex protein 1 subunit theta	0	5	5
Clk3	dual specificity protein kinase CLK3	0	5	5
Ctcf	transcriptional repressor CTCF	0	5	5
Ddx23	probable ATP-dependent RNA helicase DDX23	0	5	5
Ddx39b	spliceosome RNA helicase Ddx39b	0	5	5
Dppa4	developmental pluripotency-associated protein 4	0	5	5
Eed	polycomb protein EED	0	5	5
Eef1d	elongation factor 1-delta	0	5	5
Eef1g	elongation factor 1-gamma	0	5	5
Eif3d	eukaryotic translation initiation factor 3 subunit D	0	5	5
G3bp1	ras GTPase-activating protein-binding protein 1	0	5	5
Grwd1	glutamate-rich WD repeat-containing protein 1	0	5	5
Hat1	histone acetyltransferase type B catalytic subunit	0	5	5
Khdrbs1	KH domain-containing, RNA-binding, signal transduction-associated protein 1	0	5	5
Krr1	KRR1 small subunit processome component homolog	0	5	5
Mov10	putative helicase MOV-10	0	5	5
Ncapg2	condensin-2 complex subunit G2	0	5	5
Nono	non-POU domain-containing octamer-binding protein	0	5	5
Nup85	nuclear pore complex protein Nup85	0	5	5
Orc3	origin recognition complex subunit 3	0	5	5
Pbrm1	protein polybromo-1	0	5	5
Polr2e	DNA-directed RNA polymerases I, II, and III subunit RPABC1	0	5	5
Ppp1cb	serine/threonine-protein phosphatase PP1-beta catalytic subunit	0	5	5
Puf60	poly(U)-binding-splicing factor PUF60	0	5	5

Pwp1	periodic tryptophan protein 1 homolog	0	5	5
Rae1	mRNA export factor	0	5	5
Rfc2	replication factor C subunit 2	0	5	5
RPL27	60S ribosomal protein L27	0	5	5
RPL30	60S ribosomal protein L30	0	5	5
Rps2	40S ribosomal protein S2	0	5	5
Serbp1	plasminogen activator inhibitor 1 RNA-binding protein	0	5	5
Smu1	WD40 repeat-containing protein SMU1	0	5	5
Suz12	polycomb protein Suz12	0	5	5
Tubb4b	tubulin beta-4B chain	1	6	5
Ywhab	14-3-3 protein beta/alpha	1	6	5
1110003H02Rik	0	0	4	4
2610528E23Rik	uncharacterized protein C3orf26 homolog	0	4	4
4922501C03Rik	protein QN1 homolog	0	4	4
Aqr	intron-binding protein aquarius	0	4	4
Arpc3	actin-related protein 2/3 complex subunit 3	0	4	4
Asns	asparagine synthetase [glutamine-hydrolyzing]	0	4	4
C1qbp	complement component 1 Q subcomponent-binding protein, mitochondrial	0	4	4
Cenpi	centromere protein I	0	4	4
Ctnnb1	catenin beta-1	0	4	4
Cul4b	cullin-4B	0	4	4
Dimt1	probable dimethyladenosine transferase	0	4	4
Dnaja2	dnaJ homolog subfamily A member 2	0	4	4
Dnajc9	dnaJ homolog subfamily C member 9	0	4	4
Dnmt3a	DNA (cytosine-5)-methyltransferase 3A	0	4	4
Eef1b2	elongation factor 1-beta	0	4	4
Ehmt2	histone-lysine N-methyltransferase EHMT2	0	4	4
Esco2	N-acetyltransferase ESCO2	0	4	4
Gm10335	0	0	4	4
Gm3362	predicted gene, 100041478	0	4	4
Golgb1	golgi autoantigen, golgin subfamily b, macrogolgin 1	0	4	4
Gstm1	glutathione S-transferase Mu 1	0	4	4
Hdgfrp2	hepatoma-derived growth factor-related protein 2	0	4	4
Kif22	kinesin-like protein KIF22	0	4	4
Kri1	protein KRI1 homolog	0	4	4
Krt8	keratin, type II cytoskeletal 8	0	4	4
Lama1	laminin subunit alpha-1	0	4	4
Luc7l3	luc7-like protein 3	0	4	4
Mei4	meiosis-specific protein MEI4-like	0	4	4
Mlf1ip	centromere protein U	0	4	4
Ncaph2	condensin-2 complex subunit H2	0	4	4
Ncbp1	nuclear cap-binding protein subunit 1	0	4	4
Nol7	nucleolar protein 7	0	4	4
Npm3	nucleoplasmin-3	0	4	4
Nup214	nuclear pore complex protein Nup214	0	4	4
Nup88	nuclear pore complex protein Nup88	0	4	4
Pcm1	pericentriolar material 1 protein	0	4	4
Pdia3	protein disulfide-isomerase A3	0	4	4
Pds5b	sister chromatid cohesion protein PDS5 homolog B	0	4	4

Pdzd11	PDZ domain-containing protein 11	0	4	4
Polr2c	DNA-directed RNA polymerase II subunit RPB3	0	4	4
Ppp1cc	serine/threonine-protein phosphatase PP1-gamma catalytic subunit	0	4	4
Psmd13	26S proteasome non-ATPase regulatory subunit 13	0	4	4
Pspc1	paraspeckle component 1	0	4	4
Ranbp1	ran-specific GTPase-activating protein	0	4	4
Rfc3	replication factor C subunit 3	0	4	4
Rpl35	60S ribosomal protein L35	0	4	4
RPL36	60S ribosomal protein L36	0	4	4
Rprd1b	regulation of nuclear pre-mRNA domain-containing protein 1B	0	4	4
Rps17	40S ribosomal protein S17	0	4	4
Rps6	40S ribosomal protein S6	0	4	4
Rps6ka5	ribosomal protein S6 kinase alpha-5	0	4	4
Serpinb9	serine (or cysteine) proteinase inhibitor, clade B, member 9	0	4	4
Sin3a	paired amphipathic helix protein Sin3a	0	4	4
slc2a14	glucose transporter 14	0	4	4
Snd1	staphylococcal nuclease domain-containing protein 1	0	4	4
Snrnp40	U5 small nuclear ribonucleoprotein 40 kDa protein	0	4	4
SNRPN	small nuclear ribonucleoprotein-associated protein N	0	4	4
Snw1	SNW domain-containing protein 1	0	4	4
Srfbp1	serum response factor-binding protein 1	0	4	4
Ssfa2	sperm-specific antigen 2 homolog	0	4	4
Strap	serine-threonine kinase receptor-associated protein	0	4	4
Vps41	vacuolar protein sorting-associated protein 41 homolog	0	4	4
Xrn2	5'-3' exoribonuclease 2	0	4	4
Zdbf2	DBF4-type zinc finger-containing protein 2 homolog	0	4	4
Zfp280c	zinc finger protein 280C	0	4	4
3110082I17Rik	uncharacterized protein C7orf50 homolog	0	3	3
4930417G10Rik	UPF0638 protein C2orf84 homolog	0	3	3
Abt1	activator of basal transcription 1	0	3	3
Actl6a	actin-like protein 6A	0	3	3
Bcas2	pre-mRNA-splicing factor SPF27	0	3	3
Ccdc86	coiled-coil domain-containing protein 86	0	3	3
Cct2	T-complex protein 1 subunit beta	0	3	3
Cinp	cyclin-dependent kinase 2-interacting protein	0	3	3
Clta	clathrin light chain A	0	3	3
Cntln	centlein	0	3	3
Crat	carnitine O-acetyltransferase	0	3	3
CSNK2B	casein kinase II subunit beta	0	3	3
Ddx1	ATP-dependent RNA helicase DDX1	0	3	3
Ddx47	probable ATP-dependent RNA helicase DDX47	0	3	3
Ddx49	probable ATP-dependent RNA helicase DDX49	0	3	3
Eif2s3x	eukaryotic translation initiation factor 2 subunit 3, X-linked	0	3	3
Eif3b	eukaryotic translation initiation factor 3 subunit B	0	3	3
Exosc9	exosome complex component RRP45	0	3	3
Fmnl3	formin-like protein 3	0	3	3
Fmr1	fragile X mental retardation protein 1 homolog	0	3	3
Fscn1	fascin	0	3	3
G3bp2	ras GTPase-activating protein-binding protein 2	0	3	3

Gm10051	predicted gene, ENSMUSG00000058905	0	3	3
Gnl3l	guanine nucleotide-binding protein-like 3-like protein	0	3	3
H2afx	histone H2A.x	0	3	3
Hnrpdl	heterogeneous nuclear ribonucleoprotein D-like	0	3	3
Ik	protein Red	0	3	3
Ing5	inhibitor of growth protein 5	0	3	3
Inhba	inhibin beta A chain	0	3	3
Krt31	keratin, type I cuticular Ha1	0	3	3
Lonrf1	LON peptidase N-terminal domain and RING finger protein 1	0	3	3
Luc7l	putative RNA-binding protein Luc7-like 1	0	3	3
Magea10	melanoma-associated antigen 10	0	3	3
Magohb	protein mago nashi homolog 1-related	0	3	3
Mocs3	adenylyltransferase and sulfurtransferase MOCS3	0	3	3
Mrps15	28S ribosomal protein S15, mitochondrial	0	3	3
Mthfd1	C-1-tetrahydrofolate synthase, cytoplasmic	0	3	3
Myl12a	myosin light chain, regulatory B-like	1	4	3
Myo5a	unconventional myosin-Va	0	3	3
Nid2	nidogen-2	0	3	3
Palm3	paralemmin-3	0	3	3
Phb	prohibitin	0	3	3
Pno1	RNA-binding protein PNO1	0	3	3
Psma7	proteasome subunit alpha type-7	1	4	3
Rcc2	protein RCC2	0	3	3
Rmi1	recQ-mediated genome instability protein 1	0	3	3
Rnf2	E3 ubiquitin-protein ligase RING2	0	3	3
Rpl23	60S ribosomal protein L23	0	3	3
Rpl28-ps3	0	0	3	3
Rrp8	ribosomal RNA-processing protein 8	0	3	3
Sec13	protein SEC13 homolog	0	3	3
Slc25a13	calcium-binding mitochondrial carrier protein Aralar2	0	3	3
Snrpb	small nuclear ribonucleoprotein-associated protein B	0	3	3
Srrt	serrate RNA effector molecule homolog	0	3	3
Trim24	transcription intermediary factor 1-alpha	0	3	3
Uprt	uracil phosphoribosyltransferase homolog	1	4	3
Usp7	ubiquitin carboxyl-terminal hydrolase 7	0	3	3
Wdr81	WD repeat-containing protein 81	0	3	3
Wtap	pre-mRNA-splicing regulator WTAP	0	3	3
Zfp326	zinc finger protein 326	0	3	3
Zfp703	zinc finger protein 703	0	3	3
Zfp930	uncharacterized protein LOC234358	0	3	3
1200003J13Rik	0	0	2	2
1810008A18Rik	protein FAM207A	0	2	2
2310022A10Rik	uncharacterized protein C19orf47 homolog	0	2	2
2610027L16Rik	pumilio domain-containing protein C14orf21 homolog	0	2	2
2610509C24Rik	0	0	2	2
2700060E02Rik	UPF0568 protein C14orf166 homolog	0	2	2
4930432E11Rik	0	0	2	2
4930503B20Rik	uncharacterized protein LOC75015	0	2	2
4932418E24Rik	uncharacterized protein LOC329366	0	2	2

4933425J19Rik	0	0	2	2
4933425L11Rik	0	0	2	2
6030440G07Rik	0	0	2	2
9230104L09Rik	cystatin E2	0	2	2
Abhd11	abhydrolase domain-containing protein 11	0	2	2
Adar	double-stranded RNA-specific adenosine deaminase	0	2	2
Adnp	activity-dependent neuroprotector homeobox protein	0	2	2
Adnp2	ADNP homeobox protein 2	0	2	2
Akap8	A-kinase anchor protein 8	0	2	2
Akr1b3	aldose reductase	0	2	2
Alms1	Alstrom syndrome protein 1 homolog	0	2	2
Apol7a	apolipoprotein L 7a	0	2	2
Arap1	arf-GAP with Rho-GAP domain, ANK repeat and PH domain-containing protein 1	0	2	2
Arhgap12	rho GTPase-activating protein 12	0	2	2
Arpc1a	actin-related protein 2/3 complex subunit 1A	0	2	2
Arpc2	actin-related protein 2/3 complex subunit 2	0	2	2
Arpc5l	actin-related protein 2/3 complex subunit 5-like protein	0	2	2
Arxes1	signal peptidase complex subunit 3	0	2	2
Atad3a	ATPase family AAA domain-containing protein 3	1	3	2
Atg2a	autophagy-related protein 2 homolog A	0	2	2
Atic	bifunctional purine biosynthesis protein PURH	0	2	2
Atp13a1	probable cation-transporting ATPase 13A1	0	2	2
Atp5f1	ATP synthase subunit b, mitochondrial	0	2	2
Atxn10	ataxin-10	0	2	2
Basp1	brain acid soluble protein 1	0	2	2
Baz1a	0	0	2	2
Blzf1	Golgin-45	0	2	2
Bmp5	bone morphogenetic protein 5	0	2	2
Brd3	bromodomain-containing protein 3	0	2	2
Brd7	bromodomain-containing protein 7	0	2	2
C4a	sex-limited protein	0	2	2
Cad	carbamoyl-phosphate synthetase 2, aspartate transcarbamylase, and dihydroorotase	0	2	2
Canx	calnexin	0	2	2
Card9	caspase recruitment domain-containing protein 9	0	2	2
Carf	amyotrophic lateral sclerosis 2 chromosomal region candidate gene 8 protein homolog	0	2	2
Cars	cysteine--tRNA ligase, cytoplasmic	0	2	2
Cbx2	chromobox protein homolog 2	0	2	2
Ccdc50	coiled-coil domain-containing protein 50	0	2	2
Cct5	T-complex protein 1 subunit epsilon	0	2	2
Cd55	complement decay-accelerating factor, GPI-anchored	0	2	2
Celsr1	cadherin EGF LAG seven-pass G-type receptor 1	0	2	2
Cenpm	centromere protein M	0	2	2
Cenpt	centromere protein T	0	2	2
Cep68	centrosomal protein of 68 kDa	0	2	2
Cgnl1	cingulin-like protein 1	0	2	2
Chchd3	coiled-coil-helix-coiled-coil-helix domain-containing protein 3, mitochondrial	0	2	2
Chd1	chromodomain-helicase-DNA-binding protein 1	0	2	2
Chd2	chromodomain helicase DNA binding protein 2	0	2	2
Ciapin1	anamorsin	0	2	2

Clca3	calcium-activated chloride channel regulator 1	0	2	2
Cldn15	claudin-15	0	2	2
Cnn3	calponin-3	0	2	2
Cnnm2	metal transporter CNNM2	0	2	2
Cntnap5a	contactin-associated protein like 5-1	0	2	2
Col3a1	collagen alpha-1(III) chain	0	2	2
Col5a2	collagen alpha-2(V) chain	0	2	2
Cpne1	copine-1	0	2	2
Cpne3	copine-3	0	2	2
Csnk1a1	casein kinase I isoform alpha	0	2	2
Ctr9	RNA polymerase-associated protein CTR9 homolog	0	2	2
Cttnbp2	cortactin-binding protein 2	0	2	2
Cwc27	peptidyl-prolyl cis-trans isomerase CWC27 homolog	0	2	2
Dapk1	death-associated protein kinase 1	0	2	2
Dars	aspartate--tRNA ligase, cytoplasmic	0	2	2
Ddx25	ATP-dependent RNA helicase DDX25	0	2	2
Dhx30	putative ATP-dependent RNA helicase DHX30	0	2	2
Dmap1	DNA methyltransferase 1-associated protein 1	0	2	2
Dmwd	dystrophia myotonica WD repeat-containing protein	0	2	2
Dnahc5	dynein heavy chain 5, axonemal	0	2	2
Dnajc6	putative tyrosine-protein phosphatase auxilin	0	2	2
Dnalc4	dynein light chain 4, axonemal	0	2	2
Dock6	0	0	2	2
Dppa2	developmental pluripotency-associated protein 2	0	2	2
Dpy19l1	protein dpy-19 homolog 1	0	2	2
Dsn1	kinetochore-associated protein DSN1 homolog	0	2	2
E2f2	transcription factor E2F2	0	2	2
Edc4	enhancer of mRNA-decapping protein 4	0	2	2
Egfl6	epidermal growth factor-like protein 6	0	2	2
Ehd4	EH domain-containing protein 4	0	2	2
Ehmt1	histone-lysine N-methyltransferase EHMT1	0	2	2
Eif3c	eukaryotic translation initiation factor 3 subunit C	0	2	2
Elac1	zinc phosphodiesterase ELAC protein 1	0	2	2
Elavl3	ELAV-like protein 3	0	2	2
Emid1	EMI domain-containing protein 1	0	2	2
Eml4	echinoderm microtubule-associated protein-like 4	0	2	2
Enah	protein enabled homolog	0	2	2
Esco1	N-acetyltransferase ESCO1	0	2	2
Esrrb	steroid hormone receptor ERR2	0	2	2
Exoc6	exocyst complex component 6	0	2	2
F630043A04Rik	spindle and kinetochore-associated protein 3	0	2	2
Fam161b	protein FAM161B	0	2	2
Fam167a	protein FAM167A	0	2	2
Fam3c	protein FAM3C	0	2	2
Farsb	phenylalanine--tRNA ligase beta subunit	0	2	2
Fcf1	rRNA-processing protein FCF1 homolog	0	2	2
Fgd6	FYVE, RhoGEF and PH domain-containing protein 6	0	2	2
Fggy	FGGY carbohydrate kinase domain-containing protein	0	2	2
Flt3	receptor-type tyrosine-protein kinase FLT3	0	2	2

Fmn1	formin-1	0	2	2
Foxred1	FAD-dependent oxidoreductase domain-containing protein 1	0	2	2
Fyttd1	UAP56-interacting factor	0	2	2
Gcc2	GRIP and coiled-coil domain-containing protein 2	0	2	2
Gcnt3	beta-1,3-galactosyl-O-glycosyl-glycoprotein beta-1,6-N-acetylglucosaminyltransferase 3	0	2	2
Gdpd3	glycerophosphodiester phosphodiesterase domain-containing protein 3	0	2	2
Gfi1	zinc finger protein Gfi-1	0	2	2
Gjb3	gap junction beta-3 protein	0	2	2
Glg1	Golgi apparatus protein 1	0	2	2
Gltscr2	glioma tumor suppressor candidate region gene 2	0	2	2
Gm10725	0	0	2	2
Gm11703	0	0	2	2
Gm12569	0	0	2	2
Gm13213	0	0	2	2
Gm4617	0	0	2	2
Gm9234	predicted gene, EG668548	0	2	2
Gpatch4	G patch domain-containing protein 4	0	2	2
Gpr179	probable G-protein coupled receptor 179	0	2	2
Gramd1b	GRAM domain-containing protein 1B	0	2	2
Gstz1	maleylacetoacetate isomerase	0	2	2
Gtl3	UPF0468 protein C16orf80 homolog	0	2	2
Gzf1	GDNF-inducible zinc finger protein 1	0	2	2
H2AFZ	histone H2A.Z	0	2	2
Habp4	intracellular hyaluronan-binding protein 4	0	2	2
Hba-a1	hemoglobin subunit alpha	0	2	2
Hbegf	proheparin-binding EGF-like growth factor	0	2	2
Hist1h1c	histone H1.2	0	2	2
HIST1H2AD	histone H2A type 1-D	1	3	2
Hmgb2	high mobility group protein B2	0	2	2
Hmgn1	non-histone chromosomal protein HMG-14	0	2	2
Hsd17b2	estradiol 17-beta-dehydrogenase 2	0	2	2
Hspa4	heat shock 70 kDa protein 4	0	2	2
Iars	isoleucine--tRNA ligase, cytoplasmic	0	2	2
Ift122	intraflagellar transport protein 122 homolog	0	2	2
Igdcc4	immunoglobulin superfamily DCC subclass member 4	0	2	2
Igf2bp3	insulin-like growth factor 2 mRNA-binding protein 3	0	2	2
Il12rb2	interleukin-12 receptor subunit beta-2	0	2	2
Irgm2	interferon inducible GTPase 2	0	2	2
Itpr2	inositol 1,4,5-trisphosphate receptor type 2	0	2	2
Jarid2	protein Jumonji	0	2	2
Kif20b	kinesin-like protein KIF20B	0	2	2
Kif3a	kinesin-like protein KIF3A	0	2	2
Kif9	kinesin-like protein KIF9	0	2	2
Krt12	keratin, type I cytoskeletal 12	0	2	2
Krt28	keratin, type I cytoskeletal 28	0	2	2
Krt72-ps	keratin, type II cytoskeletal 72	0	2	2
Lce1e	late cornified envelope protein family member	0	2	2
Lgals3bp	galectin-3-binding protein	0	2	2
Lgmn	legumain	0	2	2

Lipi	lipase I	0	2	2
LOC100044627	0	0	2	2
LOC100045924	0	0	2	2
LOC100047183	0	0	2	2
LOC100047252	0	0	2	2
LOC631302	0	0	2	2
Lrig3	leucine-rich repeats and immunoglobulin-like domains protein 3	0	2	2
Lrpprc	leucine-rich PPR motif-containing protein, mitochondrial	0	2	2
Map4k3	mitogen-activated protein kinase kinase kinase kinase 3	0	2	2
Mapkapk5	MAP kinase-activated protein kinase 5	0	2	2
Marcksl1	MARCKS-related protein	0	2	2
Mdn1	midasin	0	2	2
Meaf6	chromatin modification-related protein MEAF6	0	2	2
Mettl11a	alpha N-terminal protein methyltransferase 1A	0	2	2
Mical3	protein-methionine sulfoxide oxidase MICAL3	0	2	2
Mllt4	afadin	0	2	2
Mphosph8	M-phase phosphoprotein 8	0	2	2
Mpp2	MAGUK p55 subfamily member 2	0	2	2
Mrps7	28S ribosomal protein S7, mitochondrial	0	2	2
Mta1	metastasis-associated protein MTA1	0	2	2
Mtch1	mitochondrial carrier homolog 1	0	2	2
Mtch2	mitochondrial carrier homolog 2	0	2	2
Myo9b	unconventional myosin-IXb	0	2	2
Myt1l	myelin transcription factor 1-like protein	0	2	2
N4bp3	NEDD4-binding protein 3	0	2	2
Nars2	probable asparagine--tRNA ligase, mitochondrial	0	2	2
Nes	nestin	0	2	2
Nhsl2	NHS-like protein 2	0	2	2
Nip7	60S ribosome subunit biogenesis protein NIP7 homolog	0	2	2
Nisch	nischarin	0	2	2
Nle1	notchless protein homolog 1	0	2	2
Nlrp3	NACHT, LRR and PYD domains-containing protein 3	0	2	2
Nol8	nucleolar protein 8	0	2	2
Nppb	natriuretic peptides B	0	2	2
Nrf1	nuclear respiratory factor 1	0	2	2
Nub1	NEDD8 ultimate buster 1	0	2	2
Nucks1	nuclear ubiquitous casein and cyclin-dependent kinases substrate	0	2	2
Nudt13	nucleoside diphosphate-linked moiety X motif 13	0	2	2
Nup35	nucleoporin NUP53	0	2	2
Nup50	nuclear pore complex protein Nup50	0	2	2
Odf2l	outer dense fiber protein 2-like	0	2	2
Olfr1496	olfactory receptor 1496	0	2	2
Olfr95	olfactory receptor 95	0	2	2
Pa2g4	proliferation-associated protein 2G4	0	2	2
Pabpc4	polyadenylate-binding protein 4	0	2	2
Parp2	poly [ADP-ribose] polymerase 2	0	2	2
Pcbp2	poly(rC)-binding protein 2	0	2	2
Pdcd5	programmed cell death protein 5	0	2	2
Pdgfc	platelet-derived growth factor C	0	2	2

Pgk2	phosphoglycerate kinase 2	0	2	2
Phgdh	D-3-phosphoglycerate dehydrogenase	0	2	2
Pik3cb	phosphatidylinositol-4,5-bisphosphate 3-kinase catalytic subunit beta isoform	0	2	2
Pin4	peptidyl-prolyl cis-trans isomerase NIMA-interacting 4	0	2	2
Pinx1	PIN2/TERF1-interacting telomerase inhibitor 1	0	2	2
Pitpnm3	membrane-associated phosphatidylinositol transfer protein 3	0	2	2
Plaa	phospholipase A-2-activating protein	0	2	2
Plch1	1-phosphatidylinositol-4,5-bisphosphate phosphodiesterase eta-1	0	2	2
Polk	DNA polymerase kappa	0	2	2
Polr1c	DNA-directed RNA polymerases I and III subunit RPAC1	0	2	2
Polr1d	DNA-directed RNA polymerases I and III subunit RPAC2	0	2	2
Pou5f1	POU domain, class 5, transcription factor 1	0	2	2
Ppp2cb	serine/threonine-protein phosphatase 2A catalytic subunit beta isoform	0	2	2
Ppp3cc	serine/threonine-protein phosphatase 2B catalytic subunit gamma isoform	1	3	2
Prkdc	DNA-dependent protein kinase catalytic subunit	0	2	2
Prpf38a	pre-mRNA-splicing factor 38A	0	2	2
Psat1	phosphoserine aminotransferase	0	2	2
Psma2	proteasome subunit alpha type-2	0	2	2
Psma6	proteasome subunit alpha type-6	0	2	2
Psmd14	26S proteasome non-ATPase regulatory subunit 14	0	2	2
Ptges3	prostaglandin E synthase 3	0	2	2
Ptma	prothymosin alpha	0	2	2
Qk	protein quaking	0	2	2
Rars2	probable arginine--tRNA ligase, mitochondrial	0	2	2
Rbbp7	histone-binding protein RBBP7	0	2	2
Rbm44	RNA-binding protein 44	0	2	2
Rbm8a	RNA-binding protein 8A	0	2	2
Rbpms	RNA-binding protein with multiple splicing	0	2	2
Rbpms2	RNA-binding protein with multiple splicing 2	0	2	2
Rif1	telomere-associated protein RIF1	0	2	2
Rpa1	replication protein A 70 kDa DNA-binding subunit	0	2	2
Rpa2	replication protein A 32 kDa subunit	0	2	2
Rpgrip1	X-linked retinitis pigmentosa GTPase regulator-interacting protein 1	0	2	2
Rpl29-ps5	0	0	2	2
Rpl35a	60S ribosomal protein L35a	0	2	2
Rpl38	60S ribosomal protein L38	0	2	2
Rpp30	ribonuclease P protein subunit p30	0	2	2
RPS20	40S ribosomal protein S20	0	2	2
Rps25-ps1	0	1	3	2
RPS27	40S ribosomal protein S27	0	2	2
Rras2	ras-related protein R-Ras2	0	2	2
Rwdd2b	RWD domain-containing protein 2B	0	2	2
Sae1	SUMO-activating enzyme subunit 1	0	2	2
Sall4	sal-like protein 4	0	2	2
Sap30	histone deacetylase complex subunit SAP30	0	2	2
Sart1	U4/U6.U5 tri-snRNP-associated protein 1	0	2	2
Sbno1	protein strawberry notch homolog 1	0	2	2
Scaf11	splicing factor, arginine/serine-rich 2, interacting protein	0	2	2
Scpep1	retinoid-inducible serine carboxypeptidase	0	2	2

Seh1l	nucleoporin SEH1	0	2	2
Serpinc1	antithrombin-III	0	2	2
Shf	SH2 domain-containing adapter protein F	0	2	2
Slc26a10	solute carrier family 26 member 10	0	2	2
Slc38a1	sodium-coupled neutral amino acid transporter 1	0	2	2
Slc3a2	4F2 cell-surface antigen heavy chain	0	2	2
Slfn2	schlafen family member 12-like	0	2	2
Slfn4	schlafen 4	0	2	2
Sltm	SAFB-like transcription modulator	0	2	2
Smarcd2	SWI/SNF-related matrix-associated actin-dependent regulator of chromatin subfamily D member 2	0	2	2
Smarce1	SWI/SNF-related matrix-associated actin-dependent regulator of chromatin subfamily E member 1	0	2	2
Snrk	SNF-related serine/threonine-protein kinase	0	2	2
Soat1	sterol O-acyltransferase 1	0	2	2
Son	protein SON	0	2	2
Spata18	mitochondria-eating protein	0	2	2
Spata24	spermatogenesis-associated protein 24	0	2	2
Sphk1	sphingosine kinase 1	0	2	2
Sri	sorcin	0	2	2
Srsf11	splicing factor, arginine/serine-rich 11	0	2	2
Stag2	cohesin subunit SA-2	0	2	2
Supt5h	transcription elongation factor SPT5	0	2	2
Suv39h2	histone-lysine N-methyltransferase SUV39H2	0	2	2
Syce1l	synaptonemal complex central element protein 1-like	0	2	2
Taldo1	transaldolase	0	2	2
Tcirg1	T-cell, immune regulator 1	0	2	2
Terf2	telomeric repeat-binding factor 2	0	2	2
Tet1	methylcytosine dioxygenase TET1	0	2	2
Tex11	testis-expressed sequence 11 protein	0	2	2
Tex15	testis expressed gene 15	0	2	2
Tex9	testis-expressed sequence 9 protein	0	2	2
Thoc6	THO complex subunit 6 homolog	0	2	2
Timm50	mitochondrial import inner membrane translocase subunit TIM50	0	2	2
Tmco5b	transmembrane and coiled-coil domain-containing protein 5B	0	2	2
Tmem199	transmembrane protein 199	0	2	2
Tmem209	transmembrane protein 209	0	2	2
Traf3ip1	TRAF3-interacting protein 1	0	2	2
Trim58	tripartite motif-containing protein 58	0	2	2
Trove2	60 kDa SS-A/Ro ribonucleoprotein	0	2	2
Trp53bp1	tumor suppressor p53-binding protein 1	0	2	2
Trrap	transformation/transcription domain-associated protein	0	2	2
Tshz1	teashirt homolog 1	0	2	2
Ttc14	tetratricopeptide repeat protein 14	0	2	2
Ttc30a1	tetratricopeptide repeat protein 30A1	0	2	2
Ttf1	transcription termination factor 1	0	2	2
Tulp4	tubby-related protein 4	0	2	2
Tusc5	tumor suppressor candidate 5 homolog	0	2	2
Txlna	alpha-taxilin	0	2	2
Txnl1	thioredoxin-like protein 1	0	2	2

Ube2v1	ubiquitin-conjugating enzyme E2 variant 1	0	2	2
Ubqln3	ubiquilin-3	0	2	2
Usp-ps	0	0	2	2
Vps72	vacuolar protein sorting-associated protein 72 homolog	0	2	2
Wipi2	WD repeat domain phosphoinositide-interacting protein 2	0	2	2
Xbp1	X-box-binding protein 1	0	2	2
Xpo1	exportin-1	0	2	2
Xrcc5	X-ray repair cross-complementing protein 5	0	2	2
Xrcc6	X-ray repair cross-complementing protein 6	0	2	2
Yap1	yorkie homolog	0	2	2
Zdhhc23	probable palmitoyltransferase ZDHHC23	0	2	2
Zfml	zinc finger protein 638	0	2	2
Zfp157	zinc finger protein 157	0	2	2
Zfp27	zinc finger protein 27	0	2	2
Zfp292	zinc finger protein 292	0	2	2
Zfp335	zinc finger protein 335	0	2	2
Zhx3	zinc fingers and homeoboxes protein 3	0	2	2
Zmynd12	zinc finger, MYND domain containing 12	0	2	2
Zscan10	zinc finger and SCAN domain-containing protein 10	0	2	2
1810019E15Rik	0	0	1	1
2610029M16Rik	0	0	1	1
4932429P05Rik	SMEK homolog 3, putative	0	1	1
9830107B12Rik	RIKEN cDNA 9830107B12	0	1	1
Acss1	acetyl-coenzyme A synthetase 2-like, mitochondrial	0	1	1
Adat3	tRNA-specific adenosine deaminase-like protein 3	0	1	1
Adrm1	proteasomal ubiquitin receptor ADRM1	0	1	1
Ahdc1	AT-hook DNA-binding motif-containing protein 1	0	1	1
AK020040	0	0	1	1
Ankrd60	ankyrin repeat domain-containing protein 60	0	1	1
Anp32a	acidic leucine-rich nuclear phosphoprotein 32 family member A	0	1	1
Arid3b	AT-rich interactive domain-containing protein 3B	0	1	1
Arl10	ADP-ribosylation factor-like protein 10	0	1	1
Atad2b	ATPase family AAA domain-containing protein 2B	0	1	1
Atp13a2	probable cation-transporting ATPase 13A2	0	1	1
Atp5o	ATP synthase subunit O, mitochondrial	0	1	1
Bard1	BRCA1-associated RING domain protein 1	0	1	1
Bmx	cytoplasmic tyrosine-protein kinase BMX	0	1	1
C1ra	complement C1r-A subcomponent	0	1	1
C86695	uncharacterized protein LOC97476	0	1	1
C87222	0	1	2	1
Cacng4	voltage-dependent calcium channel gamma-4 subunit	0	1	1
Cct4	T-complex protein 1 subunit delta	0	1	1
Cenpb	major centromere autoantigen B	0	1	1
Cenpq	centromere protein Q	0	1	1
Cherp	calcium homeostasis endoplasmic reticulum protein	0	1	1
Cmas	N-acylneuraminate cytidylyltransferase	0	1	1
Cox4nb	ER membrane protein complex subunit 8	0	1	1
D14Abb1e	protein FAM208A	0	1	1
Dcaf7	DDB1- and CUL4-associated factor 7	0	1	1

Ddx50	ATP-dependent RNA helicase DDX50	0	1	1
Dek	protein DEK	0	1	1
Des	desmin	0	1	1
Dnaja3	dnaJ homolog subfamily A member 3, mitochondrial	0	1	1
Drg1	developmentally-regulated GTP-binding protein 1	0	1	1
Ehhadh	peroxisomal bifunctional enzyme	0	1	1
Eif3h	eukaryotic translation initiation factor 3 subunit H	0	1	1
Eml5	echinoderm microtubule-associated protein-like 5	0	1	1
Esrra	steroid hormone receptor ERR1	0	1	1
Etf1	eukaryotic peptide chain release factor subunit 1	0	1	1
Farsa	phenylalanine--tRNA ligase alpha subunit	0	1	1
Fkbp4	peptidyl-prolyl cis-trans isomerase FKBP4	0	1	1
Fxr2	fragile X mental retardation syndrome-related protein 2	0	1	1
Gadd45gip1	growth arrest and DNA damage-inducible proteins-interacting protein 1	1	2	1
Gal3st2	galactose-3-O-sulfotransferase 2	0	1	1
Glud1	glutamate dehydrogenase 1, mitochondrial	0	1	1
Gm10044	0	0	1	1
Gm101	primary ciliary dyskinesia protein 1	1	2	1
Gm11810	predicted gene, OTTMUSG00000004420	0	1	1
Gm12335	0	0	1	1
Gm13119	uncharacterized protein LOC433779	0	1	1
Gm4764	0	0	1	1
Gm4952	glycine N-acyltransferase-like protein	0	1	1
Gm4963	0	1	2	1
Gm6091	0	0	1	1
Gm9774	0	0	1	1
Gps1	COP9 signalosome complex subunit 1	0	1	1
Grtp1	growth hormone-regulated TBC protein 1	0	1	1
Hist1h2aa	histone cluster 1, H2aa	0	1	1
Hist1h2bj	histone H2B type 1-F/J/L	0	1	1
Hmga1-rs1	high mobility group protein HMG-I/HMG-Y	0	1	1
Hnrnph2	heterogeneous nuclear ribonucleoprotein H2	0	1	1
Hnrnpr	heterogeneous nuclear ribonucleoprotein R	1	2	1
Hnrpll	heterogeneous nuclear ribonucleoprotein L-like	0	1	1
Hps3	Hermansky-Pudlak syndrome 3 protein homolog	0	1	1
Igf2bp2	insulin-like growth factor 2 mRNA-binding protein 2	0	1	1
Ina	alpha-internexin	0	1	1
Iqgap1	ras GTPase-activating-like protein IQGAP1	0	1	1
Isy1	pre-mRNA-splicing factor ISY1 homolog	0	1	1
Kars	lysine--tRNA ligase	0	1	1
Kdm1a	lysine-specific histone demethylase 1A	0	1	1
Keap1	kelch-like ECH-associated protein 1	0	1	1
Kif20a	kinesin-like protein KIF20A	0	1	1
L1td1	LINE-1 type transposase domain-containing protein 1	0	1	1
Lap3	cytosol aminopeptidase	0	1	1
LOC100046151	0	0	1	1
LOC100048062	0	0	1	1
LOC638399	0	0	1	1
Mcc	mutated in colorectal cancers	0	1	1

Mcm3ap	80 kDa MCM3-associated protein	0	1	1
Mrpl16	39S ribosomal protein L16, mitochondrial	0	1	1
Naca	nascent polypeptide-associated complex subunit alpha	1	2	1
Nap1l1	nucleosome assembly protein 1-like 1	0	1	1
Nkrf	NF-kappa-B-repressing factor	0	1	1
NOP10	H/ACA ribonucleoprotein complex subunit 3	0	1	1
Npm1	nucleophosmin	0	1	1
Nsa2	ribosome biogenesis protein NSA2 homolog	0	1	1
Nsd1	histone-lysine N-methyltransferase, H3 lysine-36 and H4 lysine-20 specific	0	1	1
Orc4	origin recognition complex subunit 4	0	1	1
Pabpn1	polyadenylate-binding protein 2	0	1	1
Paf1	RNA polymerase II-associated factor 1 homolog	0	1	1
Pcdh11x	protocadherin 11 X-linked	0	1	1
Pdia4	protein disulfide-isomerase A4	0	1	1
Pkm	pyruvate kinase isozymes M1/M2	0	1	1
Plrg1	pleiotropic regulator 1	0	1	1
Pnlip	pancreatic triacylglycerol lipase	0	1	1
Poldip3	polymerase delta-interacting protein 3	0	1	1
Ppfibp2	liprin-beta-2	0	1	1
Ppil1	peptidyl-prolyl cis-trans isomerase-like 1	0	1	1
Pramef12	PRAME family member 12	0	1	1
Prex1	phosphatidylinositol 3,4,5-trisphosphate-dependent Rac exchanger 1 protein	0	1	1
Prmt1	protein arginine N-methyltransferase 1	0	1	1
Psmc6	26S protease regulatory subunit 10B	0	1	1
Psmd2	26S proteasome non-ATPase regulatory subunit 2	0	1	1
Rab13	ras-related protein Rab-13	0	1	1
Racgap1	rac GTPase-activating protein 1	0	1	1
Rad51l1	DNA repair protein RAD51 homolog 2	0	1	1
Ralyl	RNA-binding Raly-like protein	0	1	1
Rbfox2	RNA binding protein fox-1 homolog 2	0	1	1
Rbm14	RNA-binding protein 14	0	1	1
Renbp	N-acylglucosamine 2-epimerase	0	1	1
Rgs7	regulator of G-protein signaling 7	0	1	1
Rpl28	60S ribosomal protein L28	0	1	1
Rpl31	60S ribosomal protein L31	0	1	1
Rpl36a	60S ribosomal protein L36a	0	1	1
Rpl36a-ps1	0	0	1	1
Rplp1	60S acidic ribosomal protein P1	0	1	1
RPS12	40S ribosomal protein S12	0	1	1
Rps18	40S ribosomal protein S18	1	2	1
Rps24	40S ribosomal protein S24	0	1	1
RPS28	40S ribosomal protein S28	0	1	1
Safb	scaffold attachment factor B1	0	1	1
Sh3d20	0	0	1	1
Slc25a12	calcium-binding mitochondrial carrier protein Aralar1	0	1	1
SMARCB1	SWI/SNF-related matrix-associated actin-dependent regulator of chromatin subfamily B member 1	0	1	1
Snrpd3	small nuclear ribonucleoprotein Sm D3	0	1	1
Snrpe	small nuclear ribonucleoprotein E	0	1	1
Snrpf	small nuclear ribonucleoprotein F	0	1	1

Sntb2	beta-2-syntrophin	0	1	1
Srbd1	S1 RNA-binding domain-containing protein 1	0	1	1
Sumo2	small ubiquitin-related modifier 2	0	1	1
Tex10	testis-expressed sequence 10 protein	0	1	1
Tk1	thymidine kinase, cytosolic	0	1	1
Tpt1	translationally-controlled tumor protein	0	1	1
Tpx2	targeting protein for Xklp2	0	1	1
Tspan11	tetraspanin-11	0	1	1
Ttc17	tetratricopeptide repeat domain 17	0	1	1
Tuba1a	tubulin alpha-1A chain	0	1	1
Tubb2b	tubulin beta-2B chain	0	1	1
Uba1	ubiquitin-like modifier-activating enzyme 1	0	1	1
Ubap2l	ubiquitin-associated protein 2-like	0	1	1
Uncx	homeobox protein unc-4 homolog	0	1	1
Vdac3	voltage-dependent anion-selective channel protein 3	0	1	1
Wdr65	WD repeat-containing protein 65	0	1	1
Wdr72	WD repeat domain 72	0	1	1
Xk	membrane transport protein XK	0	1	1
Yrdc	yrdC domain-containing protein, mitochondrial	0	1	1
Zc3h11a	zinc finger CCCH domain-containing protein 11A	1	2	1
Zc3h3	zinc finger CCCH domain-containing protein 3	0	1	1
Zfyve26	zinc finger FYVE domain-containing protein 26	1	2	1

Table III Mass-spec list of the Suv4-20h2 GST pulldown assays. The number of unique spectra that were identified for each protein in the mass-spec analysis is indicated (Scaffold analysis).

gene	**name**	**GST**	**M5**	**M7**	**delta**
Suv420h2	histone-lysine N-methyltransferase SUV420H2	4	112	62	108
Lmnb1	lamin-B1	1	82	75	81
Top2a	DNA topoisomerase 2-alpha	0	49	0	49
Cbx5	chromobox protein homolog 5	0	41	0	41
Hnrnpu	heterogeneous nuclear ribonucleoprotein U	2	43	4	41
CBX1	chromobox protein homolog 1	0	40	0	40
Plec	plectin	0	40	8	40
CBX3	chromobox protein homolog 3	1	40	0	39
Jup	junction plakoglobin	4	37	13	33
Mybbp1a	myb-binding protein 1A	0	30	0	30
Ahnak	AHNAK nucleoprotein	4	34	13	30
Krt31	keratin, type I cuticular Ha1	0	29	0	29
Ddx21	nucleolar RNA helicase 2	0	28	0	28
Nop58	nucleolar protein 58	0	23	0	23
Ncl	nucleolin	1	24	1	23
Nop56	nucleolar protein 56	0	23	12	23
5430421N2	type II hair keratin	1	20	2	19
Eef2	elongation factor 2	0	19	8	19
Hnrnpa3	heterogeneous nuclear ribonucleoprotein A3	4	23	12	19
Ddx5	probable ATP-dependent RNA helicase DDX5	4	22	1	18
Cltc	clathrin heavy chain 1	0	18	3	18
Vcl	vinculin	0	18	4	18
Acly	ATP-citrate synthase	0	18	5	18
Nup93	nuclear pore complex protein Nup93	0	16	0	16
Fasn	fatty acid synthase	0	16	3	16

Nolc1	nucleolar and coiled-body phosphoprotein 1	0	15	0	15
Hsp90b1	endoplasmin	2	17	8	15
Nup107	nuclear pore complex protein Nup107	0	14	0	14
Tpr	nuclear pore complex-associated protein Tpr	0	14	0	14
Nedd4	E3 ubiquitin-protein ligase NEDD4	0	14	3	14
Ddx3x	ATP-dependent RNA helicase DDX3X	2	15	0	13
Smarca5	SWI/SNF-related matrix-associated actin-dependent regulator of chromatin	0	12	0	12
Ranbp2	E3 SUMO-protein ligase RanBP2	0	12	3	12
Vcp	transitional endoplasmic reticulum ATPase	2	14	6	12
Spna2	spectrin alpha chain, brain	0	12	6	12
Vdac2	voltage-dependent anion-selective channel protein 2	3	14	1	11
Myh9	myosin-9	0	11	3	11
Atrx	transcriptional regulator ATRX	0	10	0	10
Ddost	dolichyl-diphosphooligosaccharide--protein glycosyltransferase 48 kDa subunit	0	10	0	10
Las1l	protein LAS1 homolog	0	10	0	10
Nup85	nuclear pore complex protein Nup85	0	10	0	10
Nup98	nucleoporin 98	0	10	0	10
Snrnp200	U5 small nuclear ribonucleoprotein 200 kDa helicase	0	10	0	10
Ephx1	epoxide hydrolase 1	4	14	1	10
Vars	valyl-tRNA synthetase	0	10	2	10
Col1a1	collagen alpha-1(I) chain	2	12	4	10
Actn1	alpha-actinin-1	2	12	6	10
Hnrnpul2	heterogeneous nuclear ribonucleoprotein U-like protein 2	0	9	1	9
Trim28	transcription intermediary factor 1-beta	0	9	1	9
Eef1b2	elongation factor 1-beta	3	12	3	9
Spnb2	spectrin beta chain, brain 1	0	9	4	9
Krt77	keratin, type II cytoskeletal 1b	4	13	6	9
Nat10	N-acetyltransferase 10	0	8	0	8
Orc1	origin recognition complex subunit 1	0	8	0	8
Pwp2	periodic tryptophan protein 2 homolog	0	8	0	8
Eprs	bifunctional aminoacyl-tRNA synthetase	0	8	1	8
Nup205	nucleoporin 205	0	8	1	8
Canx	calnexin	2	10	5	8
Krt78	keratin Kb40	4	12	6	8
Hist1h3e	histone H3.2	1	9	9	8
Rif1	telomere-associated protein RIF1	1	8	0	7
Mcm3	DNA replication licensing factor MCM3	0	7	0	7
Tcof1	treacle protein	0	7	0	7
Vdac1	voltage-dependent anion-selective channel protein 1	3	10	1	7
Eif3c	eukaryotic translation initiation factor 3 subunit C	0	7	1	7
Smc1a	structural maintenance of chromosomes protein 1A	0	7	1	7
Rpl5	60S ribosomal protein L5	2	8	0	6
Mki67	antigen KI-67	0	6	0	6
Ptbp1	polypyrimidine tract-binding protein 1	0	6	0	6
Ruvbl1	ruvB-like 1	0	6	0	6
Sf3b1	splicing factor 3B subunit 1	0	6	0	6
Tmpo	lamina-associated polypeptide 2	0	6	0	6
Uqcrc1	cytochrome b-c1 complex subunit 1, mitochondrial	0	6	0	6
Alb	serum albumin	2	8	2	6
Ndufs1	NADH-ubiquinone oxidoreductase 75 kDa subunit, mitochondrial	0	6	2	6
Top2b	DNA topoisomerase 2-beta	2	8	3	6
Rrbp1	ribosome-binding protein 1	0	6	3	6
Snd1	staphylococcal nuclease domain-containing protein 1	0	6	3	6
Stt3a	dolichyl-diphosphooligosaccharide--protein glycosyltransferase subunit STT3A	0	6	3	6
Aldh18a1	delta-1-pyrroline-5-carboxylate synthase	0	6	4	6
LOC10004		0	6	4	6
Krt75	keratin, type II cytoskeletal 75	1	7	5	6
Insrr	insulin receptor-related protein	2	8	7	6
Krt13	keratin, type I cytoskeletal 13	0	6	7	6
Hnrnpl	heterogeneous nuclear ribonucleoprotein L	2	7	0	5
Ddx17	probable ATP-dependent RNA helicase DDX17	0	5	0	5
Mcm5	DNA replication licensing factor MCM5	0	5	0	5

Numa1	nuclear mitotic apparatus protein 1	0	5	0	5
Otc	ornithine carbamoyltransferase, mitochondrial	0	5	0	5
Pdcd11	protein RRP5 homolog	0	5	0	5
Sf3a1	splicing factor 3A subunit 1	0	5	0	5
Sf3b2	splicing factor 3b, subunit 2	0	5	0	5
Wdr3	WD repeat-containing protein 3	0	5	0	5
Ddx3y	ATP-dependent RNA helicase DDX3Y	2	7	1	5
Lyz1	lysozyme C-1	3	8	2	5
Sfn	14-3-3 protein sigma	0	5	2	5
Dnmt3b	DNA (cytosine-5)-methyltransferase 3B	0	5	3	5
Hnrnpa2b1	heterogeneous nuclear ribonucleoproteins A2/B1	4	9	6	5
Fam161b	protein FAM161B	1	5	0	4
2610101N1	U2 snRNP-associated SURP motif-containing protein	0	4	0	4
Acin1	apoptotic chromatin condensation inducer in the nucleus	0	4	0	4
Ddx18	ATP-dependent RNA helicase DDX18	0	4	0	4
Fads2	fatty acid desaturase 2	0	4	0	4
Flnc	filamin-C	0	4	0	4
Krt33a	keratin, type I cuticular Ha3-I	0	4	0	4
Lama3	laminin subunit alpha-3	0	4	0	4
LOC10004		0	4	0	4
Nnt	NAD(P) transhydrogenase, mitochondrial	0	4	0	4
Nvl	nuclear valosin-containing protein-like	0	4	0	4
Prpf6	pre-mRNA-processing factor 6	0	4	0	4
Rpl22	60S ribosomal protein L22	0	4	0	4
Rpl23	60S ribosomal protein L23	0	4	0	4
Tln1	talin-1	0	4	0	4
Wdr36	WD repeat domain 36	0	4	0	4
D1Pas1	putative ATP-dependent RNA helicase Pl10		4	0	4
Fscn1	fascin	2	6	1	4
Hnrnph1	heterogeneous nuclear ribonucleoprotein H	2	6	1	4
Hspb1	heat shock protein beta-1	0	4	1	4
Actn4	alpha-actinin-4	0	4	2	4
Dst	dystonin	0	4	2	4
Gemin5	gem-associated protein 5	0	4	2	4
Hspa4	heat shock 70 kDa protein 4	0	4	2	4
Odf2l	outer dense fiber protein 2-like	0	4	2	4
Bicd1	protein bicaudal D homolog 1	0	4	3	4
Sarnp	SAP domain-containing ribonucleoprotein	0	4	3	4
Vps35	vacuolar protein sorting-associated protein 35	4	8	4	4
Gucy2c	heat-stable enterotoxin receptor	2	6	4	4
Krt35	keratin, type I cuticular Ha5	2	6	4	4
Plk2	serine/threonine-protein kinase PLK2	2	6	6	4
2410002O2	UPF0533 protein C5orf44 homolog	1	4	0	3
Fam98c	uncharacterized protein LOC73833	1	4	0	3
Rpl28-ps3		1	4	0	3
Shisa9	protein shisa-9	1	4	0	3
Abcc2	canalicular multispecific organic anion transporter 1	0	3	0	3
Alyref	THO complex subunit 4	0	3	0	3
Cacna2d4	voltage-dependent calcium channel subunit alpha-2/delta-4	0	3	0	3
Dsg1a	desmoglein-1-alpha	0	3	0	3
E2f2	transcription factor E2F2	0	3	0	3
Eed	polycomb protein EED	0	3	0	3
Eftud2	116 kDa U5 small nuclear ribonucleoprotein component	0	3	0	3
Fam65b	protein FAM65B	0	3	0	3
Grpel1	grpE protein homolog 1, mitochondrial	0	3	0	3
Hdac2	histone deacetylase 2	0	3	0	3
Kif1b	kinesin-like protein KIF1B	0	3	0	3
Lgals3bp	galectin-3-binding protein	0	3	0	3
Nup160	nuclear pore complex protein Nup160	0	3	0	3
P2rx3	P2X purinoceptor 3	0	3	0	3
Pcnxl3	pecanex-like protein 3	0	3	0	3
Pml	protein PML	0	3	0	3

Smc3	structural maintenance of chromosomes protein 3	0	3	0	3
Smg6	telomerase-binding protein EST1A	0	3	0	3
Tnr	tenascin-R	0	3	0	3
Vezt	vezatin	0	3	0	3
Vps16	vacuolar protein sorting-associated protein 16 homolog	0	3	0	3
Wdr46	WD repeat-containing protein 46	0	3	0	3
Yes1	tyrosine-protein kinase Yes	0	3	0	3
Arid5a	AT-rich interactive domain-containing protein 5A	0	3	1	3
Ddx58	probable ATP-dependent RNA helicase DDX58	0	3	1	3
Gdf15	growth/differentiation factor 15	0	3	1	3
Hinfp	histone H4 transcription factor	0	3	1	3
Sf3b3	splicing factor 3B subunit 3	0	3	1	3
Slc25a13	calcium-binding mitochondrial carrier protein Aralar2	0	3	1	3
Stag2	cohesin subunit SA-2	0	3	1	3
Taf1	transcription initiation factor TFIID subunit 1	0	3	1	3
Lrpprc	leucine-rich PPR motif-containing protein, mitochondrial	1	4	2	3
Herc2	E3 ubiquitin-protein ligase HERC2	0	3	2	3
Rere	arginine-glutamic acid dipeptide repeats protein	0	3	2	3
Hnrnpab	heterogeneous nuclear ribonucleoprotein A/B	4	7	3	3
Fras1	extracellular matrix protein FRAS1	2	5	3	3
Hnrnpd	heterogeneous nuclear ribonucleoprotein D0	2	5	3	3
Chrna10	neuronal acetylcholine receptor subunit alpha-10	0	3	3	3
Dock9	dedicator of cytokinesis protein 9	0	3	3	3
Erc1	ELKS/Rab6-interacting/CAST family member 1	0	3	3	3
Hnrnpa0	heterogeneous nuclear ribonucleoprotein A0	0	3	3	3
Pard6g	partitioning defective 6 homolog gamma	0	3	3	3
Prpf8	pre-mRNA-processing-splicing factor 8	0	3	3	3
Ube2t	ubiquitin-conjugating enzyme E2 T	0	3	3	3
Vash1	vasohibin-1	1	4	4	3
Mei4	UPF0623 protein	0	3	4	3

Table VI. Mass-spec list of the PrSet7 GST pulldown assays. The number of unique spectra that were identified for each protein in the mass-spec analysis is indicated (Scaffold analysis).

identified proteins (689)	**GST**	**PrSet7**
histone-lysine N-methyltransferase SETD8 [Mus musculus]	0	63
histone-lysine N-methyltransferase SUV420H2 [Mus musculus]	1	10
plakoglobin [Mus musculus]	5	10
unnamed protein product [Mus musculus]	0	5
unnamed protein product [Mus musculus]	0	4
keratin, type I cuticular Ha1 [Mus musculus]	0	4
glutathione S-transferase P 1 [Mus musculus]	0	4
unnamed protein product [Mus musculus]	2	5
mCG121875 [Mus musculus]	0	3
mCG13479, isoform CRA_a [Mus musculus]	0	3
Hist2h4 protein [Mus musculus]	17	19
mCG20427 [Mus musculus]	10	12
mCG49945 [Mus musculus]	2	4
fibronectin [Mus musculus]	2	4
mCG116671 [Mus musculus]	2	4
microtubule-actin crosslinking factor 1 [Mus musculus]	0	2
mCG141708, isoform CRA_a [Mus musculus]	0	2
Hnrpc protein [Mus musculus]	0	2

protein bicaudal D homolog 1 isoform 2 [Mus musculus]	0	2
gi|148697763	0	2
Voltage-dependent anion channel 2 [Mus musculus]	0	2
60S ribosomal protein L8 [Homo sapiens]	0	2
unnamed protein product [Mus musculus]	0	2
RIKEN cDNA 9430010O03, isoform CRA_c [Mus musculus]	0	2
60S ribosomal protein L13a [Mus musculus]	0	2
unnamed protein product [Mus musculus]	0	2
mCG113619 [Mus musculus]	0	2
mCG9260 [Mus musculus]	0	2
mCG120681 [Mus musculus]	0	2
pre-rRNA-processing protein TSR1 homolog [Mus musculus]	0	2
Hist1h3e protein [Mus musculus]	6	7
RecName: Full=Histone deacetylase 6; Short=HD6; AltName: Full=Histone deacetylase mHDA2	0	1
RIKEN cDNA 1810013C15, isoform CRA_b [Mus musculus]	1	2
epidermal keratin type I [Mus musculus]	2	3
myosin XVA isoform 1a [Mus musculus]	1	2
Cd209f protein [Mus musculus]	0	1
mCG1036780 [Mus musculus]	1	2
unnamed protein product [Mus musculus]	1	2
biorientation of chromosomes in cell division 1-like [Mus musculus]	0	1
mCG121289, isoform CRA_a [Mus musculus]	0	1
calcium channel, voltage-dependent, P/Q type, alpha 1A subunit, isoform CRA_c [Mus musculus]	0	1
mCG10523, isoform CRA_b [Mus musculus]	0	1
lysozyme C-1 precursor [Mus musculus]	1	2
L-2-hydroxyglutarate dehydrogenase [Mus musculus]	0	1
gi|12850600	1	2
histone deacetylase complex subunit SAP18 [Mus musculus]	1	2
small proline-rich protein 2B [Mus musculus]	0	1
expressed sequence AI841794 [Mus musculus]	0	1
hypothetical protein LOC240067 [Mus musculus]	0	1
gi|188497644	0	1
1200009I06Rik protein [Mus musculus]	0	1
unnamed protein product [Mus musculus]	0	1
unnamed protein product [Mus musculus]	0	1
putative GTP-binding protein Parf [Mus musculus]	0	1
RecName: Full=Putative 60S ribosomal protein L32'	0	1
mCG117386 [Mus musculus]	0	1
transmembrane channel-like gene family 6 [Mus musculus]	0	1
mCG133345, isoform CRA_a [Mus musculus]	0	1
mCG145367 [Mus musculus]	0	1
low density lipoprotein-related protein 1B (deleted in tumors) [Mus musculus]	0	1
unnamed protein product [Mus musculus]	0	1
K+ channel [Mus musculus]	0	1
low affinity cationic amino acid transporter 2 isoform 1 [Mus musculus]	0	1
cornifin-A [Mus musculus]	0	1
immunoglobulin mu heavy chain variable region [Mus musculus]	0	1
mCG8461, isoform CRA_b [Mus musculus]	0	1
ribosomal protein L26 [Mus musculus]	0	1

unnamed protein product [Mus musculus]	0	1
PREDICTED: myosin light polypeptide 6-like [Mus musculus]	0	1
mCG1230, isoform CRA_a [Mus musculus]	0	1
vacuolar protein sorting 16 (yeast) [Mus musculus]	0	1
Ribosomal protein, large, P0 [Mus musculus]	0	1
complement component 1 Q subcomponent-binding protein, mitochondrial [Mus musculus]	0	1
unnamed protein product [Mus musculus]	0	1
unnamed protein product [Mus musculus]	0	1
mCG141651 [Mus musculus]	0	1
nucleoporin 205 [Mus musculus]	0	1
myosin, heavy polypeptide 10, non-muscle [Mus musculus]	0	1
keratin, type I cuticular Ha4 [Mus musculus]	0	1
DNA segment, Chr 19, ERATO Doi 386, expressed [Mus musculus]	0	1
unnamed protein product [Mus musculus]	0	1
plakophilin 1 [Mus musculus]	0	1
protease, serine, 23, isoform CRA_c [Mus musculus]	0	1
mCG21742 [Mus musculus]	0	1
PREDICTED: dedicator of cytokinesis protein 3-like [Mus musculus]	0	1
vomeronasal 2, receptor, 122 isoform 2 [Mus musculus]	0	1
mCG49140 [Mus musculus]	0	1
unnamed protein product [Mus musculus]	0	1
arginine glutamic acid dipeptide (RE) repeats [Mus musculus]	0	1
striated muscle-specific serine/threonine protein kinase [Mus musculus]	0	1
mCG125596 [Mus musculus]	0	1
unknown [Mus musculus]	0	1
RecName: Full=Thyroid hormone receptor alpha; AltName: Full=Nuclear receptor subfamily 1 group A member 1; AltName: Full=c-erbA-1; AltName: Full=c-erbA-alpha	0	1
mCG2257 [Mus musculus]	0	1
mCG51125 [Mus musculus]	0	1
DNA-directed RNA polymerases I, II, and III subunit RPABC1 [Mus musculus]	0	1
RecName: Full=Forkhead box protein K2; AltName: Full=Cellular transcription factor ILF-1; AltName: Full=Interleukin enhancer-binding factor 1	0	1
CD84-H1 [Mus musculus]	0	1
chorion-specific transcription factor GCMb [Mus musculus]	0	1
U6 snRNA-associated Sm-like protein LSm1 [Mus musculus]	0	1
PREDICTED: 40S ribosomal protein S13-like [Mus musculus]	0	1
RecName: Full=Filamin A-interacting protein 1-like; AltName: Full=Protein down-regulated in ovarian cancer 1 homolog; Short=DOC-1	0	1
unnamed protein product [Mus musculus]	0	1
Serpinb13 protein [Mus musculus]	0	1
unnamed protein product [Mus musculus]	0	1
E2F transcription factor 7, isoform CRA_b [Mus musculus]	0	1
peptidylprolyl isomerase F (cyclophilin F), isoform CRA_c [Mus musculus]	0	1
cDNA sequence, AY616753, isoform CRA_a [Mus musculus]	0	1
DEAD/H (Asp-Glu-Ala-Asp/His) box polypeptide 31 [Mus musculus]	0	1
septin 9 [Mus musculus]	0	1
C-C motif chemokine 27 isoform 1 [Mus musculus]	0	1
immunoglobulin heavy chain [Mus musculus]	0	1
Usherin precursor [Mus musculus]	0	1
EF-hand calcium-binding domain-containing protein 7 [Mus musculus]	0	1
unnamed protein product [Mus musculus]	0	1

unnamed protein product [Mus musculus]	0	1
RIKEN cDNA 1500010J02, isoform CRA_b [Mus musculus]	0	1
unnamed protein product [Mus musculus]	0	1
novel protein [Mus musculus]	0	1
unnamed protein product [Mus musculus]	0	1
unnamed protein product [Mus musculus]	0	1
prefoldin subunit 3 [Mus musculus]	0	1
mCG117846 [Mus musculus]	0	1
RIKEN cDNA C030014K22 [Mus musculus]	0	1
ribosomal protein 10 [Mus musculus]	0	1
breast cancer susceptibility [Mus musculus]	0	1
Pwp2 protein [Mus musculus]	0	1
utrophin [Mus musculus]	0	1
gi|148674573	0	1
Zfp641 protein [Mus musculus]	0	1
Smage-3 protein [Mus musculus]	0	1
tubulin, gamma complex associated protein 2, isoform CRA_a [Mus musculus]	0	1
RecName: Full=60S ribosomal protein L3; AltName: Full=J1 protein	0	1
ADAM33 [Mus musculus]	0	1
unnamed protein product [Mus musculus]	0	1
atlastin-3 isoform 2 [Mus musculus]	0	1
mCG1032915 [Mus musculus]	0	1
unnamed protein product [Mus musculus]	0	1
mCG140660 [Mus musculus]	0	1
unknown [Mus musculus]	0	1
mCG15386 [Mus musculus]	0	1
beta,beta-carotene 9',10'-oxygenase [Mus musculus]	0	1
mCG8513 [Mus musculus]	0	1
transcription factor SOX-13 [Mus musculus]	0	1
gi|74147627	0	1
unnamed protein product [Mus musculus]	0	1
solute carrier family 13, member 4 [Mus musculus]	0	1
mCG130125, isoform CRA_b [Mus musculus]	0	1
mCG129911 [Mus musculus]	0	1
unnamed protein product [Mus musculus]	0	1
kallikrein related-peptidase 6 precursor [Mus musculus]	0	1
mCG3093, isoform CRA_b [Mus musculus]	0	1
serine/threonine-protein kinase receptor R3 precursor [Mus musculus]	0	1
mCG130959 [Mus musculus]	0	1
mCG140934 [Mus musculus]	0	1
olfactory receptor 741 [Mus musculus]	0	1
Rho GTPase activating protein 21 [Mus musculus]	0	1
mCG1463, isoform CRA_a [Mus musculus]	0	1
PDZ domain-containing protein 2 [Mus musculus]	0	1
aldehyde oxidase 3 [Mus musculus]	0	1
Tpd52 protein [Mus musculus]	0	1
serum albumin precursor [Mus musculus]	0	1
RNA/DNA-binding protein [Mus musculus]	0	1
vomeronasal 1 receptor, G1 [Mus musculus]	0	1

DEAH (Asp-Glu-Ala-His) box polypeptide 9, isoform CRA_a [Mus musculus]	0	1
mCG55273 [Mus musculus]	0	1
coiled-coil domain containing 47 [Mus musculus]	0	1
probable G-protein coupled receptor 162 [Mus musculus]	0	1
mCG147147 [Mus musculus]	0	1
unnamed protein product [Mus musculus]	0	1
olfactory receptor 1301 [Mus musculus]	0	1
ankyrin repeat domain 36 [Mus musculus]	0	1
Multimerin 1 [Mus musculus]	0	1
ATP-binding cassette 1, sub-family A, member 1 [Mus musculus]	0	1
unnamed protein product [Mus musculus]	0	1
cadherin-24 precursor [Mus musculus]	0	1
Ckap5 protein [Mus musculus]	0	1
CXXC finger 1 (PHD domain), isoform CRA_e [Mus musculus]	0	1
ret proto-oncogene [Mus musculus]	0	1
transcription factor TFIIIB component B" homolog [Mus musculus]	0	1
Stil protein [Mus musculus]	0	1
mCG148436 [Mus musculus]	0	1
RecName: Full=Serine/threonine-protein kinase 25; AltName: Full=Ste20-like kinase; AltName: Full=Sterile 20/oxidant stress-response kinase 1; Short=SOK-1; Short=Ste20/oxidant stress response kinase 1	0	1
galactose-3-O-sulfotransferase 2 [Mus musculus]	0	1
mCG117370, isoform CRA_a [Mus musculus]	0	1
unnamed protein product [Mus musculus]	0	1
unnamed protein product [Mus musculus]	0	1
RIKEN cDNA 9130019O22 gene [Mus musculus]	0	1
immunoglobulin heavy chain variable region (CDR3) [Mus musculus]	0	1
unnamed protein product [Mus musculus]	0	1
mCG129641 [Mus musculus]	0	1
paraneoplastic antigen-like protein 5 [Mus musculus]	0	1
testis-specific serine/threonine-protein kinase 5 [Mus musculus]	0	1
general transcription factor III C 1, isoform CRA_a [Mus musculus]	0	1
RecName: Full=Protein chibby homolog 3	0	1
vitamin K-dependent protein S precursor [Mus musculus]	0	1
unnamed protein product [Mus musculus]	0	1
mCG133706, isoform CRA_a [Mus musculus]	0	1
palladin [Mus musculus]	0	1
ras-related protein Rab-32 [Mus musculus]	0	1
mCG131439, isoform CRA_b [Mus musculus]	0	1
unnamed protein product [Mus musculus]	0	1
peroxisomal NADH pyrophosphatase NUDT12 [Mus musculus]	0	1
gi|10946894	0	1
RecName: Full=MAM domain-containing glycosylphosphatidylinositol anchor protein 1; Flags: Precursor	0	1
mCG5769, isoform CRA_a [Mus musculus]	0	1
unnamed protein product [Mus musculus]	0	1
HMG box domain containing 3 isoform 1 [Mus musculus]	0	1
GREB1-like protein [Mus musculus]	0	1
ATPase family AAA domain-containing protein 2 [Mus musculus]	0	1
unnamed protein product [Mus musculus]	0	1
mCG145199 [Mus musculus]	0	1
unnamed protein product [Mus musculus]	0	1

IK cytokine [Mus musculus]	0	1
centrosomal protein 135, isoform CRA_a [Mus musculus]	0	1
Ccdc60 protein [Mus musculus]	0	1
mitochondrial carnitine/acylcarnitine carrier protein [Mus musculus]	0	1
Novel RhoGAP domain containing protein [Mus musculus]	0	1
FYVE and coiled-coil domain-containing protein 1 [Mus musculus]	0	1
unnamed protein product [Mus musculus]	0	1
procollagen-proline, 2-oxoglutarate 4-dioxygenase (proline 4-hydroxylase), alpha II polypeptide, isoform CRA_a [Mus musculus]	0	1
mCG6975 [Mus musculus]	0	1
mCG127343 [Mus musculus]	0	1
serine/arginine-rich splicing factor 1 isoform 2 [Mus musculus]	0	1
urotensin-2 precursor [Mus musculus]	0	1
ephrin type-A receptor 6 [Mus musculus]	0	1
Serine carboxypeptidase 1 [Mus musculus]	0	1
fragile X mental retardation gene 1, autosomal homolog, isoform CRA_b [Mus musculus]	0	1
SWI/SNF-related matrix-associated actin-dependent regulator of chromatin subfamily D member 1 [Mus musculus]	0	1
EGF-like domain-containing protein C3orf50 homolog isoform a precursor [Mus musculus]	0	1
unnamed protein product [Mus musculus]	0	1
RecName: Full=Probable phospholipid-transporting ATPase VD; AltName: Full=ATPase class V type 10D	0	1
O-6-methylguanine-DNA methyltransferase, isoform CRA_b [Mus musculus]	0	1
kinesin 2, isoform CRA_b [Mus musculus]	0	1
RecName: Full=Brain-specific angiogenesis inhibitor 2; Flags: Precursor	0	1
mCG1031476 [Mus musculus]	0	1
env precursor [Mus musculus]	0	1
unnamed protein product [Mus musculus]	0	1
mCG19193, isoform CRA_b [Mus musculus]	0	1
RecName: Full=Porphobilinogen deaminase; Short=PBG-D; AltName: Full=Hydroxymethylbilane synthase; Short=HMBS; AltName: Full=Pre-uroporphyrinogen synthase	0	1
expressed sequence C79407 [Mus musculus]	0	1
cyclin-F [Mus musculus]	0	1
erythroid cell-specific and testis-specific protein 1(ERT-1) [Mus musculus]	0	1
mCG4144 [Mus musculus]	0	1
hypothetical protein LOC380768 [Mus musculus]	0	1
interferon alpha 6T [Mus musculus]	0	1
YTH domain containing 1 [Mus musculus]	0	1
tetratricopeptide repeat, ankyrin repeat and coiled-coil containing 2 [Mus musculus]	0	1
anti-DNA immunoglobulin heavy chain IgG [Mus musculus]	0	1
prosaposin [Mus musculus]	0	1
immunoglobulin light chain V region [Mus musculus]	0	1
metastasis associated 1, isoform CRA_a [Mus musculus]	0	1
hypothetical protein LOC214763 [Mus musculus]	0	1
novel protein similar to protein phosphatase 1, regulatory (inhibitor) subunit 2 Ppp1r2 [Mus musculus]	0	1
Rho guanine nucleotide exchange factor (GEF) 5 [Mus musculus]	0	1

CITATIONS

Aasland R, Stewart AF, Gibson T. 1996. The SANT domain: a putative DNA-binding domain in the SWI-SNF and ADA complexes, the transcriptional co-repressor N-CoR and TFIIIB. *Trends in biochemical sciences* **21**: 87-88.

Abbas T, Shibata E, Park J, Jha S, Karnani N, Dutta A. 2010. CRL4(Cdt2) regulates cell proliferation and histone gene expression by targeting PR-Set7/Set8 for degradation. *Molecular cell* **40**: 9-21.

Amato A, Schillaci T, Lentini L, Di Leonardo A. 2009. CENPA overexpression promotes genome instability in pRb-depleted human cells. *Molecular cancer* **8**: 119.

Ayadi A, Birling MC, Bottomley J, Bussell J, Fuchs H, Fray M, Gailus-Durner V, Greenaway S, Houghton R, Karp N et al. 2012. Mouse large-scale phenotyping initiatives: overview of the European Mouse Disease Clinic (EUMODIC) and of the Wellcome Trust Sanger Institute Mouse Genetics Project. *Mammalian genome : official journal of the International Mammalian Genome Society* **23**: 600-610.

Ayoub N, Jeyasekharan AD, Bernal JA, Venkitaraman AR. 2008. HP1-beta mobilization promotes chromatin changes that initiate the DNA damage response. *Nature* **453**: 682-686.

Ayoub N, Jeyasekharan AD, Venkitaraman AR. 2009. Mobilization and recruitment of HP1: a bimodal response to DNA breakage. *Cell cycle* **8**: 2945-2950.

Badugu R, Yoo Y, Singh PB, Kellum R. 2005. Mutations in the heterochromatin protein 1 (HP1) hinge domain affect HP1 protein interactions and chromosomal distribution. *Chromosoma* **113**: 370-384.

Baldeyron C, Soria G, Roche D, Cook AJ, Almouzni G. 2011. HP1alpha recruitment to DNA damage by p150CAF-1 promotes homologous recombination repair. *The Journal of cell biology* **193**: 81-95.

Bannister AJ, Zegerman P, Partridge JF, Miska EA, Thomas JO, Allshire RC, Kouzarides T. 2001. Selective recognition of methylated lysine 9 on histone H3 by the HP1 chromo domain. *Nature* **410**: 120-124.

Bartke T, Vermeulen M, Xhemalce B, Robson SC, Mann M, Kouzarides T. 2010. Nucleosome-interacting proteins regulated by DNA and histone methylation. *Cell* **143**: 470-484.

Bartova E, Kozubek S, Jirsova P, Kozubek M, Gajova H, Lukasova E, Skalnikova M, Ganova A, Koutna I, Hausmann M. 2002. Nuclear structure and gene activity in human differentiated cells. *Journal of structural biology* **139**: 76-89.

Bergmann JH, Rodriguez MG, Martins NM, Kimura H, Kelly DA, Masumoto H, Larionov V, Jansen LE, Earnshaw WC. 2011. Epigenetic engineering shows H3K4me2 is required for HJURP targeting and CENP-A assembly on a synthetic human kinetochore. *The EMBO journal* **30**: 328-340.

Bernard P, Maure JF, Partridge JF, Genier S, Javerzat JP, Allshire RC. 2001. Requirement of heterochromatin for cohesion at centromeres. *Science* **294**: 2539-2542.

Boyer LA, Latek RR, Peterson CL. 2004. The SANT domain: a unique histone-tail-binding module? *Nature reviews Molecular cell biology* **5**: 158-163.

Bradford MM. 1976. A rapid and sensitive method for the quantitation of microgram quantities of protein utilizing the principle of protein-dye binding. *Analytical biochemistry* **72**: 248-254.

Brayer KJ, Segal DJ. 2008. Keep your fingers off my DNA: protein-protein interactions mediated by C2H2 zinc finger domains. *Cell biochemistry and biophysics* **50**: 111-131.

Brown SW. 1966. Heterochromatin. *Science* **151**: 417-425.

Bulut-Karslioglu A, Perrera V, Scaranaro M, de la Rosa-Velazquez IA, van de Nobelen S, Shukeir N, Popow J, Gerle B, Opravil S, Pagani M et al. 2012. A transcription factor-based mechanism for mouse heterochromatin formation. *Nature structural & molecular biology* **19**: 1023-1030.

Cammas F, Mark M, Dolle P, Dierich A, Chambon P, Losson R. 2000. Mice lacking the transcriptional corepressor TIF1beta are defective in early postimplantation development. *Development* **127**: 2955-2963.

Canudas S, Houghtaling BR, Bhanot M, Sasa G, Savage SA, Bertuch AA, Smith S. 2011. A role for heterochromatin protein 1gamma at human telomeres. *Genes & development* **25**: 1807-1819.

Cardinale S, Bergmann JH, Kelly D, Nakano M, Valdivia MM, Kimura H, Masumoto H, Larionov V, Earnshaw WC. 2009. Hierarchical inactivation of a synthetic human kinetochore by a chromatin modifier. *Molecular biology of the cell* **20**: 4194-4204.

Carmena M, Wheelock M, Funabiki H, Earnshaw WC. 2012. The chromosomal passenger complex (CPC): from easy rider to the godfather of mitosis. *Nature reviews Molecular cell biology* **13**: 789-803.

Centore RC, Havens CG, Manning AL, Li JM, Flynn RL, Tse A, Jin J, Dyson NJ, Walter JC, Zou L. 2010. CRL4(Cdt2)-mediated destruction of the histone methyltransferase Set8 prevents premature chromatin compaction in S phase. *Molecular cell* **40**: 22-33.

Cheeseman IM, Desai A. 2008. Molecular architecture of the kinetochore-microtubule interface. *Nature reviews Molecular cell biology* **9**: 33-46.

Chen J, Fang G. 2001. MAD2B is an inhibitor of the anaphase-promoting complex. *Genes & development* **15**: 1765-1770.

Chen T, Ueda Y, Dodge JE, Wang Z, Li E. 2003. Establishment and maintenance of genomic methylation patterns in mouse embryonic stem cells by Dnmt3a and Dnmt3b. *Molecular and cellular biology* **23**: 5594-5605.

Choo KH. 2001. Domain organization at the centromere and neocentromere. *Developmental cell* **1**: 165-177.

Chung TL, Hsiao HH, Yeh YY, Shia HL, Chen YL, Liang PH, Wang AH, Khoo KH, Shoei-Lung Li S. 2004. In vitro modification of human centromere protein CENP-C fragments by small ubiquitin-like modifier (SUMO) protein: definitive identification of the modification sites by tandem mass spectrometry analysis of the isopeptides. *The Journal of biological chemistry* **279**: 39653-39662.

Coe BP, Lee EH, Chi B, Girard L, Minna JD, Gazdar AF, Lam S, MacAulay C, Lam WL. 2006. Gain of a region on 7p22.3, containing MAD1L1, is the most frequent event in small-cell lung cancer cell lines. *Genes, chromosomes & cancer* **45**: 11-19.

Compton SJ, Jones CG. 1985. Mechanism of dye response and interference in the Bradford protein assay. *Analytical biochemistry* **151**: 369-374.

Coschi CH, Dick FA. 2012. Chromosome instability and deregulated proliferation: an unavoidable duo. *Cellular and molecular life sciences : CMLS* **69**: 2009-2024.

Craig JM, Earle E, Canham P, Wong LH, Anderson M, Choo KH. 2003. Analysis of mammalian proteins involved in chromatin modification reveals new metaphase centromeric proteins and distinct chromosomal distribution patterns. *Human molecular genetics* **12**: 3109-3121.

Cutts SM, Fowler KJ, Kile BT, Hii LL, O'Dowd RA, Hudson DF, Saffery R, Kalitsis P, Earle E, Choo KH. 1999. Defective chromosome segregation, microtubule bundling and nuclear bridging in inner centromere protein gene (Incenp)-disrupted mice. *Human molecular genetics* **8**: 1145-1155.

Dambacher S, Deng W, Hahn M, Sadic D, Frohlich J, Nuber A, Hoischen C, Diekmann S, Leonhardt H, Schotta G. 2012. CENP-C facilitates the recruitment of M18BP1 to centromeric chromatin. *Nucleus* **3**: 101-110.

De Koning L, Corpet A, Haber JE, Almouzni G. 2007. Histone chaperones: an escort network regulating histone traffic. *Nature structural & molecular biology* **14**: 997-1007.

de Leeuw RJ, Davies JJ, Rosenwald A, Bebb G, Gascoyne RD, Dyer MJ, Staudt LM, Martinez-Climent JA, Lam WL. 2004. Comprehensive whole genome array CGH profiling of mantle cell lymphoma model genomes. *Human molecular genetics* **13**: 1827-1837.

Diaz-Rodriguez E, Sotillo R, Schvartzman JM, Benezra R. 2008. Hec1 overexpression hyperactivates the mitotic checkpoint and induces tumor formation in vivo. *Proceedings of the National Academy of Sciences of the United States of America* **105**: 16719-16724.

Dinant C, Luijsterburg MS. 2009. The emerging role of HP1 in the DNA damage response. *Molecular and cellular biology* **29**: 6335-6340.

Dunleavy EM, Roche D, Tagami H, Lacoste N, Ray-Gallet D, Nakamura Y, Daigo Y, Nakatani Y, Almouzni-Pettinotti G. 2009. HJURP is a cell-cycle-dependent maintenance and deposition factor of CENP-A at centromeres. *Cell* **137**: 485-497.

Earnshaw WC, Migeon BR. 1985. Three related centromere proteins are absent from the inactive centromere of a stable isodicentric chromosome. *Chromosoma* **92**: 290-296.

Eissenberg JC, James TC, Foster-Hartnett DM, Hartnett T, Ngan V, Elgin SC. 1990. Mutation in a heterochromatin-specific chromosomal protein is associated with suppression of position-effect variegation in Drosophila melanogaster. *Proceedings of the National Academy of Sciences of the United States of America* **87**: 9923-9927.

Fan Y, Nikitina T, Morin-Kensicki EM, Zhao J, Magnuson TR, Woodcock CL, Skoultchi AI. 2003. H1 linker histones are essential for mouse development and affect nucleosome spacing in vivo. *Molecular and cellular biology* **23**: 4559-4572.

Fernandez-Miranda G, Perez de Castro I, Carmena M, Aguirre-Portoles C, Ruchaud S, Fant X, Montoya G, Earnshaw WC, Malumbres M. 2010. SUMOylation modulates the function of Aurora-B kinase. *Journal of cell science* **123**: 2823-2833.

Folco HD, Pidoux AL, Urano T, Allshire RC. 2008. Heterochromatin and RNAi are required to establish CENP-A chromatin at centromeres. *Science* **319**: 94-97.

Foltz DR, Jansen LE, Bailey AO, Yates JR, 3rd, Bassett EA, Wood S, Black BE, Cleveland DW. 2009. Centromere-specific assembly of CENP-a nucleosomes is mediated by HJURP. *Cell* **137**: 472-484.

Foltz DR, Jansen LE, Black BE, Bailey AO, Yates JR, 3rd, Cleveland DW. 2006. The human CENP-A centromeric nucleosome-associated complex. *Nature cell biology* **8**: 458-469.

Fujita K, Shimazaki N, Ohta Y, Kubota T, Ibe S, Toji S, Tamai K, Fujisaki S, Hayano T, Koiwai O. 2003. Terminal deoxynucleotidyltransferase forms a ternary complex with a novel chromatin remodeling protein with 82 kDa and core histone. *Genes to cells : devoted to molecular & cellular mechanisms* **8**: 559-571.

Fujita Y, Hayashi T, Kiyomitsu T, Toyoda Y, Kokubu A, Obuse C, Yanagida M. 2007. Priming of centromere for CENP-A recruitment by human hMis18alpha, hMis18beta, and M18BP1. *Developmental cell* **12**: 17-30.

Gartenberg M. 2009. Heterochromatin and the cohesion of sister chromatids. *Chromosome research : an international journal on the molecular, supramolecular and evolutionary aspects of chromosome biology* **17**: 229-238.

Gascoigne KE, Cheeseman IM. 2011. Kinetochore assembly: if you build it, they will come. *Current opinion in cell biology* **23**: 102-108.

Gassmann R, Carvalho A, Henzing AJ, Ruchaud S, Hudson DF, Honda R, Nigg EA, Gerloff DL, Earnshaw WC. 2004. Borealin: a novel chromosomal passenger required for stability of the bipolar mitotic spindle. *The Journal of cell biology* **166**: 179-191.

Goodarzi AA, Jeggo PA. 2012. The heterochromatic barrier to DNA double strand break repair: how to get the entry visa. *International journal of molecular sciences* **13**: 11844-11860.

Gopalakrishnan S, Sullivan BA, Trazzi S, Della Valle G, Robertson KD. 2009. DNMT3B interacts with constitutive centromere protein CENP-C to modulate DNA methylation and the histone code at centromeric regions. *Human molecular genetics* **18**: 3178-3193.

Gossen M, Bujard H. 1992. Tight control of gene expression in mammalian cells by tetracycline-responsive promoters. *Proceedings of the National Academy of Sciences of the United States of America* **89**: 5547-5551.

Grigoryev SA. 2012. Nucleosome spacing and chromatin higher-order folding. *Nucleus* **3**: 493-499.

Guenatri M, Bailly D, Maison C, Almouzni G. 2004. Mouse centric and pericentric satellite repeats form distinct functional heterochromatin. *The Journal of cell biology* **166**: 493-505.

Hahn M, Dambacher S, Schotta G. 2010. Heterochromatin dysregulation in human diseases. *Journal of applied physiology* **109**: 232-242.

Hassan AH, Awad S, Al-Natour Z, Othman S, Mustafa F, Rizvi TA. 2007. Selective recognition of acetylated histones by bromodomains in transcriptional co-activators. *The Biochemical journal* **402**: 125-133.

Hauf S, Cole RW, LaTerra S, Zimmer C, Schnapp G, Walter R, Heckel A, van Meel J, Rieder CL, Peters JM. 2003. The small molecule Hesperadin reveals a role for Aurora B in correcting kinetochore-microtubule attachment and in maintaining the spindle assembly checkpoint. *The Journal of cell biology* **161**: 281-294.

Havens CG, Walter JC. 2009. Docking of a specialized PIP Box onto chromatin-bound PCNA creates a degron for the ubiquitin ligase CRL4Cdt2. *Molecular cell* **35**: 93-104.

Hayakawa T, Haraguchi T, Masumoto H, Hiraoka Y. 2003. Cell cycle behavior of human HP1 subtypes: distinct molecular domains of HP1 are required for their centromeric localization during interphase and metaphase. *Journal of cell science* **116**: 3327-3338.

Hayashi T, Fujita Y, Iwasaki O, Adachi Y, Takahashi K, Yanagida M. 2004. Mis16 and Mis18 are required for CENP-A loading and histone deacetylation at centromeres. *Cell* **118**: 715-729.

Holland AJ, Cleveland DW. 2009. Boveri revisited: chromosomal instability, aneuploidy and tumorigenesis. *Nature reviews Molecular cell biology* **10**: 478-487.

Honda S, Lewis ZA, Shimada K, Fischle W, Sack R, Selker EU. 2012. Heterochromatin protein 1 forms distinct complexes to direct histone deacetylation and DNA methylation. *Nature structural & molecular biology* **19**: 471-477, S471.

Honda Z, Suzuki T, Honda H. 2009. Identification of CENP-V as a novel microtubule-associating molecule that activates Src family kinases through SH3 domain interaction. *Genes to cells : devoted to molecular & cellular mechanisms* **14**: 1383-1394.

Hori T, Okada M, Maenaka K, Fukagawa T. 2008. CENP-O class proteins form a stable complex and are required for proper kinetochore function. *Molecular biology of the cell* **19**: 843-854.

Howman EV, Fowler KJ, Newson AJ, Redward S, MacDonald AC, Kalitsis P, Choo KH. 2000. Early disruption of centromeric chromatin organization in centromere protein A (Cenpa) null mice. *Proceedings of the National Academy of Sciences of the United States of America* **97**: 1148-1153.

Huen MS, Sy SM, van Deursen JM, Chen J. 2008. Direct interaction between SET8 and proliferating cell nuclear antigen couples H4-K20 methylation with DNA replication. *The Journal of biological chemistry* **283**: 11073-11077.

Huisinga KL, Brower-Toland B, Elgin SC. 2006. The contradictory definitions of heterochromatin: transcription and silencing. *Chromosoma* **115**: 110-122.

Huynh VA, Robinson PJ, Rhodes D. 2005. A method for the in vitro reconstitution of a defined "30 nm" chromatin fibre containing stoichiometric amounts of the linker histone. *Journal of molecular biology* **345**: 957-968.

Itoh G, Kanno S, Uchida KS, Chiba S, Sugino S, Watanabe K, Mizuno K, Yasui A, Hirota T, Tanaka K. 2011. CAMP (C13orf8, ZNF828) is a novel regulator of kinetochore-microtubule attachment. *The EMBO journal* **30**: 130-144.

Ivanov AV, Peng H, Yurchenko V, Yap KL, Negorev DG, Schultz DC, Psulkowski E, Fredericks WJ, White DE, Maul GG et al. 2007. PHD domain-mediated E3 ligase activity directs intramolecular sumoylation of an adjacent bromodomain required for gene silencing. *Molecular cell* **28**: 823-837.

Iyengar S, Farnham PJ. 2011. KAP1 protein: an enigmatic master regulator of the genome. *The Journal of biological chemistry* **286**: 26267-26276.

Jansen LE, Black BE, Foltz DR, Cleveland DW. 2007. Propagation of centromeric chromatin requires exit from mitosis. *The Journal of cell biology* **176**: 795-805.

Jenuwein T, Laible G, Dorn R, Reuter G. 1998. SET domain proteins modulate chromatin domains in eu- and heterochromatin. *Cellular and molecular life sciences : CMLS* **54**: 80-93.

Jiang WQ, Nguyen A, Cao Y, Chang AC, Reddel RR. 2011. HP1-mediated formation of alternative lengthening of telomeres-associated PML bodies requires HIRA but not ASF1a. *PloS one* **6**: e17036.

Jorgensen S, Elvers I, Trelle MB, Menzel T, Eskildsen M, Jensen ON, Helleday T, Helin K, Sorensen CS. 2007. The histone methyltransferase SET8 is required for S-phase progression. *The Journal of cell biology* **179**: 1337-1345.

Kagansky A, Folco HD, Almeida R, Pidoux AL, Boukaba A, Simmer F, Urano T, Hamilton GL, Allshire RC. 2009. Synthetic heterochromatin bypasses RNAi and centromeric repeats to establish functional centromeres. *Science* **324**: 1716-1719.

Kanda T, Sullivan KF, Wahl GM. 1998. Histone-GFP fusion protein enables sensitive analysis of chromosome dynamics in living mammalian cells. *Current biology : CB* **8**: 377-385.

Kim IS, Lee M, Park KC, Jeon Y, Park JH, Hwang EJ, Jeon TI, Ko S, Lee H, Baek SH et al. 2012. Roles of Mis18alpha in epigenetic regulation of centromeric chromatin and CENP-A loading. *Molecular cell* **46**: 260-273.

Kline SL, Cheeseman IM, Hori T, Fukagawa T, Desai A. 2006. The human Mis12 complex is required for kinetochore assembly and proper chromosome segregation. *The Journal of cell biology* **173**: 9-17.

Koch B, Kueng S, Ruckenbauer C, Wendt KS, Peters JM. 2008. The Suv39h-HP1 histone methylation pathway is dispensable for enrichment and protection of cohesin at centromeres in mammalian cells. *Chromosoma* **117**: 199-210.

Koegl M, Uetz P. 2007. Improving yeast two-hybrid screening systems. *Briefings in functional genomics & proteomics* **6**: 302-312.

Koiwai K, Noma S, Takahashi Y, Hayano T, Maezawa S, Kouda K, Matsumoto T, Suzuki M, Furuichi M, Koiwai O. 2011. TdIF2 is a nucleolar protein that promotes rRNA gene promoter activity. *Genes to cells : devoted to molecular & cellular mechanisms* **16**: 748-764.

Komori T, Pricop L, Hatakeyama A, Bona CA, Alt FW. 1996. Repertoires of antigen receptors in Tdt congenitally deficient mice. *International reviews of immunology* **13**: 317-325.

Kwon SH, Workman JL. 2011. The changing faces of HP1: From heterochromatin formation and gene silencing to euchromatic gene expression: HP1 acts as a positive regulator of transcription. *BioEssays : news and reviews in molecular, cellular and developmental biology* **33**: 280-289.

Lachner M, O'Carroll D, Rea S, Mechtler K, Jenuwein T. 2001. Methylation of histone H3 lysine 9 creates a binding site for HP1 proteins. *Nature* **410**: 116-120.

Lagana A, Dorn JF, De Rop V, Ladouceur AM, Maddox AS, Maddox PS. 2010. A small GTPase molecular switch regulates epigenetic centromere maintenance by stabilizing newly incorporated CENP-A. *Nature cell biology* **12**: 1186-1193.

Lam AL, Boivin CD, Bonney CF, Rudd MK, Sullivan BA. 2006. Human centromeric chromatin is a dynamic chromosomal domain that can spread over noncentromeric DNA. *Proceedings of the National Academy of Sciences of the United States of America* **103**: 4186-4191.

Lampson MA, Renduchitala K, Khodjakov A, Kapoor TM. 2004. Correcting improper chromosome-spindle attachments during cell division. *Nature cell biology* **6**: 232-237.

Lara-Gonzalez P, Westhorpe FG, Taylor SS. 2012. The spindle assembly checkpoint. *Current biology : CB* **22**: R966-980.

Lehnertz B, Ueda Y, Derijck AA, Braunschweig U, Perez-Burgos L, Kubicek S, Chen T, Li E, Jenuwein T, Peters AH. 2003. Suv39h-mediated histone H3 lysine 9 methylation directs DNA methylation to major satellite repeats at pericentric heterochromatin. *Current biology : CB* **13**: 1192-1200.

Li X, Lee YK, Jeng JC, Yen Y, Schultz DC, Shih HM, Ann DK. 2007. Role for KAP1 serine 824 phosphorylation and sumoylation/desumoylation switch in regulating KAP1-mediated transcriptional repression. *The Journal of biological chemistry* **282**: 36177-36189.

Liu P, Jenkins NA, Copeland NG. 2003. A highly efficient recombineering-based method for generating conditional knockout mutations. *Genome Res* **13**: 476-484.

Lomberk G, Bensi D, Fernandez-Zapico ME, Urrutia R. 2006. Evidence for the existence of an HP1-mediated subcode within the histone code. *Nature cell biology* **8**: 407-415.

Lomeli H, Ramos-Mejia V, Gertsenstein M, Lobe CG, Nagy A. 2000. Targeted insertion of Cre recombinase into the TNAP gene: excision in primordial germ cells. *Genesis* **26**: 116-117.

Losada A, Hirano M, Hirano T. 1998. Identification of Xenopus SMC protein complexes required for sister chromatid cohesion. *Genes & development* **12**: 1986-1997.

Loyola A, Tagami H, Bonaldi T, Roche D, Quivy JP, Imhof A, Nakatani Y, Dent SY, Almouzni G. 2009. The HP1alpha-CAF1-SetDB1-containing complex provides H3K9me1 for Suv39-mediated K9me3 in pericentric heterochromatin. *EMBO reports* **10**: 769-775.

Maddox PS, Hyndman F, Monen J, Oegema K, Desai A. 2007. Functional genomics identifies a Myb domain-containing protein family required for assembly of CENP-A chromatin. *The Journal of cell biology* **176**: 757-763.

Maison C, Almouzni G. 2004. HP1 and the dynamics of heterochromatin maintenance. *Nature reviews Molecular cell biology* **5**: 296-304.

Maison C, Bailly D, Roche D, Montes de Oca R, Probst AV, Vassias I, Dingli F, Lombard B, Loew D, Quivy JP et al. 2011. SUMOylation promotes de novo targeting of HP1alpha to pericentric heterochromatin. *Nature genetics* **43**: 220-227.

Martens JH, O'Sullivan RJ, Braunschweig U, Opravil S, Radolf M, Steinlein P, Jenuwein T. 2005. The profile of repeat-associated histone lysine methylation states in the mouse epigenome. *The EMBO journal* **24**: 800-812.

McLean JR, Chaix D, Ohi MD, Gould KL. 2011. State of the APC/C: organization, function, and structure. *Critical reviews in biochemistry and molecular biology* **46**: 118-136.

Mohr K, Koegl M. 2012. High-throughput yeast two-hybrid screening of complex cDNA libraries. *Methods in molecular biology* **812**: 89-102.

Morales V, Straub T, Neumann MF, Mengus G, Akhtar A, Becker PB. 2004. Functional integration of the histone acetyltransferase MOF into the dosage compensation complex. *The EMBO journal* **23**: 2258-2268.

Moree B, Meyer CB, Fuller CJ, Straight AF. 2011. CENP-C recruits M18BP1 to centromeres to promote CENP-A chromatin assembly. *The Journal of cell biology* **194**: 855-871.

Muegge K. 2005. Lsh, a guardian of heterochromatin at repeat elements. *Biochemistry and cell biology = Biochimie et biologie cellulaire* **83**: 548-554.

Murzina NV, Pei XY, Zhang W, Sparkes M, Vicente-Garcia J, Pratap JV, McLaughlin SH, Ben-Shahar TR, Verreault A, Luisi BF et al. 2008. Structural basis for the recognition of histone H4 by the histone-chaperone RbAp46. *Structure* **16**: 1077-1085.

Musselman CA, Kutateladze TG. 2011. Handpicking epigenetic marks with PHD fingers. *Nucleic acids research* **39**: 9061-9071.

Nagy A. 2000. Cre recombinase: the universal reagent for genome tailoring. *Genesis* **26**: 99-109.

Nakano M, Cardinale S, Noskov VN, Gassmann R, Vagnarelli P, Kandels-Lewis S, Larionov V, Earnshaw WC, Masumoto H. 2008. Inactivation of a human kinetochore by specific targeting of chromatin modifiers. *Developmental cell* **14**: 507-522.

Nakano M, Okamoto Y, Ohzeki J, Masumoto H. 2003. Epigenetic assembly of centromeric chromatin at ectopic alpha-satellite sites on human chromosomes. *Journal of cell science* **116**: 4021-4034.

Nakashima H, Nakano M, Ohnishi R, Hiraoka Y, Kaneda Y, Sugino A, Masumoto H. 2005. Assembly of additional heterochromatin distinct from centromere-kinetochore chromatin is required for de novo formation of human artificial chromosome. *Journal of cell science* **118**: 5885-5898.

Nakatsuji N, Chuma S. 2001. Differentiation of mouse primordial germ cells into female or male germ cells. *The International journal of developmental biology* **45**: 541-548.

Nielsen PR, Nietlispach D, Mott HR, Callaghan J, Bannister A, Kouzarides T, Murzin AG, Murzina NV, Laue ED. 2002. Structure of the HP1 chromodomain bound to histone H3 methylated at lysine 9. *Nature* **416**: 103-107.

Nishioka K, Rice JC, Sarma K, Erdjument-Bromage H, Werner J, Wang Y, Chuikov S, Valenzuela P, Tempst P, Steward R et al. 2002. PR-Set7 is a nucleosome-specific methyltransferase that modifies lysine 20 of histone H4 and is associated with silent chromatin. *Molecular cell* **9**: 1201-1213.

Nonaka N, Kitajima T, Yokobayashi S, Xiao G, Yamamoto M, Grewal SI, Watanabe Y. 2002. Recruitment of cohesin to heterochromatic regions by Swi6/HP1 in fission yeast. *Nature cell biology* **4**: 89-93.

Nousiainen M, Sillje HH, Sauer G, Nigg EA, Korner R. 2006. Phosphoproteome analysis of the human mitotic spindle. *Proceedings of the National Academy of Sciences of the United States of America* **103**: 5391-5396.

Nozawa RS, Nagao K, Masuda HT, Iwasaki O, Hirota T, Nozaki N, Kimura H, Obuse C. 2010. Human POGZ modulates dissociation of HP1alpha from mitotic chromosome arms through Aurora B activation. *Nature cell biology* **12**: 719-727.

Oceguera-Yanez F, Kimura K, Yasuda S, Higashida C, Kitamura T, Hiraoka Y, Haraguchi T, Narumiya S. 2005. Ect2 and MgcRacGAP regulate the activation and function of Cdc42 in mitosis. *The Journal of cell biology* **168**: 221-232.

Oda H, Hubner MR, Beck DB, Vermeulen M, Hurwitz J, Spector DL, Reinberg D. 2010. Regulation of the histone H4 monomethylase PR-Set7 by CRL4(Cdt2)-mediated PCNA-dependent degradation during DNA damage. *Molecular cell* **40**: 364-376.

Oda H, Okamoto I, Murphy N, Chu J, Price SM, Shen MM, Torres-Padilla ME, Heard E, Reinberg D. 2009. Monomethylation of histone H4-lysine 20 is involved in chromosome structure and stability and is essential for mouse development. *Molecular and cellular biology* **29**: 2278-2295.

Ohzeki J, Bergmann JH, Kouprina N, Noskov VN, Nakano M, Kimura H, Earnshaw WC, Larionov V, Masumoto H. 2012. Breaking the HAC Barrier: histone H3K9 acetyl/methyl balance regulates CENP-A assembly. *The EMBO journal* **31**: 2391-2402.

Okamoto Y, Nakano M, Ohzeki J, Larionov V, Masumoto H. 2007. A minimal CENP-A core is required for nucleation and maintenance of a functional human centromere. *The EMBO journal* **26**: 1279-1291.

Olsen JV, Blagoev B, Gnad F, Macek B, Kumar C, Mortensen P, Mann M. 2006. Global, in vivo, and site-specific phosphorylation dynamics in signaling networks. *Cell* **127**: 635-648.

Olszak AM, van Essen D, Pereira AJ, Diehl S, Manke T, Maiato H, Saccani S, Heun P. 2011. Heterochromatin boundaries are hotspots for de novo kinetochore formation. *Nature cell biology* **13**: 799-808.

Parelho V, Hadjur S, Spivakov M, Leleu M, Sauer S, Gregson HC, Jarmuz A, Canzonetta C, Webster Z, Nesterova T et al. 2008. Cohesins functionally associate with CTCF on mammalian chromosome arms. *Cell* **132**: 422-433.

Perpelescu M, Fukagawa T. 2011. The ABCs of CENPs. *Chromosoma* **120**: 425-446.

Perpelescu M, Nozaki N, Obuse C, Yang H, Yoda K. 2009. Active establishment of centromeric CENP-A chromatin by RSF complex. *The Journal of cell biology* **185**: 397-407.

Peters AH, O'Carroll D, Scherthan H, Mechtler K, Sauer S, Schofer C, Weipoltshammer K, Pagani M, Lachner M, Kohlmaier A et al. 2001. Loss of the Suv39h histone methyltransferases impairs mammalian heterochromatin and genome stability. *Cell* **107**: 323-337.

Peters JM, Tedeschi A, Schmitz J. 2008. The cohesin complex and its roles in chromosome biology. *Genes & development* **22**: 3089-3114.

Pfleger CM, Salic A, Lee E, Kirschner MW. 2001. Inhibition of Cdh1-APC by the MAD2-related protein MAD2L2: a novel mechanism for regulating Cdh1. *Genes & development* **15**: 1759-1764.

Pidoux AL, Allshire RC. 2004. Kinetochore and heterochromatin domains of the fission yeast centromere. *Chromosome research : an international journal on the molecular, supramolecular and evolutionary aspects of chromosome biology* **12**: 521-534.

-. 2005. The role of heterochromatin in centromere function. *Philosophical transactions of the Royal Society of London Series B, Biological sciences* **360**: 569-579.

Probst AV, Okamoto I, Casanova M, El Marjou F, Le Baccon P, Almouzni G. 2010. A strand-specific burst in transcription of pericentric satellites is required for chromocenter formation and early mouse development. *Developmental cell* **19**: 625-638.

Rea S, Eisenhaber F, O'Carroll D, Strahl BD, Sun ZW, Schmid M, Opravil S, Mechtler K, Ponting CP, Allis CD et al. 2000. Regulation of chromatin structure by site-specific histone H3 methyltransferases. *Nature* **406**: 593-599.

Regnier V, Vagnarelli P, Fukagawa T, Zerjal T, Burns E, Trouche D, Earnshaw W, Brown W. 2005. CENP-A is required for accurate chromosome segregation and sustained kinetochore association of BubR1. *Molecular and cellular biology* **25**: 3967-3981.

Ribeiro SA, Gatlin JC, Dong Y, Joglekar A, Cameron L, Hudson DF, Farr CJ, McEwen BF, Salmon ED, Earnshaw WC et al. 2009. Condensin regulates the stiffness of vertebrate centromeres. *Molecular biology of the cell* **20**: 2371-2380.

Ribeiro SA, Vagnarelli P, Dong Y, Hori T, McEwen BF, Fukagawa T, Flors C, Earnshaw WC. 2010. A super-resolution map of the vertebrate kinetochore. *Proceedings of the National Academy of Sciences of the United States of America* **107**: 10484-10489.

Routh A, Sandin S, Rhodes D. 2008. Nucleosome repeat length and linker histone stoichiometry determine chromatin fiber structure. *Proceedings of the National Academy of Sciences of the United States of America* **105**: 8872-8877.

Ruchaud S, Carmena M, Earnshaw WC. 2007. Chromosomal passengers: conducting cell division. *Nature reviews Molecular cell biology* **8**: 798-812.

Ryan DP, Sundaramoorthy R, Martin D, Singh V, Owen-Hughes T. 2011. The DNA-binding domain of the Chd1 chromatin-remodelling enzyme contains SANT and SLIDE domains. *The EMBO journal* **30**: 2596-2609.

Ryan SD, Britigan EM, Zasadil LM, Witte K, Audhya A, Roopra A, Weaver BA. 2012. Up-regulation of the mitotic checkpoint component Mad1 causes chromosomal instability and resistance to microtubule poisons. *Proceedings of the National Academy of Sciences of the United States of America* **109**: E2205-2214.

Samoshkin A, Arnaoutov A, Jansen LE, Ouspenski I, Dye L, Karpova T, McNally J, Dasso M, Cleveland DW, Strunnikov A. 2009. Human condensin function is essential for centromeric chromatin assembly and proper sister kinetochore orientation. *PloS one* **4**: e6831.

Sanyal A, Lajoie BR, Jain G, Dekker J. 2012. The long-range interaction landscape of gene promoters. *Nature* **489**: 109-113.

Sato H, Masuda F, Takayama Y, Takahashi K, Saitoh S. 2012. Epigenetic inactivation and subsequent heterochromatinization of a centromere stabilize dicentric chromosomes. *Current biology : CB* **22**: 658-667.

Schmiedeberg L, Weisshart K, Diekmann S, Meyer Zu Hoerste G, Hemmerich P. 2004. High- and low-mobility populations of HP1 in heterochromatin of mammalian cells. *Molecular biology of the cell* **15**: 2819-2833.

Schotta G, Lachner M, Sarma K, Ebert A, Sengupta R, Reuter G, Reinberg D, Jenuwein T. 2004. A silencing pathway to induce H3-K9 and H4-K20 trimethylation at constitutive heterochromatin. *Genes & development* **18**: 1251-1262.

Schotta G, Sengupta R, Kubicek S, Malin S, Kauer M, Callen E, Celeste A, Pagani M, Opravil S, De La Rosa-Velazquez IA et al. 2008. A chromatin-wide transition to H4K20 monomethylation impairs genome integrity and programmed DNA rearrangements in the mouse. *Genes & development* **22**: 2048-2061.

Schultz DC, Ayyanathan K, Negorev D, Maul GG, Rauscher FJ, 3rd. 2002. SETDB1: a novel KAP-1-associated histone H3, lysine 9-specific methyltransferase that contributes to HP1-mediated silencing of euchromatic genes by KRAB zinc-finger proteins. *Genes & development* **16**: 919-932.

Schwarz PM, Felthauser A, Fletcher TM, Hansen JC. 1996. Reversible oligonucleosome self-association: dependence on divalent cations and core histone tail domains. *Biochemistry* **35**: 4009-4015.

Schwarzacher HG. 1964. [Studies on the Nuclear Structure and Chromocenter in Tissue Culture Cells]. *Verhandlungen der Anatomischen Gesellschaft* **59**: 32-34.

Screpanti E, De Antoni A, Alushin GM, Petrovic A, Melis T, Nogales E, Musacchio A. 2011. Direct binding of Cenp-C to the Mis12 complex joins the inner and outer kinetochore. *Current biology : CB* **21**: 391-398.

Serrano A, Rodriguez-Corsino M, Losada A. 2009. Heterochromatin protein 1 (HP1) proteins do not drive pericentromeric cohesin enrichment in human cells. *PloS one* **4**: e5118.

Shah C, Vangompel MJ, Naeem V, Chen Y, Lee T, Angeloni N, Wang Y, Xu EY. 2010. Widespread presence of human BOULE homologs among animals and conservation of their ancient reproductive function. *PLoS genetics* **6**: e1001022.

Shen Z. 2011. Genomic instability and cancer: an introduction. *Journal of molecular cell biology* **3**: 1-3.

Shimada A, Murakami Y. 2010. Dynamic regulation of heterochromatin function via phosphorylation of HP1-family proteins. *Epigenetics : official journal of the DNA Methylation Society* **5**: 30-33.

Silva MC, Bodor DL, Stellfox ME, Martins NM, Hochegger H, Foltz DR, Jansen LE. 2012. Cdk activity couples epigenetic centromere inheritance to cell cycle progression. *Developmental cell* **22**: 52-63.

Singh PB. 2010. HP1 proteins--what is the essential interaction? *Genetika* **46**: 1424-1429.

Smothers JF, Henikoff S. 2000. The HP1 chromo shadow domain binds a consensus peptide pentamer. *Current biology : CB* **10**: 27-30.

Souza PP, Volkel P, Trinel D, Vandamme J, Rosnoblet C, Heliot L, Angrand PO. 2009. The histone methyltransferase SUV420H2 and Heterochromatin Proteins HP1 interact but show different dynamic behaviours. *BMC cell biology* **10**: 41.

Spektor TM, Congdon LM, Veerappan CS, Rice JC. 2011. The UBC9 E2 SUMO conjugating enzyme binds the PR-Set7 histone methyltransferase to facilitate target gene repression. *PloS one* **6**: e22785.

Steigemann P, Wurzenberger C, Schmitz MH, Held M, Guizetti J, Maar S, Gerlich DW. 2009. Aurora B-mediated abscission checkpoint protects against tetraploidization. *Cell* **136**: 473-484.

Sullivan BA, Karpen GH. 2004. Centromeric chromatin exhibits a histone modification pattern that is distinct from both euchromatin and heterochromatin. *Nature structural & molecular biology* **11**: 1076-1083.

Tachibana M, Matsumura Y, Fukuda M, Kimura H, Shinkai Y. 2008. G9a/GLP complexes independently mediate H3K9 and DNA methylation to silence transcription. *The EMBO journal* **27**: 2681-2690.

Tachibana M, Sugimoto K, Nozaki M, Ueda J, Ohta T, Ohki M, Fukuda M, Takeda N, Niida H, Kato H et al. 2002. G9a histone methyltransferase plays a dominant role in euchromatic histone H3 lysine 9 methylation and is essential for early embryogenesis. *Genes & development* **16**: 1779-1791.

Tadeu AM, Ribeiro S, Johnston J, Goldberg I, Gerloff D, Earnshaw WC. 2008. CENP-V is required for centromere organization, chromosome alignment and cytokinesis. *The EMBO journal* **27**: 2510-2522.

Tanaka TU. 2008. Bi-orienting chromosomes: acrobatics on the mitotic spindle. *Chromosoma* **117**: 521-533.

Tanaka TU, Rachidi N, Janke C, Pereira G, Galova M, Schiebel E, Stark MJ, Nasmyth K. 2002. Evidence that the Ipl1-Sli15 (Aurora kinase-INCENP) complex promotes chromosome bi-orientation by altering kinetochore-spindle pole connections. *Cell* **108**: 317-329.

Tardat M, Brustel J, Kirsh O, Lefevbre C, Callanan M, Sardet C, Julien E. 2010. The histone H4 Lys 20 methyltransferase PR-Set7 regulates replication origins in mammalian cells. *Nature cell biology* **12**: 1086-1093.

Thiru A, Nietlispach D, Mott HR, Okuwaki M, Lyon D, Nielsen PR, Hirshberg M, Verreault A, Murzina NV, Laue ED. 2004. Structural basis of HP1/PXVXL motif peptide interactions and HP1 localisation to heterochromatin. *The EMBO journal* **23**: 489-499.

Toth A, Ciosk R, Uhlmann F, Galova M, Schleiffer A, Nasmyth K. 1999. Yeast cohesin complex requires a conserved protein, Eco1p(Ctf7), to establish cohesion between sister chromatids during DNA replication. *Genes & development* **13**: 320-333.

Trazzi S, Bernardoni R, Diolaiti D, Politi V, Earnshaw WC, Perini G, Della Valle G. 2002. In vivo functional dissection of human inner kinetochore protein CENP-C. *Journal of structural biology* **140**: 39-48.

Trazzi S, Perini G, Bernardoni R, Zoli M, Reese JC, Musacchio A, Della Valle G. 2009. The C-terminal domain of CENP-C displays multiple and critical functions for mammalian centromere formation. *PloS one* **4**: e5832.

Trievel RC, Beach BM, Dirk LM, Houtz RL, Hurley JH. 2002. Structure and catalytic mechanism of a SET domain protein methyltransferase. *Cell* **111**: 91-103.

Tschiersch B, Hofmann A, Krauss V, Dorn R, Korge G, Reuter G. 1994. The protein encoded by the Drosophila position-effect variegation suppressor gene Su(var)3-9 combines domains of antagonistic regulators of homeotic gene complexes. *The EMBO journal* **13**: 3822-3831.

Uren AG, Wong L, Pakusch M, Fowler KJ, Burrows FJ, Vaux DL, Choo KH. 2000. Survivin and the inner centromere protein INCENP show similar cell-cycle localization and gene knockout phenotype. *Current biology : CB* **10**: 1319-1328.

Vagnarelli P, Hudson DF, Ribeiro SA, Trinkle-Mulcahy L, Spence JM, Lai F, Farr CJ, Lamond AI, Earnshaw WC. 2006. Condensin and Repo-Man-PP1 co-operate in the regulation of chromosome architecture during mitosis. *Nature cell biology* **8**: 1133-1142.

van der Waal MS, Hengeveld RC, van der Horst A, Lens SM. 2012. Cell division control by the Chromosomal Passenger Complex. *Experimental cell research* **318**: 1407-1420.

Van Hooser AA, Ouspenski, II, Gregson HC, Starr DA, Yen TJ, Goldberg ML, Yokomori K, Earnshaw WC, Sullivan KF, Brinkley BR. 2001. Specification of kinetochore-forming chromatin by the histone H3 variant CENP-A. *Journal of cell science* **114**: 3529-3542.

Vandesompele J, De Preter K, Pattyn F, Poppe B, Van Roy N, De Paepe A, Speleman F. 2002. Accurate normalization of real-time quantitative RT-PCR data by geometric averaging of multiple internal control genes. *Genome Biol* **3**: RESEARCH0034.

VanGompel MJ, Xu EY. 2010. A novel requirement in mammalian spermatid differentiation for the DAZ-family protein Boule. *Human molecular genetics* **19**: 2360-2369.

Vermeulen M, Eberl HC, Matarese F, Marks H, Denissov S, Butter F, Lee KK, Olsen JV, Hyman AA, Stunnenberg HG et al. 2010. Quantitative interaction proteomics and genome-wide profiling of epigenetic histone marks and their readers. *Cell* **142**: 967-980.

Wendt KS, Yoshida K, Itoh T, Bando M, Koch B, Schirghuber E, Tsutsumi S, Nagae G, Ishihara K, Mishiro T et al. 2008. Cohesin mediates transcriptional insulation by CCCTC-binding factor. *Nature* **451**: 796-801.

Whelan G, Kreidl E, Wutz G, Egner A, Peters JM, Eichele G. 2012. Cohesin acetyltransferase Esco2 is a cell viability factor and is required for cohesion in pericentric heterochromatin. *The EMBO journal* **31**: 71-82.

Yamagata K, Yamazaki T, Miki H, Ogonuki N, Inoue K, Ogura A, Baba T. 2007. Centromeric DNA hypomethylation as an epigenetic signature discriminates between germ and somatic cell lineages. *Developmental biology* **312**: 419-426.

Yamagishi Y, Sakuno T, Shimura M, Watanabe Y. 2008. Heterochromatin links to centromeric protection by recruiting shugoshin. *Nature* **455**: 251-255.

Yan Q, Cho E, Lockett S, Muegge K. 2003. Association of Lsh, a regulator of DNA methylation, with pericentromeric heterochromatin is dependent on intact heterochromatin. *Molecular and cellular biology* **23**: 8416-8428.

Yang L, Xia L, Wu DY, Wang H, Chansky HA, Schubach WH, Hickstein DD, Zhang Y. 2002. Molecular cloning of ESET, a novel histone H3-specific methyltransferase that interacts with ERG transcription factor. *Oncogene* **21**: 148-152.

Yap KL, Zhou MM. 2010. Keeping it in the family: diverse histone recognition by conserved structural folds. *Critical reviews in biochemistry and molecular biology* **45**: 488-505.

Yeates TO. 2002. Structures of SET domain proteins: protein lysine methyltransferases make their mark. *Cell* **111**: 5-7.

Yuan B, Xu Y, Woo JH, Wang Y, Bae YK, Yoon DS, Wersto RP, Tully E, Wilsbach K, Gabrielson E. 2006. Increased expression of mitotic checkpoint genes in breast cancer cells with chromosomal instability. *Clinical cancer research : an official journal of the American Association for Cancer Research* **12**: 405-410.

Zeng W, Ball AR, Jr., Yokomori K. 2010. HP1: heterochromatin binding proteins working the genome. *Epigenetics : official journal of the DNA Methylation Society* **5**: 287-292.

Zhang D, Martyniuk CJ, Trudeau VL. 2006. SANTA domain: a novel conserved protein module in Eukaryota with potential involvement in chromatin regulation. *Bioinformatics* **22**: 2459-2462.

Zolghadr K, Rothbauer U, Leonhardt H. 2012. The fluorescent two-hybrid (F2H) assay for direct analysis of protein-protein interactions in living cells. *Methods in molecular biology* **812**: 275-282.